



Land use effects on geochemical properties and their control
on soil organic matter in volcanic soils in Java, Indonesia

Sastrika Anindita

2023

Land use effects on geochemical properties and their control on soil organic matter in volcanic soils in Java, Indonesia

Sastrika Anindita

Members of the examination committee:

Prof. dr. ir. Peter Bossier (chairman)

Faculty of Bioscience Engineering, Ghent university

Prof. dr. ir. Erik Meers

Faculty of Bioscience Engineering, Ghent University

Prof. dr. ir. Stefaan De Neve

Faculty of Bioscience Engineering, Ghent University

Prof. dr. Johan De Grave

Faculty of Science, Ghent University

Prof. dr. Bas Van Wesemael

Faculty of Science, Université Catholique de Louvain

Supervisors:

Prof. dr. Peter Finke (promoter)

Department of Environment

Faculty of Bioscience Engineering

Ghent University

Prof. dr. ir. Steven Sleutel (promoter)

Department of Environment

Faculty of Bioscience Engineering

Ghent University

Dean: Prof. dr. Els Van Damme

Rector: Prof. dr. Rik Van de Walle

Land use effects on geochemical properties and their control on soil organic carbon in volcanic soils in Java, Indonesia

Doctoral dissertation presented by

Sastrika Anindita

DISSERTATION SUBMITTED IN FULFILLMENT OF THE REQUIREMENT FOR THE DEGREE OF
DOCTOR IN BIOSCIENCE ENGINEERING: NATURAL RESOURCES

DEPARTMENT OF ENVIRONMENT
FACULTY OF BIOSCIENCE ENGINEERING
GHENT UNIVERSITY

Dutch translation of the title:

Effecten van landgebruik op geochemische eigenschappen en hun beïnvloeding van organische koolstof in de bodem in vulkanische bodems in Java, Indonesië.

Cover illustration:

Mount Tangkuban Perahu and soil minerals.

Citation of the dissertation:

ISBN number:

Copyright statement: All rights reserved. No part of this document may be reproduced or transmitted in any form or by any means, electronic, mechanical, photocopying, scanning, recording, or otherwise, without prior written permission of the author and/or dissertation promoter(s). A written permission of the author is also required to use the methods, products, schematics and programs described in this work for industrial or commercial use, and for submitting any part of this dissertation in scientific contests. Every other use is subjected to the copyright laws.

Acknowledgements

My sincere gratitude is expressed to my supervisor, Prof. dr. Peter Finke. This dissertation is an expanded research of my master's thesis, and I could not ask for a better supervisor than him, who has guided me during research. It all started seven years ago when I came and asked you to supervise my research on volcanic soils in Indonesia. He agreed, and we tried to simulate the development of soil properties using the SoilGen model, which was unfamiliar to me. Nevertheless, his inevitable support and knowledge helped me become familiar with soil genesis modelling. I also sincerely thank him for entrusting me with the opportunity to do PhD research under your supervision. During my doctoral journey, he gave me a great deal of freedom, and it stimulated my decision-making ability. He is always available and responds fast whenever I need him to discuss my research, and I appreciate everything he has taught me. Also, I highly appreciate Prof. Steven Sleutel, my second supervisor, for his enormous assistance during the laboratory experiment and for spending much time reading, checking, and correcting my manuscript. Thank you for your support and knowledge.

I would like to express my gratitude to the members of my examination committee: Prof. dr. ir Peter Bossier (chairman), Prof. dr. ir. Stefaan De Neve, Prof. dr. Johan De Grave, Prof. dr. Bas Van Wesemael, Prof. dr. ir. Erik Meers for their appreciation on this dissertation. They have thoroughly screened this thesis and their suggestions have highly improved the quality of this work. I also thank Prof. dr. Johan De Grave for giving me access to analyse my samples in the Department of Geology and Dimitri, Veerle, Tina, Sophie, Matthieu, Anne-Mie for the help and assistance in the laboratory. My gratitude also goes to Indonesia Endowment Fund for Education (LPDP) for financial support during my stay in Belgium and to the Soil Department, Universitas Padjadjaran, for allowing me to use the instrument during field sampling.

My special thanks also go to my colleagues in the Soil research group, Department of Environment: Nirmani, Tizitha, Haichao, Orly, Oka, Wenjing, Patria, Heleen, Tamir, Scynthia, Umehani, Junwei, Lin lin, and others for the fruitful discussion, pleasant and interactive lunch. My sincere appreciation goes to OBSG for providing me a very warm stay in Ghent and to all the members of the Indonesian Student Association in Ghent (PPI Ghent) for making the city like home. My hearth-felt thanks go to Uwa Ann Djuzman, Ko Juliando, Pak Bakhtiar, and Mommy Lely for being parents of all the Indonesian students in Ghent.

To my mom, Diah Ratna Surjati, and my sisters (Sasmita and Satwika), thank you for your support and unconditional love. My mother probably does not know exactly what I aimed for in my research, but her prayer always gives me calm and earns me luck. To my beloved father, my role model, thank you for everything. Finally, to my dearest husband, Arfah Durahman, thank you for the love and patience. He has given everything he could – his career and his time – to stand behind me during my scientific journey in Belgium. His love and encouragement continuously sustain me, help me bounce back from a setback and get back to my work. This dissertation is dedicated to all of them.

Sastrika Anindita
2023, Ghent, Belgium

Table of contents

Table of contents	i
List of tables	v
List of figures.....	vi
List of abbreviations.....	viii
Summary	xi
Samenvatting	xiv
CHAPTER 1 GENERAL INTRODUCTION	1
1.1 Broader framework.....	3
1.1.1 Organic matter in soils	3
1.1.2 Volcanic soils and interaction with soil organic carbon	4
1.1.3 Land use and interactions with SOC	6
1.1.4 Soil genoforms and phenoforms.....	7
1.1.5 Climate change and its effect on soil carbon	8
1.2 Specific objectives and research questions	9
1.3 Study area	10
1.3.1 Geography.....	10
1.3.2 Geology of Mt. Tangkuban Perahu and Mt. Burangrang.....	10
1.3.3 Land use	12
1.4 Outline of thesis.....	13
CHAPTER 2 LAND USE IMPACTS ON WEATHERING, SOIL PROPERTIES, AND CARBON STORAGE IN WET ANDOSOLS, INDONESIA	3
2.1 Introduction	19
2.2 Materials and methods.....	20
2.2.1 Environmental setting.....	20
2.2.2 Site description and soil sampling.....	20
2.2.3 Physico-chemical analyses	22
2.2.4 Selective extraction data.....	23
2.2.5 Total elemental analysis and quantification of minerals	23
2.2.6 Soil specific surface area	24
2.2.7 Statistical analysis	24
2.3 Results.....	25

2.3.1 Soil morphology	25
2.3.2 Soil physiochemical properties	25
2.3.3 Total elemental analysis, degree of weathering, and estimation of acid neutralizing capacity	27
2.3.4 XRD-mineralogy	27
2.3.5 Soil specific surface area	29
2.4 Discussion	32
2.4.1 Verifying the anthropo-chronosequence and soil weathering stage as affected by deposition age.....	32
2.4.2 Effects of land use on weathering and acid-neutralizing capacities.....	33
2.4.3 Effects of land use on soil properties.....	34
2.4.4 Soil organic carbon and its association with minerals	35
2.5 Conclusions and research perspective	37

CHAPTER 3 TROPICAL ANDOSOL ORGANIC CARBON QUALITY AND DEGRADABILITY IN RELATION TO SOIL GEOCHEMISTRY AS AFFECTED BY LAND USE **39**

3.1 Introduction	43
3.2 Materials and methods.....	44
3.2.1 Site description and soil sampling.....	44
3.2.2 Soil organic matter fractionation	46
3.2.3 Soil incubation experiment and isotopic signature measurements	47
3.2.4 Statistics	48
3.3 Results.....	48
3.3.1 Organic carbon in soil fractions	48
3.3.2 C:N ratio, amorphous aluminum and iron in the sand-aggregates (S+A) and silt-clay (s+c) fractions.....	50
3.3.3 Correlations between SOC fractions and selected chemical properties.	51
3.3.4 Carbon mineralization experiment	52
3.3.4.1 Gross soil carbon mineralization.....	52
3.3.4.2 Grass C-mineralization	52
3.3.4.3 Native SOC mineralization	52
3.4 Discussion	55
3.4.1 Land use effects on free and aggregate protected OC	55
3.4.2 Effect of land use on SOC in the silt and clay fraction	56
3.4.3 Land use effects on native SOC degradability.....	57

3.4.4 Land use effects of exogenous organic matter decomposition and net priming of SOC	58
3.5 Conclusions	59
CHAPTER 4 SIMULATING SOIL ORGANIC CARBON STOCK AS AFFECTED BY LAND USE AND CLIMATE CHANGE ON VOLCANIC SOILS IN INDONESIA	61
4.1 Introduction	65
4.2 Materials and methods.....	66
4.2.1 Study area	66
4.2.2 SoilGen model	67
4.2.2.1 Water, solute, and heat transfer	67
4.2.2.2 Clay migration process	67
4.2.2.3 Chemical weathering of primary minerals.....	69
4.2.2.4 Vegetation, carbon cycling and plant uptake processes	69
4.2.2.5 Soil phases redistribution processes.....	70
4.2.3 Input data	70
4.2.4 Measured data	71
4.2.5 Research steps	71
4.2.5.1 Calibration of important parameters.....	71
4.2.5.2 Identification of geochemical proxies for SOC-pool decay rates.....	74
4.2.5.3 Model projections	74
4.3 Results and discussion	75
4.3.1 Calibration.....	75
4.3.1.1 Clay migration	75
4.3.1.2 Weathering of primary minerals.....	77
4.3.1.3 Soil organic carbon pool.....	79
4.3.2 Identification of geochemical proxies.....	81
4.3.3 Comparison of simulations quality	83
4.3.4 Effects of different climate projection scenarios on SOC	84
4.3.5 Limitation of this study	87
4.4 Conclusions	88
CHAPTER 5 GENERAL CONCLUSION	89
5.1 General conclusions and discussion	91
5.2 Challenges and recommendations	94
5.2.1 Samples collection	94

5.2.2 Laboratory method	94
5.2.3 Model input data	96
5.2.4 Model process coverage	97
5.2.5 Model calibration	98
5.3 Areas for future research.....	98
5.3.1 Assessing the effect of different agricultural practices on geochemical soil properties.....	98
5.3.2 Improving soil fractionation method and conversion of SOC fractions to SOC pool in the Roth-C model (Zimmermann et al., 2007) for tropical Andosols....	99
5.3.3 Calibrating of non-crystalline materials in tropical volcanic soil using chrono-sequence study.....	99
5.3.4 Improving soil-vegetation-climate simulation in the SoilGen model	100
Appendix for chapter 2	102
Appendix for chapter 3	109
Appendix for chapter 4	110
References	117
Curriculum vitae.....	136

List of tables

Table 2-1	Location of sampling sites, land use, slope, altitude, and age of soils	21
Table 2-2	Selected physicochemical properties in surface and sub-surface horizon of soils.....	26
Table 2-3	Geochemical characteristics (oxide content, weathering intensity, acid-neutralizing capacity)	30
Table 2-4	Comparison of mean soil properties across all depth in the pine forest and agricultural soils (independent samples t-test).....	35
Table 3-1	Physicochemical soil properties of 6 sampled soil profiles in the Sunda Volcanic complex in West Java, Indonesia (partly taken from (Anindita et al., 2022b))	45
Table 3-2	Mass proportion, C concentration, and total content of SOC contained in soil fractions isolated by a modified version of the Zimmermann et al. (2007) method.....	49
Table 3-3	Ratio of C:N, oxalate extractable-aluminum (Al_o) and iron (Fe_o) in S+A and s+c fractions. 51	
Table 4-1	The order of calibrated parameters and their range of parameter values	73
Table 4-2	A summary of the calibrated parameters and best calibrated parameter values.....	76
Table 4-3	Pearson correlation coefficients between calibrated rate constants (k_{RPM} , k_{DPM} , k_{HUM} , and k_{BIO} in y^{-1}) and measured soil properties in the PF and AG soils (5 sites). Double underlined coefficients are significant at $\alpha = 5\%$, whereas underlined means are significant at $\alpha = 10\%$	82

List of figures

Figure 1-1 Illustration of stabilization soil organic matter via physical protection within soil aggregates and organo-mineral association.....	6
Figure 1-2 Location of study area and sampling sites.....	11
Figure 1-3 Typical pine forest (left) and agricultural land use (right) in study area.	13
Figure 2-1 Lithology map of Mt. Tangkuban Perahu and Mt. Burangrang areas with sample points. Simplify from geology map (Silitonga, 1973).	23
Figure 2-2 Geochemical classification (i.e. Total Alkali Silica (TAS) diagram) of total elements of SiO ₂ (%) in function to Na ₂ O + K ₂ O (%) in all soils. Analyses recalculated to 100% on a volatile free basis.	28
Figure 2-3 Relative proportions of mineral constituents as inferred by XRD data at each depth in all soils.....	28
Figure 2-4 Correlations between the means of XRD-amorphous materials and contents of Al _o and Al _o +1/2Fe _o . Correlation coefficient is applied for pine forest and agricultural soils.	29
Figure 2-5 Powder diffractogram of soil samples (< 2 mm) at depth 0 – 20 cm in forest (bottom) and agriculture (top). Peak d-spacing are indicated in nm. Mineral abbreviations: 1:1: 1:1 clay minerals, Hbl: hornblende, Trd: tridymite, Alb: albite, Crs: cristobalite, Gbs: gibbsite, Fsp: feldspar, Qz: quartz, Rtl: rutile, Alu: alunite, Mag: magnetite.....	31
Figure 2-6 Depth evolution soil specific surface area (left) and micropores volume (right) in the different soils at each site.....	31
Figure 2-7 The means of specific surface area and micropores volume as plotted against Al _o content in all soils. Correlation coefficient is applied for pine forest and agricultural soils.	32
Figure 2-8 Plot of molar ratio SiO ₂ /R ₂ O ₃ versus TRB at each soil depth (0 – 20, 20 – 40, and ± 60 – 80 cm) of all soils.....	34
Figure 2-9 Relation between SOC and Al _o content at all measured depths of pine forest and agricultural soils (n per depth = 5). Coefficients of determination at depths of 0 – 20, 20 – 40, and ± 60 – 80 cm are indicated in black, red, and blue fonts, respectively.....	37
Figure 3-1 The distribution of OC over soil fractions obtained by a modified version of the Zimmerman et al. (2007) procedure for 6 sampled soil profiles at each depth of 0 – 20, 20 – 40, ± 60 – 80 cm in the Sunda Volcanic complex in West Java, Indonesia. Vertical bars indicate standard deviations for three lab-replicates (n = 3)	50
Figure 3-2 Scatter plots of the SOC proportion of the S+A fraction and the amounts of Al _o (in bulk soil and sand-aggregate fraction) and amorphous materials. Symbols and Pearson correlation coefficients are in black, red, and blue represent correlations at depths of 0 – 20, 20 – 40, and ± 60 – 80 cm, respectively. Sites under agriculture and pine forest are indicated by ▲ and ●, respectively (n per depth = 5).	52
Figure 3-3 Gross cumulative amount of C mineralized in soil with and without 1 g C kg ⁻¹ ryegrass added. Vertical bars indicate standard deviations of three lab replicates (n = 3) and are presented for the grass amended soils only. Sites under forest and agriculture are indicated by ● and ▲, respectively.	53

Figure 3-4	The percentage of C_{grass} (left) and C_{SOC} (right) mineralized during 120 days of incubation in soils with 1 g kg^{-1} grass or no grass added, respectively. Vertical bars indicate standard deviations of triplicate lab repetitions. Sites under forest and agriculture are indicated by ● and ▲, respectively.	53
Figure 3-5	Net effect of grass addition (1 g kg^{-1}) on cumulative native SOC mineralization. Positive and negative figures denote net positive or net negative cumulative priming of SOC mineralization. Dotted lines present the temporal evolution of mean net cumulative priming effect for either primary forest, pine forest, or agricultural land use, with respectively only upper or lower error bars representing the standard deviations on the data. The dash lines represent the net cumulative priming effect at each site.	54
Figure 3-6	Relation between the proportion of SOC that was oxidizable by 6% NaOCl in the pine forest and agricultural soils with the soil A_{lo} , micropores volume, and soil specific surface area (at each depth $n = 5$). Sites under agriculture and pine forest are indicated by ▲ and ●, respectively. Symbols and Pearson correlation coefficients in black, red, and blue represent correlations at depths of 0 – 20, 20 – 40, and ± 60 – 80 cm, respectively (n per depth = 5).....	57
Figure 4-1	Variation of scaled dissimilarities (Eq. 4-9) between measured and simulated clay content in the calibration of clay migration.	78
Figure 4-2	Variation of scaled dissimilarities between measured (i.e. derived from SOC fractions following Zimmerman et al. (2007) based on data by (Anindita et al., 2022a) and simulated SOC pool in the calibration of the SOC pool decay rates of the four-pool SOC model in SoilGen.	80
Figure 4-3	SOC pool sizes derived from the distribution of SOC across measured soil fractions following Zimmerman et al. (2007) using data from (Anindita et al., 2022a) (meas) and from SOC pool simulation using site-specific process rates (sim) for the five-pool (top) and the four-pool (bottom) SOC model in SoilGen.....	81
Figure 4-4	Comparison of total SOC in each model pool between measured pools (estimated from soil fractionation carried out by (Anindita et al., 2022a) and simulations using (i) site-specific rate constants, (ii) average rate constants, and (iii) geochemical proxy based modification of rates at depths of 0 – 20, 20 - 40, and ± 60 – 80 cm in the four-pool model version of SoilGen	83
Figure 4-5	The trend of OC stock (0 – 20, 20 - 40, and ± 60-80 cm) calculated with three different decay rates, viz. site-specific rate constants, average rate constants, and average rate constant modified by geochemical proxy in sites NF-y, PF-i, PF-o, AG-y, AG-i, and AG-o from 2020 to 2100 under climate scenarios RCP 2.6 (solid line) and 8.5 (dashed line).	85
Figure 4-6	Simulation on the amount and distribution of each SOC pool i.e. RPM, DPM, HUM, BIO using site-specific calibration in response to different climate scenarios: RCP 2.6 (solid line) and RCP 8.5 (dashed line).	86

List of abbreviations

μm	Micrometer
AG	Agriculture
Al	Aluminium
Al^{3+}	Aluminium ions
Al_o	Aluminium extracted by NH_4 -oxalate
Al_p	Aluminium extracted by Na-pyrophosphate
ANC	Acid neutralizing capacity
BD	Bulk density
BIO	Microbial biomass
C:N	Ratio of carbon to nitrogen
Ca	Calcium
Ca^{2+}	Calcium ions
CEC	Cation exchange capacities
$\text{C}_{\text{grass-min}}$	Mineralization of carbon derived from grass
CIA	Chemical index of alteration
C-min	Carbon mineralization
CO_2	Carbon dioxide
$\text{C}_{\text{SOC-min}}$	Mineralization of carbon derived from native soil organic carbon
DIS	Dissimilarity
DOC	Dissolved organic carbon
DPM	Decomposable plant material
Fe	Iron
Fe^{3+}	Iron ions
Fe_d	Iron extracted by dithionite-citrate-bicarbonate
Fe_h	Iron extracted by hydroxylamine hydrochloride
Fe_o	Iron extracted by NH_4 -oxalate
HUM	Humified organic matter
h- θ macro	Pressure head at which macropores empty
IOM	Inert organic matter
kBIO	Decay rate of microbial biomass
k_d	Soil detachability coefficient
kDPM	Decay rate of decomposable plant material
k_H	Dissolution rate constant at acidic condition
kHUM	Decay rate of humified organic matter
k_{OH}	Dissolution rate constant at basic condition
kRPM	Decay rate of resistant plant material
LGM	Last glacial maximum
Ma	Million years
Mg	Magnesium
Mt.	Mountain
n	Filter coefficient
Na	Sodium
NaCl	Sodium chloride
NaOCl	Sodium hypochlorite

NF	Primary forest
OC	Organic carbon
OM	Organic matter
PF	Pine forest
POM	Particulate organic matter
PS _{max}	Maximum particle splitting probability
R ₂ O ₃	Al ₂ O ₃ +Fe ₂ O ₃ +TiO ₂
RCP	Representative concentration pathway
RPM	Resistant plant material
rSOC	Resistant soil organic carbon
S+A	Sand and aggregates fraction
s+c	Silt and clay fraction
Si	Silicon
Si _o	Silicon extracted by NH ₄ -oxalate
SOC	Soil organic carbon
SOM	Soil organic matter
SRO	Short-range order
SSA	Specific surface area
TAS	Total alkali silica
TRB	Total reserve of bases
WRB	World Reference Base for Soil Resources
XRD	X-ray diffraction
yBP	Years before present
δ ¹³ C	Delta carbon thirteen

Summary

Soil organic carbon (SOC) is the main component in global carbon cycling and has important functions in many ecosystem services, such as climate regulation and soil fertility. The ability of soils to retain organic carbon is crucial as the soil stores three times more carbon than the atmosphere. Volcanic soils are amongst the soils that have a large ability to retain a substantial amount of organic carbon. The ability of these soils to store SOC is due to their unique physical and chemical properties. In these soils, the large amounts of non-crystalline and poorly crystalline materials formed by weathering are considered to be responsible for organic carbon stabilization. Meanwhile, the amount and stability of SOC are also influenced by other factors, such as vegetation and climate. In Indonesia, volcanic soils are susceptible to land use conversion, mainly from forest to agricultural land, due to their favourable soil properties for agricultural production. This land use conversion may likely affect the SOC content in these soils, but the knowledge of the relations between land use, geochemical properties, and SOC is still limited. In addition, on-going climate change likely also determines the fate of SOC in the future. Therefore, this research aims to improve our understanding of the effect of land use on SOC through its relation to current geochemical properties and to explore future SOC under different climate scenarios. The research was conducted in volcanic soils near Mt. Tangkuban Perahu and Mt. Burangrang, Java, Indonesia. The study covered six sites with expected different ages based on lithology maps and land use (tropical primary forest, secondary pine forest, and agricultural land).

As a first step, in **chapter 2**, we evaluated the effect of land use on geochemical properties on forest and agricultural sites in Java Indonesia. Analytical data showed that most study sites have similar parent materials indicated by a comparable weathering stage, total element levels, and mineralogy. The site with the primary forest was however found to have a different parent material and thus was excluded from the comparison of soil properties. A difference in soil properties was found between both land-uses with a higher pH, exchangeable base contents, and base saturation in the agricultural soils than in the pine forest. These results highlight the existence of phenofoms (management-related sub-soil type) within the general genoforms (genetic soil types), which were expressed in terms of soil classification by the modifier *dystric* (pine forest soil) and *eutric* (agricultural soil). Besides those properties, a higher content of short-range order aluminium (indicated by NH_4 -oxalate extractable Al_o , Al_o) was also found under agricultural soils and it positively correlated to SOC content. We conclude that land use affects soil properties, and postulate that enhanced Al_o formation under agricultural land-use would partly contribute to the relatively high SOC stock in these soils also after conversion from forest land-use.

In **chapter 3**, the effect of land use on the stability and quality of SOC was evaluated by a modified soil fractionation method by Zimmermann et al. (2007). This method separated the soils into fractions corresponding to different physical and chemical stabilization mechanisms. Our results showed that most of the SOC was present in the silt-clay fraction. Interestingly, there was a threefold larger amount of SOC in strong ultrasonication resistant sand-sized aggregates under agricultural vs. forest land use. Positive correlations existed between SOC content in this stable aggregate fraction and some soil properties, such as the contents of Al_o and amorphous materials. These results suggest that Al_o plays

an essential role in the aggregation of soil particles and alongside in aggregate-occlusion of SOC. In addition, the role of Al_0 on silt clay associated SOC was also observed, particularly at subsoil. Thus, the positive role of Al_0 on SOC as postulated in Chapter 2 was supported. Furthermore, we also examined the degradability of native and exogenous SOC of topsoil (0 – 20 cm) in an incubation experiment. We applied a single ^{13}C -isotope labelled substrate to the topsoils to investigate the effects of geochemical properties or soil aggregation on the decomposition of fresh organic matter. The results showed no differential effects on the mineralization of fresh organic matter (ryegrass) between forest and agricultural land use. However, the effect of geochemical properties, texture, and structure on the stability of native SOC was observed, as indicated by the negative correlation between SOC in sand-aggregate fractions and mineralization of native SOC. Thus, we could conclude the roles of Al_0 on soil aggregation and organo-mineral association apparently play important role in stabilizing SOC in at these tropical Andosols.

In **Chapter 4**, the research was extended to model SOC using a process-based genesis model, the SoilGen model. First, the soil model was calibrated for essential soil processes in volcanic soils, such as clay migration, weathering of primary minerals, and SOC pool decay rate, to maximize the reliability of the model output. The calibration ran for over $\pm 8 - 10$ kyrs, being the approximate age of the soils. The results showed that the clay migration calibration was in reasonable agreement with the range of literature values. In contrast, the optimum parameter values derived from calibration of weathering rates were not within the range of reference values. The uncertainty of initial stocks of minerals and limited soil process coverage, such as the formation of secondary minerals, possibly caused the inaccuracy in the model output in the minerals' calibration. Accurate initial minerals content and the process of secondary minerals formation need to be included to improve the model output. Furthermore, the calibration of SOC pools was analysed in more detail. In this calibration, we compared four-pool (without inert organic matter) vs five-pool models (including inert organic matter) and three calibration methods: a site-specific calibration, a generic calibration, and a generic calibration modified by a geochemical proxy. The geochemical proxy was identified to represent the effects of geochemical composition on the decay rate of SOC. Results showed that the measured SOC pools and total SOC were better reproduced with a four-pool model and a site-specific calibration. This result illustrates that there is uncertainty on the presence of an inert organic pool over a millennial time scale and also the differences in SOC decay rate under different land use. The calibration method using a geochemical proxy generally improved the simulated total SOC and HUM pool than calibration with a generic rate. Furthermore, the effect of global warming (i.e., climate scenario RCP 8.5) was generally more pronounced in agricultural soils than forest soils. This work overall highlighted the importance of the calibration method in estimating future SOC and the susceptibility of forest and agricultural soils to global warming.

General conclusions and challenges are summarized in **chapter 5**. Overall, our work investigated the relations between land use, geochemical soil properties, and SOC using analytical data and a process-based genesis model (SoilGen). This research highlights that the difference in geochemical properties mediated by land use potentially contributes to the accumulation and stabilization of SOC, and the calibration approach on the SOC model affects the accuracy of the result with respect to current and future SOC. The largest challenge was related to particle size analyses, whereas the uncertainty of

initial data (stocks) and the inaccurate SOC model pool partitioning may contribute to the inaccuracy of model output in the modelling study. The laboratory analyses and soil model remain to be improved for the precise output as described in this chapter. In the future, it will now be needed to affirm the robustness of the found effect of agricultural practice on the formation of non-crystalline materials in volcanic soils. Larger sets of sites with comparable parent material and age but differing land use will need to be looked included. In this PhD research, the positive effect of soil aggregates on SOC storage was suggested. However, from the likeness in C:N ratios and contents of pedogenic oxides between isolated 'aggregate' and 'silt and clay' fractions, it emerges that soil fractionation methods need to be further developed still for Andosols to more efficiently isolate functional SOC pools. Lastly, there is a need to integrate the formation of non-crystalline materials in the SoilGen model, along with their impacts on SOC stabilization.

Samenvatting

Organische koolstof in de bodem (SOC) is de belangrijkste component in de wereldwijde koolstofcyclus en heeft belangrijke functies in veel ecosysteemdiensten, zoals klimaatregulering en bodemvruchtbaarheid. Het vermogen van bodems om organische koolstof vast te houden is cruciaal, aangezien de bodem drie keer meer koolstof opslaat dan de atmosfeer. Vulkanische bodems behoren tot de bodems die een groot vermogen hebben om een aanzienlijke hoeveelheid organische koolstof vast te houden. Het vermogen van deze bodems om SOC op te slaan is te danken aan hun unieke fysische en chemische eigenschappen. In deze bodems worden de grote hoeveelheden niet-kristallijne en slecht kristallijne materialen gevormd door verwerking verantwoordelijk geacht voor de stabilisatie van organische koolstof. Ondertussen worden de hoeveelheid en de stabiliteit van SOC ook beïnvloed door andere factoren, zoals vegetatie en klimaat. In Indonesië zijn vulkanische bodems vatbaar voor conversie van landgebruik, voornamelijk van bos naar landbouwgrond, vanwege hun gunstige bodemeigenschappen voor landbouwproductie. Deze conversie van landgebruik kan waarschijnlijk het SOC-gehalte in deze bodems beïnvloeden, maar de kennis van de relaties tussen landgebruik, geochemische eigenschappen en SOC is nog beperkt. Bovendien bepaalt de aanhoudende klimaatverandering waarschijnlijk ook het lot van SOC in de toekomst. Daarom heeft dit onderzoek tot doel ons begrip van het effect van landgebruik op SOC te verbeteren als functie van zijn relatie met de huidige geochemische eigenschappen en om toekomstige SOC onder verschillende klimaatscenario's te verkennen. Het onderzoek werd uitgevoerd in vulkanische bodems nabij de berg Tangkuban Perahu en de berg Burangrang, Java, Indonesië. De studie omvatte zes locaties met verwachte verschillende leeftijden op basis van lithologische kaarten en landgebruik (tropisch oerbos, secundair dennenbos en landbouwgrond).

Als eerste stap evalueerden we in hoofdstuk 2 het effect van landgebruik op geochemische eigenschappen op bos- en landbouwgebieden in Java, Indonesië. Analytische gegevens toonden aan dat de meeste onderzoekslocaties vergelijkbaar moedermateriaal hebben, blijkens een vergelijkbaar verweringsstadium, totale elementniveaus en mineralogie. De site met het oerbos bleek echter een ander moedermateriaal te hebben en werd daarom uitgesloten van de vergelijking van bodemeigenschappen. Er werd een verschil in bodemeigenschappen gevonden tussen beide landgebruiken met hogere pH, uitwisselbare basegehalten en baseverzadiging in de landbouwbodems dan in het dennenbos. Deze resultaten benadrukken het bestaan van fenovormen (beheergerelateerd sub-bodemtype) binnen de algemene genovormen (genetische bodemtypen), die werden uitgedrukt in termen van bodemclassificatie door de modifier *dystric* (dennenbosbodem) en *eutric* (landbouwgrond). Naast deze eigenschappen werd ook een hoger gehalte aan aluminium-mineralen met korte-afstand kristalstructuur (*short range order*, aangegeven door NH_4 -oxalaat extraheerbaar Al, Al_o) gevonden onder landbouwbodems en dit correleerde positief met het SOC-gehalte. We concluderen dat landgebruik de bodemeigenschappen beïnvloedt, en postuleren dat verbeterde Al_o -vorming onder agrarisch landgebruik gedeeltelijk zou bijdragen aan de relatief hoge SOC-voorraad in deze bodems, ook na conversie van boslandgebruik.

In hoofdstuk 3 werd het effect van landgebruik op de stabiliteit en kwaliteit van SOC geëvalueerd met een gemodificeerde bodemfractioneringsmethode door Zimmermann et al. (2007). Deze methode scheidde de bodems in fracties die overeenkomen met verschillende fysische en chemische stabilisatiemechanismen. Onze resultaten toonden aan dat het grootste deel van de SOC aanwezig was in de silt-kleifractie. Interessant is dat er een drievoudig grotere hoeveelheid SOC was in sterke ultrasone trillingen-resistente aggregaten ter grootte van zand bij gebruik van landbouwgrond versus bosgrond. Er waren positieve correlaties tussen het SOC-gehalte in deze stabiele aggregaatfractie en sommige bodemeigenschappen, zoals het gehalte aan Al_0 en amorfe materialen. Deze resultaten suggereren dat Al_0 een essentiële rol speelt bij de aggregatie van bodemdeeltjes en daarnaast bij de aggregatie-occlusie van SOC. Daarnaast werd ook de rol van Al_0 op silt-klei-geassocieerde SOC waargenomen, vooral in de ondergrond. De positieve rol van Al_0 op de SOC, zoals gepostuleerd in hoofdstuk 2, werd dus ondersteund. Verder onderzochten we ook de afbreekbaarheid van inheemse en toegevoegde SOC in de bovengrond (0 – 20 cm) in een incubatie-experiment. We hebben éénmaal een ^{13}C -isotoop gelabeld substraat op de bovengrond aangebracht om de effecten van geochemische eigenschappen of bodemaggregatie op de afbraak van vers organisch materiaal te onderzoeken. De resultaten lieten geen differentiële effecten zien op de mineralisatie van vers organisch materiaal (raaigras) tussen bos- en landbouwgrondgebruik. Het effect van geochemische eigenschappen, textuur en structuur op de stabiliteit van inheemse SOC werd echter waargenomen, zoals aangegeven door de negatieve correlatie tussen SOC in zand-aggregaatfracties en mineralisatie van native SOC. We zouden dus kunnen concluderen dat het effect van Al_0 op bodemaggregatie en organo-minerale associatie blijkbaar een belangrijke rol speelt bij het stabiliseren van SOC in deze tropische Andosols.

In Hoofdstuk 4 werd het onderzoek uitgebreid naar het modelleren van SOC met behulp van een proces-gebaseerd bodemvormingsmodel, het SoilGen-model. Eerst werd het bodemmodel gekalibreerd voor essentiële bodemprocessen in vulkanische bodems, zoals kleimigratie, verwerking van primaire mineralen en SOC-poelvervalsnelheid, om de betrouwbaarheid van de modeloutput te maximaliseren. De kalibratie weerspiegelde een periode van meer dan $\pm 8 - 10$ kyr, zijnde de geschatte leeftijd van de bodems. De resultaten toonden aan dat de kalibratie van de kleimigratie redelijk overeenkwam met waarden in de literatuur. Daarentegen lagen de optimale parameterwaarden afgeleid van kalibratie van verwerkingssnelheden niet binnen het bereik van referentiewaarden. De onzekerheid van de initiële voorraden van mineralen en de beperkte procesdekking van het bodemmodel, met name de vorming van secundaire mineralen, veroorzaakten mogelijk de onnauwkeurigheid in de modeloutput bij de kalibratie van de mineralen. Nauwkeurige initiële mineraleninhoud en het proces van vorming van secundaire mineralen moeten worden opgenomen in de modellering om de modeloutput te verbeteren. Verder werd de kalibratie van SOC-poelen in meer detail geanalyseerd. In deze kalibratie vergeleken we modellen met vier poelen (zonder inert organisch materiaal) versus modellen met vijf poelen (inclusief inert organisch materiaal) en drie kalibratiemethoden: een locatiespecifieke kalibratie, een generieke kalibratie en een generieke kalibratie aangepast door een geochemische proxy. De geochemische proxy werd geïdentificeerd om de effecten van geochemische samenstelling op de afbraaksnelheid van SOC weer te geven. De resultaten toonden aan dat de gemeten SOC-poelen en de totale SOC beter werden gereproduceerd met een model met vier poelen en een locatiespecifieke kalibratie. Dit resultaat illustreert dat er onzekerheid bestaat over de aanwezigheid van een inerte organische poel over een

millenniumtijdschaal en ook over de verschillen in SOC-vervalsnelheid bij verschillend landgebruik. De kalibratiemethode met behulp van een geochemische proxy verbeterde over het algemeen de gesimuleerde totale SOC en HUM-pool ten opzichte van kalibratie met een generieke snelheid. Bovendien was het effect van de opwarming van de aarde (d.w.z. klimaatscenario RCP 8.5) over het algemeen meer uitgesproken in landbouwbodems dan in bosbodems. Dit werk benadrukte het belang van de kalibratiemethode bij het schatten van toekomstige SOC en de gevoeligheid van bos- en landbouwbodems voor het broeikaseffect.

Algemene conclusies en uitdagingen zijn samengevat in hoofdstuk 5. Over het algemeen onderzocht ons werk de relaties tussen landgebruik, geochemische bodemeigenschappen en SOC met behulp van analytische gegevens en een procesgebaseerd bodemvormingsmodel (SoilGen). Dit onderzoek benadrukt dat het verschil in geochemische eigenschappen gemedieerd door landgebruik mogelijk bijdraagt aan de accumulatie en stabilisatie van SOC, en de kalibratiebenadering van het SOC-model beïnvloedt de nauwkeurigheid van het resultaat met betrekking tot de huidige en toekomstige SOC. De grootste uitdaging had betrekking op de analyse van de deeltjesgrootte, terwijl de onzekerheid van de initiële gegevens (voorraden) en de onnauwkeurige verdeling van de SOC-modelpoelen kunnen bijdragen aan de onnauwkeurigheid van de modeloutput in het modelleringsonderzoek. De laboratoriumanalyses en het bodemmodel moeten nog worden verbeterd voor de precieze output zoals beschreven in dit hoofdstuk. In de toekomst zal het nu nodig zijn om de robuustheid te bevestigen van het gevonden effect van landbouwpraktijken op de vorming van niet-kristallijne materialen in vulkanische bodems. Er moet worden gekeken naar grotere aantallen sites met vergelijkbaar moeder materiaal en leeftijd, maar met een verschillend landgebruik. In dit doctoraatsonderzoek werd een positief effect van bodemaggregaten op SOC-opslag gesuggereerd. Echter, uit de gelijkenis in C:N-verhoudingen en gehalten aan pedogene oxiden tussen geïsoleerde 'aggregaat'- en 'silt- en klei'-fracties, blijkt dat bodemfractioneringsmethoden nog verder moeten worden ontwikkeld voor Andosols om functionele SOC-poelen efficiënter te isoleren. Ten slotte is er behoefte om de vorming van niet-kristallijne materialen in het SoilGen-model te integreren, samen met hun impact op SOC-stabilisatie.

CHAPTER 1

GENERAL INTRODUCTION

1.1 Broader framework

1.1.1 Organic matter in soils

Soil organic matter (SOM) is the foundation of terrestrial life and a main component of the global carbon cycle. Globally, there is approximately 1500 Pg of organic carbon in the top one-meter soil, of which one-quarter is in tropical soils (Craswell and Lefroy, 2001). SOM represents the largest terrestrial carbon reservoir (Jobbágy and Jackson, 2000) and has effects on many ecosystem services, such as on climate regulation (Lal, 2003), and soil fertility (Craswell and Lefroy, 2001). Carbon constitutes about 50% of SOM and the content of soil organic carbon (SOC) is mostly used to quantify OM in soil or its fractions. SOM is derived from organic materials entering soil, mainly from plant and animal debris. The breakdown of these inputs drives biological processes in soils which provide many functions, such as providing of nutrients for crops, stimulating soil aggregation, retaining moisture, and reducing compaction (Craswell and Lefroy, 2001).

The amount of organic matter (OM) in soil results from a dynamic balance between the organic inputs and the decomposition process (Schimel, 1995). Decomposition is the process of the breakdown of dead OM that includes physical, chemical, and biological mechanisms transforming OM into an increasingly stable form and releasing CO₂, organic trace gases, mineral nutrients, water, and energy (Berg and McLaugherty, 2003). This process has been described as the primary key in nutrient and carbon cycling and is the major pathway of carbon release and inputs from and to soils. The decomposition process is influenced by biotic, abiotic, and anthropogenic factors (Berg and McLaugherty, 2003). The biotic factors include the amount and quality of litter input and the presence of soil microorganisms, whereas the abiotic factors comprise the geochemical composition, climate, and relief aspects. Anthropogenic factors like change of land use, soil tillage, and the addition of chemical fertilizer, also greatly affect SOM. Understanding the ecological control on soil organic carbon (SOC) is important to assess and forecast the fate of SOC to function optimally in supporting ecosystem service.

The heterogeneous OM derived from plant litter input consists of different chemical composition with distinct decomposition rates. The order of OM compounds from most stable to least are lignin and tannin > starch and waxes > hemicellulose > cellulose > proteins > amino acids > simple sugar (Quideau, 2006), with the most stable or recalcitrant organic compounds having a lower decomposition rate (Hall et al., 2020). However, studies showed that the stability of SOC does not depend primarily on litter biochemistry. The relations between SOC and soil properties overridingly determine the stability of SOC (Kleber et al., 2015; Lehmann and Kleber, 2015). Plant litter with high rates of mineralisation indicated by rapid decomposition rates and low C:N ratio in fact often display faster and more interaction with minerals, e.g. association SOM and clay particles, than plant litters with slow decomposition rates because litter with high mineralisation rate synthesise microbial products (Kallenbach et al., 2015). Such microbial products and dissolved OM released during decomposition of litter can go in association with minerals, through which 'stable SOM' is formed that persists for a long time (Torn et al., 1997). The stability of SOC related to its subjection to various stabilization mechanisms and turnover times can be studied by identifying measurable and functional

SOM fractions using physical fractionation, chemical fractionation, or a combination of physical and chemical fractionation methods (von Lützow et al., 2007).

In general, two main mechanisms of SOC stability are organo-mineral interaction and occlusion of SOC within soil aggregates. Organo-mineral interactions have been acknowledged as a key factor in SOC stabilization for the last decades (Lehmann and Kleber, 2015; Schmidt et al., 2011). The smallest minerals, i.e. clay particle size, possess a great surface reactivity and large specific surface area and are thereby mainly involved in organo-mineral interaction. In general, the clay fraction contains a large proportion of total SOC in most soils and thus serves as an indicator of SOC storage over wider range of soils (Beare et al., 2014). This particle size includes a different variety of minerals, such as phyllosilicates, different forms of metal oxyhydroxides, and poorly crystalline aluminosilicates (Basile-Doelsch et al., 2015; Kleber et al., 2015; Schneider et al., 2010). These minerals and poorly crystalline minerals stabilize SOC via several processes, such as the adsorption of OM on the surface of minerals, interactions between iron or aluminium cations (Fe^{3+} , Al^{3+}) and organic ligands which form organo-mineral complexes, and cationic bridging by di- or trivalent ions (Kleber et al., 2015; Mikutta et al., 2009; Rowley et al., 2018; Tamrat et al., 2019; Wagai and Mayer, 2007; Wiseman and Püttmann, 2005).

Physical protection of SOC in aggregates is considered to be another important mechanism for SOC stabilization. The protection of OC within stable aggregates limits the accessibility of decomposers, e.g. fungi, microbes, or enzymes, due to a reduced diffusion of oxygen into aggregates (Lehmann et al., 2007; Totsche et al., 2018). Aggregates can be divided into macro- and micro-aggregates with different SOC retention mechanisms. Macroaggregates (usually soil particles $> 250 \mu\text{m}$) generally contain OC from fresh litter substrate and have higher OC content than microaggregates, but the turnover time of carbon in macroaggregates is less than microaggregates (Churchman et al., 2020; Pronk et al., 2012). On the other hand, the occlusion of OC by adsorption and entrapment in microaggregates can become stable OC promoting long-term SOC sequestration (Chenu and Plante, 2006; Witzgall et al., 2021). Some cementing agents that influence the stability of aggregates are oxides, hydroxides, and oxyhydroxides of iron, aluminium, manganese, carbonates, and aluminosilicates (Totsche et al., 2018).

1.1.2 Volcanic soils and interaction with soil organic carbon

Andosols (IUSS, 2015) or Andisols (Soil Survey Staff, 2014) are a soil type typically formed from the weathering of volcanic materials. These soils cover 0.84% of terrestrial land and usually stores more SOC than non-volcanic soils under comparable conditions (Dahlgren et al., 2004; Eswaran et al., 1993). Accumulation and stabilization of SOC in Andosols are mainly attributed to the presence of non-crystalline materials, such as active aluminium and iron compounds, allophane, imogolite, and ferrihydrite. The formation of non-crystalline materials is related to the characteristics of volcanic ejecta, e.g. small, glassy, high porosity and permeability, as parent materials (Dahlgren et al., 1999). Rapid weathering of the volcanic ejecta releases elements, such as aluminium (Al), silicon (Si), and iron (Fe), resulting in over-saturated metastable, non-crystalline materials in soil solution (Ugolini and

Dahlgren, 2002). The availability of Al and Si influences the formation of secondary minerals, e.g. allophane, (Parfitt, 2009).

The stability of SOC in Andosols can occur through the complexation of SOC by non-crystalline materials or metal (Ugolini and Dahlgren, 2002). In the organo-mineral complex, the presence of non-crystalline materials which have high reactive surface area provides an abundance of charge sites on the mineral surface available for organo-mineral interactions (Basile-Doelsch et al., 2007; Bruun et al., 2010; Lyu et al., 2021; McNally et al., 2017; Mikutta et al., 2006; Nanzyo et al., 1993a; Rasmussen et al., 2005; Reichenbach et al., 2021). The sorption mechanism of humic substances by variable charge minerals is through ligand exchange reaction (Yuan et al., 2000). In this process, a hydroxyl group is attached to Al in the allophane structure and a carboxylate group of humic acid. The presence of electrolytes such as NaCl would promote humic acid sorption. On the other hand, the study of volcanic soils in New Zealand and Chile showed the important role of Al oxides rather than clay (having 50% of allophane) in stabilizing SOC (Matus et al., 2006; Percival et al., 2000). Al in monomers or polymeric forms can interact with carboxyl groups of organic matter which may play an important role in stabilizing SOC. Al^{3+} and Fe^{3+} are likely important cations for bridging the negative charge minerals and organic surface (Rasmussen et al., 2005).

The physical protection of SOC within stable soil aggregates is an important mechanism of SOC stabilization in Andosols (Tonnejck et al., 2010). In this soil, the formation of stable aggregates is related to the presence of non-crystalline materials that plays an essential role as cementing or gluing agent (Huygens et al., 2005; Nanzyo et al., 1993a; Rasmussen et al., 2005). The abundance and chemistry of small particles (< 0.2 and 0.2 – 2 μm fractions) in Andosols likely act as strong binding agents to form both micro- and macroaggregates (Asano et al., 2018; Asano and Wagai, 2014). How the organic carbon and non-crystalline materials are assembled to form aggregate structure is still poorly understood. Previous studies reported a lack of aggregate hierarchy in Andosols due to a lack of size-dependent change in carbon concentration after weak dispersion (Hoyos and Comerford, 2005; Huygens et al., 2005). The use of particle size fractionation with ultrasonication to disperse aggregates and without wet chemical reagents showed no clear difference or minimum alteration of carbon composition in sand- to clay-sized particles (Edwards and Bremner, 1967; Perdrial et al., 2010). These results imply that the high stability of aggregates in Andosols may obscure the relations between OM and aggregate size.

Other factors also contribute to the accumulation of SOC in Andosols, such as a possible inhibition of the microbial activity due to aluminium toxicity, low pH, or change in nutrient availability (Doetterl et al., 2015; Tonnejck et al., 2010), and the diverse volcanic materials which release macro- and micro-nutrients after weathering, e.g. Ca, Na, K, Mg, Zn, Fe, Cu, and Mn (Anda and Sarwani, 2012), sustaining the high productivity of ecosystems in Andosols.

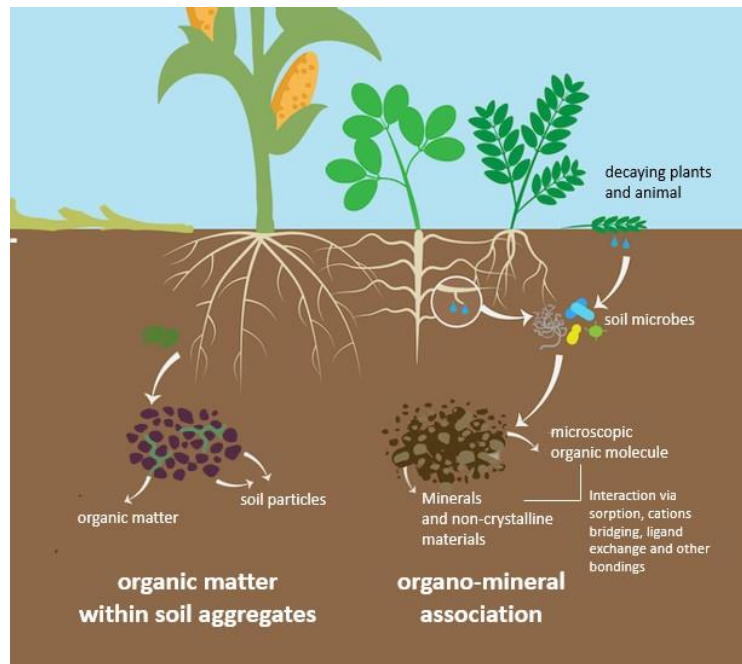


Figure 1-1 Illustration of stabilization soil organic matter via physical protection within soil aggregates and organo-mineral association.

1.1.3 Land use and interactions with SOC

Land use, climate, topography, and soils all interact, determining the amount and composition of carbon inputs to soil. Land use is assumed to be the most dynamic factor influencing the amount of SOC (Guo and Gifford, 2002; Post and Kwon, 2000) and vertical distribution of SOC (Jobbágy and Jackson, 2000). Land use and its vegetation often correspond to different plant diversity and plant litter biochemistry. Plant diversity has been observed to correlate positively with soil microorganisms and SOC storage (Lange et al., 2015), whereas litter chemistry affects OM decomposition (Chenu et al., 2019; Cyle et al., 2016). Besides vegetation, land management was found to have impacts on chemical and physical soil properties, such as pH, bulk density, and moisture content affecting SOC storage (Malik et al., 2018; Wiesmeier et al., 2019).

For the last century, the conversion of forest to other land uses has occurred worldwide, affecting SOC storage and CO₂ emissions into the atmosphere (Guo and Gifford, 2002; Smith et al., 2012). A reduction of SOC stocks after the conversion of native forest to plantation and agricultural land was reported at 13% and 42%, respectively (Guo and Gifford, 2002), which is consistent with an increase in CO₂ emissions due to human-induced activities (Cox et al., 2000; Sanderman et al., 2017). The reduced SOC in agricultural land is mainly due to the low amount of carbon input (Chenu et al., 2019). In addition, tillage practice can promote OM decomposition by mixing and loosening soil. Tillage specifically affects the stability and arrangement of soil aggregates, with consequent adverse effects on SOM preservation potential (Guo et al., 2020). In Andosols, land management can obviously likewise affect the physical structure of soil (Dec et al., 2012; Dörner et al., 2012; Seguel and Horn, 2005), which may influence the physical protection of SOC. Abera and Wolde-Meskel (2013) found a significant decrease in SOC in soil aggregates under intensive cultivation. On the other hand, some studies showed little impact on SOC by land use change due to an inherent high structural stability in

Andosols (Candan and Broquen, 2009; Hoyos and Comerford, 2005; Linlin et al., 2016). However, it is not well resolved to what extent cultivation of volcanic land induces changes in the proportion of various SOC pools. Finally, the reduction of SOC can also occur when Andosols lose their andic properties due to continuous drying and rewetting (Woignier et al., 2008).

In agricultural systems, the use of multiple crops, e.g. perennial crops and cover crops, or application of organic fertilizer in high amount cause a distinctly high SOC stock (Gross and Glaser, 2021; Paustian et al., 1997; Poeplau and Don, 2015; Yu et al., 2012). Application of organic fertilizers can influence the concentration of exchangeable cations that indirectly affect the SOC stabilization (Kaiser et al., 2012; Lützow et al., 2006). The availability of polyvalent cations, e.g. Ca and Mg, from organic fertilizer or liming can increase SOC stabilization via electrostatic bridging between soil mineral surface and SOM (mineral – cations – SOM) (Lützow et al., 2006) and by promoting aggregation (Rowley et al., 2018). Calcium is reported to be a good predictor of SOC (Rasmussen et al., 2018), likely because it is involved in both organo-mineral association as well as aggregate occlusion of OM in that Ca^{2+} acts as polyvalent cation bridge between negatively charged mineral surface and OM and also enhances clay flocculation and soil aggregate stability. A high content of calcium was furthermore documented to align with greater SOC across land uses, such as forest, agriculture, and pasture (Fornara et al., 2011; Kaiser et al., 2012; Morris et al., 2007). On the other hand, radiocarbon dating on bulk SOC showed a decrease of recent carbon retention in agricultural sites (Cusack et al., 2013), which is in line with the priming effect where an increase of organic carbon input can lead to the decrease of SOC stabilization within aggregates (Shahbaz et al., 2017). Combination of organic and mineral fertilizer was also found to increase carbon mineralization in aggregates (Yu et al., 2012).

1.1.4 Soil genoforms and phenoforms

In the last century, the impacts of human activities on soils have accelerated (Richter, 2007). To boost crop production, humans apply soil management which has significant effects on soil properties. In agricultural systems, humans modify physical and chemical soil properties by loosening soils, and using liming, organic and chemical fertilizer (Richter, 2007; Richter et al., 2015). To describe the effect of management inducing changes and persistent differences in soil functions in soils with the same pedogenesis, the terms of soil genoforms and phenoforms were proposed (Droogers and Bouma, 1997). Soil genoforms refer to soil classes as identified by soil classification system, whereas soil phenoforms are persistent variants of soil genoforms with different physical and chemical properties that considerably affect soil functions (Rossiter and Bouma, 2018). The human factor often has a more significant impact on soil properties than other soil-forming factors i.e. parent materials, relief, climate, organism, time. Soil genoforms generally alter slowly, but with management, soils may change at medium (decadal) time scale. Several studies reported change of the magnitude of soil development processes due to human activities. Examples are: (i) differences in clay mineralogy in albeluvisols under forest and agriculture (Cornu et al., 2012), (ii) change in the classification of black soil as an effect of agriculture (Veenstra and Lee Burras, 2012), (iii) alteration of soil properties after deforestation in tropical soil that strongly affect soil functions (Veldkamp et al., 2020), (iv) soil erosion that affects land productivity (Holz et al., 2015). A more limited number of studies also showed that the change of geochemical composition due to weathering in turn affects SOC stock and mineral-

related carbon stabilization mechanisms (Doetterl et al., 2015; Reichenbach et al., 2021). However, little is known about if and how strongly the effect of land-use on SOC is actually manifested indirectly via such accelerated or modified soil formation.

1.1.5 Climate change and its effect on soil carbon

Climate change refers to the alteration in temperature, precipitation patterns resulting from atmospheric greenhouse gas levels. This phenomenon has become a major issue for sustenance of ecosystems over the last decades. SOC has been considered as a possible solution to mitigate climate change by storing substantial amounts of CO₂ from the atmosphere. The response of SOC to climate change is critically important since soil contains more organic carbon than vegetation and atmosphere (IPCC WGI, 2001). Therefore, a small change in SOC can have a large impact on the global carbon cycle. A global climate agreement has been set to reduce global warming by limiting the increase of temperature to 1.5°C. Recently, at COP21, the 4 per mille program was introduced to increase global SOC stock by 0.4% per year as a compensation of the greenhouse gasses emitted by anthropogenic sources (Minasny et al., 2017).

Understanding how future climate change affects soil development and SOC stock should provide useful information to improve management needed to maintain or increase SOC stocks. However, the effect of climate on SOC stocks is complex. First, a change in climate variables, i.e. temperature and precipitation, can affect the balance of net carbon input and loss of carbon over time. Temperature largely affects carbon input by controlling plant productivity (Madani et al., 2018; Rustad et al., 2001; Yu et al., 2020) and also indirectly affects SOC by changing the microbial decomposer environment (Boddy et al., 2008; Conant et al., 2011; von Lützow and Kögel-Knabner, 2009). As the temperature rises, the associated higher respiration is assumed to increase more than the photosynthesis, leading to the decrease SOC storage (Crowther et al., 2016; Sleutel et al., 2007; Zhao et al., 2021). Meanwhile, the precipitation controls the SOC stock as it determines net primary productivity (Niu et al., 2008). Secondly, changes in climate influence the mineral weathering, affecting SOC stabilization (Doetterl et al., 2015; Meier and Leuschner, 2010). Since a change in temperature or precipitation can affect almost any soil process, the result on the stability of SOC derives from multiple co-occurring changes in soil properties. A positive relation between SOC and precipitation may for instance be explained by increased release of organic acids under increased precipitation, e.g. in forests, increasing the leaching of base cations leading to lower pH and higher Al toxicity, which contribute to SOC accumulation (Tonneijck et al., 2010).

The response of SOC to climate change can be estimated using mechanistic models. As setting up field trials for various climate scenarios is difficult and the cost of field-related work is expensive, the use of climate and SOC models to predict SOC can partially address these disadvantages, although the models still need real data for the input and validation. Several SOC models have been developed to describe soil carbon cycling e.g. RothC-26.3 (Coleman and Jenkinson, 1999), Century (Parton, 1996), and are used both at various temporal (e.g. Smith et al., 2006) and spatial scales (e.g. Smith et al., 1998). Previous studies documented that the estimated effect of climate change on SOC using SOC models varied between models and differed between regions, thus it is necessary to assess the impact

for particular regions (Gottschalk et al., 2012). In addition, the effect of climate change on SOC also varies depending on land management (Minasny et al., 2011; Wiesmeier et al., 2013) and soil properties (Hartley et al., 2021). Doetterl et al. (2018) found that temperature and soil minerals, through changes in mineral reactivity and nutrient availability, control the composition of microbial communities affecting carbon stabilization. The advantage of using geochemical proxy into SOC model was reported in previous studies (Finke et al., 2019; Shirato et al., 2004).

1.2 Specific objectives and research questions

Volcanic soils have the potential to store large amounts of organic carbon. Understanding what drives accumulation of SOC in these volcanic soils can help in setting out SOC-storage management for climate regulation and other soil functions. The dynamics of SOC in tropical volcanic soils cannot be separated from the significant role of soil geochemistry and land use. To obtain a complete picture of the interrelations between land use, geochemistry and climate, first, the effect of land use on soil geochemistry should be evaluated. Thereafter, the effect of land use on stability of organic matter with the mediation of soil geochemistry can be assessed. The interaction of these processes may provide information on whether different land uses, including their history and management in volcanic soils, can have impact on soil being either a carbon source or a carbon sink. Although many studies on the impact of land use on soil geochemistry and SOC have been carried out, the mechanism and the impact vary between soils and are still limited for tropical volcanic soils. In addition, some of the soil processes such as the effect of soil geochemistry on SOC dynamics, is still rarely present in carbon turnover models (Reichenbach et al., 2021), creating substantial uncertainty in estimating SOC. Thus, there is a need to have a model that integrates different factors that influence SOC, e.g. soil geochemistry, climate, litter input, agricultural practices, to estimate SOC stock. The process-based soil genesis model, SoilGen (described in detail in chapter 4), simulates the combined soil-development processes simultaneously to produce soil properties, including SOC. Furthermore, different calibration approaches of SOC models, more specifically the decay rates, have impact on the model accuracy of calculated current and future SOC stocks. By improving the SOC calibration methods, the future SOC stock under different climate projection scenarios can be better forecasted. Overall, this study is about relating geochemistry to land use, applying and testing an integrated process model while improving calibration methods on volcanic soils. An understanding on these processes can provide scientific contribution to the land management in tropical volcanic soils.

Therefore, the specific objectives addressed in this study include:

1. To assess the impact of land use change on weathering, soil geochemical properties, and SOC storage in volcanic soils in Indonesia (Chapter 2)
2. To assess the effect of land use, with existing soil development phase, on quality and stability of SOC in these soils (Chapter 3)
3. To calibrate important soil processes on volcanic soils in an integrated soil development model, such as clay migration, weathering rates of primary minerals, and decay rates of soil organic carbon (Chapter 4)
4. To assess the impact of different calibration approaches, including the effect of geochemical properties, on the accuracy of simulated SOC (Chapter 4)

5. To forecast the change of SOC pools under different climate projection scenarios (Chapter 4)

This study is accordingly designed to answer the following research questions:

1. Is there any effect of land use on soil geochemical properties? Do, in tropical volcanic soils, phenofoms (management-related soil sub-types) exist within the more general genoforms (genetic soil types)? (Chapter 2)
2. Does land use through its impact on soil geochemistry indirectly control the distribution of SOC across various pools (like mineral-associated OM and physically occluded OM) and how does the OM degradability differ in function to land use? (Chapter 3)
3. How well do simulated soil properties match the measured soil properties (i.e. the content of clay, minerals, and SOC in each pool) by calibrating soil model (in SoilGen) parameters? (Chapter 4)
4. Do different information levels used to calibrate model SOC decomposition rate constants affect the prediction of current and future SOC? (Chapter 4)
5. What is the effect of global warming on SOC stock in tropical volcanic soils under different land uses? (Chapter 4)

1.3 Study area

1.3.1 Geography

The study area is located in the Mt. Tangkuban Perahu (2084 asl) and Mt. Burangrang (2054 asl) areas (Fig. 1-2). The geographical position of Mt. Tangkuban Perahu ranges from longitude 107°29'03" to 107°47'47" east and latitude 6°54'03" to 6°40'00" south. The study area administratively belongs to the Lembang, Cisarua, and Cikalong Wetan Districts, West Bandung Regency, around 30 km north of Bandung city, West Java. The area receives an annual precipitation around 2000 – 3000 mm year⁻¹ and mean annual temperature is around 19 - 21°C. According to the Köppen climate classification (Köppen, 1936), the areas has the *Am* subtype. There are two seasons: The rainy season occurs from October to May with the highest rainfall amount in November. The dry season occurs from June to September with the lowest amount in August.

1.3.2 Geology of Mt. Tangkuban Perahu and Mt. Burangrang

Approximately 80% of the active volcanoes in Indonesia archipelago are located in the western part mainly on Sumatra and Java (Hall and Smyth, 2008). The Sumatra and Java islands are part of the Sunda arc that displays features of subduction zones. This area represents part of the convergent plate boundary of the Eurasian plate in the north and the Indian-Australian oceanic plate in the South creating an east-west volcanic chain. The Sunda arc has existed in its current configuration for about 5 Ma with Quaternary volcanoes generally overlying late Miocene-Pliocene volcanic rocks and sediments (Soeria-Atmadja and Noeradi, 2005). These Quaternary volcanoes were formed on the eroded surface of the uplifted Miocene basement sedimentary rocks (Nasution et al., 2004; Van Bemmelen, 1949). On Java Island, at least 28 volcanoes are still active. Various rocks are produced from the volcanic activities ranging from tholeiitic to high-alkaline basalts, but mostly the volcanic rocks are classified into calc-alkaline basaltic-andesite and andesite volcanic rocks (Handley, 2006).

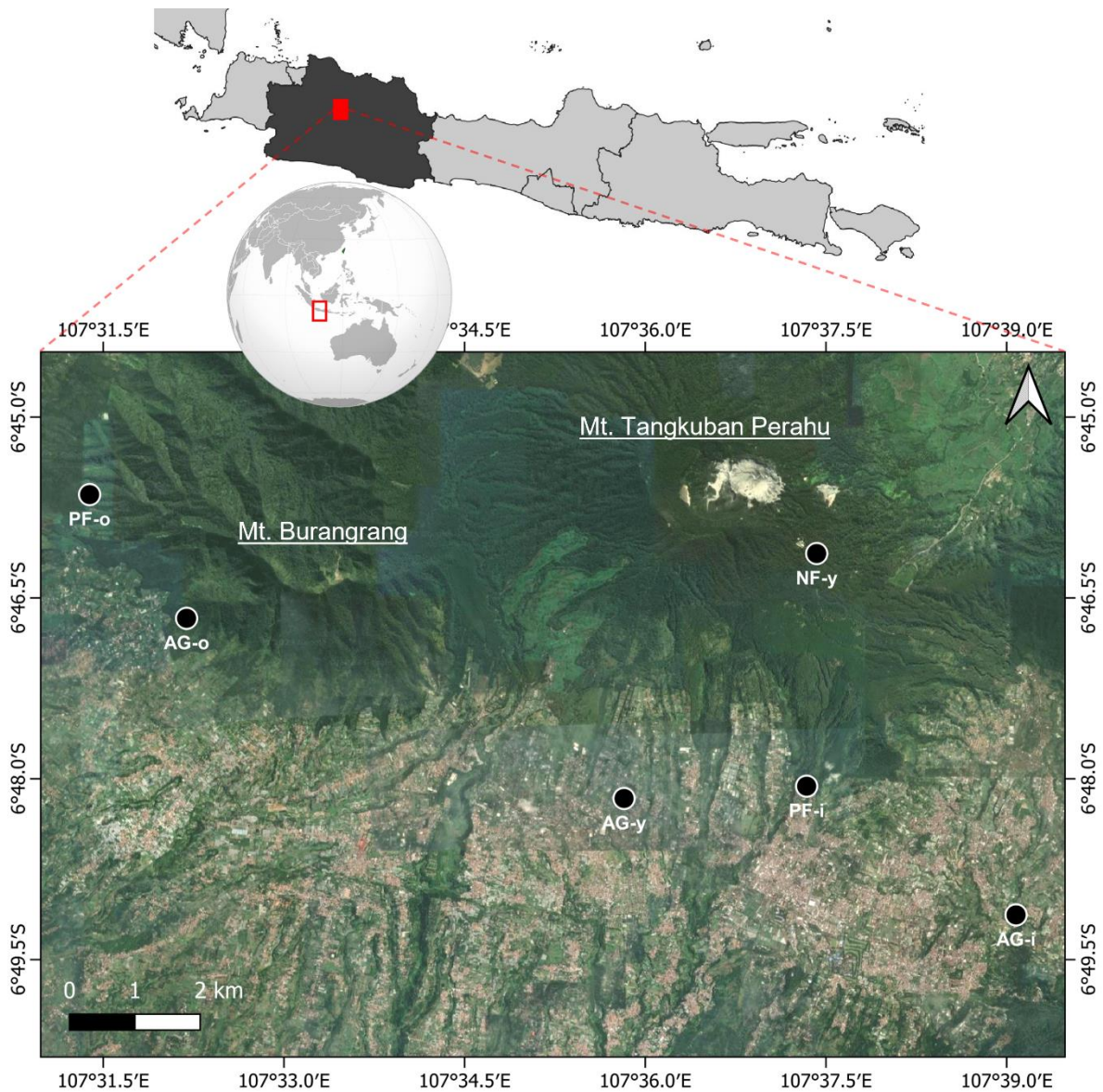


Figure 1-2 Location of study area and sampling sites.

Mt. Tangkuban Perahu is an active well-preserved stratovolcano which is located in the Sunda volcanic arc (Van Bemmelen, 1949). The formation of Mt. Tangkuban Perahu is related to the volcanic activity series in the Mt. Sunda volcanic complex. This mountain was formed in the eastern rim caldera of ancient Mt. Sunda which existed in the Pleistocene until a violent Plinian eruption caused its summit to collapse. Mt. Burangrang is situated in the southwest of Mt. Tangkuban Perahu and is characterized by older volcanic material (Nasution et al., 2004; Silitonga, 1973). There were three main periods of activity in the Mt. Sunda volcanic complex, viz. a (i) Pre-Sunda volcano, (ii) Sunda volcano, and (iii) Tangkuban Perahu volcano (Nasution et al., 2004). The first series volcanic activities are poorly known but possibly predate the Quaternary. In the second series, the ancient Sunda volcano was formed on Neogene sedimentary basement rocks, and the third series is characterized by the formation of Mt. Tangkuban Perahu. The volcanic successions of the latter are divided into two main formations, old and young Tangkuban Perahu. The materials from old Tangkuban were derived from magmatic – phreatomagmatic eruptions with ages of $40,750 \pm 270$ and $22,380 \pm 80$ yBP, whereas the materials of

the young Tangkuban Perahu are generally from phreatic to phreatomagmatic eruptions with ages around 9,000 – 9,980 yBP (Nasution et al., 2004). The buried horizons in eastern Mt. Tangkuban Perahu showed a radiocarbon dating around 8,700 ± 200 and 14,500 for horizons 2A and 3A, respectively (Chartres and Van Reuler, 1985). The maximum age of Andesitic Tuffaceous ash in southwest of Mt. Tangkuban Perahu, Mt. Burangrang area, was around 10,000 years (Utami et al., 2019). Mt. Tangkuban Perahu is still active today, indicating that most of the terrain developed in the Late Quaternary (Dam et al., 1996). The main volcanic materials associated with Tangkuban Perahu are andesitic rocks with calc-alkaline lavas, pyroclastic flow deposits and air-fall deposits of basaltic-andesitic composition (Nasution et al., 2004). Sunardy and Kimura (1998) also found basaltic to dacitic materials in volcanic products of Mt. Tangkuban Perahu with SiO₂ contents between 51 – 63 wt%.

1.3.3 Land use

From marine pollen records the occurrence of rainforest in Indonesia has been confirmed to have already started at around 17 kyr BP, after the last glacial maximum (LGM). There was an abrupt pollen shift from glacial to interglacial conditions suggesting a response of vegetation to climate change. At the end of the LGM, montane trees such as *Dacrycarpus*, *Podocarpus* dominated, indicating a drier and cooler climate (Walker and Flenley, 1979) than at present. The pollen records from Sumatra and West Java show a lowering of forest altitudinal zones in the Late Pleistocene compared to the Holocene, as indicated by the fact that similar Late Pleistocene vegetation occurred at altitudes of 1300 to 1500 m, while at present this is found above 1800 m (Stuitjs et al., 1988). This implies a cooler climate at moderate elevation during the Late Pleistocene than during the Holocene and also marks the beginning of upland vegetation in West Java (Van Der Kaars and Dam, 1997). The increase of temperature and rainfall started around 17 kyr BP (Kershaw et al., 2007). Abundant pollen of *Altingia*, *Castanopsis*, and *Quercus* characterize the early Holocene in Sumatra and Java, indicating a wet and warm climate (Stuitjs et al., 1988). The occurrence of rainforest in Java during the Holocene period was also reported in other studies (e.g. Kershaw et al., 2007; Sémah and Sémah, 2012). Rainforest possibly reached its maximum surface area in the Early-Middle Holocene (Kershaw et al., 2007). The rainforest recession was detected at 2800 BP, and this has been attributed to climate change, whereas human effects on vegetation are found only since 1500 BP (Sémah and Sémah, 2012). In general, the presence of rainforest within the South China Sea region has seen little overall change in most of the area through most of the Quaternary (Kershaw et al., 2007).

Rainforest has overall demonstrated a remarkable resilience in variable climatic conditions. However, the past centuries humans exerted major impact on the Holocene rainforest (Lumbanraja et al., 1998). Firstly, part of the native rainforest had been converted into secondary forest, often with pine trees, particularly with *Pinus merkusii*, the only pine naturally occurring in Indonesia and the Southern hemisphere as a whole. It is also often present on volcanic soils as a pioneer species (Stuitjs et al., 1988). *Pinus merkusii* has become one of the important tree species in Indonesia as it produces pulp, paper, timber, and non-wood products such as turpentine and resin (Imanuddin et al., 2020). This pine species was planted during the era of Dutch government in Sumatra, Java, and Bali as production forest (Ferguson, 1954). One of the research centres about pine was located in Lembang, southern part of Mt. Tangkuban Perahu. Before pine, the Lembang area was planted with *Acacia* and mixed

broadleaved forest. From around 1960, pine trees are also widely planted for the purpose of reforestation with the status of protected forest in 2017 (Perhutani, 2014).

Next to secondary forest there has also been conversion of native forest into agricultural land. In the Lembang and Cisarua Districts this has widely occurred around 1990 (Ruswandi et al., 2007), but settlements with dry rice fields were already present since 1917 (Topographical Service Batavia, 1941). Currently, Lembang is one of the most intensively cultivated areas for horticultural crops in West Java. Agricultural lands in the study area were converted from forest or coffee plantation between 1970 – 1988. Farmers in these areas generally applied horticultural crops with multiple (2 – 4) crops per year, such as tomatoes, cabbage, broccoli, cauliflower. Soil tillage is done every crop rotation and fertilization is applied using both chemical and organic fertilizers. Lastly a smaller part of the native forest has been converted into coffee plantations. In the study area this has not been for massive commercial production, but mainly for local use. This form of land-use was not considered in this PhD research, while conversions from native forest to secondary pine forest and cropland for vegetable production are.



Figure 1-3 Typical pine forest (left) and agricultural land use (right) in study area.

1.4 Outline of thesis

This study has been organised into five chapters. Chapter 1, introduction, consists of three parts. In the first part (1.1.), the knowledge of the soil organic matter, interaction between volcanic soils and land use on SOC, and the effect of climate change on SOC evaluated using mechanistic models are presented. In the second part (1.2) goals of this PhD research and emerging research questions are formulated. The third part (1.3.), describes the geology and land use history of the study area, the Sunda volcanic complex in Indonesia. Chapters 2 – 4 cover the main research objectives mentioned above. The last chapter, chapter 5, gives general conclusions, challenges, and topic for future research. Only relatively recently there have been land-use changes from native forest to secondary forest or agricultural land. This makes that the evolution of land use can be traced back with confidence, offering the opportunity to study land-use change effects on volcanic soil development and SOC.

Authors contributions

This chapter was designed and written by Sastrika Anindita. Peter Finke and Steven Sleutel had a significant contribution through commenting, reviewing, and giving suggestions for improving this chapter.

CHAPTER 2

LAND USE IMPACTS ON WEATHERING, SOIL PROPERTIES, AND CARBON STORAGE IN WET ANDOSOLS, INDONESIA

Based on:

Anindita, S., Sleutel, S., Vandenberghe, D., Grave, J. De, Vandenhende, V., Finke, P., 2022. Land use impacts on weathering, soil properties, and carbon storage in wet Andosols, Indonesia. *Geoderma* 423, 115963. <https://doi.org/10.1016/j.geoderma.2022.115963>

Abstract

We investigated changes in geochemical soil properties in response to deposition age and land use management over 30–50 years on tropical volcanic soils. Our purpose was to find out how weathering stage and land use interactively affect soil properties and organic carbon, and to check if phenofoms (management-related soil subtypes) exist within the genoforms (genetic soil types). Soil samples were taken at land uses that have been converted (pine forest and agricultural land) and a natural forest as the original land use. The results showed that pine forest and agricultural soils displayed similar weathering intensity. Intensive agricultural practices also improved soil chemical properties such as pH, exchangeable base cations, and base saturation leading to WRB-qualifier of “*eutric*” in cultivated soils, whereas the averages of bulk density and organic carbon stock were relatively similar between forests and agricultural soils. Positive correlations were found between amorphous materials and Al_o , specific surface area, and micropore volume. Correlations between the content of short-range order Al (hydr-) oxides (indicated by Al_o) and organic carbon were found in pine forest and agricultural soils, particularly in subsoils. Our results clearly indicate the increase of base cations retention due to less acidification and an increase of organic carbon stock under agricultural land use, likely due to stabilization with non-crystalline materials.

Keywords: land use change, volcanic soils, weathering, geochemical soil properties

2.1 Introduction

Soil weathering is one of the main processes in soil formation (Birkeland, 1999). This process can affect physical and chemical soil properties, storage of nutrients, and carbon. Volcanic ash soils generally weather following a sequence from primary minerals to short-range order (SRO) minerals, halloysite, and kaolinite (Parfitt et al., 1983). The rates of weathering from primary to secondary minerals depend on environmental conditions. Humid climate can enhance desilication and loss of base cations (Chadwick et al., 2003). Land use can modify the fate of weatherable minerals by serving as H⁺ sink (Acid Neutralizing Capacity; Van Breemen et al., 1983) and by physical weathering, such as tillage (Wei et al., 2006).

Volcanic soils are susceptible to land use change, especially conversion to cultivated land, due to their inherent good chemical fertility. In cropland management, soil tillage creates a warmer and dryer soil climate and disrupts aggregates, which increases organic matter (OM) turnover (Bandyopadhyay, 2019) and enhances the chemical weathering (Li et al., 2021). Converting forest area to cropland in which tillage is practiced may affect Andosols, and thus deserves attention because of their fertility and intense agricultural use. Several studies reported negative effects such as disturbance of the geochemical cycle and less organic carbon (OC) storage (Lemenih et al., 2005; Sosnowska, 2012). However, manure application under agricultural management can increase soil OC stocks (Maillard and Angers, 2014). The conversion to cropland was reported to improve soil chemical properties such as the increase of K, Ca, Mg (Asio et al., 1999), but in contrast net acidification may also occur if nutrient export by harvesting is not compensated (Van Breemen et al., 1983).

The formation of SRO aluminosilicate materials, iron oxide, and accumulation of OM are the main pedogenic processes in allophanic Andosols (Shoji et al., 1993). Interactions between nano-sized SRO minerals and soil OM play a significant role in the retention and stabilization of carbon (Basile-Doelsch et al., 2015; Kleber et al., 2015; Lehmann and Kleber, 2015; Tamrat et al., 2019). Their presence also contributes to unique chemical and physical soil properties in Andosols, such as variable charge, low bulk density, high water holding capacity, and formation of stable soil aggregates. There is still no decisive information related to how weathering and geochemical properties are driven by land use in these soils.

Here, we investigated the change of geochemical soil properties as impacted by land use in Andosols from the Sunda volcanic arc region (Mt. Tangkuban Parahu and Mt. Burangrang), West Java, Indonesia. In particular, we tested the assumption that phenoforms (management-related soil subtypes) exist within the more general genoforms (genetic soil types; Droogers and Bouma, 1997; Rossiter and Bouma, 2018) of these specific Andosols. Phenoforms are identified by observing differences in soil properties, such as soil structure, bulk density, carbon concentration, nutrient retention, content of Fe and Al, soil color, and soil horizons, which sufficiently affect soil function in the medium term (Rossiter and Bouma, 2018). By analysing their weathering statuses both geochemically and mineralogically, and OC contents, we aim at testing our assumption about age and parent materials, relating weathering, land use, and OC status.

2.2 Materials and methods

2.2.1 Environmental setting

The study areas were situated in the Mount Tangkuban Perahu and Mount Burangrang regions, which are part of the Sunda Volcanic Complex (SVC) in West Java, Indonesia (Fig. 1-2). Mt. Tangkuban Perahu is an active stratovolcano that was formed in the eastern rim caldera of ancient Mt. Sunda. Over the last 10,000 years, the dominant type of Tangkuban Perahu eruption is small scale phreatic. Only in 1910 there was a magmatic eruption affecting a small area with ejected volcanic ash and scoria rock. Mt. Burangrang is also part of the remaining Mt. Sunda, but is situated in the western part of the caldera rim and has older volcanic edifices (Silitonga, 1973). Soils in these areas were derived from similar parent material (basaltic-andesitic (ash) tuff), which originated from Holocene to Late Pleistocene activity (Dam et al., 1996; BBSDLP, 2017). The soil type was classified as Typic hapludands based on the soil map scale 1:50,000 (BBSDLP, 2017). The areas have a mean annual precipitation of 2000 – 3000 mm year⁻¹ and mean annual temperature around 19-21°C.

The study areas were located in deposits of different lithology and age i.e. Qyd (young deposition age), Qyt (intermediate deposition age), Qvu (old deposition age) (Silitonga, 1973) (Table 2-1; Fig. 2-1). Soil samples taken from Qyd and Qyt were located in Lembang district near Mt. Tangkuban Perahu. The radiocarbon dating of buried organic horizon in the Lembang district yielded age 8700 ± 200 and 14500 ± 300 yrs BP for 2A and 3A horizons, respectively (Chartres and Van Reuler, 1985). Soil samples from Qvu were located near Mt. Burangrang, in the border of Cisarua district. The maximum age of volcanic ash in this area was expected to be 10,000 yrs (Utami et al., 2019).

Most of the areas were under forest before 1900 but have been gradually opened since 20th century and subjected to high anthropic pressures. Currently, the primary forest occupies only the upper slopes within a distance of around 1 km surrounding the crater of Mt. Tangkuban Perahu. Pine forest is a secondary forest planted in 1962 for restoration purposes (Perhutani, 2014). Agricultural practices date back 30 – 50 years and involve mainly rotations of horticultural crops. The history of land use and management was obtained by collecting data from historical land use maps, queries to government institutions, and interviews with landowners (Table 2-1).

2.2.2 Site description and soil sampling

We sampled an anthropo-chronosequence of volcanic soils in the Mt. Tangkuban Perahu and Mt. Burangrang, representing deposition age and land use histories as known from geological and historical land use maps. Six sites representing different land use (i.e. primary forest, pine forest, agricultural land) and lithology (i.e. Qyd, Qyt, Qvu) were selected. In Qyd, land use encompasses primary forest (NF-y) and agricultural fields (AG-y). The site of Qyt consists of pine forest (PF-i) and agricultural site (AG-i), whereas Qvu covers pine forest (PF-o) and agricultural site (AG-o). All the sampling sites were situated on slopes near ± 17° and the agricultural sites were under terrace. At each site, bulk undisturbed and disturbed core samples were taken at the depths of 0 – 20, 20 – 40, and ± 60 – 80 cm. A single composite soil sample was collected for each depth from different walls of soil pit, bringing the total number of replicates per land use (forest vs. agriculture) at n = 3.

Table 2-1 Location of sampling sites, land use, slope, altitude, and age of soils

Coordinates	Slope (°)	Elevation (m)	Present vegetation and management	Land use history	Parent material	
					Lithology ^{b)}	Approximate age (yrs) ^{c)}
<i>Primary forest (NF-y)^a</i>						
6°46'15.69"S 107°37'21.98"E	15	1710	<i>Altingia excels</i> , <i>Schima wallichii</i> , <i>Astronia spectabilis</i> , <i>Castanopsis argenta</i> , <i>Quercus spp</i> ,	Natural forest	Qyd (phase C-young eruption)	Holocene max. 8700±200
<i>Agricultural land (AG-y)</i>						
6°48'9.00"S 107°35'47.60"E	15	1313	- Annual crops: tomatoes, cabbage, broccoli, chilly - Three crops rotation per year - Intensive tillage - Fertilizer: (1) mix of chicken, cow manure and rice husk = ±76 Mg/ha/year (2) inorganic fertilizer= 307 kg N ha ⁻¹ , 307 kg P ha ⁻¹ , 307 kg K ha ⁻¹	- 1909-1917: degraded forest (shrub) (Topographical Service Batavia, 1941) - Ca. 1940-1950: Unmanaged plantation (possibly coffee). - Ca. 1970: Intensive cultivation (horticulture)	Qyd (phase C-young eruption)	Holocene max. 8700±200
<i>Pine forest (PF-i)</i>						
6°47'54.80"S 107°37'21.50"E	18	1343	- <i>Pinus merkusii</i> - No fertilizer	- < 1900: Degraded (Dutch colonial era: wood production) - Ca. 1960: Pine forest (production forest, pine sap/resin capture, locally coffee; agro forestry). - Ca. 2007: protected forest	Qyt (phase A-old eruption)	Holocene max. 8700±200
<i>Agricultural land (AG-i)</i>						
6°48'48.60"S 107°38'30.30"E	16	1163	- Annual crops: potatoes, broccoli, cabbage - Max. three crops rotation per year - Intensive tillage - Fertilizer: (1) mix of chicken manure and rice husk = ±20 Mg/ha/year (2) inorganic fertilizer = 144 kg N ha ⁻¹ , 144 kg P ha ⁻¹ , 144 kg K ha ⁻¹ as NPK fertilizer	- 1909-1917: Bamboo forest (Topographical Service Batavia, 1941) - 1940-ca.1980: unmanaged plantation, possibly coffee. - Ca. 1980: Intensive cultivation (horticulture)	Qyt (phase A-old eruption)	Holocene max. 8700±200
<i>Pine forest (PF-o)</i>						
6°45'38.50"S 107°31'3.00"E	18	1128	- <i>Pinus merkusii</i> - No fertilizer	- < 1900: Degraded (Dutch colonial era: wood production)	Qvu	Holocene 10000

- Ca. 1960: conversion to pine forest. Previously and locally, pine trees with horticulture for 5 years, then agroforestry of pine trees with coffee, but because of low production, change to protected forest locally for tourism.

Agricultural land (AG-o)

6°46'26.80"S	14	1132	-	Annual crops: chayote, cabbage, green bean	-	1909-1917: Degraded forest (Topographical Service Batavia, 1941)	Qvu	Holocene 10000
107°31'20.30"E			-	One or two crops rotation per year	-	1940-ca.1988: Conversion to unmanaged coffee plantation.		
			-	Fertilizer: (1) mix of chicken manure and rice husk = ± 18 Mg/ha/year (2) inorganic fertilizer = 90 kg N ha ⁻¹ , 90 kg P ha ⁻¹ , 90 kg K ha ⁻¹	-	Ca.1988: Intensive cultivation (horticulture)		

^{a)} -y: young soil age; -i: intermediate soil age; -o: old soil age

^{b)} Based on Silitonga (1973). Qyd is defined as brownish sandy tuff from Mt. Dano and Mt. Tangkuban Parahu (eruption "C"; Van Bemmelen (1934)), which is very porous and contains very coarse hornblende crystals as well as lahar deposit, lapilli layers, and breccia; Qyt is tuffaceous sand with lapilli, bombs, scoriaceous lava, angular fragments of dense andesite-basalt, and many pumice fragments, mostly from Mt. Tangkuban Parahu (eruption "A"; Van Bemmelen (1934)) and Mt. Tampomas; Qvu is undifferentiated old volcanic product consist of volcanic breccia, lahar deposit and repeated interlayer lava. The eruption of phase A has older formation than the eruption of phase C (Arifin, 1994; Van Bemmelen, 1949)

^{c)} Based on (Chartres and Van Reuler, 1985; Kartadinata et al., 2002; Sunardy and Kimura, 1998; Utami et al., 2019)

2.2.3 Physico-chemical analyses

Selected physical and chemical soil analyses were used to compare soil characteristics among land use and deposition age. All analyses were made on air-dried fine earth (< 2- mm) and the fraction > 2 mm was accounted as coarse fragments. Bulk density was measured on undisturbed samples taken at field-moist condition using the core method (Blake and Hartge, 1986). Particle size analysis was achieved after sonication, dispersion with Na⁺ resin, and raising the pH until 8 – 9 without any pretreatment with H₂O₂ oxidation of organic matter (Bartoli et al., 1991; Delvaux et al., 1989; Rouiller et al., 1972). Sand was measured after separating it using wet sieving from the sonicated soil slurries. The silt and clay were determined by the pipet method after full dispersion of the < 50 µm by Na⁺ resin. The pH was measured both in H₂O and 1 M KCl with a glass electrode pH meter at 1:5 and 1:2.5 soil:solution ratios, respectively. The total cation exchange capacity (CEC_T) and cations present on the exchange complex were determined using the compulsive exchange method at pH ± 4.1 – 5.3 (Gillman and Sumpter, 1986). Phosphate retention was analyzed following method by Blakemore et al. (1981). Total carbon contents were measured on bulk soil < 2 mm samples by the dry combustion method at 1100 – 1450 °C using LECO 928 series carbon/nitrogen analyzer. Total carbon corresponded to OC due to the absence of carbonates.

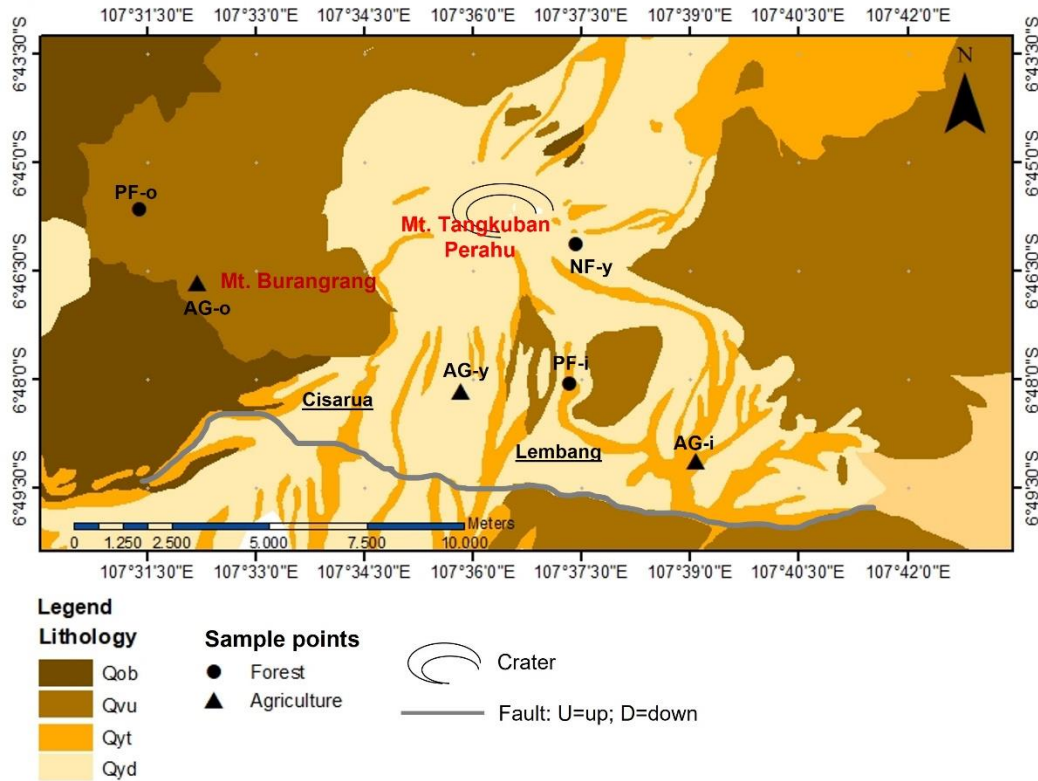


Figure 2-1 Lithology map of Mt. Tangkuban Perahu and Mt. Burangrang areas with sample points. Simplify from geology map (Silitonga, 1973).

2.2.4 Selective extraction data

Selective dissolution was used to estimate levels of SRO minerals, and -metal-humus complexes. Sodium dithionite-citrate-bicarbonate (DCB) was used to extract free iron (Fe_d) (Mehra and Jackson, 1958). Sodium pyrophosphate extracted (Fe, Al)-humus complexes (Al_p , Fe_p) (McKeague, 1967). Silicon, aluminum, and iron extractable by dark ammonium oxalate (Al_o , Fe_o , Si_o) were used to estimate allophanic substances and ferrihydrite. Estimating OC bound onto SRO Fe oxide (OC_h) was done by extraction OC and Fe (Fe_h) with hydroxylamine hydrochloride ($NH_2OH.HCl$), after removing aqueous OC with deionized water. In the various extracts, Si, Al, and Fe concentrations were determined by ICP-OESn. The OC concentration of the $NH_2OH.HCl$ extracts was determined with a FORMACS^{HT/TN-I} TOC-analyser (Skalar, The Netherlands). The OC stock per measured depth was calculated as follow:

$$OC\ stock\ (Mg\ ha^{-1}) = SD \times BD \times 10000\ m^2 \times \left(\frac{SOC}{100}\right) \quad (Eq. 2-1)$$

Where SD is soil depth (m), BD is bulk density ($Mg\ m^{-3}$), SOC is soil organic carbon (%).

2.2.5 Total elemental analysis and quantification of minerals

Major elements (Si, Al, Fe, Ti, Ca, Mg, K, Na, Mn, P) were measured by ICP-OES Varian 720-ES after dissolving the soil samples following the ISO14869-2 procedure. The weathering indices were derived

from computing the molar ratios ($\text{SiO}_2 / (\text{Al}_2\text{O}_3 + \text{Fe}_2\text{O}_3 + \text{TiO}_2)$) (Birkeland, 1999), $(\text{K}+\text{Ca})/\text{Ti}$ (Harrington and Whitney, 1987), the chemical index of alteration ($\text{CIA} = 100\% * \text{Al}_2\text{O}_3 / (\text{Al}_2\text{O}_3 + \text{CaO} + \text{Na}_2\text{O} + \text{K}_2\text{O})$) (Nesbitt and Young, 1982), and the total reserve in bases (TRB), which sums up the concentrations of alkaline and alkaline-earth cations, thus representing both their non-exchangeable and exchangeable pools (Herbillon, 1986). Acid-neutralizing capacity (ANC) was calculated at pH reference 3 following Brahy et al. (2000):

$$\text{ANC} = \text{TRB} + 6(\text{Al}_2\text{O}_3) + 6(\text{Fe}_2\text{O}_{3\text{tot}} - \text{Fe}_2\text{O}_{3\text{d}}) \quad (\text{Eq. 2-2})$$

Where TRB is expressed as $2(\text{CaO}) + 2(\text{MgO}) + 2(\text{K}_2\text{O}) + 2(\text{Na}_2\text{O})$ and $6(\text{Fe}_2\text{O}_{3\text{tot}} - \text{Fe}_2\text{O}_{3\text{d}})$ reflects Fe_2O_3 content of Fe-bearing silicates.

Identification and semi-quantification of minerals in the bulk soil (< 2 mm) was done using X-ray diffraction (XRD) after removing OC with sodium hypochlorite (Anderson, 1961). The samples were pulverized until all grains passed a 500 μm mesh sieve. For each sample, a 2 g sub-sample was mixed with 20% zincite as internal standard and further micronized (grain size of 10 μm or less) by wet grinding with ethanol using a McCrone Micronizing mill. The obtained slurry was dried to obtain a powder for XRD analysis with a Bruker D8 ECO Advance apparatus, equipped with a Cu-anode (40 kV, 25mA) and an energy-dispersive position sensitive LynxEye XE detector. The incoming beam was collimated to a fixed beam length of 17 mm. Phases were identified using the DIFFRAC.EVA suite. The spectra were interpreted semi quantitatively using the BGMN Rietveld method with Profex version 4.0 as user interface (Bergmann et al., 1998; Doebelin and Kleeberg, 2015). The amount of amorphous material was estimated from the mismatch between the obtained and the real amount of internal standard (20% of zincite).

2.2.6 Soil specific surface area

The specific surface area (SSA) was assessed on samples (< 2 mm). First, OM was removed with 6% H_2O_2 at 80°C, then dried at 100°C under vacuum, from N_2 adsorption-desorption at 77°K using a Micromeritics Tristar I following the Brunauer–Emmet–Teller (BET) approach. Furthermore, the SSA of micropores was evaluated using t-plot analysis (Mayer and Xing, 2001; Sing et al., 1985).

2.2.7 Statistical analysis

Statistical data analysis was done using IBM SPSS Statistics for Windows, version 27 (IBM Corp., Armonk, N.Y., USA). The data was grouped to identify differences in soil properties based on soil deposition ages (Qyd vs. Qyt vs. Qvu) ($n = 2$) and land use (pine forest ($n = 2$) vs. agricultural land use ($n = 3$)). As will be explained further on putative deposition ages proved inaccurate, evidenced by very limited contrasts in the parent materials of these age classes, and so this factor was omitted from the statistical analysis. Means of soil properties between land uses were compared using independent sample t-tests across all depths or based on total stocks calculated using bulk densities (i.e. SOC stock). Relations between geochemical soil properties were investigated by calculating Pearson correlation

coefficients for pine forest and agricultural land use classes separately, across depths or per depth increment.

2.3 Results

2.3.1 Soil morphology

The pedons consist of A, AB, and Bw horizons followed by a lithologic discontinuity (i.e. horizon 2AB) indicated by darker soil color than the above soil horizon. Soils are deep (> 150 cm), well drained, and non-sticky. Field assessment of texture indicated little clay, but high sand and silt content. Distinct features occurred in forest sites which had ectorganic layers, dark black surface soil horizons (i.e. horizon Ah), and concentration of boulders at depth 84-118 cm at site NF-y (Appendix 2-1).

2.3.2 Soil physiochemical properties

Major physical and chemical soil properties are presented in Table 2-2. The bulk density was invariably below 0.8 g cm^{-3} in all soil horizons, which had P-retention $\geq 85\%$, except in NF-y (A, AB), PF-i (A1), AG-y and AG-i (Ap1). The $\text{pH}_{\text{H}_2\text{O}}$ was acidic ranging from 4.08 – 5.91 and did not follow distinct depth gradients. The pH_{KCl} was mostly below 5 and was associated with KCl-extractable aluminum (Al_{KCl}) contents which increases with the decrease of pH_{KCl} . Delta pH values ($\text{pH}_{\text{H}_2\text{O}} - \text{pH}_{\text{KCl}}$) in sites NF-y and PF-o were < 0.5 , indicating the dominance of variable charge constituents while other sites had delta $\text{pH} \pm 0.5 - 1.0$ which may denote either a large dominance of variable charge or a mix (Uehara and Gillman, 1981). Soil $\text{pH}_{\text{H}_2\text{O}}$ and pH_{KCl} were higher in the agricultural soils than in pine forest ($p < 0.05$), as well as primary forest soils, coinciding with higher contents of base cations. Exchangeable Ca was the dominant base cation in all soils followed by Mg, K, and Na. Base saturation in agricultural soils ($> 100\%$) was higher than that under pine forest ($< 45\%$) ($p < 0.05$) and primary forest ($< 5\%$). Low amounts of exchangeable basic cations in forest soils were accompanied with substantial Al_{KCl} levels, as expected from pH_{KCl} values below 4.7. In all soils, the CEC_T was generally low regardless of land use ($5.6 - 10.7 \text{ cmol}_{(+) } \text{ kg}^{-1}$) and was higher in topsoil than in subsoil. Using the WRB textural classes (IUSS, 2015), texture is clay in all soil horizons (clay content = 47 – 71%), except in NF-y, A-AB-Bw (loam), AG-i, Ap1 (loam) and Ap2 (silty clay loam). The OC concentration was clearly higher in the topsoil (0 – 20 cm), viz. 23.6 – 54.4 g kg^{-1} , and decreased with depth in all soil profiles. In subsoil, the OC concentration at pine forest soils and agricultural soils were lower than that in soils under primary forest. In pine forest soils, however, OC concentration was invariably lower than that in agricultural soils. Volcanic glass was observed in all soils and ranged between 0.1 – 5.4% by grain count.

Table 2-2 Selected physicochemical properties in surface and sub-surface horizon of soils

Depth (cm)	pH		BD	O.C	Particle-size distribution			Exchangeable cations					CEC _T	BS	P-ret.	Oxalate			Fe _d	Fe _o /Fe _d	Fe _h	Al _p	Al _p / Al _o	OC _h	Allo +imo ^a	Volc. glass
	H ₂ O	KCl	g cm ⁻³	g kg ⁻¹	Sand	Silt	Clay	Ca	K	Mg	Na	Al	cmol ₍₊₎ kg ⁻¹	%	%	Al _o	Fe _o	Si _o	g kg ⁻¹					% of SOC	%	%
Primary forest (NF-y)																										
0-20 (A)	4.08	3.86	0.77	37.1	42.8	38.50	18.70	0.22	0.03	0.06	0.05	3.64	10.1	4	68.5	3.51	15.50	0.06	7.70	2.01	13.33	3.43	0.98	33.99	0.04	4.5
20-40 (AB)	4.39	3.94	0.78	26.0	40.0	40.18	19.81	0.13	0.03	0.05	0.04	2.04	7.48	4	71.3	2.34	25.42	0.04	16.92	1.50	23.93	3.52	1.50	34.05	0.03	2.3
60-80 (Bw)	4.26	4.00	0.65	28.6	29.2	41.28	29.51	0.13	0.01	0.04	0.03	2.06	7.94	3	85.9	4.83	52.43	0.13	42.58	1.23	51.30	2.81	0.58	62.58	0.09	5.4
Agricultural land (AG-y)																										
0-20 (Ap1)	5.09	4.36	0.67	29.9	8.2	23.58	68.21	7.67	1.29	1.19	0.72	1.08	7.96	137	83.5	14.35	21.08	0.85	42.51	0.50	22.74	26.30	1.83	15.81	0.61	1.3
20-40 (Ap2)	4.97	4.39	0.66	13.0	3.1	33.84	63.06	5.67	0.12	0.84	1.13	0.75	5.64	137	85.6	16.52	12.95	1.42	36.56	0.35	13.10	19.71	1.19	21.59	1.01	1.8
60-80 (Bw)	4.80	4.26	0.64	11.2	5.7	32.87	61.43	4.71	0.21	0.64	0.71	1.24	6.21	101	87.9	22.34	18.13	2.26	57.37	0.32	13.64	12.94	0.58	19.51	1.61	1.7
Pine forest (PF-i)																										
0-20 (A1)	4.54	3.65	0.64	23.6	8.0	24.73	67.27	1.77	0.08	0.59	0.24	4.79	10.7	25	84.9	8.11	11.89	0.45	33.23	0.36	13.44	41.00	5.06	17.47	0.32	1.9
20-40 (A2)	4.40	3.69	0.61	13.0	6.1	28.44	71.56	0.49	0.05	0.16	0.25	5.59	10.5	9	85.6	10.36	12.15	0.79	40.72	0.30	14.95	32.23	2.97	21.32	0.56	1.9
70-90 (Bw)	4.44	3.60	0.69	5.9	6.4	29.25	64.35	0.22	0.08	0.06	0.38	5.17	10.1	7	87.4	13.73	21.11	1.36	46.13	0.46	19.74	13.70	1.00	31.45	0.97	0.9
Agricultural land (AG-i)																										
0-20 (Ap1)	5.40	4.65	0.66	54.4	25.0	47.77	27.24	6.61	0.62	0.93	0.13	0.59	7.44	111	77.8	31.40	12.28	2.37	31.30	0.39	14.16	7.60	0.24	21.38	1.68	1.1
20-40 (Ap2)	5.75	5.32	0.47	42.6	12.1	52.29	35.62	9.97	0.95	1.75	0.14	0.04	6.00	219	88.1	33.24	12.08	2.66	35.16	0.34	14.81	5.81	0.17	14.17	1.89	1.6
50-70 (Bw)	5.91	5.50	0.52	26.9	12.5	40.44	47.07	6.99	0.63	1.46	0.17	0.03	5.44	172	90.7	36.40	11.57	3.01	29.47	0.39	15.79	5.07	0.14	22.05	2.14	0.1
Pine forest (PF-o)																										
0-20 (A1)	4.73	4.57	0.50	33.3	9.5	35.03	55.48	0.74	0.07	0.15	0.06	1.55	6.98	14	91.0	28.45	17.54	2.19	38.42	0.46	22.89	10.12	0.36	29.41	1.55	0.9
20-40 (A2)	4.88	4.68	0.56	18.2	10.7	42.88	46.63	0.39	0.03	0.11	0.09	1.48	6.43	10	89.3	27.73	17.19	2.22	41.18	0.42	25.88	9.75	0.35	31.60	1.57	1.6
60-80 (AB)	4.42	4.38	0.60	15.7	10.8	40.38	48.82	0.35	0.03	0.16	0.12	2.30	7.25	9	88.3	25.92	17.51	1.04	39.10	0.45	35.06	9.39	0.36	26.62	0.74	0.9
Agricultural land (AG-o)																										
0-20 (Ap1)	5.38	4.52	0.65	47.0	14.5	30.59	54.91	10.45	1.55	1.64	0.14	0.30	9.15	151	86.6	17.07	9.68	1.04	28.14	0.34	14.20	9.00	0.53	15.17	0.74	2.0
20-40 (Ap2)	5.60	4.68	0.61	28.8	12.7	37.27	50.02	6.97	1.62	1.25	0.18	0.10	7.98	126	84.6	15.59	9.46	1.15	28.28	0.33	14.32	8.56	0.55	18.87	0.81	1.9
60-80 (Bw)	5.77	4.73	0.62	7.8	4.9	32.29	62.81	5.99	1.79	0.97	0.23	0.07	7.44	121	87.7	9.08	7.96	0.81	31.68	0.25	13.03	10.66	1.17	16.15	0.58	1.3

^aAllophane and imogolite = Si_o% x 7.1 (Nanzyo et al., 1993a)

2.3.3 Total elemental analysis, degree of weathering, and estimation of acid neutralizing capacity

The NF-y soil horizons were clearly set apart with the highest SiO_2 (435 – 699 g kg^{-1}) and $\text{SiO}_2/\text{R}_2\text{O}_3$ molar ratio ranging from 4.7 to 8.6 (Table 2-3). In contrast, this ratio was invariably below 2 in all other soils, in which SiO_2 content ranged from 177 to 361 g kg^{-1} (Fig. 2-2). SiO_2 content was inversely proportional to Al_2O_3 , and Fe_2O_3 contents. Notable concentrations of Al_2O_3 and Fe_2O_3 were measured in soil horizons under pine forest and agricultural soil with no significant differences between these land uses. All soils generally had low total contents of CaO, MgO, K_2O , Na_2O , with slightly higher levels in NF-y soil horizons. Loss on ignition (LOI) was generally high (12.3 to 43.1%), suggesting that these soils contained substantial amounts of amorphous phases, organic matter, and water.

The weathering indices using ratios of $\text{SiO}_2/\text{R}_2\text{O}_3$, $(\text{K}+\text{Ca})/\text{Ti}$, CIA, and TRB demonstrated the distinctly lower weathering degree of the NF-y soils compared to other soils (Table 2-3). The NF-y soils had higher $\text{SiO}_2/\text{R}_2\text{O}_3$ (4.7-8.9), $(\text{K}+\text{Ca})/\text{Ti}$ (0.9 – 1.5), and lower Fe_0/Fe_t (0.25 – 0.45), and CIA (66 – 71%). In contrast, these weathering indices were low and the CIA was high in other sites indicating more severe weathering close to the ferrallitic domain (Herbillon, 1986). TRB was higher in NF-y (91 – 106 $\text{cmol}_{(+)} \text{kg}^{-1}$), AG-i (61 – 118.4 $\text{cmol}_{(+)} \text{kg}^{-1}$), and, but in lesser extent, AG-o (43 – 99 $\text{cmol}_{(+)} \text{kg}^{-1}$), whereas AG-y, PF-i, and PF-o contained TRB ranging from 30 – 60 $\text{cmol}_{(+)} \text{kg}^{-1}$. Our data further showed that, apart from NF-y and AG-y, TRB was always higher in agricultural soils than in their counterparts under pine forest. TRB was negatively correlated with clay ($r = -0.84$). The percentage of non-exchangeable base pool relative to TRB reached more than 95% in both primary and pine forest soils, whereas it ranged from 72 – 93% in agricultural soils.

Soil ANC ranged from 574.2 – 1387.1 $\text{cmol}_{(+)} \text{kg}^{-1}$. The NF-y soil clearly had the lowest ANC compared to other soils (574.2 – 600 $\text{cmol}_{(+)} \text{kg}^{-1}$). Apart from NF-y, the ANC was comparable between sites regardless deposition age. The mean of ANC was found to be slightly higher in the pine forest (1279.8 $\text{cmol}_{(+)}$) than agricultural soils (1209.9 $\text{cmol}_{(+)}$). Soil ANC was positively correlated to Al_2O_3 and Fe_2O_3 , $r = 0.67$ and $r = 0.68$, respectively.

2.3.4 XRD-mineralogy

Semi quantitative identification of the mineral phase using XRD revealed the dominance of amorphous materials in most soils (Fig. 2-3). Amorphous materials in XRD can be defined as all phases that do not produce XRD-peaks (Jones et al., 2000). Their content varied across deposition age and land use. The lowest amorphous content was found in NF-y soils, particularly in the topsoil ($\pm 25\%$). Conversely, other soils contained more amorphous materials with the largest content in the AG-i ($\pm 64\%$). These observations were also supported by high LOI values and a high $\text{Al}_0+1/2\text{Fe}_0$ content. Estimated contents of amorphous materials were positively correlated with Al_0 and $\text{Al}_0+1/2\text{Fe}_0$ ($r \pm 0.70$, $p < 0.1$) (Fig. 2-4), and negatively with SiO_2 ($r = -0.53$). There was generally no clear depth gradient in amorphous material content.

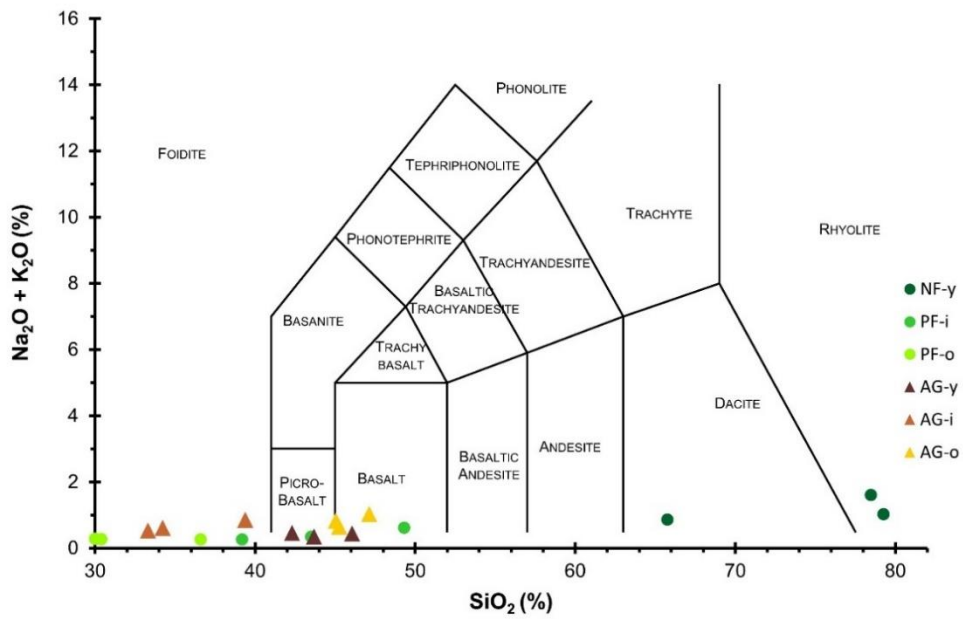


Figure 2-2 Geochemical classification (i.e. Total Alkali Silica (TAS) diagram) of total elements of SiO_2 (%) in function to $\text{Na}_2\text{O} + \text{K}_2\text{O}$ (%) in all soils. Analyses recalculated to 100% on a volatile free basis.

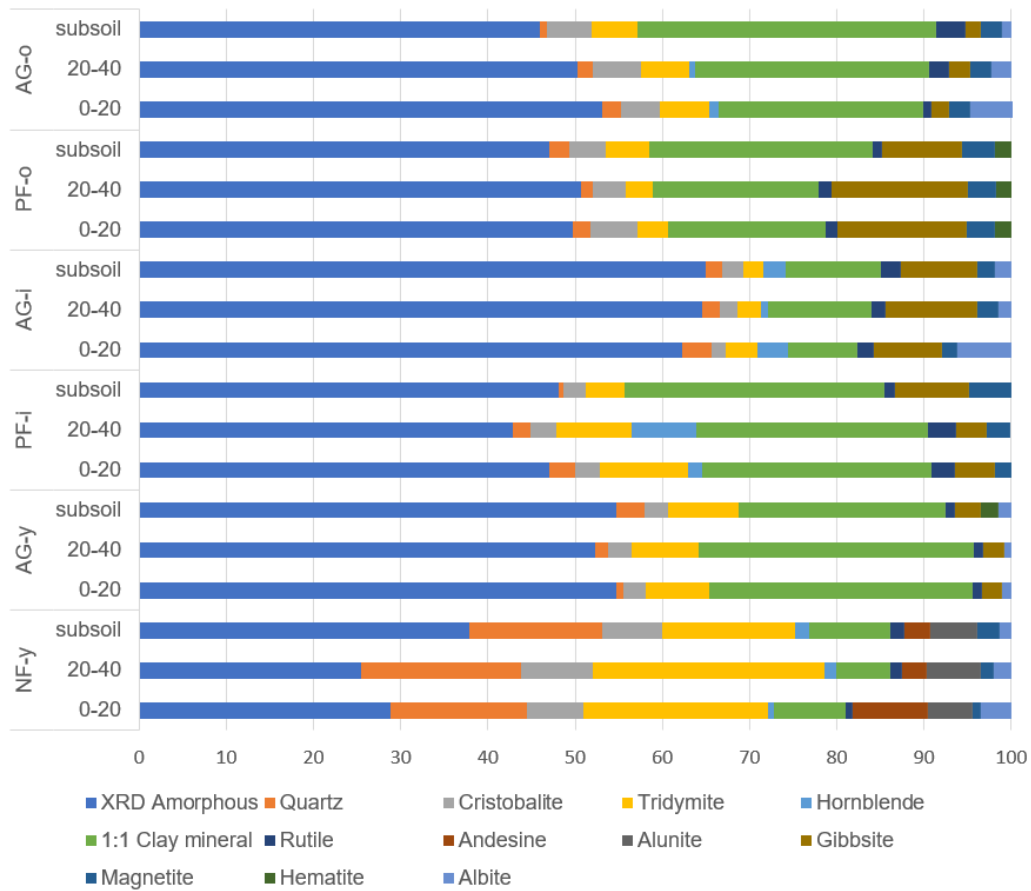


Figure 2-3 Relative proportions of mineral constituents as inferred by XRD data at each depth in all soils.

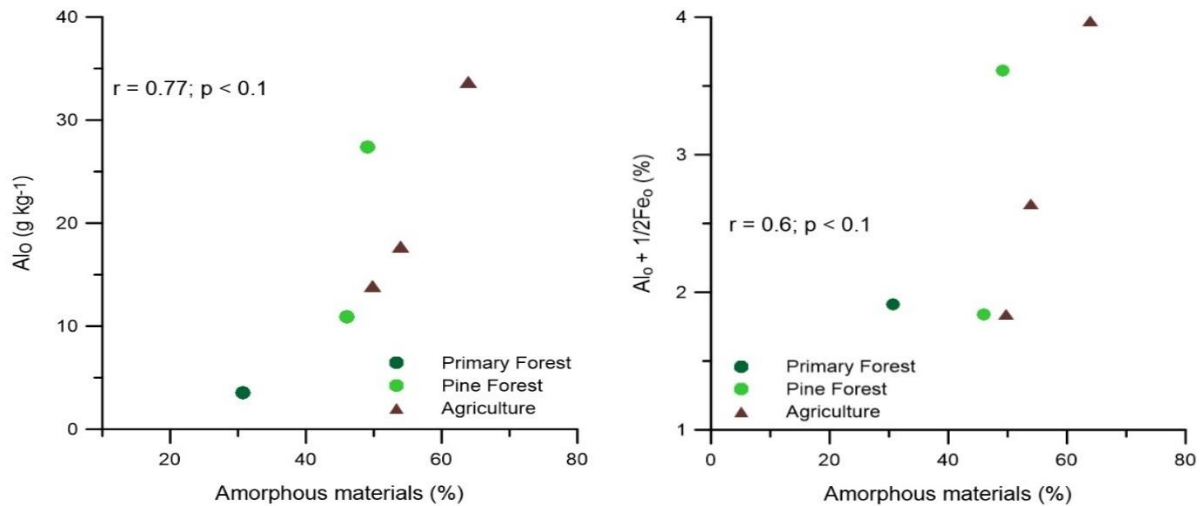


Figure 2-4 Correlations between the means of XRD-amorphous materials and contents of Al_o and Al_o+1/2Fe_o. Correlation coefficient is applied for pine forest and agricultural soils.

As indicated by a broad 0.7-nm peak, 1:1 clay mineral was present in all samples (Fig. 2-5). The 0.7-nm peak was only weakly expressed (< 10%) at NF-y, while in contrast the derived 1:1 clay mineral content was 12% to as much as 34 % in other sites. High contents of this mineral were detected in the topsoil at AG-y and subsoil at AG-o. Minerals from the quartz group, such as quartz, tridymite, and cristobalite/opal were present in notable quantities, especially at NF-y (> 30%; sum of the identified minerals). Conversely, the proportion of these minerals ranged only between 7% – 14% at other soils. Other minerals, such as hornblende, andesine, magnetite, gibbsite, albite, and rutile were detected in minor proportions and were not found in all soils. A notable quantity of gibbsite was found at the AG-i and PF-o (8 – 15%), whereas it was found in small amount in NF-y (0.1 – 0.3%). These minerals also showed no clear trend with depth. Grouping the minerals identified by Q-XRD in either primary minerals (Albite, Cristobalite, Trydimite, Quartz, Rutile, Andesine, Alunite and Hornblende) or secondary minerals (Gibbsite, 1:1 minerals; Magnetite and Hematite) showed clearly higher amounts of primary minerals and lower amounts of secondary minerals in NF-y, compared to the other soils.

2.3.5 Soil specific surface area

Soil SSA and micropores volume did not differ among soils, except for a contrast between NF-y and the other soils (Fig. 2-6). Natural forest nevertheless did exhibit a low SSA (8 – 58 m² g⁻¹) compared to pine forest and agricultural soils (66 – 198 m² g⁻¹). The largest surface area was detected in the subsoil of AG-i (198 m² g⁻¹), in accordance with high contents of Al_o and amorphous materials. Most of the subsoil had higher SSA than in topsoil. The volume of micropores was between 0 – 19.4 mm³ g⁻¹ and large micropore volume was detected in AG-y, AG-i, and PF-o soils. The C_{BET} constant, which relates to the affinity of sorption of N₂ gas molecules on solid surfaces, ranged from 75 to 213 indicating high energy surface sites or the filling of narrow micropores (Thommes et al., 2015). This high value (> 150) was detected in most of the soils, except NF-y and AG-o. SSA and micropores volume were positively correlated with Al_o (r ≤ 0.80; p ≤ 0.1) (Fig. 2-7).

Table 2-3 Geochemical characteristics (oxide content, weathering intensity, acid-neutralizing capacity)

Site	Depth	Al ₂ O ₃	SiO ₂	TiO ₂	CaO	MgO	K ₂ O	Na ₂ O	Fe ₂ O ₃	MnO	P ₂ O ₅	LOI	Weathering index			Percentage non-exch. base pool to TRB	Acid neutralizing capacity (ANC)		
													SiO ₂ /R ₂ O ₃	(K+Ca)/Ti	CIA			TRB	Fe _d /Fe _t
weight %													%	cmol ₍₊₎ kg ⁻¹	%	cmol ₍₊₎ kg ⁻¹			
NF-y	0-20 (A)	6.9	59.6	1.4	1.1	0.7	0.7	0.6	4.6	0.0	0.3	24.1	8.6	1.5	66	106.5	0.24	99.7	580.1
	20-40 (AB)	6.3	69.9	1.9	0.8	0.9	0.6	0.3	7.1	0.1	0.3	12.3	8.9	0.9	71	95.8	0.25	99.7	574.2
	60-80 (Bw)	4.8	43.5	1.7	0.8	0.9	0.4	0.3	13.5	0.1	0.3	33.8	4.7	0.9	68	90.9	0.45	99.8	599.9
AG-y	0-20 (Ap1)	23.3	28.7	1.5	0.3	0.5	0.2	0.1	12.7	0.2	0.4	31.4	1.5	0.2	96	38.9	0.48	72.1	1204.0
	20-40 (Ap2)	22.9	28.7	1.4	0.2	0.4	0.1	0.1	11.3	0.2	0.4	34.0	1.5	0.2	97	33.2	0.46	76.6	1156.7
	60-80 (Bw)	22.2	30.3	1.3	0.3	0.6	0.2	0.1	10.4	0.2	0.4	33.5	1.7	0.3	96	45.6	0.79	86.2	1156.7
PF-i	0-20 (A1)	22.6	36.1	1.4	0.6	0.7	0.2	0.2	11.2	0.2	0.4	25.9	1.9	0.7	93	69.1	0.43	96.1	1076.5
	20-40 (A2)	23.9	30.8	1.6	0.2	0.5	0.1	0.1	13.1	0.2	0.2	28.3	1.5	0.3	97	38.6	0.44	97.5	1212.2
	70-90 (Bw)	24.2	26.5	1.7	0.03	0.5	0.1	0.1	14.2	0.2	0.2	32.0	1.3	0.1	99	30.0	0.46	97.5	1242.3
AG-i	0-20 (Ap1)	21.4	25.1	1.3	1.3	1.2	0.2	0.3	11.7	0.3	1.0	35.4	1.4	1.2	88	118.4	0.39	93.0	1248.5
	20-40 (Ap2)	22.8	18.8	1.3	0.5	0.7	0.2	0.1	11.4	0.2	0.5	42.9	1.0	0.4	95	61.1	0.44	79.0	1295.4
	50-70 (Bw)	22.6	19.5	1.2	0.5	1.2	0.2	0.1	11.1	0.2	0.3	43.1	1.1	0.5	94	84.3	0.38	89.0	1213.3
PF-o	0-20 (A1)	24.8	17.7	1.7	0.1	0.5	0.1	0.1	13.5	0.2	0.4	40.6	0.8	0.1	98	34.7	0.41	97.0	1258.7
	20-40 (A2)	26.4	19.4	1.8	0.2	0.7	0.1	0.1	14.5	0.3	0.4	35.4	0.9	0.2	98	45.2	0.41	98.6	1282.6
	60-80 (AB)	25.4	24.4	1.7	0.1	0.5	0.1	0.1	13.7	0.3	0.3	32.8	1.1	0.1	99	31.1	0.41	97.9	1387.1
AG-o	0-20 (Ap1)	21.3	32.4	1.3	1.1	0.9	0.4	0.3	10.0	0.3	0.8	30.4	1.9	1.1	88	99.1	0.40	86.1	1305.9
	20-40 (Ap2)	21.6	29.7	1.3	0.6	0.7	0.4	0.2	10.8	0.3	0.5	33.6	1.7	0.7	92	71.1	0.38	85.9	1188.9
	60-80 (Bw)	24.8	33.0	1.5	0.2	0.5	0.4	0.1	12.0	0.3	0.3	26.9	1.6	0.3	96	42.7	0.38	79.0	1279.7

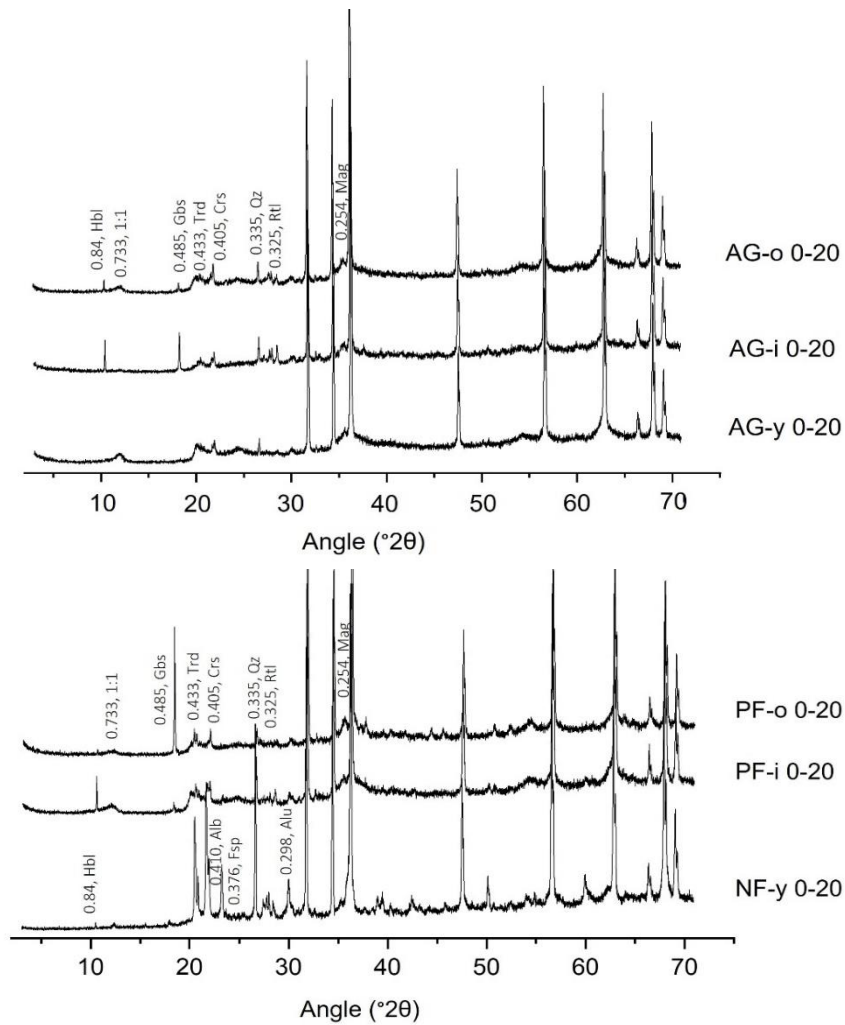


Figure 2-5 Powder diffractogram of soil samples (< 2 mm) at depth 0 – 20 cm in forest (bottom) and agriculture (top). Peak d-spacing are indicated in nm. Mineral abbreviations: 1:1: 1:1 clay minerals, Hbl: hornblende, Trd: tridymite, Alb: albite, Crs: cristobalite, Gbs: gibbsite, Fsp: feldspar, Qz: quartz, Rtl: rutile, Alu: alunite, Mag: magnetite.

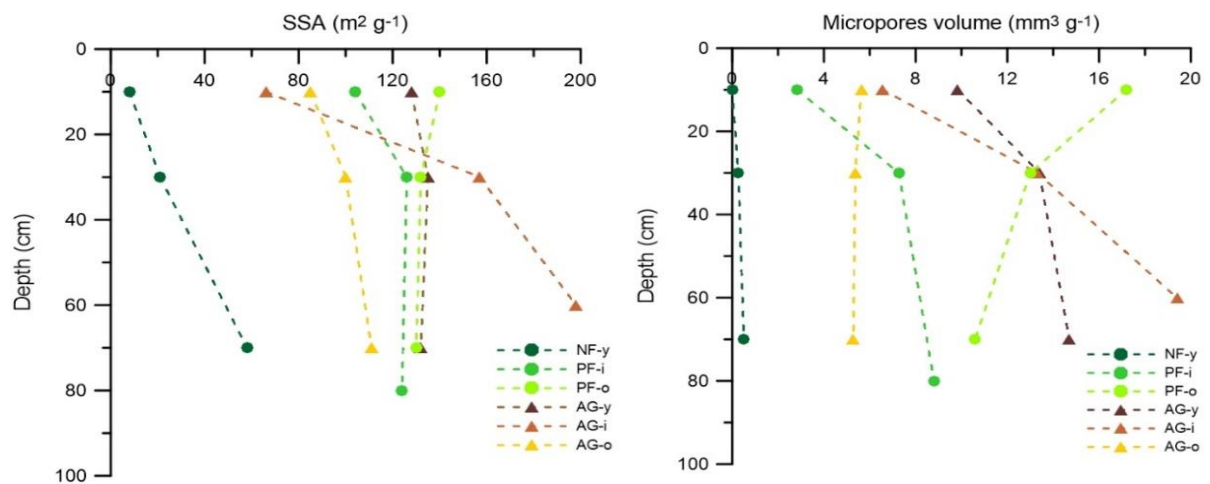


Figure 2-6 Depth evolution soil specific surface area (left) and micropores volume (right) in the different soils at each site.

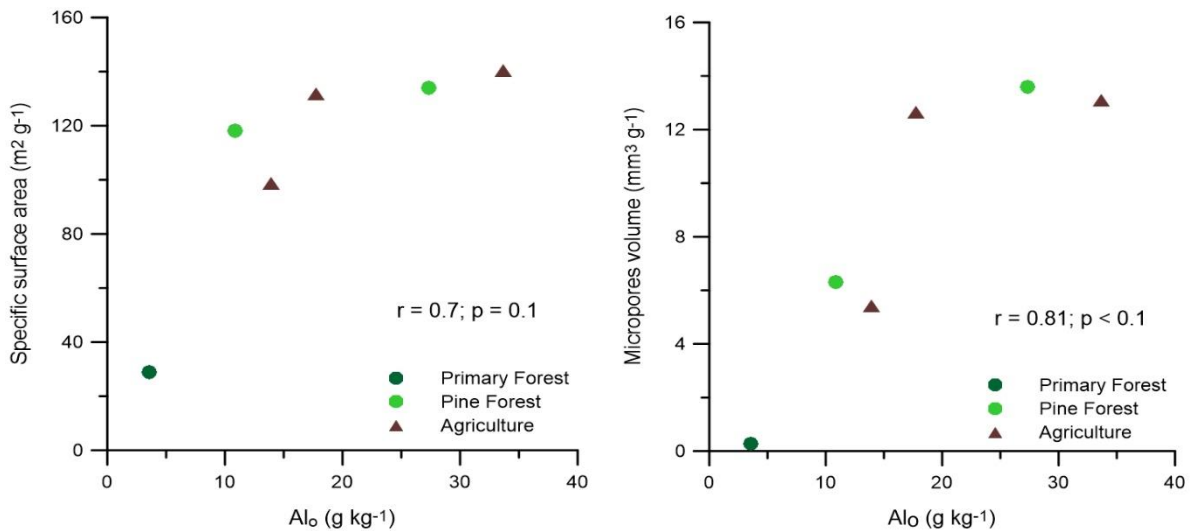


Figure 2-7 The means of specific surface area and micropores volume as plotted against Al_o content in all soils. Correlation coefficient is applied for pine forest and agricultural soils.

2.4 Discussion

2.4.1 Verifying the anthropo-chronosequence and soil weathering stage as affected by deposition age

Though soil sampling was based on geological maps and land use data, we verify here whether our analytical results confirm or not that the sequence is an anthropo-chronosequence. Clearly, NF-y is an outlier in its mineralogical composition, having higher amounts of primary minerals with notably higher amounts of Si-rich minerals, and having lower amounts of amorphous material and 1:1 mineral but slightly higher amounts of crystalline Fe-minerals (Fig. 2-3). Based on the weathering indices and silica oxide contents (Table 2-3), it is also clear that the NF-y soil is less weathered than all other soils. The high amount of SiO₂ ($\pm 60\%$) and less Al₂O₃ (6%) are characteristic of a more siliceous composition of the ash. A significant portion of SiO₂ content was possibly derived from volcanic glass and other silicate minerals (i.e. tridymite, cristobalite and quartz). The low SSA at NF-y further indicates a limited degree of physical weathering, which is known to lift the surface area of minerals (e.g. quartz < potassium feldspar < anorthite), probably due to the development of internal porosity (Brantley and Mellott, 2000). In addition, the coarser texture ($\pm 29 - 40\%$ sand particle), particularly in the topsoil of NF-y also denoted a low weathering intensity. Given the divergent mineralogical composition and total elements in NF-y soil, it is likely that this soil was influenced by the small-scale, more dacitic, eruption of nearby (1.3 km) Mt. Tangkuban Perahu in 1910 (Surmayadi et al., 2011), and that the parent material at this site was rejuvenated by younger ash of more siliceous composition. As a conclusion, the NF-y soils is developed from another parent material. This means that NF-y should be kept out of the comparison between different land uses because NF-y and the rest of soils are in different parent materials.

Apart from the different weathering intensity of NF-y soils, all the weathering indices between sites including ratios of SiO₂/R₂O₃, (K+Ca)/Ti, Fe_d/Fe_t, CIA, and TRB were similar regardless deposition age

(i.e. intermediate and old deposition age). The proportion of various identified minerals in the study soils, except NF-y, were also comparable. Solleiro-Rebolledo et al. (2015) suggested that the Andosol stage remains stable as long as the parent materials still contain sufficient materials to form allophane. Indeed, we found that volcanic glass was not exhausted at any of the soils (Table 2-2). The limited contrast in weathering between young, intermediate, and old deposition ages of pine forest and agricultural soils may be due to the relatively small deposition age differences: i.e. possibly from the Holocene to Late Pleistocene, $\pm 8000 - 10000$ yrs old (Table 2-1). Therefore, instead of anthropo – chronosequence, the comparable parent materials, and relatively small age differences between sites under pine forest and agricultural land, formed a strong base to study the effect of land use (anthropocene) on soil properties.

2.4.2 Effects of land use on weathering and acid-neutralizing capacities

Agricultural soils were detected to have slightly higher (K+Ca)/Ti ratio, TRB, and lower CIA than pine forest soils. Another weathering index, ratio Fe_d/Fe_t , which is independent from the total content of Si, Al, Ca, Mg, Na, K also showed no significant difference between soils in these land use. These results indicated the contribution of cropland management on the total base cations and the similar weathering intensity between pine forest and agricultural soils.

The TRB followed a sequence $AG-y < PF-o < PF-i < AG-o < AG-i < NF-y$ indicating that the most and least weathered soil was found in AG-y and NF-y, respectively. All soils generally have reached an advanced weathering stage since fresh andesitic materials can have TRB values as high as $500 \text{ cmol}_{(+) } \text{ kg}^{-1}$, with some being close to ferralitic domain as computed at $\leq 40 - 60 \text{ cmol}_{(+) } \text{ kg}^{-1}$ (e.g. PF soil) (Herbillon, 1986) (Fig. 2-8). High rainfall was possibly one of the reasons of advanced weathering stage, similar to the recent study by Vander Linden et al. (2021). Higher weathering degrees of pine forests soils based on the low TRB possibly links to the effect of deforestation. Clear-cutting was observed to increase export of base cations from forest soils (Richardson et al., 2017). In addition, the acidic condition in pine forest soils ($\text{pH}_{\text{H}_2\text{O}} 4.4 - 4.7$) was evidently reflected in increased ‘acid’ cations and decreased ‘base’ cation contents. On the other hand, different weathering levels on agricultural soils likely occur because not all croplands have been equally managed in term of the intensities of tillage, fertilization, and type of crops, thus the cultivation age alone is not the sole determinant of weathering stage.

The ability of soil to neutralize net acidification (ANC) is commonly linked to the release of alkaline cations through mineral weathering. Since the major component of ANC is TRB, we expected a high ANC in cultivated soils. Interestingly, a slightly higher ANC was detected in pine forest soils than agricultural soils. A decrease of ANC is linked to net acidification of soil (Van Breemen et al., 1983) which causes a significant leaching of Fe, Al, and Mn (Nawaz et al., 2013). However, our study showed no significant correlation between ANC and pH, and higher Al_2O_3 and Fe_2O_3 contents in pine forest than agricultural soils ($p < 0.05$). This result was also concomitant with the similar amount of base cations in the non-exchangeable pool between those soils. The fact that pine forest soil had more Al_2O_3 and Fe_2O_3 , and similar amount of non-exchangeable base cations suggested that not all minerals weathered faster at low pH in these soils.

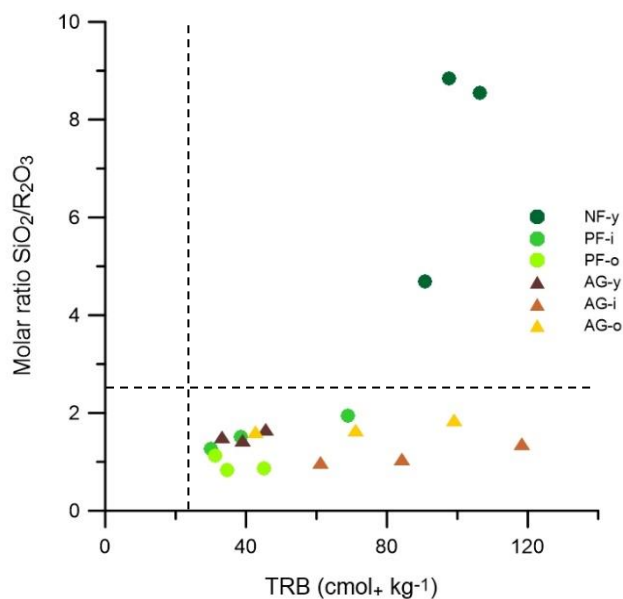


Figure 2-8 Plot of molar ratio SiO₂/R₂O₃ versus TRB at each soil depth (0 – 20, 20 – 40, and ± 60 – 80 cm) of all soils

2.4.3 Effects of land use on soil properties

Several soil properties were clearly distinct in cultivated soil compared to forest (i.e. excluding NF-y). Agricultural soils had a generally higher pH, exchangeable bases, and base saturation ($p < 0.05$) than the pine forest (Table 2-4). Lime and substantial annual input of manure explain the higher pH and so the exchangeable bases and TRB, particularly Ca, of the agricultural soils (Table 2-1). Likewise, the higher P levels logically derive from substantial annual inputs of fertilizers and manure. Continuous nutrient loss through leaching with insufficient replenishment by weathering likely acidified the forest soils with consequent lower base saturation. Conversely, higher SOC stock was detected in agricultural soils, although not significantly different, in line with the recent study by Ouédraogo et al. (2020). Similar effects of agricultural practices on soil properties were also found by Anda and Dahlgren (2020), who recently compared cropland and pine forest soils in the same region. Other properties that were expected to be equally sensitive to agricultural practices (i.e. master properties) (Kuzyakov and Zamanian, 2019) such as bulk density, surprisingly did not differ between forest and cultivated soils. Anda and Dahlgren (2020) did find a somewhat lower bulk density in pine forest (0.4 g cm^{-3}) than in agricultural soils ($0.5 - 0.8 \text{ g cm}^{-3}$) but regardless both studies show that bulk density is inherently very low in these soils, as expected for Andosols, with little further effect of land-use. Shoji and Takahashi (2002) also confirmed that a low bulk density remains in Andosols even after long-term cultivation.

Other than the land-use effects described above, the content of SRO Al (hydr-) oxides (indicated by Al_o) in agricultural soil was 14% higher than in pine forest, but with limited replication this difference could not be statistically demonstrated. Nevertheless, this outcome is well in line with a study of Andosols on the Galápagos by Gerzabek et al. (2019) who likewise documented Al_o in cropland topsoils to be 9% higher when compared to directly adjacent forest from which the agricultural land was

developed. Formation of aluminum oxides as a result of agricultural practices in volcanic soils was reported by Hernández et al. (2012) as well. Firstly, long term organic amendments were reported to increase amorphous Al and pH (Yu et al., 2017; Zhang et al., 2017). These organic amendments would promote the formation of short-range order materials possibly due to production of low molecular weight organic acids by roots or the degradation of organic amendments (Yu et al., 2017). Secondly, deforestation and soil tillage possibly cause an increase of soil temperature (Shen et al., 2018), enhancing chemical weathering (Li et al., 2021).

Our study then showed that within similar soil genoforms, a soil phenoform developed over agricultural periods in less than 50 years. These phenoforms are expressed in the soil classification by either the WRB-qualifier *dystric* (forest soils) or *eutric* (agricultural soils). In the agricultural soils, the qualifier *aric* was assigned, but not in forest soils. At the level of soil variables, the soil phenoforms were expressed by a difference in attributes such as pH, exchangeable cations, and base saturation. The change of these attributes will possibly affect nutrient cycling. Generally, agriculture practices will alter the “master properties” to reach their maximum or minimum with time, but the rate of alteration is still under discussion (Kuzyakov and Zamanian, 2019).

Table 2-4 Comparison of mean soil properties across all depth in the pine forest and agricultural soils (independent samples t-test)

Soil properties	Unit	Pine forest (n = 2)	Agriculture (n = 3)	p-value
pH _{H2O}	-	4.57 ± 1.15	5.41 ± 1.11	0.048
Exchangeable Ca	cmol ₍₊₎ kg ⁻¹	0.83 ± 0.47	7.23 ± 1.05	0.004
Exchangeable Mg	cmol ₍₊₎ kg ⁻¹	0.21 ± 0.09	1.19 ± 0.26	0.016
Exchangeable K	cmol ₍₊₎ kg ⁻¹	0.55 ± 0.02	0.98 ± 0.60	0.057
Exchangeable Na	cmol ₍₊₎ kg ⁻¹	0.19 ± 0.14	0.40 ± 0.36	0.552
Exchangeable Al	cmol ₍₊₎ kg ⁻¹	3.48 ± 2.40	0.47 ± 0.46	0.069
CEC _T	cmol ₍₊₎ kg ⁻¹	8.66 ± 1.90	7.03 ± 1.30	0.021
SOC stock ^a	Mg ha ⁻¹	63.21 ± 12.51	105.61 ± 33.56	0.200
Base saturation	%	12.51 ± 1.84	142 ± 22.87	0.005
Al _o	g kg ⁻¹	19.13 ± 11.63	21.78 ± 10.47	0.301
Al _o +1/2Fe _o	%	2.24 ± 1.25	2.60 ± 1.08	0.257
P ₂ O ₅	%	0.30 ± 0.14	0.49 ± 0.09	0.141
Amorphous materials	%	47.57 ± 2.18	55.78 ± 7.28	0.231

^a SOC stock is calculated as the sum of OC stock at depths of 0 – 20, 20 – 40, ± 60 – 80 cm

2.4.4 Soil organic carbon and its association with minerals

The total OC stocks at 0-20, 20-40, and ± 60-80 cm varied in the order of (Mg ha⁻¹): AG-i (139) > NF-y (135) > AG-o (106) > AG-y (72) ~ PF-o (72) > PF-i (54). Pine forest soils thus generally had lower SOC stocks than agricultural and primary forest soils, in accordance with other studies (Anda and Dahlgren, 2020; La Manna et al., 2018). The particularly low SOC stocks in pine forest were unexpected because usually the more polyphenol and lipid-rich residues from coniferous species give rise to accumulation of OM in soil, owing to their inherent low decomposability (McTiernan et al., 2003). The resulting ectorganic layers can in turn further limit accumulation of SOC in the underlying mineral soil because then plant litter is not completely incorporated. In any case it is striking that there was apparently no

OC depletion after conversion from forest to agricultural land-use as otherwise generally expected (Murty et al., 2002; Don et al., 2011). It seems improbable that the inputs of OC via manure and vegetable crops residues would have sufficed to explain the absence of a contrast in OC content with the pine forest soils. In fact, the OC content at AG-y was substantially lower than at AG-i and AG-o, although at the former site huge amounts of organic and NPK fertilizers (76 and 2 Mg ha⁻¹ y⁻¹, respectively) are being applied. The SOC content is obviously the resultant of the balancing of both OC inputs as well as outputs, of which microbially mediated decomposition is by far most important. Various mechanisms simultaneously limit OM decomposition in soil, of which sorption onto reactive minerals and metals has been long recognized for volcanic soils. More specifically, direct ligand exchange between organic functional groups and hydroxylated surfaces on short-range ordered mineral phases and the formation of organo-metal complexes have been shown to be very effective carbon retention mechanisms in volcanic soils (Basile-Doelsch et al., 2015, 2005; Kleber et al., 2015; Lehmann and Kleber, 2015; Sanderman and Kramer, 2017; Tamrat et al., 2019)

In pine forest and agricultural soils, Al_o correlated positively with OC content across the different sampled depths (Fig. 2-9). This suggests that, as reported by previous studies (Hernández et al., 2012; Ouédraogo et al., 2020), association by non-crystalline materials was likely a significant OC stabilization mechanism. Al_o content also correlated well with SSA and even a bit stronger with micropores volume (Fig. 2-7). Soils with high microporosity generally have high C_{BET} (Mayer and Xing, 2001; Wagai et al., 2009), thus clearly a substantial share of colloidal surface was provided by pedogenic Al. The limited microbial accessibility of OM held in micropores on pedogenic oxides has been particularly forwarded to raise long-term stability of mineral-retained OM (Zimmerman et al., 2004). So, we hypothesize that the larger surface and micropore volume provided by the higher Al_o under agricultural soil in part explains their elevated OC content compared to pine forest soil. A likewise promoted formation of Fe_o by land-use conversion was not observed and the here estimated pedogenic Fe-bound C levels remained comparable between pine forest and cultivated soils. The interaction between non-crystalline Al and OC was furthermore probably stronger at depth ± 60 – 80 cm (R² = 0.89; p < 0.05) than at 0 – 20 and 20 – 40 cm (R² = 0.46) (Fig. 2-9). The greater of organo-mineral interaction in subsoil than topsoil was also found by Poirier et al. (2020). Probably, at the lower SOC concentrations found in the subsoils (Fig. 2-9), more reactive mineral surface could be occupied by the OM, while high OM levels in topsoil may have overloaded the available reactive mineral surface, as also suggested by Gulde et al. (2008). Di et al. (2017) also found that in Chinese cropland soils with high manure inputs, the potential to store additional SOC declined, which these authors attributed to a lower SOC saturation deficit.

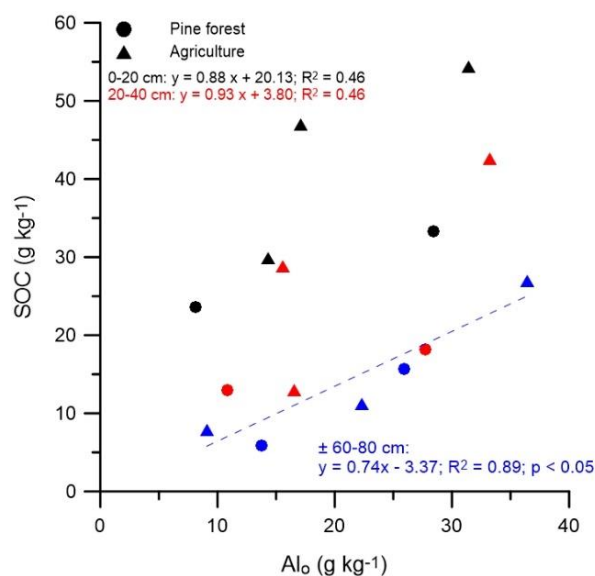


Figure 2-9 Relation between SOC and Al_o content at all measured depths of pine forest and agricultural soils (n per depth = 5). Coefficients of determination at depths of 0 – 20, 20 – 40, and ± 60 – 80 cm are indicated in black, red, and blue fonts, respectively.

2.5 Conclusions and research perspective

Apart from one rejuvenated volcanic ash soil, the anthropo-chronosequence in our study had comparable ages and parent materials, and thus are suitable to determine the effect of human land use. The data presented in this study clearly indicate the increase of base cations retention due to the decrease of acidification as natural forest is converted into managed ecosystems. Under agricultural practices (30 – 50 years), chemical soil properties such as pH, exchangeable cations, and base saturation were changed and can be considered to be an expression of soil phenofoms. Strikingly, we found no significant loss of OC stock or change in bulk density under agricultural soils. We hypothesize that the higher observed Al_o, SSA, and micropores volume under anthropogenic sites (i.e. pine forest and agriculture) promoted retention of SOC, particularly in the subsoil. The relation between minerals and OC may be better clarified by taking into account (i) the rate of mineral weathering, (ii) the capacity of soils to absorb OC relative to the OC-input via agricultural practices, and (iii) the OM turnover as function of mineralogical properties.

Authors contributions

The first author (Sastrika Anindita) performed the field research, laboratory experiment, data analyses, interpretation of the results, and writing of the paper. Peter Finke reviewed, co-wrote the paper, and supervised the research. Steven Sleutel supervised laboratory analyses in the Department of Environment, reviewed the paper, and supervised the research. Johan De Grave facilitated the laboratory analyses in the Department of Geology and reviewed the paper. Dimitri Vandenberghe provided assistance in minerals quantification and reviewed the paper. Veerle Vandenhende provided assistance during laboratory analyses in Department of Geology.

Acknowledgement

This research is supported and funded by Indonesia Endowment Fund for Education (LPDP). The XRD facilities were subsidized by the Hercules foundation and the research foundation – Flanders (FWO-Vlaanderen) through grant numbers AUGÉ/13/05 – G0F2714N and G028714N.

CHAPTER 3

TROPICAL ANDOSOL ORGANIC CARBON QUALITY AND
DEGRADABILITY IN RELATION TO SOIL GEOCHEMISTRY AS
AFFECTED BY LAND USE

Based on:

Anindita, S., Finke, P., Sleutel, S. Tropical Andosol organic carbon quality and degradability in relation to soil geochemistry as affected by land use. This manuscript is under review in the journal of SOIL.

Abstract

Land use is recognized to impact soil geochemistry on the centennial to millennial time scale, with implications for the distribution and stability of soil organic carbon (SOC). Volcanic soils in tropical areas are subject to faster pedogenesis, with also possibly mediated by land use on much shorter centennial or even decadal scale. Very scarce observational evidence exists and so such indirect implications of land use on SOC cycling are largely unknown. We here investigated SOC fractions, substrate specific mineralization (SOC or added plant residue), and net priming of SOC in function of forest or agricultural land use on Indonesian volcanic soils. The results showed that the content of oxalate-extracted Al (Al_o) and amorphous materials correlated well with OC associated with sand-sized aggregates, particularly in subsoil. The proportion of SOC in sand-sized 400 J ml^{-1} ultrasonication resistant aggregates was found to be higher in agricultural than pine forest soils, likewise the contrasts in Al_o suggest that enhanced formation of Al-(hydr)oxides promoted aggregation and physical occlusion of OC. This was importantly also consistent with a relatively lesser degradability of SOC in the agricultural than pine forest soils, though the net priming of SOC and degradability of added ^{13}C -labelled ryegrass was not found to depend on land use. We expected that amorphous Al content under agricultural land use would mainly have promoted mineral-association of SOC compared to under pine forest but found no indications for this. Improved small scale aggregation of tropical Andosols caused by conversion to agriculture and high carbon input via organic fertilizer may thus partially counter the otherwise expectable decline of SOC stocks following cultivation. Such indirect land use effects on the SOC balance appeared relevant for correct interpretation and prediction of the long-term C-balance of (agro)ecosystems with soil subject to intense development, like this research in tropical Andosols.

Keywords: land use, amorphous aluminum, soil aggregates, SOC mineralization, Andosols

3.1 Introduction

Storage of SOC in terrestrial ecosystems can improve ecosystem services such as soil health, agricultural productivity, and climate change mitigation (Baldock, 2007; Lehmann and Kleber, 2015). The storage of SOC is influenced by the interaction of ecological processes with net primary productivity and heterotrophic respiration usually being most important terms of the SOC balance. Land use determines the net-C input to soil and in doing so often bears an overriding control on the SOC balance, compared to other drivers of the carbon cycle at ecosystem level. Forest ecosystems usually have relatively high net primary productivity compared to agricultural land use (Smith et al., 2014). The net result of cultivation then typically leads to a decline in SOC stock and increased human-induced CO₂ emission (Don et al., 2011; Wei et al., 2014). The long-term SOC balance of ecosystems also depends on the capacity of soils to stabilize newly entering OC against microbial decomposition, resulting from heterotrophic respiration. Physical occlusion of OC at the microaggregate scale as well as binding of OC onto reactive mineral surfaces constitute two major mechanisms for stabilization of SOC (Matus et al., 2014). Soil characteristics such as content of non-crystalline materials, specific surface area, clay content and degree of soil micro-aggregation have all been linked to the capacity of soils to accumulate SOC (Hernández et al., 2012; Kleber et al., 2015; Mikutta et al., 2009, 2006; Poirier et al., 2020). While soil mineralogy itself is thus a well-recognized controller of SOC stabilization (Basile-Doelsch et al., 2005; Hernández et al., 2012; Lyu et al., 2021; Tamrat et al., 2019), surprisingly little attention has gone into understanding how land use history, through its impact on soil geochemistry might in turn indirectly control stability of SOC and OM entering soil.

The geochemistry of the reactive mineral phase of a soil is the resultant of both the composition of its parent material and soil weathering status (Mikutta et al., 2009). Weathering status is crucially driven by the time since the onset of weathering, local climate and hydrologic conditions, resilience of minerals to weathering and vegetation cover (Doetterl et al., 2015). Land use, through its control on vegetation, can impact the weathering process by modifying the pH, influencing soil biological activity and nutrient levels, and releasing organic complexing compounds (Cronan, 2018; Van Breemen et al., 1983). On agricultural lands, fertilizer addition and soil disturbance caused by tillage have also been reported to significantly enhance weathering (Churchman and Lowe, 2012; Li et al., 2021; Taylor et al., 2016). While an extensive and still growing number of studies considered land use impacts on SOC stock, soil OM quality and its degradability (Covaleda et al., 2011; Cusack et al., 2013; Huygens et al., 2005), just very few of them have considered the potential indirect impact of land use on SOC stability through its effect on the geochemical properties. Moreover, the coverage remains limited for several soil groups, including tropical Andosols. A recent study on the Gálápagos islands demonstrated that even after maximum of fifteen years conversion of native forest to cultivated land strikingly accelerated soil weathering (Gerzabek et al., 2019). In particular, formation of secondary minerals should impact SOC retention in volcanic soils as their high capacity to do so is acknowledged to emerge from abundantly present poorly crystalline Al and Fe oxides. Indeed, Asano and Wagai (2014) concluded the importance of short-range order minerals or organo-Al complexes for SOC stabilization in Andosols from correlations with OC stock (Miyazawa et al., 2013), mean residence time (reviewed by Parfitt (2009)), and by chemical characterization of organo-mineral associations (Basile-Doelsch et al., 2007; Mikutta et al., 2009). Next to a large specific surface area, also microaggregation and occlusion therein of intra-microaggregate particulate OM (iPOM) is known to grant a degree of

protection against its microbial decay (Six et al., 2000a), particularly in Andosols (Asano et al., 2018; Asano and Wagai, 2014). Introduction of tillage and removal of permanent vegetative coverage usually adversely affect iPOM-induced physical protection (Besnard et al., 1996). However, differences between untilled native vegetation or secondary forest on the one hand and tilled cropland might not be significant for volcanic soils (Dörner et al., 2012; Huygens et al., 2005; Linlin et al., 2016) as abundant nano sized organo–mineral composites overridingly act as binding agents in microaggregates in Andosols (Asano and Wagai, 2015).

In Indonesia, the Sunda volcanic arc region (Mt. Tangkuban Perahu and Mt. Burangrang) in West Java, was covered by native forest until only about two centuries back but has since then been largely replaced by secondary pine forest or agricultural land use. The co-occurrence of native forest, secondary forest and agricultural land forms a useful means to understand how land use would influence geochemical properties, and impact SOC storage and stability in this Andosol. A first objective was to further investigate how cultivation history in this region would have resulted in differential soil aggregation and levels of iPOM, and mineral associated OM vs. free relatively unprotected OM. We did so by assessing soil OM fractions for a set of 6 Indonesian volcanic soil (Cambisols and Andosols) with native forest, secondary pine forest or agricultural land use. A second goal was to infer how OM degradability in the topsoil of these tropical volcanic soils itself differs in function of forest vs. agricultural land use. Assessing the indirect effect of land use on SOC degradability through its mediation of soil mineralogy is, however, complicated by the fact that quality of native SOC itself is also function of land use. We therefore assessed the degradability of a single model exogenous OM source (^{13}C -labelled ryegrass residues) to see how land use changes affect stability of OC in soil. We hypothesize that the enhanced formation of pedogenic short-range order Al under agricultural land use, as we previously confirmed (Anindita et al., 2022b), results in a relative stabilization of the exogenous OM as compared to native forest or secondary forest. In doing so we take account for the well-known phenomenon that labile OC-inputs can accelerate the decomposition of native SOC, a process called positive priming (Chen et al., 2014), or conversely restrain decomposition of SOC and induce negative priming (Blagodatskaya et al., 2014; Qiao et al., 2014). By using a C-isotope mixing model (Werth and Kuzyakov, 2010), the contribution of two different sources of CO_2 to total emitted CO_2 can be distinguished, and therefore, the carbon mineralization derived from exogenous OM (i.e. ryegrass) and native SOC can be estimated.

3.2 Materials and methods

3.2.1 Site description and soil sampling

Our study covered soils from the Mount Tangkuban Perahu and Mount Burangrang regions that are part of the Sunda Volcanic complex in West Java, Indonesia. Six sites were selected to represent the dominant land use types in the area, viz. primary forest (NF-y), pine forest (PF-i and PF-o) and horticulture (AG-y, AG-i, and AG-o) (Fig. 1-2). The mean annual temperature in the study sites is 19–21°C and mean annual precipitation ranges around 2000–3000 mm per year. Soils at sites NF-y and PF-i are andic Cambisols and at the PF-o, AG-y, AG-i, AG-o sites aluandic Andosols (Anindita et al., 2022b). All soils contain non-crystalline materials and crystalline minerals, i.e. quartz, cristobalite,

tridymite, gibbsite, albite, hornblende, 1:1 clay minerals (Anindita et al., 2022b). The proportion of primary minerals is higher in the younger NF-y soil as it is closer (within 1.5 km) to the crater of Mt. Tangkuban Perahu and received ash more recently. The pine forest and agricultural sites were originally all under the primary forest vegetation. At PF-i and PF-o, secondary forests were planted in 1962 for restoration purposes, following earlier deforestation. Agricultural land use at AG-y, AG-i, and AG-o dates back to just 30–50 years ago with mainly diverse horticultural crop rotations with crops potatoes (*Solanum tuberosum*), cabbage (*Brassica oleracea*), green bean (*Phaseolus vulgaris*), tomatoes (*Solanum lycopersicum*), and chayote (*Sechium edule*). Detailed information about land use history, and land management are given in (Anindita et al., 2022b).

At every site, soil samples were taken at 0–20, 20–40, and 60–80 cm depth. At each depth, the bulk samples were mixed into composite ones, which were then dried to the air, homogenised and sieved (< 2 mm) until further analysis at the Dept. of Environment of Ghent University (Belgium). The pH H₂O was measured using a glass electrode pH meter in a 1:5 soil solution slurry. The estimated clay content was determined using the pipet method after full soil dispersion with Na⁺-resin (Bartoli et al., 1991), after testing several other procedures for soil texture analysis that proved incompatible with the investigated set of volcanic soils. The concentrations of total C and N were determined by dry combustion at 1100°C using a LECO 928 series CN-analyser. Aluminum extracted by 0.1 M pyrophosphate solution (Al_p) was taken as measure of complexed Al to OM (McKeague, 1967). Iron and aluminum extractable by ammonium oxalate (Al_o, Fe_o) were used as estimates of X-ray amorphous Al and Fe. We previously quantified crystalline minerals using X-ray diffraction analysis. The amount of amorphous materials undetectable by X-ray diffraction was semi-quantitatively estimated from the difference between the obtained and the real amount of internal standard (Zincite 20%) after semi-quantification of crystalline minerals using BGMN Rietveld and Profex as user interface. Soil specific surface area (SSA) was assessed from adsorption-desorption of N₂ at 77°C following Brunauer–Emmett–Teller (BET) approach. Detailed methods and the results of geochemical analyses of the samples were documented in (Anindita et al., 2022b) Selected physicochemical soil properties are given in Table 3-1. More detailed information of geochemical soil properties can be found in (Anindita et al., 2022b).

Table 3-1 Physicochemical soil properties of 6 sampled soil profiles in the Sunda Volcanic complex in West Java, Indonesia (partly taken from (Anindita et al., 2022b))

Depth (cm)	pH H ₂ O	BD ^a (g cm ⁻³)	OC stock ^a Mg ha ⁻¹	δ ¹³ C ‰	C/N ratio	Clay %	NH ₄ -oxalate extractable		Al _p ^a mg g ⁻¹	SSA ^a m ² g ⁻¹	Amorphous materials g kg ⁻¹	Land use & estimated annual C-inputs ^b
							Al _o ^a mg g ⁻¹	Fe _o ^a mg g ⁻¹				
Primary forest (NF-y)												
0–20	4.1	0.77	56.9	-27.0	15.1	18.70	3.5	15.5	3.4	9	288	Natural vegetation (estimated plant C input: 6.7 – 12.2 Mg ha ⁻¹ yr ⁻¹)
20–40	4.4	0.78	43.1		20.2	19.81	2.3	25.4	3.5	27	254	
60–80	4.3	0.65	37.4		20.0	29.51	4.8	52.4	2.8	69	378	
Agriculture (AG-y)												
0–20	5.1	0.67	40.2	-13.6	18.2	68.21	14.4	21.1	26.3	114	548	Intensive horticulture ± 50 years (estimated plant C input = 1.8 Mg ha ⁻¹ yr ⁻¹ , organic fertilizer C- input = 11.5 Mg ha ⁻¹ yr ⁻¹)
20–40	4.9	0.66	17.3		11.9	63.06	16.5	13.0	19.7	125	523	
60–80	4.8	0.64	14.4		10.8	61.43	22.3	18.1	12.9	134	547	
Pine forest (PF-i)												
0–20	4.5	0.64	30.4	-24.3	10.8	67.27	8.1	11.9	41.0	91	471	Pine forest

20–40	4.4	0.61	15.9		10.2	71.56	10.4	12.2	32.2	117	429	(estimated plant C input: 3.6 – 9.1 Mg ha ⁻¹ yr ⁻¹)
70–90	4.4	0.69	8.1		10.0	64.35	13.7	21.1	13.7	124	481	
Agriculture (AG-i)												
0–20	5.4	0.66	71.4	-15.4	14.7	27.24	31.4	12.3	7.6	48	623	Intensive horticulture ± 40 years (estimated plant C input = 1.6 Mg ha ⁻¹ yr ⁻¹ , organic fertilizer C-input = 6.42 Mg ha ⁻¹ yr ⁻¹)
20–40	5.8	0.47	39.6		17.9	35.62	33.2	12.1	5.8	128	645	
50–70	5.9	0.52	28.1		16.9	47.07	36.4	11.6	5.1	185	650	
Pine forest (PF-o)												
0–20	4.7	0.50	33.0	-24.2	12.6	55.48	28.5	17.5	10.1	107	497	Pine forest (estimated plant C input: 3.6 – 9.1 Mg ha ⁻¹ yr ⁻¹)
20–40	4.9	0.56	20.4		12.2	46.43	27.7	17.2	9.8	145	506	
60–80	4.4	0.60	18.8		11.9	48.82	25.9	17.5	9.4	127	447	
Agriculture (AG-o)												
0–20	5.4	0.65	61.1	-24.0	10.5	54.91	17.1	9.7	9.0	74	531	Horticulture < 30 years (estimated plant C input = 0.98 Mg ha ⁻¹ yr ⁻¹ , organic fertilizer C-input = 6.8 Mg ha ⁻¹ yr ⁻¹)
20–40	5.6	0.61	35.0		9.8	50.02	15.6	9.5	8.6	91	502	
60–80	5.8	0.62	9.7		8.4	62.81	9.1	8.0	10.7	108	460	

^a BD = bulk density; OC = organic carbon; Al_o = aluminium extracted by NH₄-oxalate; Fe_o = iron extracted by NH₄-oxalate; Al_p = aluminum extracted by Na-pyrophosphate; SSA = specific surface area

^b C-inputs from vegetation (forest or annual crops) and organic amendments. Forest C-inputs estimated from studies on Indonesian pine forest (Bruijnzeel, 1985) and Indonesian tropical primary forest (Guillaume et al., 2018; Hertel et al., 2009). Crop C-inputs based on farmer interviews and SSB & UGhent (2008). C-inputs from organic amendments were based on farmer interviews and lab-analyses.

3.2.2 Soil organic matter fractionation

Soils were fractionated using size, density and chemical separation steps according to a modified version of a fractionation scheme proposed by Zimmermann et al. (2007) (Fig. A3-1 in Appendix 3). This procedure separates SOC into five pools, namely into i) OC contained in soil aggregates and associated with sand (S+A), ii) in free particulate organic matter (POM), iii) in water dissolvable OC (DOC), iv) in oxidizable OC associated with the silt and clay (s+c – rSOC) fraction, and v) in a chemically resistant SOC (rSOC) pool. Briefly, 30 g of equivalent dry soil (< 2 mm) was initially dispersed in water by a calibrated ultrasonic probe with an output energy of 22 J ml⁻¹. The resulting slurries were wet-sieved over a 63 µm sieve and rinsed with deionized water until the rinsing water became clear. In the original Zimmermann et al. (2007) method the > 63 µm fraction is further separated into S+A and POM based on density differences using sodium polytungstate at 1.8 g cm⁻³. However, several samples could not be well separated into free OM on the one hand and predominantly mineral material of the S+A fraction on the other. After pre-tests we instead used a 1.5 g cm⁻³ sodium polytungstate solution to separate free POM from the S+A soil fraction, as per Cerli et al. (2012)'s advise to per soil optimize density cut-off for best separation of free and occluded POM. A subsample of the < 63 µm suspension (± 10 ml) derived from the wet sieving step was filtered through a 0.45 µm nylon membrane filter. The filtrate was analyzed for its dissolved OC concentration using a HT-I Formacs TOC-analyzer (Skalar, The Netherlands). The DOC pool was calculated by multiplying this OC concentration with the volume of flush water used in the preceding wet sieving step. The < 63 µm suspension was dried at 40°C and weighted to constitute the overall silt+clay (s+c) fraction. A chemically inert share of the SOC (rSOC) was isolated by subjecting the s+c fraction to oxidation by 6 % NaOCl. To this end, one gram of s+c material was weighted inside a 65 ml Nalgene centrifuge tube and 50 ml 6 % NaOCl adjusted to pH 8 was added and allowed to react for 18 h at 25°C. After centrifugation, remnant NaOCl was discarded by decantation. This procedure was repeated three times, the pellet was washed three more times with deionized water, transferred to a pre-weighted aluminum cup, dried at 40°C and weighted. The

obtained S+A fraction remains composite as it contains s+c associated OC next to occluded POM. In addition to the original scheme proposed by Zimmermann et al. (2007) and Poeplau et al. (2013), a further fractionation of the S+A into s+c and POM and sand-associated OM was included: A 3 g subsample of the obtained S+A fraction was further dispersed by ultrasonication at 400 J ml⁻¹ and then separated into two size fractions by passing the obtained slurries over a 63 µm sieve. The obtained < 63 µm fraction contains s+c OM and the > 63 µm fraction primarily occluded POM and sand-bound OM contained in S+A as well as OM contained in > 63 µm aggregates resistant to dispersal at 400 J ml⁻¹. The S+A and s+c fraction was further on considered as to constitute a single joint OM fraction with s+c obtained after the first 22 J ml⁻¹ and 63 µm sieving step. All fractions were analyzed for their carbon concentration using a LECO 928 series CN-analyzer.

3.2.3 Soil incubation experiment and isotopic signature measurements

Soils were incubated in a standardized way to compare degradability of a model plant-C substrate and SOC in the topsoil (0 – 20 cm) of the 6 considered sites. Decomposition of either substrate was derived by regular measurement of the soil CO₂ efflux and inference of its δ¹³C signature. Soil mesocosms were prepared by repacking approximately 150 g of soil (depending on bulk density) into PVC tubes (diameter: 6.8 cm, height: 7 cm) to reach a height of 6.2 cm and bulk density as encountered at the field sites, around 0.6 g cm⁻³. Soil moisture content was set to 50 % water-filled pore space by addition of deionized water. A ¹³C-labelled plant-substrate, i.e. pulse-labelled ryegrass (*Lolium perenne*) with δ¹³C of +54.25 ± 0.3‰ (n = 6), and C and N contents 43.9±0.5% and 4.3 ± 0.3% (n = 3), yielding a C:N ratio of 10±0.5, was applied at a dose of 1 g kg⁻¹ (0.44 g C kg⁻¹). The contrast in δ¹³C with SOC (Table 3-1) allowed to distinguish emitted CO₂ into parts stemming from either native SOC or grass-C mineralization. The δ¹³C of topsoil (expressed as δ¹³C value (‰) vs. the international Vienna Pee Dee Belemnite standard) was measured using a PDZ Europe ANCA-GSL elemental analyser, interfaced with a Sercon 20–22 IRMS with SysCon electronics (SetCon, Ceshire, UK).

Soils were incubated at 20°C for 120 days. On days 1, 3, 5, 8, 12, 17, 24, 32, 38, 47, 59, 73, 87, 101, 111, 120 soil CO₂ emission was inferred by measuring CO₂ build-up in a cylindrical closed-chamber attached consecutively on top of each PVC tube for at least 10 min. The evolution of the headspace CO₂ concentration and its δ¹³C was measured every 4 sec by connecting the closed-chamber with a cavity ring-down spectrometer (G2201-i CRDS isotopic CO₂ analyser, Picarro, USA) in a loop via Teflon tubing. Soil CO₂ efflux rate in mg C kg⁻¹ h⁻¹ was calculated from the slope of the accumulating CO₂ concentration in function of time using the ideal gas law. The δ¹³C of emitted CO₂ was estimated from the y-axis intercept of derived Keeling plots (Keeling, 1958). The fraction of CO₂ derived from grass was calculated using the following equations introduced by Werth and Kuzyakov (2010):

$$f_{grass-CO_2} = \frac{\delta^{13}C_{total-CO_2} - \delta^{13}C_{SOC-CO_2}}{\delta^{13}C_{grass-CO_2} - \delta^{13}C_{SOC-CO_2}} \quad (\text{Eq. 3-1})$$

$$\delta^{13}C_{grass-CO_2} = \delta^{13}C_{grass} - \epsilon_{grass} \quad (\text{Eq. 3-2})$$

$$\delta^{13}C_{SOC-CO_2} = \delta^{13}C_{SOC} - \epsilon_{SOC} \quad (\text{Eq. 3-3})$$

with ϵ_{SOC} (in ‰) the net C-isotopic fractionation resulting from native SOC mineralization and diffusive CO_2 transport in soil until its efflux into the headspace air. The ϵ_{SOC} was obtained from CO_2 -efflux monitoring parallel triplicate sets of control soils without grass added. A third parallel set of soils were amended with a very high dose of grass (viz. 6 g kg^{-1} added grass, i.e. about 4 t C ha^{-1}) to estimate ϵ_{grass} . This value was operationally calculated by subtracting $\delta^{13}\text{C}_{\text{grass}}$ from the peak CO_2 emission $\delta^{13}\text{C-CO}_2$ of soil with 6 g kg^{-1} grass under the assumption that virtually any emitted CO_2 was then derived from grass mineralization.

Using Eq. 3-1, 3-2 and 3-3 the fraction of emitted CO_2 derived from grass-C mineralization was calculated per soil and per point in time. The rate of grass-C mineralization ($C_{\text{grass-min}}$, in $\text{mg C kg}^{-1} \text{ h}^{-1}$) for each measurement day was calculated by multiplying the f_{grass} value with the total CO_2 emission. The rate of SOC mineralization ($C_{\text{SOC min}}$, in $\text{mg C kg}^{-1} \text{ h}^{-1}$) was calculated by subtracting the rate of $C_{\text{grass-min}}$ from the total CO_2 -C emission rate. Cumulative CO_2 emissions derived from native SOC-C and grass-C were obtained by consecutively summing up $C_{\text{SOC-CO}_2}$ and $C_{\text{grass-CO}_2}$ respectively per time increment between flux measurements. The % of mineralized C_{SOC} was then derived from dividing $C_{\text{SOC-CO}_2}$ by C_{SOC} .

3.2.4 Statistics

2-way ANOVA was used to compare the distribution of OC over soil fractions and soil properties with depth increment and land-use as fixed factors. For individual increments (0 – 20, 20 – 40, and ± 60 – 80 cm) additional t-tests were used as well to test for differences between pine forest and agricultural land use. For the total cumulative carbon mineralization, grass and native C -mineralized, and net cumulative priming of native SOC, the comparison was only at depth 0 – 20 cm by t-tests between the pine forest and agricultural soil groups. The primary forest was excluded from this comparison due to its different parent materials as found in previous study (Anindita et al., 2022b). Pearson correlation coefficients were used to investigate relations between soil carbon fraction, carbon mineralization, and geochemical properties for pine forest and agricultural soils at each measured depth. Analyses were completed in IBM SPSS Statistics 27.

3.3 Results

3.3.1 Organic carbon in soil fractions

From all soils, a greater part of soil material was found as s+c fraction ($\pm 73\%$) (Table 3-2). There were particularly large proportions of s+c in the PF-i, PF-o, and AG-o soils ($> 80\%$). Conversely, in the AG-i at depths of 20 – 40 and ± 60 – 80 cm, the S+A fraction was the largest (64 – 66%). The OC concentration of soil fractions decreased in the order: POM $>$ s+c (including rSOC) $>$ S+A $>$ DOC and was generally higher at the depth of 0 – 20 than 20 – 40 and ± 60 – 80 cm. The mean OC concentration of the S+A fraction was higher under agricultural than pine forest soils ($p < 0.05$), particularly at depth 0 – 20 cm of agricultural land use ($36.8 \pm 10 \text{ g C kg}^{-1}$ fraction). The OC concentration of s+c and s+c – rSOC were generally higher in the agricultural compared to the pine forest soils ($p < 0.1$), but there was no significant difference in rSOC fraction between these land uses. On the other hand, in primary

forest, the OC concentration in s+c fraction was generally higher than in S+A fraction. The size of the DOC fraction was negligibly small ($\pm 0.002 \text{ g C kg}^{-1}$ fraction) in all soils and was further disregarded. The mean total SOC content in all fractions was higher in agricultural soils ($29.6 \pm 15.7 \text{ g C kg}^{-1}$ soil) than pine forest (16.3 ± 8.04) ($p < 0.05$).

Overall, the bulk of SOC across depths was present in the s+c ($\pm 78\%$) with higher proportion in rSOC ($\pm 44\%$) than in the s+c - rSOC ($\pm 35\%$) fraction, followed by S+A ($\pm 21\%$) and POM ($\pm 2\%$) fractions (Fig. 3-1). The mean OC content in the S+A fraction were higher in the agricultural ($11 \pm 10 \text{ g C kg}^{-1}$ soil) than pine forest soils ($1.5 \pm 0.6 \text{ g C kg}^{-1}$ soil, respectively) (but only at $p = 0.09$). Likewise, its relative contribution to SOC was larger in the agricultural soils ($31.7 \pm 25\%$ of SOC) compared to pine forest soils ($9 \pm 1.5\%$ of SOC) (but only at $p = 0.08$). In the upper layer of the agricultural soils, a large share of the SOC was present in the S+A fraction of AG-i at the depths of 0 – 20 cm (22.3 g C kg^{-1} soil) and 20 – 40 cm (30.6 g C kg^{-1} soil). The s+c followed an opposite trend with a larger SOC proportion under pine forest ($89 \pm 2.1\%$ of SOC) than under agricultural land-use ($68 \pm 24.4\%$ of SOC) (though only at $p = 0.08$). The mean resistant SOC (rSOC) fraction accounted for approximately a third to half of SOC and its proportion was likewise higher under pine forest ($52.1 \pm 4.6\%$) than agricultural land use (34.3 ± 5.8) ($p < 0.01$). Free POM contributed on average less than 5 % of SOC. The occasional low POM C-concentrations (Table 3-2) indicate that some mineral matter was left in the isolated POM fraction. However, given its very small mass proportion (median 0.1%), this artefact has negligible further impact on the overall distribution of SOC across soil fractions. The SOC proportion of free POM (% of SOC) was generally higher under pine forest than agricultural land use, but they did not differ significantly. For the primary forest, the proportions of SOC at all depths were found to be higher in order: rSOC > s+c – rSOC > S+A > POM > DOC fractions.

Table 3-2 Mass proportion, C concentration, and total content of SOC contained in soil fractions isolated by a modified version of the Zimmermann et al. (2007) method.

Depth (cm)	Soil mass proportion (%)			C concentration (g kg^{-1} fraction)				Amount of C (g kg^{-1} soil)				Total SOC in bulk soil	
	POM	S+A	s+c	POM	S+A	s+c	DOC	POM	S+A	s+c			
						s+c - rSOC	rSOC				s+c - rSOC	rSOC	
Primary forest (NF-y)													
0–20	0.2	37.6	62.2	412.5	4.6	31.1	30.5	1.0	0.9	1.7	19.4	18.9	37.1
20–40	1.1	31.0	67.9	393.0	2.9	12.9	24.9	0.7	4.4	0.9	8.8	16.9	26.0
60–80	0.1	27.3	72.6	367.5	12.9	16.0	36.3	0.8	0.5	3.6	11.5	26.3	28.6
Agriculture (AG-y)													
0–20	0.1	39.6	60.3	206.0	32.2	12.7	17.8	1.5	0.1	12.8	7.7	10.7	29.9
20–40	0.04	34.8	65.2	63.7	15.5	6.6	9.5	0.3	0.02	5.4	4.3	6.2	13.0
60–80	0.04	30.5	69.4	15.6	12.2	5.8	7.6	0.4	0.01	3.7	4.0	5.2	11.2
Pine forest (PF-i)													
0–20	0.1	9.2	90.7	227.0	11.5	12.2	9.8	1.9	0.3	1.1	11.1	8.9	23.6
20–40	0.1	16.5	83.5	162.0	11.6	5.6	7.1	1.0	0.1	1.9	4.7	6.0	13.0
70–90	0.0	7.1	92.9	103.6	3.6	2.9	4.1	0.4	0.1	0.3	2.7	3.8	5.9
Agriculture (AG-i)													
0–20	0.1	45.7	54.2	350.0	48.7	26.7	36.1	0.6	0.2	22.3	14.5	19.6	54.4
20–40	0.04	66.3	33.7	401.0	46.2	16.1	31.4	1.1	0.04	30.6	5.5	10.6	42.6
50–70	0.03	64.1	35.8	587.5	26.3	10.4	19.7	0.8	0.1	16.9	3.7	7.1	26.9
Pine forest (PF-o)													
0–20	0.4	16.3	83.3	188.3	19.0	12.9	17.6	1.7	0.8	3.1	10.8	14.6	33.3

20–40	0.2	15.5	84.3	148.7	10.3	7.4	10.4	1.5	0.2	1.6	6.2	8.8	18.2
60–80	0.1	11.5	88.4	135.6	9.6	3.3	8.0	1.1	0.1	1.1	2.9	7.1	15.7
Agriculture (AG-o)													
0–20	0.2	9.2	90.6	420.7	29.6	21.7	17.2	1.8	0.8	2.7	19.7	15.6	47.0
20–40	0.2	8.2	91.6	311.3	19.0	14.4	12.5	1.3	0.5	1.6	13.2	11.5	28.8
60–80	0.04	4.6	95.4	92.6	7.1	7.0	3.0	1.2	0.1	0.3	6.7	2.8	7.8

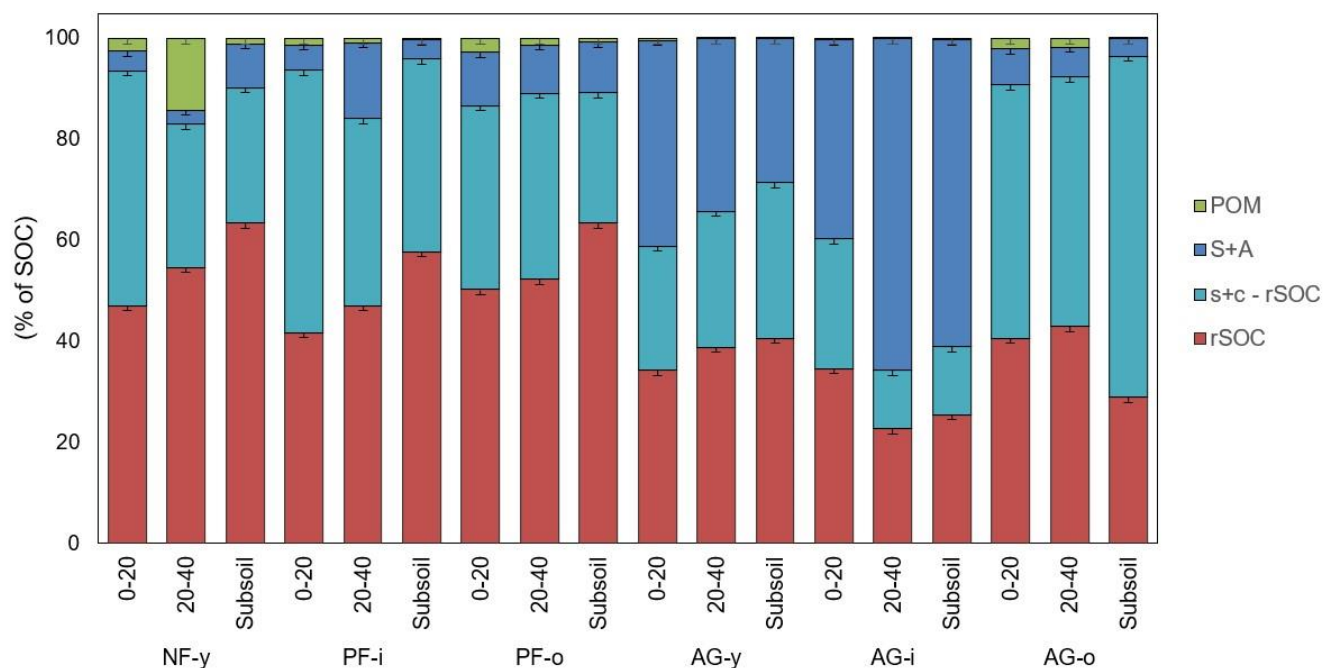


Figure 3-1 The distribution of OC over soil fractions obtained by a modified version of the Zimmerman et al. (2007) procedure for 6 sampled soil profiles at each depth of 0 – 20, 20 – 40, ± 60 – 80 cm in the Sunda Volcanic complex in West Java, Indonesia. Vertical bars indicate standard deviations for three lab-replicates (n = 3)

3.3.2 C:N ratio, amorphous aluminum and iron in the sand-aggregates (S+A) and silt-clay (s+c) fractions

The ratios of C:N at 0 – 20, 20 – 40, and ± 60 – 80 in S+A fraction ranged from 9.5 – 19.6, 9.1 – 19.8, and 7.3 – 18, respectively, similar to C:N ratios in s+c fraction, 9.3 – 15.5, 8.1 – 19.8, and 7.5 – 20.1, respectively (Table 3-3). Their mean values did not differ. The S+A C:N-ratio was generally higher in the agriculture than in the pine forest soils ($p = 0.07$). The content of Al_o at all depths varied between 1.5 to 56.6 $g\ kg^{-1}$ and 3.2 to 46.6 $g\ kg^{-1}$ in the S+A and s+c fractions, respectively, whereas Fe_o ranged from 9.6 to 34.3 $g\ kg^{-1}$ and 7.6 to 74.2 $g\ kg^{-1}$ in the S+A and s+c fractions, respectively. A much lower content of Al_o in s+c and S+A fractions in NF-y soil compared to all other soils was in line with its distinctive total elemental composition previously reported by (Anindita et al., 2022b). The mean Al_o content in S+A fraction was generally higher under agriculture ($28.9 \pm 20.8\ g\ kg^{-1}$) than pine forest ($20.9 \pm 14.6\ g\ kg^{-1}$) (though only at $p = 0.09$). Meanwhile, the Al_o content in s+c fraction was similar between agriculture and pine forest soils. The Fe_o contents in S+A and s+c fraction were generally higher under pine forest than agricultural soils, particularly at depth 20 – 40 and ± 60 – 80 cm, with no significant difference. For the primary forest, the C:N ratio of S+A fraction was slightly higher than in

s+c fraction at 0–20 cm, but slightly lower at 20–40 and ±60–80 cm depths. The Al_o and Fe_o contents in primary forest were higher in the s+c than S+A fractions at all depths.

Table 3-3 Ratio of C:N, oxalate extractable-aluminum (Al_o) and iron (Fe_o) in S+A and s+c fractions

Depth	S+A fraction			s+c fraction		
	C:N ratio	Al _o	Fe _o	C:N ratio	Al _o	Fe _o
		g kg ⁻¹			g kg ⁻¹	
Primary forest (NF-y)						
0–20	16.5	1.7	17.5	15.5	4.2	26.6
20–40	18.6	1.7	28.1	19.8	3.2	39.3
60–80	15.0	1.5	20.0	20.1	7.6	74.2
Agriculture (AG-y)						
0–20	18.7	19.9	30.1	17.0	18.6	31.9
20–40	12.1	25.7	24.0	11.1	19.3	16.5
60–80	11.0	29.4	22.1	10.6	26.5	20.5
Pine forest (PF-i)						
0–20	9.5	11.0	19.9	9.3	11.1	15.8
20–40	9.1	15.3	21.1	8.9	15.3	20.3
70–90	7.3	10.2	28.5	9.7	16.7	29.8
Agriculture (AG-i)						
0–20	19.6	44.8	11.8	11.7	44.5	13.7
20–40	19.8	53.0	11.0	15.6	45.7	10.2
50–70	18.0	56.6	9.6	16.2	46.6	7.6
Pine forest (PF-o)						
0–20	12.0	34.6	24.9	11.2	37.1	21.6
20–40	10.5	28.5	27.9	10.7	34.9	20.2
60–80	10.6	10.6	26.1	10.0	28.1	21.9
Agriculture (AG-o)						
0–20	12.6	21.7	27.4	9.4	22.0	14.0
20–40	9.5	23.1	34.3	8.1	21.6	15.3
60–80	7.5	16.1	33.5	7.5	14.5	22.7

3.3.3 Correlations between SOC fractions and selected chemical properties.

The proportion of several of the isolated SOC fractions correlated to some of the geochemical soil properties (Fig. 3-2). By considering only pine forest and agricultural soils, the SOC proportion of the S+A fraction was positively correlated with Al_o (in bulk soil as well as in the S+A fraction) and content of amorphous materials, particularly at depth of ±60–80 cm ($p < 0.05$), and C:N ratio of S+A fraction at all depths ($p < 0.05$). These soil properties were also positively correlated with the amount of OC in S+A fraction (g C kg⁻¹ soil) and OC concentration in S+A fraction (g C kg⁻¹ fraction). The SOC proportion in s+c fraction was detected to positively correlate with Fe_o s+c fraction at depth of ±60–80 cm ($p < 0.05$), but the amount of OC in s+c fraction (g C kg⁻¹ soil) and OC concentration (g C kg⁻¹ fraction) in s+c fraction correlated negatively to Fe_o s+c fraction at all depths. The proportion of rSOC in s+c fraction (i.e. rSOC / s+c x 100) correlated positively to micropores volume at 0–20 and 20–40 cm, ($r = 0.7$ and $r = 0.86$, respectively), and to SSA at 20–40 cm ($r = 0.9$) ($p < 0.05$).

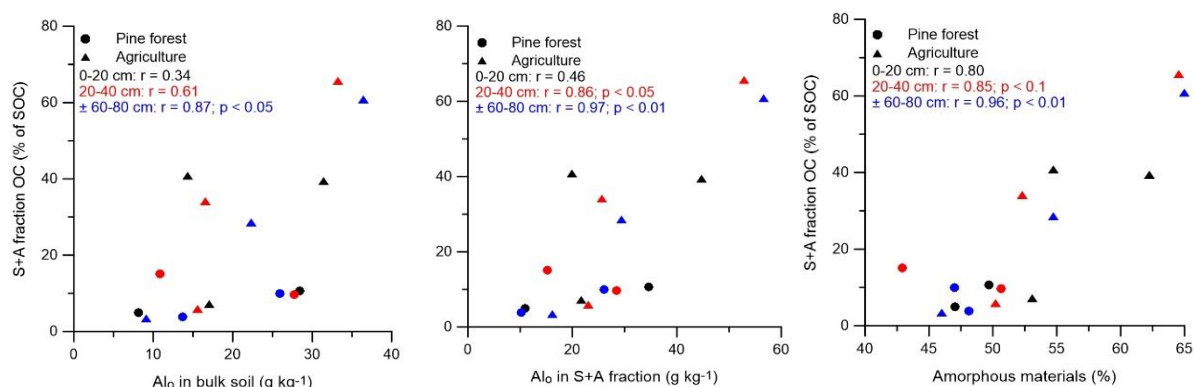


Figure 3-2 Scatter plots of the SOC proportion of the S+A fraction and the amounts of Al_o (in bulk soil and sand-aggregate fraction) and amorphous materials. Symbols and Pearson correlation coefficients are in black, red, and blue represent correlations at depths of 0 – 20, 20 – 40, and ± 60 – 80 cm, respectively. Sites under agriculture and pine forest are indicated by ▲ and ●, respectively (n per depth = 5).

3.3.4 Carbon mineralization experiment

3.3.4.1 Gross soil carbon mineralization

Across all sites, carbon mineralization (C-min) rates were highest for AG-i and AG-o and peaked already during the first day of incubation, while for the other soils rates peaked at day 3 or 5 only. After day 38, the C-min rates stabilized across time. The cumulative total CO₂-C emission and derived amount of C-mineralized (SOC + ryegrass) generally followed a sequence NF-y < AG-y < AG-i < PF-i < AG-o < PF-o. Pine forest soils displayed higher cumulative C-min than agricultural soils (p < 0.05). Overall, the 120-day cumulative C-min was 194–419 mg kg⁻¹ higher in soil with grass added than without (Fig. 3-3).

3.3.4.2 Grass C-mineralization

The C_{grass}-min rates peaked within 12 days after the start of the incubation, and they dropped thereafter to just half to one third of the initial rates. The C_{grass} mineralization rate was conspicuously high on the first day of incubation in soils AG-i and AG-o, whereas for the other soils mineralization peaked on day 5 only. From day 38 onwards, the C_{grass}-min rate had become more or less similar in all six sites. By the end of the 120-days incubations, 22 – 38% of the added ryegrass had been mineralized (Fig. 3-4). The highest cumulative C_{grass}-min was found for PF-o (389 mg kg⁻¹), followed by AG-i > AG-o ≈ PF-i ≈ AG-y > NF-y. There were no significant differences in C_{grass}-min between the sets of agricultural and pine forest soils.

3.3.4.3 Native SOC mineralization

Mineralization of SOC (C_{SOC}-min) contributed more to gross soil C mineralization than C_{grass}-min did. There were large differences in C_{SOC}-min between the 0-20 cm soil layers of the six sites. By the end of the incubation, the highest cumulative amount of SOC mineralized was found for PF-o (953 ± 13 mg kg⁻¹) while a fourfold lower amount was mineralized in case of NF-y (195 ± 17 mg kg⁻¹). Significantly

less SOC was mineralized in the agricultural soils ($517 \pm 90 \text{ mg kg}^{-1}$) than in the pine forest soils ($813 \pm 156 \text{ mg kg}^{-1}$) ($p < 0.01$). Relatively, 0.5–2.9 % of the SOC had been mineralized within the 120 days incubations (Fig. 3-4). A larger % of SOC was mineralized in the pine forest soils ($2.9\% \pm 0.1$) than in the agricultural soils ($1.2\% \pm 0.3$) ($p < 0.01$).

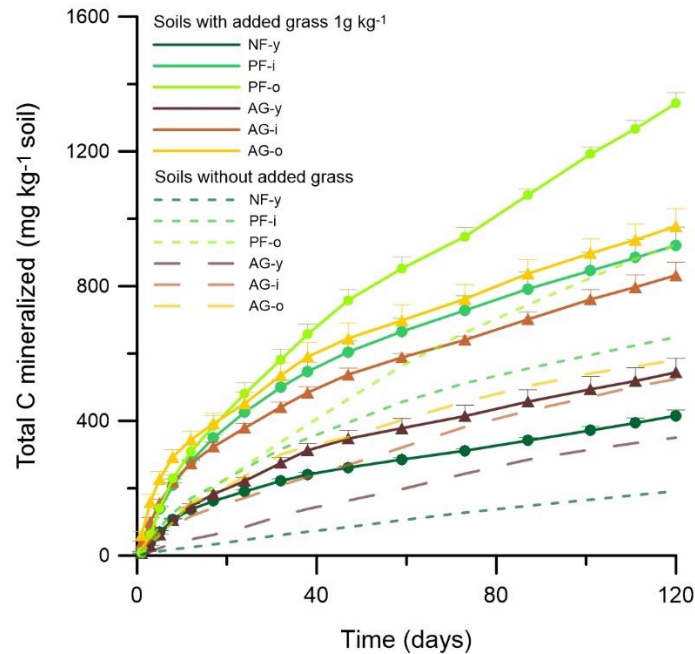


Figure 3-3 Gross cumulative amount of C mineralized in soil with and without 1 g C kg^{-1} ryegrass added. Vertical bars indicate standard deviations of three lab replicates ($n = 3$) and are presented for the grass amended soils only. Sites under forest and agriculture are indicated by ● and ▲, respectively.

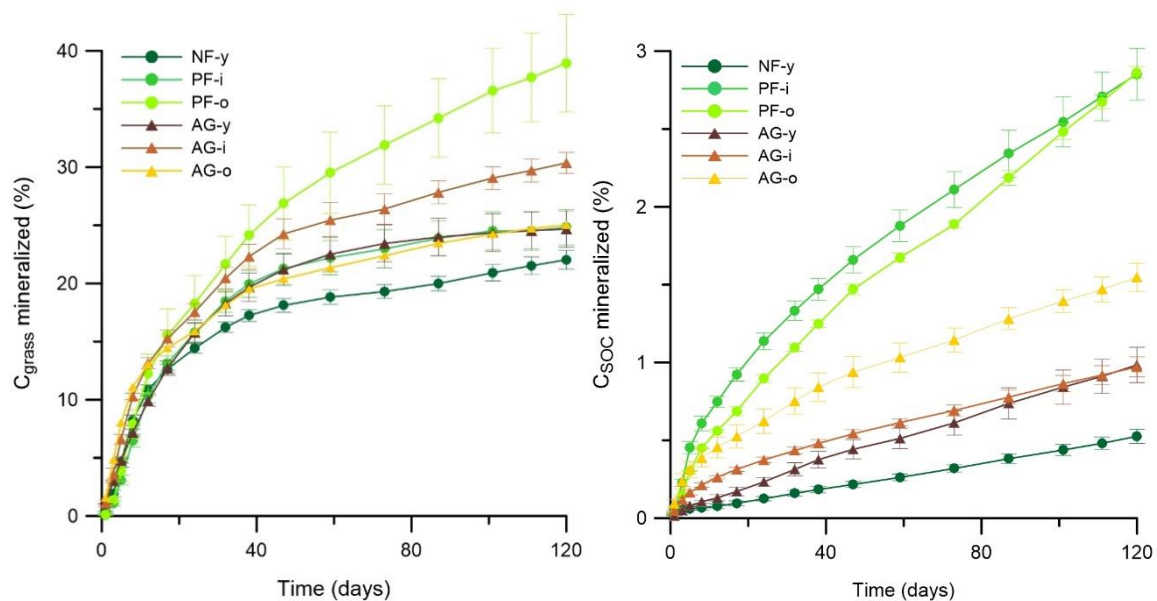


Figure 3-4 The percentage of C_{grass} (left) and C_{SOC} (right) mineralized during 120 days of incubation in soils with 1 g kg^{-1} grass or no grass added, respectively. Vertical bars indicate standard deviations of triplicate lab repetitions. Sites under forest and agriculture are indicated by ● and ▲, respectively.

Priming of native SOC mineralization was assessed by comparing $C_{\text{SOC-min}}$ between the soils with and without 1 g kg^{-1} grass added (Fig. 3-5). During the first week, grass addition tended to increase the $C_{\text{SOC-min}}$ rate in most soils, i.e. there was positive priming of native SOC. Along the 120-days experiment, however, the direction and magnitude of the net cumulative priming effect varied strongly among soils. Little or no net priming of $C_{\text{SOC-min}}$ occurred in the NF-y soil, as a result of initial positive priming until day 17 but negative priming afterwards. In the pine forest soils likewise periods of positive and negative priming alternated, with at the end of the 120-days period an alike limited net positive priming of SOC at both PF sites. Priming of SOC was diverse among the three agricultural soils. While strong positive priming throughout the 120-days period in the AG-o soil, the opposite was true for AG-y and no net priming occurred in case of AG-i. On average, the net 120-days cumulative priming of SOC in forest ($19.3 \text{ mg CO}_2\text{-C kg}^{-1} \text{ day}^{-1}$) was lower than agricultural ($31.2 \text{ mg CO}_2\text{-C kg}^{-1} \text{ day}^{-1}$) land use, but due to wide variation between replicate sites this difference proved insignificant and moreover net priming rates were not significantly different from zero.

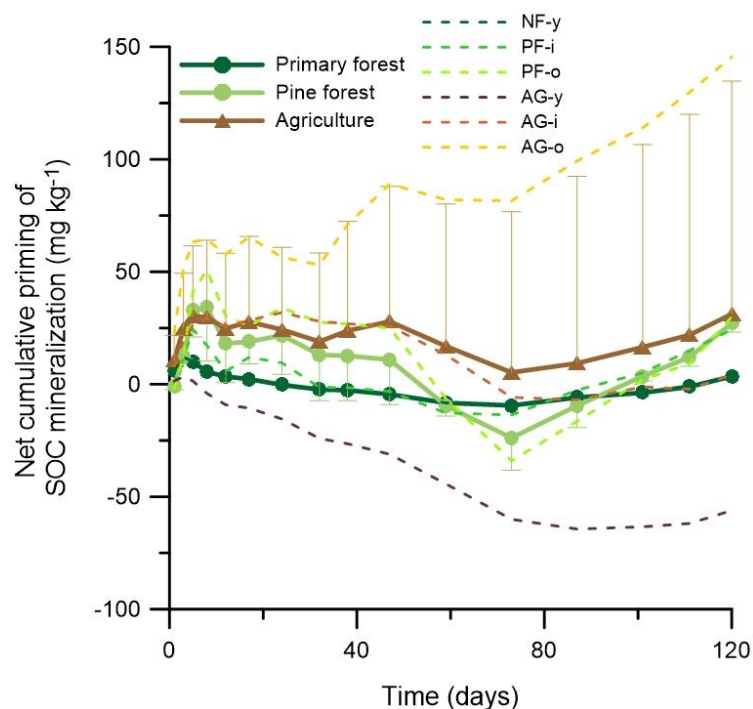


Figure 3-5 Net effect of grass addition (1 g kg^{-1}) on cumulative native SOC mineralization. Positive and negative figures denote net positive or net negative cumulative priming of SOC mineralization. Dotted lines present the temporal evolution of mean net cumulative priming effect for either primary forest, pine forest, or agricultural land use, with respectively only upper or lower error bars representing the standard deviations on the data. The dash lines represent the net cumulative priming effect at each site.

3.4 Discussion

3.4.1 Land use effects on free and aggregate protected OC

Overall, the mean portion of S+A fraction material (i.e. > 63 μm 400 J ml^{-1} ultrasonication resistant aggregates and sand particles) was more than double in the agricultural ($33 \pm 26\%$) than pine forest soils ($13 \pm 3\%$), and nearly double compared to all forest, including primary forest ($19 \pm 11\%$) (though only at $p = 0.1$, probably due to the small sample number). This indicated stronger soil aggregation and aggregate stability under agriculture. In line, a nearly fourfold share of SOC resided in the S+A fraction at all depths under agriculture ($32 \pm 25\%$) than pine forest ($9 \pm 4\%$) ($p = 0.08$), and more than fourfold than all forests ($7.7 \pm 4.3\%$). The important role of soil microaggregates for SOC storage has been displayed by numerous studies (Dungait et al., 2012; Rabbi et al., 2016; Six et al., 2002). We expected a lesser share of SOC to be occluded inside aggregates in the tilled agricultural soils, as absence of tillage results in less disruption of macroaggregates with increased formation of microaggregates and occlusion of POM (Six et al., 2000b; Zheng et al., 2018). However, tillage is not the only determinant of soil aggregate formation and breakdown as aggregate stability also depends on presence of binding agents that cluster mineral and organic particles into aggregates. Repeated addition of labile carbon via manure and compost amendments was shown to result in greater formation of macroaggregate (Du et al., 2014; Mikha and Rice, 2004; Yu et al., 2012) by increased production of microbial-derived binding agents. Manure and compost amendments to the AG sites were vast (Table 3-1), and so the enhanced addition of labile C as compared to the pine forest sites may have boosted aggregate formation with more SOC storage in the S+A fraction under agricultural land use. Next to organic binding agents, Wagai et al. (2018) also found reactive metal phases to be important binding agents in Allophanic Andisols. With high to very high levels of Al_0 (up to 4% of the soil mass), it seems very likely that amorphous to poorly crystalline Al-containing minerals would have been prominent binding agents in our set of soils. The S+A fraction contents of Al_0 were also larger in the agricultural than in the pine forest soils ($p = 0.09$). Moreover, the SOC proportion of the S+A fraction and its OC concentration (g C kg^{-1} S+A fraction) correlated positively with contents of Al_0 and the % of X-ray amorphous materials, particularly at depths of 20 – 40 and \pm 60 – 80 cm. This indicates that higher levels of Al_0 under agriculture than pine forest would have enhanced aggregation, and in doing so occluded a larger share of SOC inside these aggregates. When comparing the agricultural sites and all forest sites, including primary forest, likewise differences existed. In other words, the results were not biased by the deviating mineralogical composition and texture of the NF site. Notwithstanding, when considering only pine forest and agricultural sites, the S+A SOC proportion sole best correlated to the S+A Al_0 content, particularly at depths of 20 – 40 and \pm 60 – 80 cm ($r > 0.80$; $p < 0.05$), strengthening the view that to a substantial extent enhanced Al_0 content under agriculture promoted storage of SOC inside stable aggregates. By expanding the Zimmerman et al. (2007) fractionation procedure with a stronger (400 J ml^{-1}) ultrasonic dispersion step, we attempted to further isolate s+c associated OC from POM contained in the S+A fraction. The intermediate C:N ratio of the final 400 J ml^{-1} S+A fraction at all depths were around 13 ± 4.2 , indicated that it still contained likely mineral associated OM next to POM, complicating further interpretation of mechanisms for S+A SOC storage in the agricultural sites. Nevertheless, the higher (but non-significantly) S+A fraction C:N ratio of the agriculture vs. pine forest and all forests sites demonstrates that at least to some extent enhanced SOC storage in aggregates under agricultural land-use resulted from extra occluded POM

storage. Particularly, for the 0 – 20 cm layer the contrast in the S+A C:N ratio (agriculture: 17.0 vs. pine forest: 11) supports this view. Lastly, less free POM was found in the agricultural than forest soils, likely as a logical consequence of more POM occlusion under agriculture. However, we cannot exclude that also a better degradability of crop-derived residues vs. pine or native forest litter co-explains these trends. It is well established that litter rich in cutin, waxes and lignin such as derived from pine forests is less degradable than plant litter richer in carbohydrates and organic nitrogen like most crop residues (Berg and McClaugherty, 2003).

3.4.2 Effect of land use on SOC in the silt and clay fraction

Interaction of SOC with silt and clay provides long-term stabilization to SOC against decomposition and therefore forms a key mechanism for SOC sequestration (De Clercq et al., 2015). SOC sorbs to phyllosilicate clays, Al-, Fe- and Mn-oxides, poorly crystalline minerals, as well as polyvalent cations that form a bridge between minerals and organic constituents (Blanco-Canqui and Lal, 2004). However, for our soils, we found that despite higher concentrations of Al_o under agriculture, a lesser share of the SOC was present in the s+c fraction (as % of SOC) compared to the pine forest soils (though only at $p = 0.08$). Thus, association of OC with Al_o -containing minerals could not explain the higher SOC proportion of OC in s+c under pine forest. As the amount of s+c OC (in $g\ C\ kg^{-1}$ soil) was in fact slightly higher in the agricultural than pine forest soils. It appears that a lower s+c SOC contribution in the agricultural soils was instead simply mirroring trends in the S+A fraction. A positive correlation between the s+c SOC proportion and Fe_o in s+c at $\pm 60 - 80$ cm ($r = 0.93$; $p < 0.05$) could indicate that association with poorly crystalline Fe stabilizes OC in the s+c fraction at this depth. However, as OC concentration ($g\ kg^{-1}$ fraction) and OC content ($g\ kg^{-1}$ soil) was slightly higher in the agriculture than pine forest soils at all depths, and Fe_o in s+c fraction correlated negatively with OC concentration ($g\ kg^{-1}$ fraction) and OC content ($g\ kg^{-1}$ soil) of s+c fraction, such land-use control on s+c Fe_o associated SOC seems unlikely. On the other hand, the higher SOC content ($g\ C\ kg^{-1}$ soil) in s+c fraction of NF-y than other soils, particularly at depth of $\pm 60 - 80$ cm, might be due to the differences in mineralogy. At this depth, the amorphous Fe content (Fe_o and Fe_h) in NF-y was very high compared to the other soils. In the Zimmerman et al. (2007) fractionation procedure, the s+c fraction was subdivided into oxidizable and resistant parts, expected to coincide roughly with SOC stabilized by mineral-association as opposed to its own biochemical inertness, respectively. Negative correlations existed between the share of s+c OC (% of s+c OC) that was oxidizable by 6% NaOCl (i.e. s+c - rSOC) with the contents of Al_o , the bulk soil of SSA, and micropores volume (Fig. 3-6). The correlation with these properties were strong, especially in subsoils (Fig. 3-6). These correlations suggest that the association of SOC with short-range order Al (hydr)oxides has been found to limit oxidation of SOC by 6% of NaOCl (Mikutta et al., 2006). It appears that geochemical properties influence the degree of mineral association of OC and its content in these Andosols. However, neither the mean of chemical inertness of the s+c OC (agriculture: 53% of s+c vs. pine forest: 59% of s+c), nor the s+c Al_o , bulk soil SSA, and micropore volume differed between both land uses. This outcome at least contradicts that more s+c OC would accumulate under pine forest because of a more biochemical inertness of the OC inputs compared to agriculture.

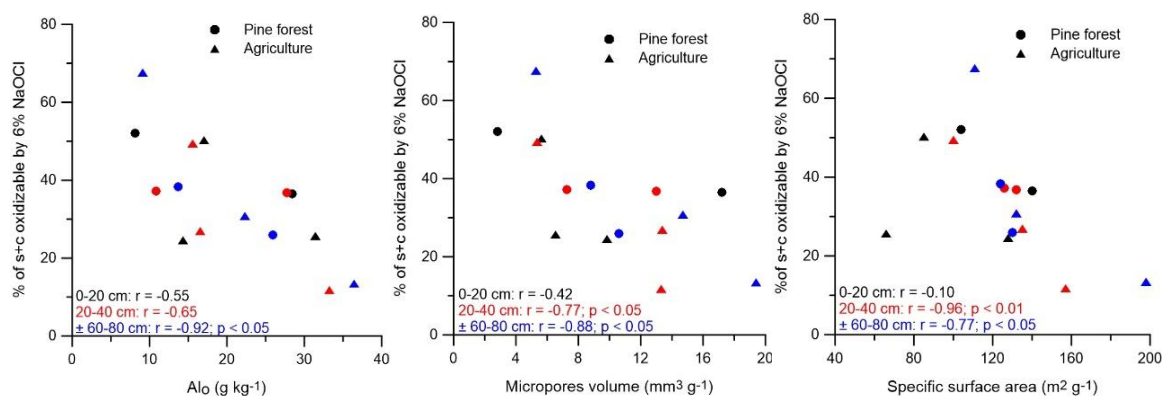


Figure 3-6 Relation between the proportion of SOC that was oxidizable by 6% NaOCl in the pine forest and agricultural soils with the soil Al_o, micropores volume, and soil specific surface area (at each depth n = 5). Sites under agriculture and pine forest are indicated by ▲ and ●, respectively. Symbols and Pearson correlation coefficients in black, red, and blue represent correlations at depths of 0 – 20, 20 – 40, and ± 60 – 80 cm, respectively (n per depth = 5)

3.4.3 Land use effects on native SOC degradability

The percentage of SOC mineralized after 120 days of incubation was less than half in the agricultural soils (1.2 %) than in the pine forest soils (2.9 %) ($p < 0.01$). This result was rather unexpected given the lower soil pH by 0.8 under pine forest, as acidic conditions are well known to retard SOC decomposition of SOC (Högberg et al., 2007; Malik et al., 2018) in line with Anda and Dahlgren (2020). To understand the apparent relative stabilization of SOC in the agricultural soils, we again consider the distribution of SOC across soil fractions. We (Anindita et al., 2022b) previously hypothesized that the higher Al_o content in the agricultural soils (21.8 g kg⁻¹ on average) compared to the pine forest soils (19.1 g kg⁻¹) would partially explain the relatively elevated SOC stocks under agriculture for our study area due to enhanced organo–mineral association. Basile-Doelsch et al. (2005) likewise found that volcanic ash soil horizons containing much poorly crystalline materials (proto–imogolite and proto–imogolite allophane). These materials store large amounts of organic matter which turns over very slowly. But as no significant negative correlations existed between the amount or proportion of SOC mineralized and Al_o content, this hypothesis was not confirmed. As mentioned above, we did find a higher proportion of SOC (%) to be present in the rSOC fraction under forest but its content (g kg⁻¹ soil) was not higher than under agricultural land use and again no correlation existed with SOC mineralization. Mikutta et al. (2006) indeed demonstrated that a larger chemical recalcitrance of SOC does not really translate into a larger biological stability. Once more, it appears that the larger SOC proportion of rSOC seems to simply result from less accumulation of SOC in the S+A fraction under pine forest.

The proportion and concentration of the S+A fraction OC were higher under agriculture, so enhanced soil aggregation and occlusion of SOC might have significantly physically protected SOC against microbially mediated decomposition compared to pine forest land use. A study of Andosols in Colombia by Gijsman and Sanz (1998) also reported that aggregation holds considerable control on SOC decomposability as these authors observed a significant increase of carbon mineralization after crushing large and small macroaggregates (> 53 μm). Indeed, we found that the amount of OC (g C kg⁻¹

¹ soil) in the S+A fraction negatively correlated to the percentage of C_{SOC} mineralized for the set of soils with agricultural and pine forest land use ($r = -0.78$; $p < 0.01$). It then appears that enhanced soil aggregation and occlusion of SOC under agricultural land use in part limited degradability of SOC, rather than enhanced association of SOC with soil minerals, including poorly crystalline or amorphous Al-containing minerals. As argued in 4.2, we can add to this that formation of amorphous materials and Al_o in the agricultural soils most likely promoted soil aggregation. Hence, we hypothesize that enhanced pedogenesis forms a relevant indirect mechanism via which conversion to agricultural land use impacts the SOC balance of these relatively young tropical volcanic soils. However, since large amounts of exogenous OM are annually being applied to the investigated agricultural fields in this study (Table 3-1), we cannot unequivocally exclude that these instead explain the high SOC stocks and contribution of aggregate associated OC here and more observations on an expanded set of sites will be required to test this hypothesis.

3.4.4 Land use effects of exogenous organic matter decomposition and net priming of SOC

In contrast to native SOC mineralization, added grass C mineralization did not differ between forest and agricultural soils. Therefore, apparently protection of ryegrass OC either by mineral association or occlusion inside aggregates must have been similar between both land uses and, in any case, did not impact its degradability in soil. Laboratory incubations with disturbed soils do not necessarily adequately reproduce field conditions in terms of soil structure, microclimate, and food webs. For instance, only 20 – 40% of ryegrass degraded after 120-days, somewhat less than usually observed in laboratory incubations; Mendoza et al. (2022) found that 30 – 50% of the exact same ryegrass as used here had decomposition after 90 days. Nevertheless, in contrast to Mendoza et al. (2022) ryegrass mineralization was indicated to steadily continue beyond the incubation experiment duration. Perhaps the microbial community in these tropical Andosols require time to adapt to degrading the applied substrate that originated from a grassland field in Belgium, i.e. the temperate zone. The observed similar degradability of ryegrass-C does not suggest a likewise enhanced storage of freshly added OM like for native SOC under agriculture than under forest. Possibly, such impact only emerges on the longer term when the added OM has been subject to sufficient diminution into smaller POM that could be occluded in microaggregates. Six et al. (2002) summarized that particularly 50 – 250 μm scaled microaggregates grant sizable physical protection to POM, while the macroaggregate ($> 250 \mu m$) structure exerts little control on POM decomposability. Adding ryegrass to the 0 – 20 cm soils initially seemed to impact mineralization of native SOC with a general positive priming effect in first week of incubation, in line with many other studies, e.g. Liu et al. (2017). Thereafter, however, in four of the six soils net negative priming countered this initial stimulation of SOC mineralization. Such adverse impact of adding fresh OM on SOC mineralization could be due to a preferential utilization of the added substrate by microorganisms (Derrien et al., 2014). Regardless, the net result was that after 120 days SOC mineralization was not significantly stimulated (on average by 1.6 %). There was also no land use effect on the net priming of SOC after 120 days. Hence, in spite of differences in SOC quality under both land uses, as inferred from different SOC proportions of S+A and free POM, no differential stimulation of SOC mineralization by addition of a relatively labile plant-C substrate existed between agricultural or forest land use. These observations imply that no adverse effect is to be expected of

the addition of generally relatively labile C (above ground crop residues, animal manure) on stability of the native SOC present under agricultural land use.

3.5 Conclusions

Following the fractionation of SOC by Zimmermann et al., (2007), the silt and clay associated OC forms the dominant SOC pool in tropical volcanic soils in Indonesia, regardless of land-use. However, land-use strongly impacts SOC contained within 400 J m⁻¹ ultrasonic dispersion resistant soil aggregates as its contribution to SOC rose from 9% of SOC in pine forest to as much as 32% of SOC several decades after conversion to agricultural use, with alongside also more OC stored in this fraction. The S+A SOC proportion was positively related to Al_o and the amount of amorphous materials (%). Our study thus indicates the presence of Al_o in agricultural land use promoted soil aggregation and physical occlusion of OC compared to pine forest land use. A negative correlation between relative decomposability of the SOC and the portion of SOC that is physically occluded further suggests that enhanced soil aggregation under cropland effectively stabilizes part of the SOC compared to pine forest land use. Contrary to our hypothesis, however, we found no proof that stimulated formation of Al_o and amorphous minerals would have increased association of SOC with soil minerals under agriculture. Based on the present study, we postulate that the presence of amorphous materials and Al_o under agriculture with high OM inputs promoted development of stable soil aggregates and OC occlusion therein and this would in part counter otherwise expected losses of SOC compared to primary and secondary forest. However, the contribution of large OM inputs vs. land-use conversion per sé could not be elucidated here and this will require study of other tropical Andosol forest-agricultural land use pairs with detailed inventory of OC inputs. To the least, our study points at the overall need to account for potential indirect land use effects on stability of SOC via its control on pedogenesis. Especially, this is so for pedoclimatic combinations where weathering can be very fast, like in tropical Andosols that have only relatively recently been cultivated.

Authors contributions

Sastrika Anindita performed the laboratory experiment, data analyses, interpretation of the results, and writing of the manuscript. Steven Sleutel co-wrote and reviewed the manuscript and supervised the research. Peter Finke reviewed the paper and supervised the research.

Acknowledgement

This research is supported and funded by Indonesia Endowment Fund for Education (LPDP).

CHAPTER 4

SIMULATING SOIL ORGANIC CARBON STOCK AS AFFECTED BY LAND USE AND CLIMATE CHANGE ON VOLCANIC SOILS IN INDONESIA

Based on:

Anindita, S., Sleutel, S., Finke, P. Simulating soil organic carbon stock as affected by land use and climate change on volcanic soils in Indonesia. This manuscript is submitted to the journal of Geoderma Regional and currently under review.

Abstract

We assessed long-term trends in soil organic carbon (SOC) in volcanic soils with a process-based soil genesis model, SoilGen2.25. The relation between soil geochemistry and SOC was applied in a model context by using found influential soil properties to modify the decay rates of SOC pools. We used data from Indonesian sites with different land use (tropical primary forest, secondary pine forest, and agricultural land) and calibrated major soil processes in volcanic soils, viz. clay migration and weathering of primary minerals. The model evaluated the decay rates of SOC pools using three calibration approaches: (i) a site-specific calibration, (ii) a generic calibration, and (iii) a generic calibration modified by geochemical proxy. The best calibration for each approach was then used to estimate the future of SOC under different climate projection scenarios, viz. representative concentration pathways (RCP) 2.6 and 8.5. SoilGen2.25 model was generally sensitive to the change of selected soil process parameters. A four-pool SOC model (Roth-C) with site-specific decay rates best reproduced total SOC with percentage difference between measured and simulated SOC between 1 – 10%. Application of a geochemical proxy to modify the generic rate calibration also improved, relative to a generic calibration, the simulation quality of the included HUM and total SOC in most study site. In forest soils, global warming (i.e. RCP 8.5) did not affect SOC stocks, while agricultural soil showed higher susceptibility, with a 3 – 5% reduced SOC stock compared to the RCP 2.6 scenario. Projective scenarios based on the three calibration scenarios highlighted the importance of the calibration method on the accuracy of SOC projection.

Keywords: soil organic carbon (SOC), SoilGen model, soil geochemistry, global warming, volcanic soil

4.1 Introduction

Soil organic carbon (SOC) is an important component of biogeochemical cycling and a major component of the global carbon budget (Eswaran et al., 1999, 2000). The organic carbon (OC) retained in soils is more than the carbon in global vegetation and atmosphere combined (Lehman and Kleber, 2015). However, climate change such as the elevation of global temperature and the change of precipitation may affect SOC storage (Pendall et al., 2008) due to their influence on the amount of organic matter supply and rate of decomposition (Soleimani et al., 2017). Studies found variable responses to climate change on SOC stock (Lu et al., 2013; Riggers et al., 2021; Yigini and Panagos, 2016; Zhao et al., 2021) whereas few studies emphasized that the bulk SOC fraction can persist via various mechanisms and evaluating the response of SOC fraction to this global change is equally important (Poeplau et al., 2017; Rocci et al., 2021). Understanding the SOC dynamics and the response of SOC to climate change is necessary to help mitigate the effect of human-induced climate change.

The dynamics of SOC are controlled by several factors, such as parent materials (Mayes et al., 2014) including soil geochemical composition (Doetterl et al., 2018; Lawrence et al., 2015), climate (Gray et al., 2016), topography (Araujo et al., 2017), organisms (Jobbágy and Jackson, 2000; Poeplau and Don, 2015), and pedogenic time (Dümig et al., 2011). These factors interactively affect the amount of SOC stored in ecosystems. To estimate the change of SOC stock over time as the result of these factors process-based soil C models could be employed. However, while several of such models account for the impact of environmental and fixed soil factors onto SOC dynamics, simulation of changes in soil geochemistry or soil profile development and feedbacks on SOC stocks are not possible. Especially in contexts where appreciable soil development is to be expected such feedbacks would need to be incorporated to properly simulate SOC stock evolution. For instance, soil development in young tropical volcanic soils proceeds at such a fast pace that it may be needed to account for changing soil specific surface area over time when projecting the temporal evolution of SOC stocks. The SoilGen2 model (Finke, 2012) considers the physical, geochemical, and biological processes, including the external factors, such as climate, land use, and land management as boundary conditions (Opolot et al., 2015) to simulate soil genesis. In addition, this model has been calibrated for carbon cycling processes (Finke et al., 2019; Yu et al., 2013) and was tested for the impact of human activities, e.g. ploughing and fertilizer (Keyvanshokouhi et al., 2016), thus it should be suitable for simulation of SOC projection.

Volcanic soils are characterized by their ability to retain SOC (Nanzyo et al., 1993a). The retention of SOC in these soils occurs through several mechanisms such as physical protection of OC within aggregates, physiochemical sorption of organic carbon on minerals, and chemical interaction between soil minerals and organic matter (Matus et al., 2014). Soil geochemical composition, e.g. clay content, mineralogy, the content of pedogenic Si, Al, and Fe, total reserve of bases and reactive surface area were found to influence the amount of SOC (Doetterl et al., 2015) and to affect the composition of soil microorganisms as well as the aboveground net primary productivity (Doetterl et al., 2018). To better estimate the amount and distribution of SOC over time, the effect of soil geochemical composition as the result of mineral weathering on SOC degradation needs to be included and

converted in a model context. Finke et al. (2019) successfully reproduced the effect of geochemistry and mineralogy on SOC decomposition rate in a modelling study on the same site as Doetterl et al. (2018)'s study. They also evaluated that more precise information (i.e. site-specific calibration) produced better quality of model-estimated SOC pools than less precise information (i.e. generic calibration).

The studies by Doetterl et al. (2018) and Finke et al. (2019) raise a number of questions: Are decomposition rates, in a modelling context, in other parent materials also a function of geochemical or mineralogical properties? Is the difference between an accurate assessment of these rates (site-specific calibration) and a less accurate assessment (generic calibration) relevant in a projection context? i.e. does the information level on decomposition rates influence the outcomes and comparison of future climate scenarios? The information level is directly related to the effort of a projective modelling study: site-specific calibration is much more labour- and data-intensive than generic calibration or correction of generic decay rates with geochemical proxies. Our objective is to evaluate these questions in the context of volcanic ash soils in Java (Anindita et al., 2022b), using the SoilGen2.25 model. This leads to the following detailed objectives:

1. To investigate the effect of soil geochemical composition on SOC decomposition as simulated by the SoilGen2.25 model for volcanic ash soils. Hereto, we calibrate the major soil forming processes, viz. clay migration and weathering of primary minerals, in volcanic soils.
2. To evaluate if a site-specific calibration, a generic calibration, and a generic calibration modified by rate corrections with geochemical proxies lead to similar accuracy of SOC-decay rates. We did a model calibration, comparing the laboratory assessments of SOC-pools as identified by Zimmermann et al. (2007) after conversion to RothC-pools with the simulated SOC. Calibration is done (i) at 6 sites individually, (ii) at 6 sites simultaneously, and (iii) by correcting the found rates in (ii) with geochemical proxies. The most informative proxy is identified by relating the rates found in (i) with measured geochemical proxies, as in Finke et al. (2019).
3. To forecast the change of SOC-pools under different climate projection scenarios while comparing the 3 calibration methods. Purpose of this comparison is to find if the available information impacts the conclusions of a projected climate scenario.

4.2 Materials and methods

4.2.1 Study area

The study area was close to Mount Tangkuban Perahu and Burangrang which are part of the Sunda Volcanic complex in West Java, Indonesia (Fig. 1-2). The area has a tropical monsoon climate (Am) according to Köppen climate classification (Köppen, 1936) with mean annual temperature and precipitation ranging from 19 – 21°C and 2000 – 3000 mm per year, respectively. Six sites representing the dominant land uses in these areas were selected, namely primary forest (NF-y), pine forest (PF-i, PF-o), and agriculture (AG-y, AG-i, AG-o) (Fig. 1-2). The soils are all derived from basaltic-andesitic (ash) tuff originated from Holocene to Late Pleistocene activity (BBSDLP, 2017; Dam et al., 1996), but previous research found recent volcanic admixtures at site NF-y, concluding that this site has different parent materials (Anindita et al., 2022b). The soil ages are approximately between 8000 – 10000 years (Chartres and Van Reuler, 1985; Utami et al., 2019), except NF-y which was rejuvenated by recent

volcanic ash. The study soils are classified as Cambisols (NF-y, PF-i) and Andosols (AG-y, AG-i, PF-o, AG-o) (IUSS, 2015). The sites were situated on slopes around $\pm 17^\circ$. At each site, soil samples were taken at depth 0 – 20, 20 – 40, and ± 60 – 80 cm. Land use history and land management of these sites are described in Anindita et al. (2022b).

4.2.2 SoilGen model

The SoilGen model (Finke, 2012; Finke and Hutson, 2008) is a pedon scale model that simulates the vertical change of soil properties as a result of pedogenic processes and external factors such as climate and vegetation over the millennium time scale. According to a review by Samouëlian et al. (2012), the SoilGen model (Finke, 2012; Finke and Hutson, 2008) is one of the more complete soil evolution models. The model simulates the interacting soil formation processes, i.e. biological, geochemical, and physical processes, by considering soil formation factors (climate, organisms, relief, parent material, time). Major soil processes, such as clay migration, physical and chemical weathering, chemical equilibria, erosion, sedimentation, carbon cycling, bioturbation, and the impact of human activity, e.g. ploughing and fertilizing are simulated and have been tested in SoilGen (Finke et al., 2019, 2015; Keyvanshokouhi et al., 2016; Opolot and Finke, 2015; Ranathunga et al., 2022; Yu et al., 2013). The simulation time steps in SoilGen vary depending on simulated processes, e.g. the simulations of water and solutes flows are every second to hours, the physical weathering and heat flow is every hour, carbon cycling is every day, while erosion, deposition, and sedimentation is every year. Thus, soil properties are produced from the interactions between solid (mineral and organic matter), liquid, and air phases. Detailed model description and model input can be referred to (Finke, 2012; Finke and Hutson, 2008; Opolot et al., 2015). Below we summarize several soil processes simulated in the SoilGen model.

4.2.2.1 Water, solute, and heat transfer

In SoilGen, the flows of heat, water and solutes through the soil profile are simulated following the scheme of the LEACHC model (Hutson and Wagenet, 1995). Richards' equation is used to calculate unsaturated water flow, the heat flow equation is applied to simulate the distribution of heat and temperature in the soil profile, and the convection-dispersion equation is used to describe transfer of solutes (Finke and Hutson, 2008). The diffusive flow of CO₂ is also added in SoilGen2 (Finke and Hutson, 2008).

4.2.2.2 Clay migration process

Clay migration is the process that leaches clay from the topsoil to a deeper depth. This process is defined by detachment, dispersion, transportation, and filtering processes. The clay migration process is initiated by splash detachment at the soil surface due to raindrops and carries part of the particles in the topsoil in the transportable state. The splash detachment process is simulated following Jarvis et al. (1999) but modified by (Finke, 2012) to include the effect of humus layer or vegetation cover on splash detachment and the effect of bioturbation on distribution of clay. Furthermore, clay dispersion and flocculation may occur in any soil compartment, depending on salt concentration. The mass balance of dispersible particles at the surface layer is estimated from (Eq. 4-1)

$$\frac{dA_s}{dt} = -D + P \quad (\text{Eq. 4-1})$$

where A_s is the mass dispersible particles at the soil surface (g m^{-2}), D is the splash detachment rate ($\text{g m}^{-2} \text{h}^{-1}$), and P is the replenishment rate ($\text{g m}^{-2} \text{h}^{-1}$). To calculate the mass balance, the dispersible clay in the topsoil compartment (5 cm) is calculated. The maximal % of dispersible clay (DC_{max}) is estimated based on the regression equation of Brubaker et al. (1992), which consider cation exchange capacity, organic carbon content, and clay content. The splash detachment rate (D) in each rainfall event and replenishment rate (P) are calculated using Eq. 4-2 and 4-3.

$$D = k_d * E * R * (1 - sc) * DC_s \quad (\text{Eq. 4-2})$$

$$P = k_r * \left(1 - \frac{DC_s}{DC_{max}}\right) \quad (\text{Eq. 4-3})$$

Where k_d represents the soil detachability coefficient (g J^{-1}), R is rainfall intensity (mm h^{-1}), sc (-) is the proportion of the soil covered by ground vegetation or the humus profile, E is kinetic energy of the rainfall calculated from the revised universal soil loss equation (Brown and Foster, 1986). The parameter DC_s represents the amount of readily available dispersible particles (g g^{-1} soil) at the surface with the initial value equal to DC_{max} , and k_r is the replenishment rate coefficient ($\text{g m}^{-2} \text{h}^{-1}$). Furthermore, the transportable dispersed clay follows the convection-dispersion equation with modification to include the filtering process.

$$fDC = \left\{1 - \left(\frac{SC}{CSC}\right)\right\} * \theta_{macro} * fVC \quad (\text{Eq. 4-4})$$

where the amount of clay in the transportable dispersed state (fDC) is a function of total electrolyte concentration (SC ; $\text{mmol}_c \text{dm}^{-3}$ water) and critical salt concentration (CSC ; $\text{mmol}_c \text{dm}^{-3}$ water) at which soil clay mixture stays flocculated. The θ_{macro} is the volumetric water fraction ($\text{m}^3 \text{m}^{-3}$) in macropores estimated from the water retention curve at pressure head h (hPa) near saturation, and fVC is the fraction of soil volume taken by clay. Additionally, the filtering process is added to the SoilGen model. It is the sink term in the model to estimate the amount of clay that is not transported, e.g. due to surface roughness or entrapment in small pores at a certain point. The removal of particles from soil water transport by filtering is calculated following the approach by Jarvis et al. (1999)

$$F = f_{ref} * v_{ref}^n * v^{1-n} * c * \theta \quad (\text{Eq. 4-5})$$

where the reference filter coefficient (f_{ref} ; m^{-1}) and the pore water velocity (v_{ref} ; m h^{-1}) use the values of 2 m^{-1} and 0.1 m h^{-1} , respectively taken from (Jarvis et al., 1999). Furthermore, v is the current pore water velocity. The parameters n and c represent an empirical exponent and the particle concentration (g m^{-3} water), respectively. In SoilGen, c is a vector containing the dispersible and transportable clay calculated using Eq. 4-4.

4.2.2.3 Chemical weathering of primary minerals

Weathering of primary minerals and atmospheric inputs provides the main source of cations in natural, non-fertilized soils. In the chemical weathering processes, the model simulates the dissolution kinetics of some predefined minerals, such as albite, anorthite, augite, biotite, chlorite, fayalite, forsterite, hornblende, illite, muscovite, k-feldspar, and quartz. The dissolution of two user-defined extra minerals can be simulated as well. SoilGen2 model calculates the dissolution rate of each mineral, assuming far from equilibrium conditions, as a function of pH (Brantley, 2008):

$$r_k = k_H a_{H^+}^n + k_{H_2O} + k_{OH} a_{OH^-}^m \quad (\text{Eq. 4-6})$$

where r_k is the dissolution rate of a given mineral and k_H and k_{OH} are mineral dissolution constants at acidic and basic conditions, respectively. The a_{H^+} and a_{OH^-} are the activities of H^+ and OH^- , respectively, and superscript n and m indicate the reaction order. k_{H_2O} is a parameter describing the dissolution rate at neutral pH and was considered equal to zero here (Brantley, 2003). The dissolution reactions, enthalpies of the reaction and equilibrium constant of these minerals are based on values reported in PHREEQC.dat database (Parkhurst and Appelo, 1999) and other literature (e.g. Godd ris et al., 2006). The dissolution of primary minerals is the major source of cations in non-agricultural soils, and the amounts of primary minerals (cations pools) decrease over time as weathering continues. The cation release $r_{i,k}$ ($\text{mol m}^{-2} \text{s}^{-1}$) from k minerals is computed as below

$$r_{i,k} = \sum_{k=1}^N A_k v_{i,k} r_k m_k T \quad (\text{Eq. 4-7})$$

where A_k ($\text{m}^2 \text{mol}^{-1}$) is the reactive surface area of the k^{th} mineral, $v_{i,k}$ (-) is the stoichiometric number of the i^{th} element in mineral k , r_k ($\text{mol m}^{-2} \text{s}^{-1}$) is the dissolution rate of the k^{th} mineral ($\text{mol m}^{-3} \text{soil}$), m_k is the amount of the k^{th} mineral ($\text{mol m}^{-3} \text{soil}$) in the parent material, and T (m) is the thickness of soil compartment. Currently, formation of secondary minerals is not simulated in SoilGen (far-from-equilibrium condition, which is a reasonable assumption for most leaching climates, but perhaps less so in volcanic ash soils).

4.2.2.4 Vegetation, carbon cycling and plant uptake processes

The interaction between the vegetation and the soil in SoilGen occur through annual litter input, carbon cycling, and ion uptake. The model distinguishes four vegetation types: grass or scrub, agriculture, deciduous, and coniferous wood, characterized by maximum rooting density, cation uptake, and parameters related to soil organic carbon cycling, e.g. partitioning of plant litter to above and below ground. The uptake of cations (Al, Ca, Mg, Na, K) by vegetation is assumed to occur via transpiration stream by preferential uptake to reflect the relative fractions of those elements measured in the plant. Relative concentrations of those elements in four vegetation types has been documented in a study by Finke (2012). In addition, the amount of fertilizer as well as the cations content in fertilizer can be inputted into the model.

The carbon cycling follows the concepts and pools of the RothC26.3 model (Coleman and Jenkinson, 1999). Five SOC pools are simulated in the SoilGen model, viz. resistant plant material (RPM),

decomposable plant material (DPM), humified organic matter (HUM), and microbial biomass (BIO). These pools degrade according to first-order kinetics with specific decay rate constants modified by soil moisture and temperature in each soil compartment to calculate the loss of SOC from each SOC pool:

$$loss = Y * (1 - e^{-x1*x2*k_p*t}) \quad (\text{Eq. 4-8})$$

where Y is the pool size (RPM, DPM, BIO, HUM) at the start of the daily time step for the C-cycle sub-model ($\text{Mg ha}^{-1} \text{y}^{-1}$), k_p is the average rate constant (y^{-1}) derived for each pool p by calibration, $x1$ is a dynamic decay rate modifier for the combined effect of moisture, soil cover and temperature, $x2$ is additional geochemical rate modifier representing the physico-chemical protection, and t is the period of decay (1/365 year). The inert organic matter (IOM) pool is inactive (non-decaying) and present from the start of the simulation period and invariable during the period of simulation. The incoming litter is split by a ratio of DPM/RPM into RPM and DPM pools, and both decay at rates k_{RPM} and k_{DPM} . The resulting products from RPM and DPM decay are divided using the clay content and fixed BIO/HUM ratio into HUM, BIO, and mineralized CO_2 with rates k_{HUM} and k_{BIO} .

4.2.2.5 Soil phases redistribution processes

Besides the clay migration process, SoilGen also considers some soil processes that influence the distribution of soil phases (solid and liquid) in the soil profile, such as bioturbation, tillage, erosion, sedimentation, dissolution and precipitation of calcite and gypsum. Bioturbation is described as the mixing of soils caused by meso and macro-fauna. The input mass fraction is used to vertically mix and distribute soil masses to the bioturbated soil compartments. The effect of soil tillage is also implemented in SoilGen, where the mass fraction involved in the mixing process over the ploughing depth can be adjusted depending on tillage intensity. Erosion and sedimentation processes are also implemented as event at the upper boundary by removing and adding soil layers.

4.2.3 Input data

For the SoilGen model, the input data consist of initial and boundary conditions representing major soil-forming factors (climate, organisms, relief, parent materials) (Table A4-1 to A4-4, Fig. A4-1 in Appendix 4):

- Climate data time series, viz. precipitation, potential evapotranspiration, and temperature were derived from the LOVECLIM climate model (Goosse et al., 2010). The monthly cumulative precipitation and evaporation were corrected for bias with the ratio between observed and simulated values in the period 1980-2019, while the monthly average temperature was corrected with the difference between observed and simulated values from 1980 till 2019. Later, bias-corrected temperature, precipitation, and potential evapotranspiration data were downscaled to local-scale climate data using either a difference or a ratio correction based on local temperature, precipitation, and potential evapotranspiration maps to reflect the differences between sites before input to SoilGen.
- The initial parent materials are defined from the dominant crystalline minerals and amorphous materials present in topsoil and subsoil (Anindita et al., 2022b) since no unweathered C-horizons

were found because the deeper subsoil contained buried older soil profiles. In this study, the parent materials consist of crystalline minerals (i.e. quartz, hornblende, gibbsite, kaolinite, albite, anorthite, alunite, magnetite) and amorphous materials, based on semi-quantitative Q-XRD analysis (Anindita et al., 2022b). The chemical composition of amorphous materials is not well known, and thus it was estimated based on the difference of the total elements derived from laboratory analysis (i.e. total elemental analysis) and elements in minerals identified by X-ray diffraction at present times.

- For the initial texture, we used field estimated texture while recognising that often pseudo-sand and pseudo-silt are determined in the field in which these are actually stable clay aggregate. This was done because pseudo-sand and pseudo-silt determine the hydraulic properties to large degree. However, for evaluation, we also measured the true clay content by sonication and Na⁺ resin (Anindita et al., 2022b)
- The plant carbon input of forest was derived from the reference value for typical carbon input in rainforest (Guillaume et al., 2018; Hertel et al., 2009) and pine forest (Bruijnzeel, 1985) in Indonesia. The OC input at agricultural sites, in the form of manure and crop residues, was inputted based on results from laboratory analyses and interviews with farmers.
- Bioturbation, the soil mixing by soil meso- and macrofauna was reported to be an important factor in soil horizonation (Finke, 2012; Phillips, 2007). No bioturbation data exist for the study area. The estimated amount of 30 Mg ha⁻¹ yr⁻¹ was chosen referring to measured mixing rate of earthworms in Ivory Coast (Bétard, 2021), with higher values in topsoils compared to subsoils.
- Agricultural practices are characterized by input fertilization, planting and harvesting date, and tillage, as derived from (Anindita et al., 2022b) and interviews with farmers.

4.2.4 Measured data

To test the performance of simulated SOC, we compared the simulated and the estimated SOC pool sizes based on measurements of C-distribution across soil fractions. Specifically, we previously used the Zimmermann et al., (2007) soil fractionation method to subdivide SOC into dissolved organic carbon (DOC), particulate organic matter (POM), OC in the so-termed sand-aggregates fraction (S+A), OC in silt+clay fraction (s+c - rSOC) that is oxidizable by 6% NaOCl, and silt and clay sized oxidation-resistant organic carbon (rSOC). The proportion of these fractions to total SOC was used to partition SOC across the Roth-C model RPM, DPM, BIO, HUM, IOM pools following Zimmermann et al. (2007). The sum of POM and DOC fraction is split into DPM and RPM pools at a ratio of 0.1190, whereas the sum of s+c - rSOC and S+A fractions is split into BIO and HUM pools at a ratio 0.0260 (Zimmermann et al., 2007). The rSOC was set to equal IOM.

4.2.5 Research steps

4.2.5.1 Calibration of important parameters

Calibration was started from 8000 yrs BP (NF-y, PF-i, AG-y, AG-i) and 10000 yrs BP (PF-o, AG-o) as the approximate age of the soils developed over the top 1 m depth. The calibration was done per soil process in a sequence i.e. clay migration followed by weathering, and finally SOC decay. The order of calibration of parameters associated to each soil process was based on their sensitivity found in earlier studies (Table 4-1). Clay content is used to calculate mineral surface area which is then used to

determine cation release rate during mineral dissolution, thus it is necessary to first calibrate clay migration and thereafter weathering of minerals. The mineralogical composition may in turn influence the chemical protection of SOC, so the SOC-decay rates were calibrated after the mineralogy is calibrated. Therefore, the order of calibration is (i) clay migration, (ii) weathering of minerals, and (iii) decay rate of each SOC pool. The optimal value for a parameter in each soil process was selected by comparing the dissimilarity between the measured and simulated soil properties at the profile scale (scaled $DIS_{profile}$) (Gower, 1971):

$$scaled\ DIS_{profile} = \frac{1}{k(X_{r,max} - X_{r,min})} \sum_{k=1}^K abs(X_{r,k} - X_{s,k}) \quad (Eq. 4-9)$$

where X represents the soil property of interest, k is the number soil compartments, s refers to the value for the simulation, and r for the reference (measurement). The scaled DIS ranges from 0 (perfect) to 1 (very poor). In each calibration process, the best parameter value was obtained by comparing the simulated and measured soil properties over the measured depth, $\pm 0 - 80$ cm. The values of all parameters were adjusted until we found the minimum average of DIS over all study sites, except the calibration of SOC where we selected the best value based on the minimum average of DIS over all study sites or the minimum of DIS in each study site, depending on the calibration approach. Only the calibrating parameters were changed within the value range, while other parameters were kept the same as the previously calibrated values. Simultaneous change of all involved parameters via Monte Carlo-like approaches was unfeasible because of the large simulation time of individual model runs.

Clay migration processes were calibrated by tuning some individual parameters, viz. (i) thickness of the ectorganic layer, (ii) soil detachability coefficient (k_d), (iii) pressure head at which macropores empty, $h-\theta_{macro}$, (iv) filter coefficients (n), and (v) maximum particle splitting probability and soil temperature change at which this occurs (PS_{max} and B). Thickness of the surface litter layer has a role on reducing splash detachment. Soil detachability coefficient relates to the inherent susceptibility to breakdown of aggregates which depends on other properties like clay mineralogy, organic matter content, and cations on exchange sites (e.g. Ca^{2+} , Na^+) (Jarvis et al., 1999) and is used to calculate the splash detachment rate ($g\ m^{-2}\ h^{-1}$). The $h-\theta_{macro}$ is related to the transport of clay in macropores (Eq. 4-4). Filter coefficient is an empirical exponent from 0 – 1 to describe the loss of dispersed clay by filtering in relation to pore water velocities (Eq. 4-5). Particle splitting probability is the maximum probability that soil particles will break due to physical weathering as temperature changes.

Calibration of weathering of primary minerals was done in an order from the most sensitive to the stable mineral: (i) amorphous materials, (ii) alunite, (iii) anorthite, (iv) albite, (v) hornblende, (vi) quartz (Churchman and Lowe, 2012). Not all the sites contained all these minerals, thus for each site we only calibrated the minerals that were present (Table 4-1). The calibration processes were done by tuning the parameters, namely mineral dissolution rate constant at acidic and/or basic condition (i.e. k_H and k_{OH} , respectively), and reaction orders with respect to H^+ and OH^- promoted dissolution (i.e. n and m , respectively) (Eq. 4-6).

The decay rate of SOC pools was calibrated by following a downstream scheme which means that the pathway of SOC-decay via RPM and DPM to HUM and BIO determines the calibration order of the decay rate (k) factors. The pools with slower rates are calibrated first, thus the sequence of calibration is $k_{RPM} - k_{DPM} - k_{HUM} - k_{BIO}$. For each rate, the range of values are taken based on previous calibration studies (Finke et al., 2019; Yu et al., 2013) and adjustments in these ranges were made to reach minimum error. We ran the calibration in four- and five- SOC pools models. In the four-pool model, the Inert Organic Matter (IOM) pool was absent, and all SOC was subject to decay. Conversely, the OC in the IOM pool did not decay in the five-pool model. The best rate value was selected based on (i) the minimum DIS at each specific site (i.e. site-specific rate) and (ii) the average minimum error for all sites (i.e. generic rate).

Table 4-1 The order of calibrated parameters and their range of parameter values

Soil forming process	Order	Process parameter with units	Default/range of parameter values		Application on sites
			Reference	this study	
Clay migration	(1)	Thickness of ectorganic layer (mm)	0.5 – 3.5 ⁽¹⁾	5 – 30	All six sites
	(2)	Soil detachability coefficients (k_d ; $g J^{-1}$)	0.05 – 2 ⁽²⁾	0.0175 – 0.1	All six sites
	(3)	Pressure head (hPa) at which macropores empty ($h - \theta_{macro}$)	0 – -35 ^(1,2)	-6 – -30	All six sites
	(4)	Filter coefficient of clay (n ; -)	0 – 1 ^(1,2)	0.2 – 0.7	All six sites
	(5)	Particle splitting probability and soil temperature change (PS_{max} and B ; - and $^{\circ}C hour^{-1}$, respectively) (4 x 4 combination)	1.338 x 10 ⁻⁶ – 2.163 x 10 ⁻⁶ ; 0.45 – 1.95 ⁽¹⁻²⁾	1.338 x 10 ⁻⁶ – 2.163 x 10 ⁻⁶ ; 0.45 – 1.95	All six sites
Weathering rate of amorphous materials	(6)	Dissolution rate constant at acid ($\log kH_{25}$; $mol m^{-2} s^{-1}$)	-9.07 – -11.5 ⁽³⁾	-10 – -11.8	All six sites
	(7)	Reaction order of H ⁺ (n ; -)	-	0.28 – 0.44	All six sites
	(8)	Dissolution rate constant at basic ($\log kOH_{25}$; $mol m^{-2} s^{-1}$)	-8.15 – -10.3 ⁽³⁾	-10.4 – -13.4	All six sites
	(9)	Reaction order of OH ⁻ (m ; -)	-	0.12 – 0.28	All six sites
Weathering of alunite	(10)	Dissolution rate constant at acid ($\log kH_{25}$; $mol m^{-2} s^{-1}$)	-10.8 – -11.6 ⁽⁴⁾	-10.8 – -12.8	NF-y
	(11)	Reaction order of H ⁺ (n ; -)	-	0.42 – 0.58	NF-y
	(12)	Dissolution rate constant at basic ($\log kOH_{25}$; $mol m^{-2} s^{-1}$)	-10.8 – -11.6 ⁽⁴⁾	-11.2 – -13.4	NF-y
	(13)	Reaction order of OH ⁻ (m ; -)	-	0.23 – 0.35	NF-y
Weathering of anorthite	(14)	Dissolution rate constant at acid ($\log kH_{25}$; $mol m^{-2} s^{-1}$)	-5.9 ⁽⁵⁾	-5 – -7.1	NF-y
	(15)	Reaction order of H ⁺ (n ; -)	0.9 ⁽⁵⁾	0.72 – 0.93	NF-y
Weathering of albite	(16)	Dissolution rate constant at acid ($\log kH_{25}$; $mol m^{-2} s^{-1}$)	-9.7 ⁽⁵⁾	-7.7 – -9.7	NF-y, AG-y, AG-i, AG-o

	(17)	Reaction order of H ⁺ (<i>n</i> ; -)	0.5 ⁽⁵⁾	0.44 – 0.56	NF-y, AG-y, AG-i, AG-o
	(18)	Dissolution rate constant at basic (log <i>kOH</i> ₂₅ ; mol m ⁻² s ⁻¹)	-9.95 ⁽⁵⁾	-8.1 – -10.1	NF-y, AG-y, AG-i, AG-o
	(19)	Reaction order of OH ⁻ (<i>m</i> ; -)	0.5 ⁽⁵⁾	0.44 – 0.56	NF-y, AG-y, AG-i, AG-o
Weathering of hornblende	(20)	Dissolution rate constant at acid (log <i>kH</i> ₂₅ ; mol m ⁻² s ⁻¹)	-10.20 ⁽⁶⁾	-8 – -10.2	NF-y, PF-i, AG-i, AG-o
	(21)	Reaction order of H ⁺ (<i>n</i> ; -)	0.55 ⁽⁶⁾	0.49 – 0.61	NF-y, PF-i, AG-i, AG-o
Weathering of quartz	(22)	Dissolution rate constant at basic (log <i>kOH</i> ₂₅ ; mol m ⁻² s ⁻¹)	-11 ⁽⁶⁾	-9.6 – -11	All six sites
	(23)	Reaction order of OH ⁻ (<i>m</i> ; -)	0.25 ⁽⁶⁾		All six sites
SOC pool	(24)	Decay rate of RPM pool (yr ⁻¹)	0.075 – 0.525 ^(7,8)	0.075 – 6	All six sites
	(25)	Decay rate of DPM pool (yr ⁻¹)	0.100 – 1.600 ⁽⁸⁾	0.1 – 23	All six sites
	(26)	Decay rate of HUM pool (yr ⁻¹)	0.005 – 0.035 ^(7,8)	0.001 – 0.01	All six sites
	(27)	Decay rate of BIO pool (yr ⁻¹)	0.100 – 0.800 ⁽⁸⁾	0.05 – 0.50	All six sites

¹Ranathunga et al (2022); ²Finke et al (2015), ³Data reported for volcanic glass (Wolff-Boenisch et al., 2004); ⁴Dissolution rate of alunite at pH 1-8 (Miller et al., 2016); ⁵Godd ris et al (2006) reported in Opolot (2016); ⁶Violette et al. (2010) reported in Opolot (2016); ⁷Yu et al. (2013); ⁸Finke et al (2019)

4.2.5.2 Identification of geochemical proxies for SOC-pool decay rates

Geochemical proxies to possibly improve SOC-pool decay rates in a modelling context were identified in two steps (Finke et al., 2019). First, by correlating the rates obtained by calibration with measured geochemical data from the same profiles the most informative candidate proxies were identified. Such proxy reflects the degree of physico-chemical protection of SOC. Candidate proxies were selected using the strongest and most significant correlations. These proxies were then used for the second step where rate modifiers are calculated by linear regression. The value of geochemical rate modifier (x_2) in Eq. 4-8 is calculated for each site i using Eq. 4-10 and applied to each pool.

$$x_2 = \frac{\beta_0 + \beta_1 * G_i}{k} \quad (\text{Eq. 4-10})$$

where β_0 and β_1 are regression coefficients, G_i is geochemical proxy at site i and k is the average of the calibrated rate constants (yr⁻¹) at all sites. The geochemical rate correction was applied for simulations that used a generic rate in the SOC calibration. The latter situation reflects a lower information level (no local calibration), which we attempt to improve by using the proxy correction.

4.2.5.3 Model projections

Simulations for future projection were conducted using different climate scenarios as climate boundary conditions to the model. Two extreme emission scenarios were used, viz. (i) the Representative Concentration Pathway (RCP) 2.6 and the RCP 8.5 derived from Coordinated Regional Climate Downscaling Experiment (CORDEX) for South-East Asia (CORDEX-SEA) domain using climate model from MPI-ESM-LR_REMO2015 (Giorgetta et al., 2013; Remedio et al., 2019). The MPI-ESM

model considers El Nino Southern Oscillation phenomenon (Giorgetta et al., 2013) which influences the rainfall variability in Indonesia (Nur'utami and Hidayat, 2016), whereas CORDEX delivered downscaled simulations from global climate model to higher resolution of regional models with spatial resolution 25 km. The performance of CORDEX-SEA has been evaluated in other studies (e.g. Nguyen et al., 2022; Tangang et al., 2020). In this study, the atmospheric variables derived from both RCP 2.6 and 8.5 were downscaled to local climate data as described in section 4.2.3 (input climate data). The RCP 2.6 showed a stabilized climate until 2100, while the RCP 8.5 scenario displayed an increase of average temperature and a slight decrease of precipitation in our study area (Fig. A4-2 in Appendix 4). We used the temperature and precipitation from RCP 2.6 and 8.5 to estimate net primary productivity (NPP in Mg dry matter ha⁻¹ y⁻¹) using the Miami model (Lieth, 1975):

$$NPP = 30 * MIN\left(\frac{1}{1+e^{1.315-0.119*MAT}}, 1 - e^{-0.00064*MAP}\right) \quad (\text{Eq. 4-11})$$

where MAT is the Mean Annual Temperature (°C) and MAP is Mean Annual Precipitation (mm). Our study did not consider the effect of increased atmospheric CO₂ concentration on NPP, so climate projection scenarios were only based on the change of precipitation and temperature. The SoilGen model calculate litter input via NPP as a function of climate in every year. For forest land use, we assumed that forest is in equilibrium (i.e. mature), so the amount of biomass that is produced becomes plant litter. For agricultural land use, the estimation of litter input was calculated in SoilGen as follow:

$$\text{Litter input (Mg C ha}^{-1}\text{)} = NPP \times (1 - \text{harvested product}) \quad (\text{Eq. 4-12})$$

Where harvested product is a fraction of NPP that is harvested (Mg C ha⁻¹).

For the evaluation of the effect of different climate scenarios on SOC stocks, these were simulated for 80 years, from 2021 onwards using the SoilGen model. In this period, we evaluated the amount of SOC and its distribution over SOC pools. The input includes soil data, minerals, vegetation at the final year of the best calibration simulation (i.e. SOC-decay rate: i. site-specific rate, ii. generic rate, iii. generic rate modified by geochemical proxy). Boundary conditions such as type of vegetation, bioturbation, fertilization, and ploughing were assumed to be the same as at present time. We also assumed there were no destructive events such as eruptions or landslides.

4.3 Results and discussion

4.3.1 Calibration

4.3.1.1 Clay migration

The clay migration process was sensitive to four parameters, i.e. soil detachability coefficient (k_d), pressure head at which macropores empty ($h-\theta_{macro}$), filter coefficient (n), and max splitting probability and temperature gradient (PS_{max} and B), whereas the difference of thickness of the ectorganic layer showed no effect on clay translocation (Fig. 4-1). The limited sensitivity of the ectorganic layer in our study might be due to the high precipitation in our study area (± 2000 mm yr⁻¹) and also ploughing of

agricultural sites, which may have led to a lesser influence of ectorganic layer thickness to the clay detachment process. Unlike the study by Finke et al. (2015) who demonstrated the limited sensitivity of k_d in SoilGen2, our study showed a change in the dissimilarity of clay amount (%) between measured vs. simulated clay content in the soil profile after shifting of the k_d value, particularly in the forest. The calibrated optimal value of k_d was 0.023 (Table 4-2). This value was smaller than found in studies by Jarvis et al. (1999), who obtained a value of 15, and Morgan (2001), who proposed k_d to range from 0.05 to 2. The low k_d value implied just a small detachment rate in these soils. In line, Andosols are known to have good aggregate stability and thereby they are relatively resistant to water drop impact (Nanzyo et al., 1993b) even after long-term cultivation (Shoji and Takahashi, 2002). The depth distribution of the clay in the agricultural soil profiles seemed to be insensitive to the change of k_d parameter and had higher dissimilarity than in case of the forest soils. This might be because of the ploughing activities, which may have caused local (but unknown) variation in aggregate stability, resulting in a lesser influence of the detachability coefficient on clay dispersion.

The $h-\theta_{macro}$ parameter is used to calculate the fraction of clay that is in a transportable dispersed state (Eq. 4-4). The best calibrated value of $h-\theta_{macro}$ in our soils was -24 hPa, lower than values predicted for Western Europe, viz. -1 hPa (Finke, 2012) and -18.3 (Finke et al., 2015). Clay translocation was sensitive to $h-\theta_{macro}$, in contrast to Ranathunga et al. (2022) who found clay distribution in semi-arid climates to be unrelated to this parameter. This emphasizes that as expected, the amount of precipitation would be a critical determinant of clay mobility. With high precipitation in our study area logically there is a larger chance of water-clay contact and for flow thereof through the macropores. The result showed a low $h-\theta_{macro}$ value indicating that, nevertheless but a relatively low fraction of clay was transported downwards. The filter coefficient n also relates to the clay migration, specifically to calculate the amount of clay that is not leached due to filtering. The best calibrated value was 0.5, similar to the value proposed by Ranathunga et al. (2022), and comparable with estimates for silty clay soil in Sweden (0.71; (Jarvis et al. 1999)) and loess soils in Belgium (0.51; (Finke et al., 2015)). Lastly, the optimum calibrated values of PS_{max} and B were 1.65×10^{-6} and $1.95^\circ\text{C hour}^{-1}$, respectively. These values were in between values reported from the study of loess soil in semi-arid climate (2.163×10^{-6} and $0.95^\circ\text{C hour}^{-1}$) (Ranathunga et al., 2022) and for French soils, i.e. Paris Basin, for which Finke et al. (2015) found the best value at 1.338×10^{-6} and $1.95^\circ\text{C hour}^{-1}$.

Table 4-2 A summary of the calibrated parameters and best calibrated parameter values

Soil processes	Process parameters with units	Best values
Clay migration	1. Soil detachability coefficients (k_d ; g J^{-1})	0.023
	2. Pressure head (hPa) at which macropores empty ($h\theta$ -macro)	-24
	3. Filter coefficient of clay (n ; -)	0.5
	4. Particle splitting probability and soil temperature change (PS_{max} and B ; - and $^\circ\text{C hour}^{-1}$) (4 x 4 combination)	1.61×10^{-6} ; 1.95
Weathering rate of amorphous materials	5. Dissolution rate constant at acid ($\log kH_{25}$; $\text{mol m}^{-2} \text{s}^{-1}$)	-11.4

	6.	Dissolution rate constant at basic ($\log k_{OH_{25}}$; mol m ⁻² s ⁻¹)	-13	
Weathering rate of alunite	7.	Dissolution rate constant at acid ($\log k_{H_{25}}$; mol m ⁻² s ⁻¹)	-12	
	8.	Dissolution rate constant at basic ($\log k_{OH_{25}}$; mol m ⁻² s ⁻¹)	-13	
Weathering of anorthite	9.	Dissolution rate constant at acid ($\log k_{H_{25}}$; mol m ⁻² s ⁻¹)	-5.3	
	10.	Reaction order of H ⁺ (n ; -)	0.9	
Weathering of albite	11.	Dissolution rate constant at acid ($\log k_{H_{25}}$; mol m ⁻² s ⁻¹)	-8.3	
	12.	Reaction order of H ⁺ (n ; -)	0.5	
	13.	Dissolution rate constant at basic ($\log k_{OH_{25}}$; mol m ⁻² s ⁻¹)	-8.3	
	14.	Reaction order of OH ⁻ (m ; -)	0.5	
Weathering of Hornblende	15.	Dissolution rate constant at acid ($\log k_{H_{25}}$; mol m ⁻² s ⁻¹)	-8.4	
	16.	Reaction order of H ⁺ (n ; -)	0.55	
Weathering of quartz	17.	Dissolution rate constant at basic ($\log k_{OH_{25}}$; mol m ⁻² s ⁻¹)	-10.6	
	18.	Reaction order of OH ⁻ (m ; -)	0.25	
SOC pool (4-pool model)	19.	Decay rate of RPM pool (k_{RPM} ; yr ⁻¹)		Generic rate = 0.15 Site-specific rate = NF-y (0.075); PF-i (0.325); PF-o (0.125); AG-y (4.5); AG-i (1.5); AG-o (0.55)
	20.	Decay rate of DPM pool (k_{DPM} ; yr ⁻¹)		Generic rate = 0.25 Site-specific rate = NF-y (0.10); PF-i (0.25); PF-o (0.10); AG-y (23); AG-i (5); AG-o (3.5)
	21.	Decay rate of HUM pool (k_{HUM} ; yr ⁻¹)		Generic rate = 0.0035 Site-specific rate = NF-y (0.0025); PF-i (0.005); PF-o (0.005); AG-y (0.005); AG-i (0.0025); AG-o (0.0025)
	22.	Decay rate of BIO pool (k_{BIO} ; yr ⁻¹)		Generic rate = 0.10 Site-specific rate = NF-y (0.05); PF-i (0.05); PF-o (0.05); AG-y (0.35); AG-i (0.1); AG-o (0.2)

4.3.1.2 Weathering of primary minerals

The simulation of minerals weathering was sensitive to the parameters of dissolution rates constant at acid and/or basic conditions of mineral (k_H and k_{OH} , respectively) (Fig. A4-3 to A4-8 in Appendix 4). Conversely, not all parameters of reaction orders with respect to H⁺ and OH⁻ (n and m , respectively) were sensitive enough to influence the dissolution rate of minerals (r_k , see eq. 1). Best calibrated values of k_H and k_{OH} for amorphous materials were -11.4 and -13 log mol m⁻² s⁻¹, respectively (Table 4-2). Compared to the dissolution rate constant of volcanic glass ((Wolff-Boenisch et al., 2004); Table 4-1), these values were much lower implying a slower dissolution rate. Possibly, this results from that

amorphous materials in our study refer to all phases that did not produce XRD peaks. For instance, the % of amorphous materials correlated well with the content of SRO Al (hydr-) oxides (Anindita et al., 2022b). This material forms after rapid dissolution of volcanic glass and can persist for relatively long time periods until all the non-crystalline materials transform to crystalline phase (Rasmussen et al., 2007). The current SoilGen model assumes that dissolution occurs at far from equilibrium conditions and does not account for the formation of secondary minerals. Changing parameters n and m did not bear any effect on the modelled dissolution of amorphous materials (Fig. A4-3 in Appendix 4).

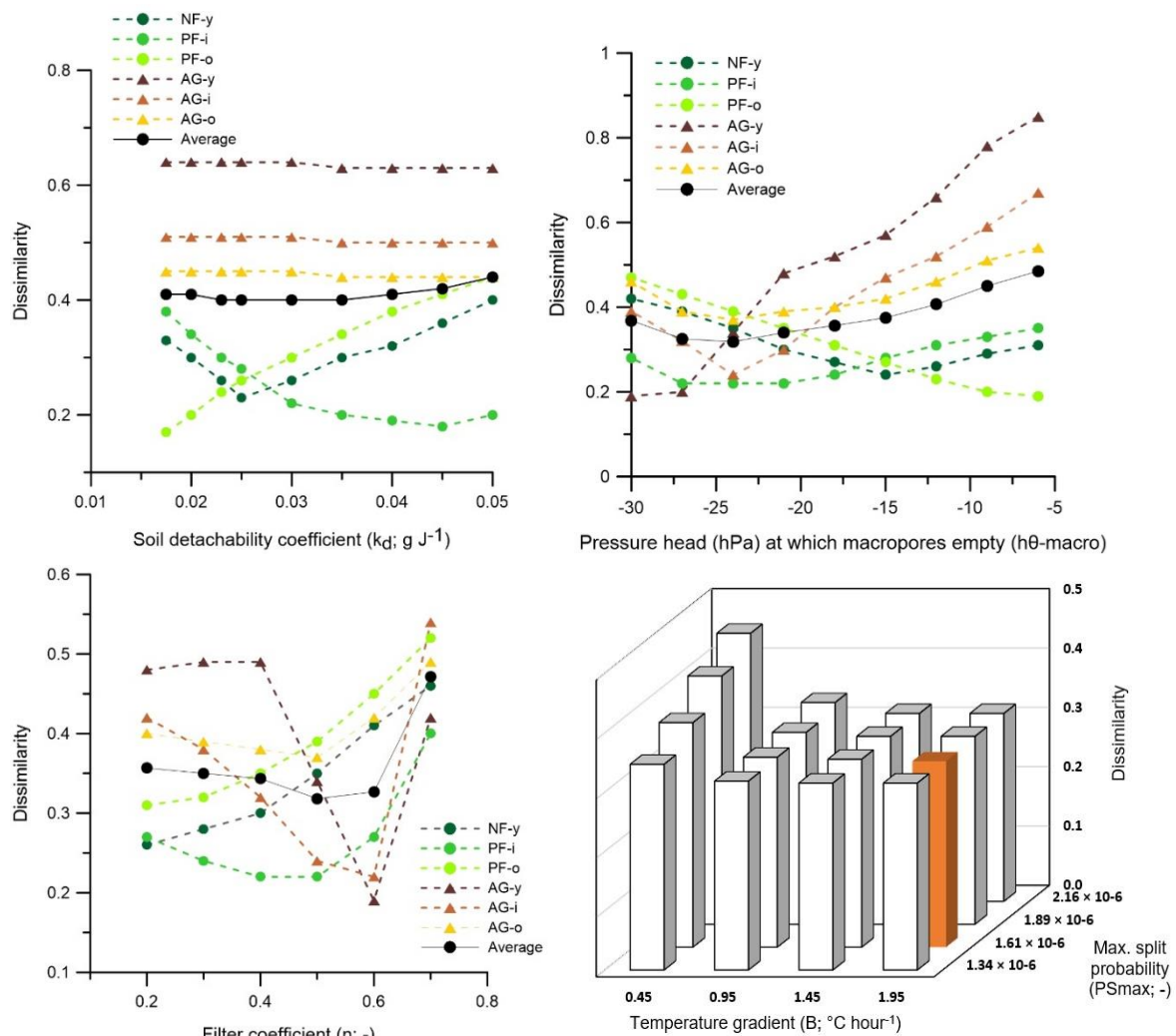


Figure 4-1 Variation of scaled dissimilarities (Eq. 4-9) between measured and simulated clay content in the calibration of clay migration.

The optimum k_H and k_{OH} of alunite in NF-y soil were -12 and -13 $\log mol m^{-2} s^{-1}$, respectively (Table 4-2). These values were lower than in a previous study by (Miller et al., 2016) where obtained dissolution rates were -10.8 to -11.4 from pH 1 till pH 8. In line to their study, our result also showed the inflection point "V" in the alunite dissolution rate versus pH occurs at a minimum for pH 6 - 7 (Fig A4-8 in

Appendix 4). Such shifting of dissolution mechanism from H^+ to OH^- is due to Al^{3+} hydrolysis at higher pH (Miller et al., 2016). Again, variation in the reaction orders n and m did not influence the modelled dissolution of alunite. For anorthite, the best value of k_H was $-5.3 \log \text{mol m}^{-2} \text{s}^{-1}$. This value was higher than found in previous studies: -5.9 (Godd ris et al., 2006) and -6.64 (Palandri and Kharaka, 2004). The optimum derived value for parameter n of anorthite minerals was similar to the SoilGen reference value of 0.9 (Table 4-1). The optimum calibrated k_H and k_{OH} for albite was $-8.3 \log \text{mol m}^{-2} \text{s}^{-1}$ (Table 4-2). These rate constants were faster than documented in previous studies, e.g. -9.62 and -9.64 (Bandstra and Brantley, 2008) and -9.7 and -9.95 (Godd ris et al., 2006), for k_H and k_{OH} respectively. However, we noticed that the difference of the dissimilarity value between k_{OH} -8.3 and -9.95 was in fact very small, viz. 0.005 (Fig. A4-5 in Appendix 4). The optimum values for parameters n and m in albite were both 0.5 , the same as the reference value. The best calibrated value for k_H of hornblende was $-8.4 \log \text{mol m}^{-2} \text{s}^{-1}$. This rate was faster than found in studies of hornblende dissolution rate compiled by Bandstra and Brantley (2008). On the other hand, the optimum value for n was 0.55 , the same as the reference value. The best calibrated value of k_{OH} for quartz was $-10.6 \log \text{mol m}^{-2} \text{s}^{-1}$ which was faster than the study by Violette et al. (2010) who obtained the value of -11 .

Overall, our study showed either slower or faster dissolution rate constant (k_H , k_{OH}) than the reference values of other studies. The comparison of minerals' dissolution rates obtained in various studies with different time scales remains a challenge and this could have partly contributed to the spread in reported results (White and Brantley, 2003). Another factor which also influences this disparity is the initial amount of parent material, as will be further described in section 4.3.5. The optimum values for parameters n and m were same as the reference values (Table 4-1). It might be because the simulated soils had neutral pH, $6 - 7$, thus the reaction order which mainly affects the dissolution rate at acid (± 4) or basic (± 9) pH did not have much effect when the dissolution rate constant (k_H and k_{OH}) has been adjusted.

4.3.1.3 Soil organic carbon pool

The site-specific calibration showed that the optimal decay rates for the various OC pools varied among the soils (Table 4-2; Fig. 4-2). The optimal values obtained from our SOC calibration were not entirely within the range of the rates reported in previous studies (Finke et al., 2019; Yu et al., 2013). The calibrated k_{RPM} and k_{DPM} were similar in the four- and five-pool models because both the carbon input and the measured amount of OC in DPM and RPM pools were the same. The optimum calibrated k_{RPM} and k_{DPM} in forest soils were within the range of reference values (Table 4-1). However, for the agricultural soils, calibrated k_{RPM} and k_{DPM} values were much higher and also beyond ranges of reference values. The contrast in k_{RPM} and k_{DPM} in agricultural soils than in the forest soils was to be expected as forest soils generally contain more recalcitrant materials (McTiernan et al., 2003), while added OC in agricultural soils, which is mainly derived from organic fertilizer, is better decomposable. In addition, management practice, e.g. soil tillage, creates higher turnover rate, particularly for decomposable plant materials, while fertilization and liming enhance nutrient availability and improve soil pH for heterotrophs to operate. There are no N-availability or pH modifiers in the Roth-C model and so these effects translate into best calibrated values for C-model pool in our study.

Both k_{HUM} and k_{BIO} in the four-pool model generally had slower decay rate than five pool model, which was expected because in the four-pool model the recalcitrant SOC is entirely part of the HUM pool, and not spread across IOM and HUM. The site-specific k_{HUM} and k_{BIO} calibrated values were slightly below or within the range of reference values reported in literature. Our study showed a better calibration of SOC pools using the four-pool than five-pool model as was shown by the closer approximation of modelled and measured total SOC in most of the sites using the four-pool model (Fig. 4-3), in line with Finke et al. (2019) who found better simulation using a SOC four-pool model for a chronosequence study. In the five-pool model, there was an overestimation or underestimation of the HUM and IOM pools, indicating an uncertainty of the model whether OC is subjected to decay or not. The OC may be relatively stable but assuming that IOM will exist over millennium time scales may be also not completely correct. Sanderman et al. (2016) concluded that IOM is hardly inert at the millennium time scale, and it depends on the carbon flow through the soils. In general, HUM was the dominant SOC pool and accounted for about 90% of total SOC, then followed by RPM (0.1 – 5%) or BIO (1.5 – 5.4%) and the lowest was DPM (0 – 1%).

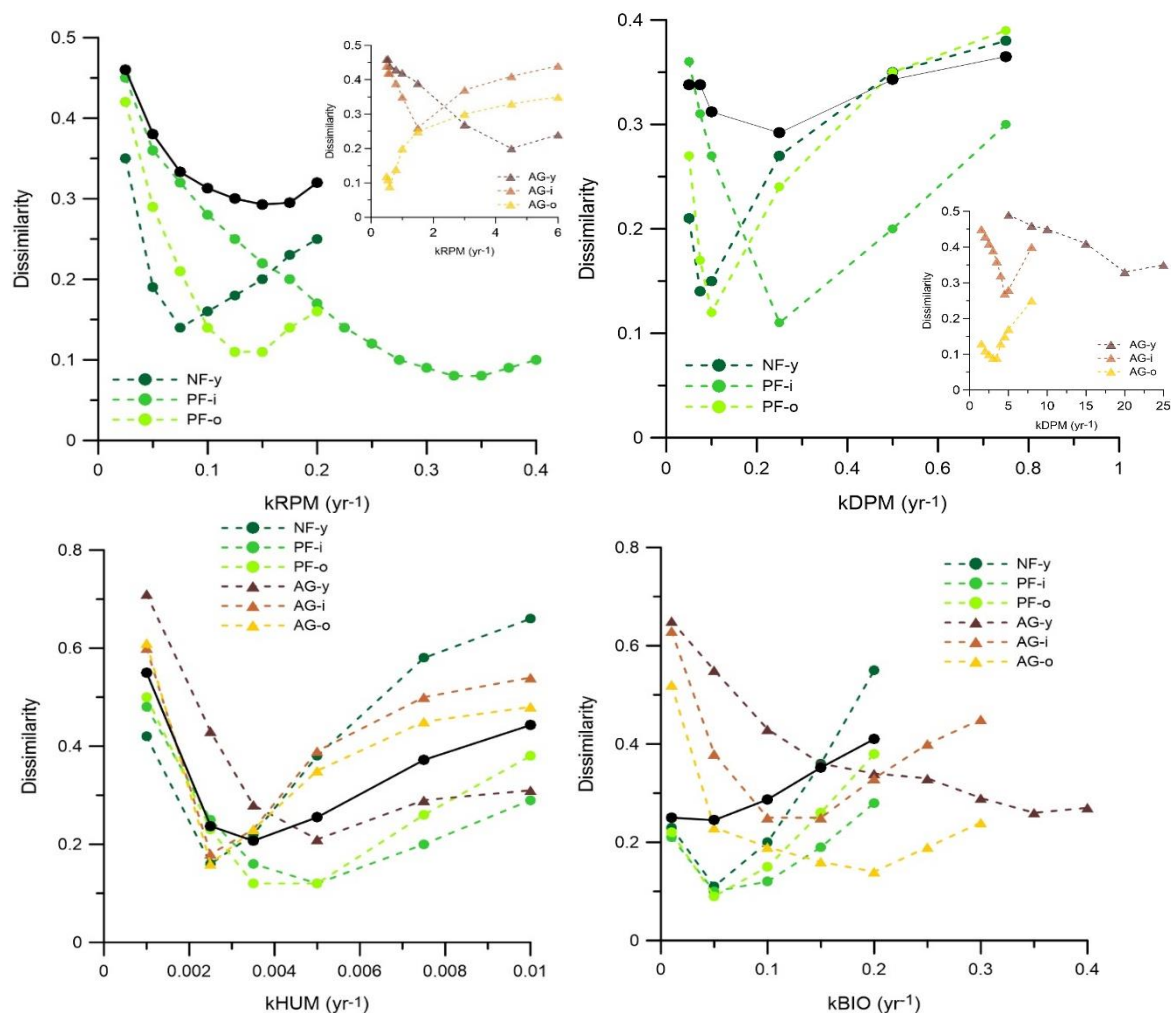


Figure 4-2 Variation of scaled dissimilarities between measured (i.e. derived from SOC fractions following Zimmerman et al. (2007) based on data by (Anindita et al., 2022a) and simulated SOC pool in the calibration of the SOC pool decay rates of the four-pool SOC model in SoilGen.

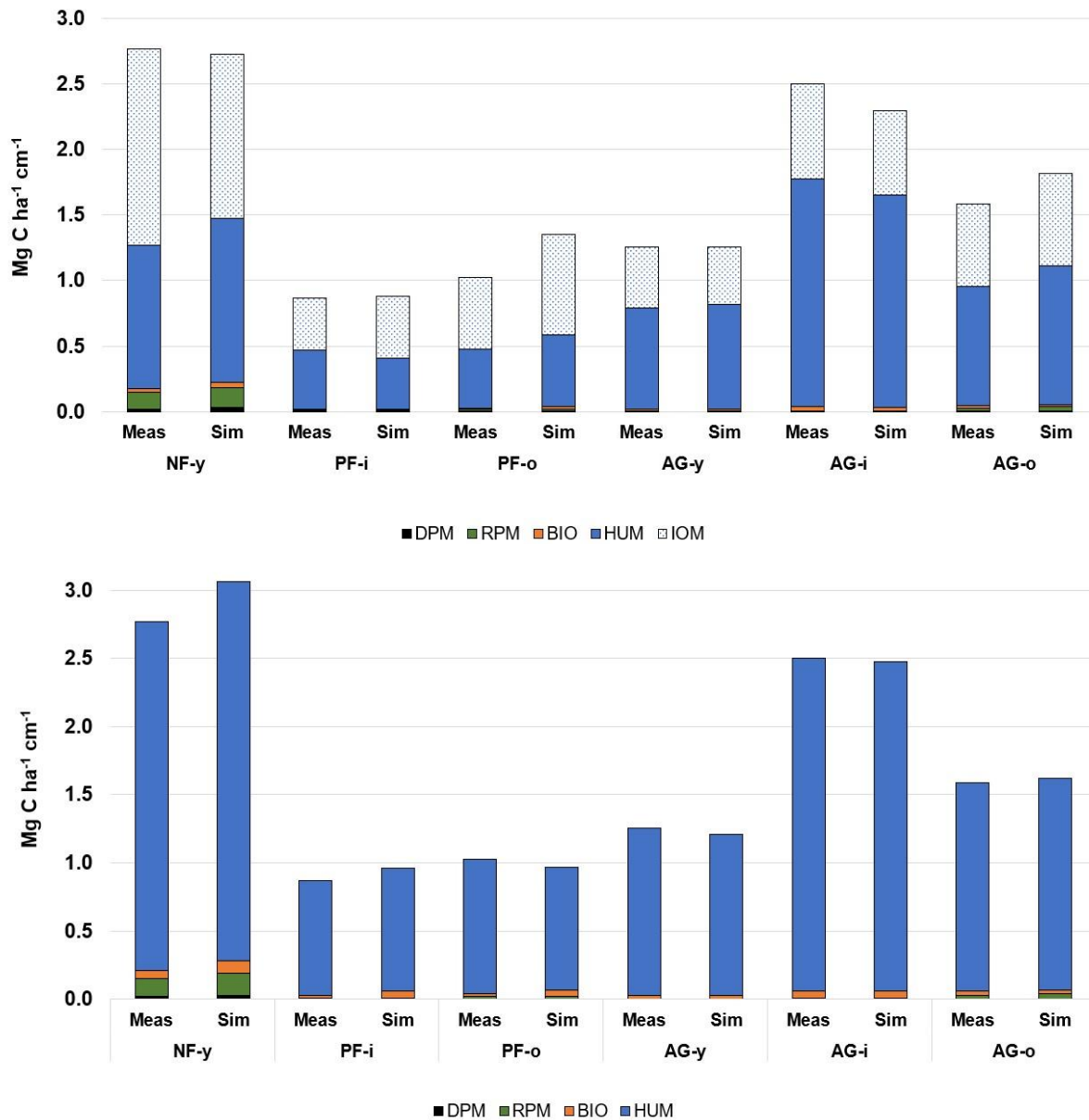


Figure 4-3 SOC pool sizes derived from the distribution of SOC across measured soil fractions following Zimmerman et al. (2007) using data from (Anindita et al., 2022a) (meas) and from SOC pool simulation using site-specific process rates (sim) for the five-pool (top) and the four-pool (bottom) SOC model in SoilGen.

4.3.2 Identification of geochemical proxies

Correlations between measured soil properties and calibrated SOC pool decay rate constants were used to identify candidate geochemical rate modifiers and these are presented in Table 4-3. The results from the five- and four- pool models were similar. We found a negative correlation between k_{HUM} and the soil pH H₂O, the base saturation, the exchangeable Ca content, and the total reserve of bases (TRB) for both four- and five-pool models across the PF and AG soils, excluding NF-y. These negative relations between TRB and exchangeable Ca in particular and SOC-breakdown kinetics is originated from the fact that polyvalent cations act as bridges between soil mineral surface and organic matter or stimulate soil aggregation, thus promoting the stabilization of SOC (Rowley et al.,

2018). Doetterl et al. (2015) found positive correlations between TRB and SOC stocks and interpreted that a slower degradation of SOC occurs as more cations are available for organo-mineral association. But it remains difficult to unequivocally confirm such connections between TRB or base saturation and stability of SOC. Indeed, relations between contents of ‘basic’ cations and SOC need to be interpreted carefully, because fertilizer addition to agricultural soils artificially lifts their levels, while at the same time alongside soils also receive OC-inputs of distinct quality, in contrast to forested sites.

Soil parameters, such as the content of Al_o and amorphous materials also displayed a tendency towards a negative correlation with model pool decomposition rates, but none of these were statistically significant. This is surprising as poorly crystalline Al is known to be one of the principal factors for immobilization of OM in acid volcanic soils and is known to have a role in SOC stabilization in other soils as well (Hernández et al., 2012; Kramer et al., 2012). Perhaps this absence of a relation between mineralization rates and Al_o or content of amorphous materials is explained by the high clay content (27-67%) (Anindita et al., 2022b) acting as primary surfaces for organo-mineral association. This also adds up to the presumed role of basic cations in SOC stabilization as suggested above, to act as bridges between net negatively charged organic matter and most clay minerals at the prevailing soil pH.

We did not find significant correlations between soil properties and k_{RPM} and k_{DPM} and no further modification of these parameters based on soil geochemical proxy was attempted. Unsurprisingly there was a positive correlation between the carbon input amounts and the size of the DPM or RPM pools ($r = 0.98$; $p < 0.01$), but by default the model structure assumes that SOC mineralization rates themselves are independent of C-inputs. In conclusion, we selected TRB as geochemical modifier for the rate of HUM pool only in the simulation of four-pool model. We only did so for five sites i.e. PF-i, PF-o, AG-y, AG-i, AG-o (see next section).

Table 4-3 Pearson correlation coefficients between calibrated rate constants (k_{RPM} , k_{DPM} , k_{HUM} , and k_{BIO} in y^{-1}) and measured soil properties in the PF and AG soils (5 sites). Double underlined coefficients are significant at $\alpha = 5\%$, whereas underlined means are significant at $\alpha = 10\%$

Pearson correlations	Five pool model				Four pool model			
	k_{RPM}	k_{DPM}	k_{HUM}	k_{BIO}	k_{RPM}	k_{DPM}	k_{HUM}	k_{BIO}
Clay (%)	0.39	0.28	0.37	-0.03	0.39	0.28	0.48	-0.85
Silt (%)	0.42	0.54	0.20	0.72	0.44	0.53	0.11	0.50
Sand (%)	-0.30	-0.39	-0.27	-0.57	-0.30	-0.39	-0.11	-0.37
pH H ₂ O	0.23	0.09	<u>-0.98</u>	0.20	0.23	0.09	<u>-0.94</u>	-0.77
Exchangeable Ca (cmol _c kg ⁻¹)	0.53	0.42	<u>-0.85</u>	0.54	0.53	0.42	-0.80	0.81
Oxalate-extracted Al (Al_o ; mg g ⁻¹)	0.10	-0.08	-0.45	-0.28	-0.10	-0.08	-0.30	-0.23
TRB (cmol _c kg ⁻¹ soil)	-0.01	-0.22	<u>-0.84</u>	<u>-0.13</u>	-0.01	-0.22	<u>-0.95</u>	0.60
Specific surface area (m ² g ⁻¹)	0.38	0.24	0.13	-0.06	0.38	0.24	0.28	-0.69
Amorphous materials (%)	0.52	0.29	-0.64	-0.18	0.52	0.29	-0.56	0.13
Al/Si	-0.26	-0.33	-0.07	-0.55	-0.26	-0.33	0.10	-0.54
Base saturation (%)	0.61	0.48	<u>-0.81</u>	0.60	0.61	0.48	-0.76	0.70
Cation exchange capacity (cmol kg ⁻¹)	-0.53	-0.45	0.54	-0.32	-0.53	-0.45	0.24	-0.12

4.3.3 Comparison of simulations quality

The amount of SOC over the pools was calculated using: (i) site-specific pool decay rates, (ii) generic rates, and (iii) average rate constants modified by geochemical proxy. These C pool contributions to SOC were then compared to measured pools (Fig. 4-4), from SOC-fractionation data reported by Anindita et al. (2022a). Results showed that site-specific calibration led to the best simulation of both measured total SOC stock and stock of each of the individual SOC pools, in line with previous study (Finke et al., 2019). The percentage difference of total SOC stock in topsoils (0 – 20, 20 – 40 cm) and subsoil (\pm 60 - 80 cm) between simulation with site-specific rates and measured SOC pools were 3.9%, 10.4%, 5.5%, 3.9%, 1.0%, and 2.2% in NF-y, PF-i, PF-o, AG-y, AG-i and AG-o, respectively. Simulations using both generic decomposition rates and generic rates modified by geochemical proxy generally overestimated total SOC, particularly for the agricultural soils. This was mainly due to an overestimation of the RPM and DPM pools for this land use. This implies that the RPM and DPM of forest and agricultural land use have different quality or are subject to variable degree of stabilization under these land-uses. In our previous study (Anindita et al., 2022a) we found that C-mineralization of a model plant residue (^{13}C labelled aboveground ryegrass parts) did not differ between the agricultural and forest sites. This then demonstrates that not the mode of stabilization of C-inputs per se but rather their differing quality between forest and agricultural land-use determined their contrasting mineralization. A further calibration of DPM and RPM decomposition rates should thus not be based on geochemical proxy, but rather from indicators of the quality of the C-inputs. Alternatively, the partitioning between both labile C pools could be based on such quality indices as already successfully demonstrated by Peltre et al. (2012). Regardless, this outcome stresses the need for site-specific or rather land-use specific decomposition rates for these pools.

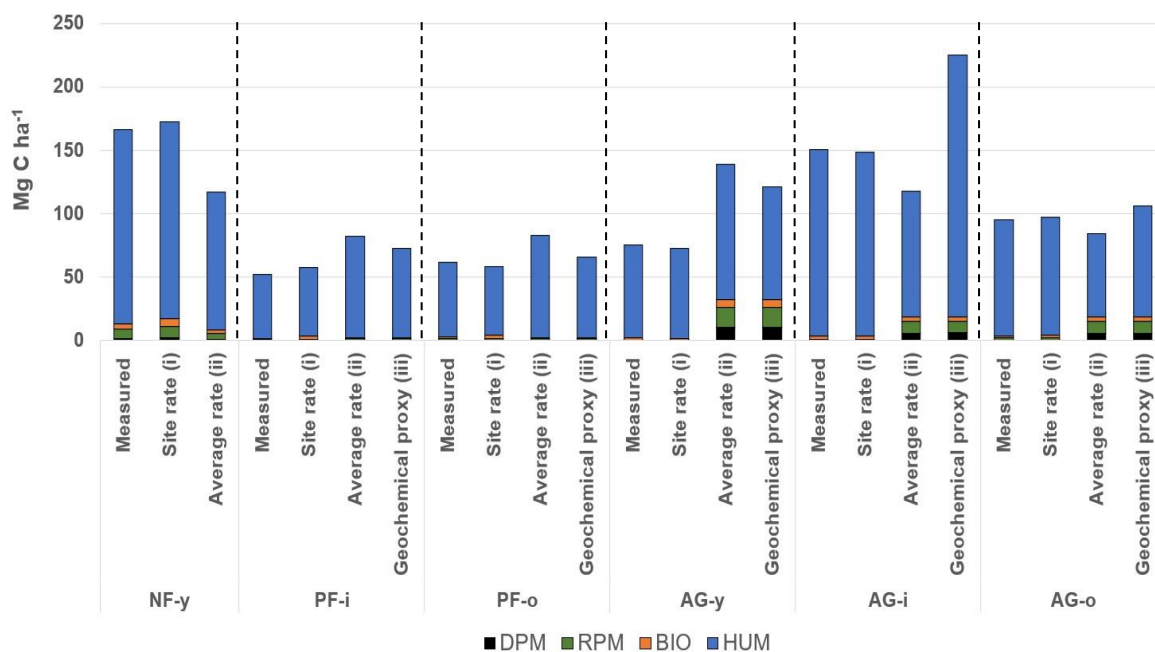


Figure 4-4 Comparison of total SOC in each model pool between measured pools (estimated from soil fractionation carried out by (Anindita et al., 2022a) and simulations using (i) site-specific rate constants, (ii) average rate constants, and (iii) geochemical proxy based modification of rates at depths of 0 – 20, 20 - 40, and \pm 60 – 80 cm in the four-pool model version of SoilGen

The percentage differences of simulation with geochemical proxy and the measured pool for HUM pool were 20%, 40%, 2%; 5%, 39% and 7% in AG-y, AG-i, AG-o, PF-i, and PF-o soils, respectively. The use of a geochemical proxy (i.e. TRB in this study) produced a better estimate of HUM than the simulation with a generic rate in PF-i, PF-o, AG-y, and AG-o soils, with reduction of percentage difference about 18 - 24% on HUM pool. However, this proxy tended to overestimate the HUM pool in AG-i. The advantage of using geochemical proxy to modify the decay rate of HUM pools in SOC simulation was found in other studies as well (Finke et al., 2019; Shirato et al., 2004). For the PF-i, PF-o, AG-y and AG-o, in particular adjustment of k_{HUM} based on geochemical proxy improved simulation of SOC in HUM as well as total SOC compared to simulation with only generic decomposition rates. For the AG-i soil the proxy-based modification of k_{HUM} did not correctly reproduce the HUM pool as well as total SOC. We conclude that simulation with C-pool rate modification based on the here selected geochemical proxy (TRB) thus led to incorrect SOC-pool partitioning and overestimated total SOC stock, although this method did outperform the simulation using generic rates in most study sites.

4.3.4 Effects of different climate projection scenarios on SOC

The trend of estimated total SOC stocks (0 – 20, 20 - 40 cm, and \pm 60 – 80 cm) under two extreme climate scenarios, i.e. RCP 2.6 and RCP 8.5, from years 2021 – 2100 using different decay rate constants is presented in Fig. 4-5. The results showed that the use of different decay rate constants (i.e. site-specific, generic, generic + geochemical proxy) can lead to different directions of the future predicted trend in SOC stock. The selection of type of calibration proved to be very important as the difference of simulated SOC stock evolution between calibration scenarios was generally much larger than the difference between two RCP scenarios (Fig. 4-5). Based on the dissimilarity analysis made (and presented in 4.3.3), the best calibrated SOC model was using the site-specific decomposition rate modification, thus this rate is expected to produce more reliable future simulation. Missing site-specific information or using generic rate calibration can lead to over- or under-estimation of SOC.

The estimated future total SOC also varied among sites. In the simulation with site-specific calibration, the NF-y, AG-y, and AG-o soils showed a further increase of SOC content by 5.7, 26.8, and 12.8% under RCP 2.6 and an increase of 6.1, 20.5, and 9.1% under RCP 8.5, respectively, compared to total SOC at present. On the other hand, the SOC content in PF-i, PF-o, and AG-i soils displayed a decreasing trend by 9.2, 7.7, and 5.2% under RCP 2.6, and 10.6, 7.3, 8.5% under RCP 8.5, respectively. The results suggested that regardless of climate scenario the estimated SOC stock in future is probably not solely dependent on land use. Trends in SOC evidently depend on initially present SOC stock and on C-inputs. Godde et al. (2016) found that initial SOC content explains 66% of SOC variation in model output for agricultural soils. Within the agricultural land-use group a distinction can be made for both aspects. The lower and very high initially present SOC stocks for the AG-y and AG-i sites, respectively probably explain contrasting further increases and decreases in simulated SOC stocks for both respective sites. The expected SOC stock increase of the AG-o site contrasting to the AG-i site is likewise explained by its lower initial SOC but to a lesser degree. The decrease of SOC stock in the planted pine forests for all climate scenarios at the end of projection simulation might indicate that the SOC input was not sufficient to compensate SOC decomposition, regardless of the climate scenario considered.

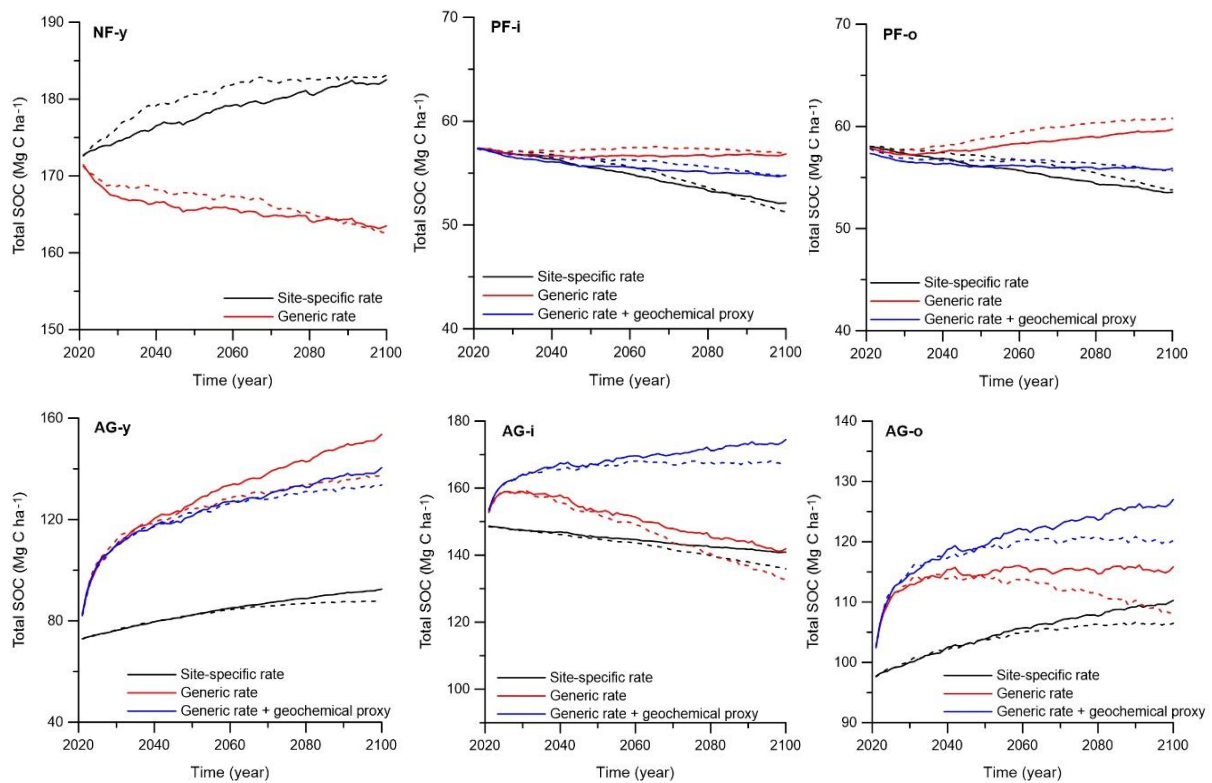


Figure 4-5 The trend of OC stock (0 – 20, 20 - 40, and ± 60-80 cm) calculated with three different decay rates, viz. site-specific rate constants, average rate constants, and average rate constant modified by geochemical proxy in sites NF-y, PF-i, PF-o, AG-y, AG-i, and AG-o from 2020 to 2100 under climate scenarios RCP 2.6 (solid line) and 8.5 (dashed line).

The effect of global warming is represented by the deviating SOC trends between the RCP 8.5 and RCP 2.6 scenarios in Fig. 4-5. At the forest sites, the SOC trend tended to increase in the beginning years but was stagnant or declined by ± 2080 with then final predicted 2100 SOC stocks similar to the RCP 2.6. A general negative impact of global warming on SOC stock was in contrast expected for the agricultural soils, where already from year ± 2040, a discrepancy in SOC stock evolution emerged between the RCP 2.6 and 8.5 scenarios to result in between 3 – 5% lower SOC stock in agricultural soils by 2100 with climate change. The susceptibility of SOC in the agricultural soils to the increase of temperature has been reported in other studies as well, owing to enhanced SOC decomposition that is not met by alongside proportional increased C-inputs (Riggers et al., 2021; Wang et al., 2022). Particularly, in the here intensively managed agricultural lands, organic fertilizers make up for a very substantial share of the overall C-input. Organic fertilizer inputs would evidently not become larger with increasing temperature, in contrast to plant-C inputs. This most probably explains why the impact of global warming was less for the forest soils in our study. In general, our study simulated a decreased trend of SOC under RCP 8.5 as the increased decomposition of SOC was not compensated by the rise in NPP or the amount of additional carbon input, i.e. organic fertilizer. We found a maximum of 5% lower SOC stock under global warming scenario from all soils. The low effect of global warming on SOC storage was also reported in other areas with warm climate (Crowther et al., 2016; Hartley et al., 2021). However, this small effect might also be partly due to the use of stable decomposition rate

constant (k_p) in our model. This effect is difficult to quantify since, field or laboratory experiments generally show that soil warming increases decomposition (Hou et al., 2016; Stuble et al., 2019), where this is the combined effect of k_p and the temperature correction of the decomposition rate in SoilGen.

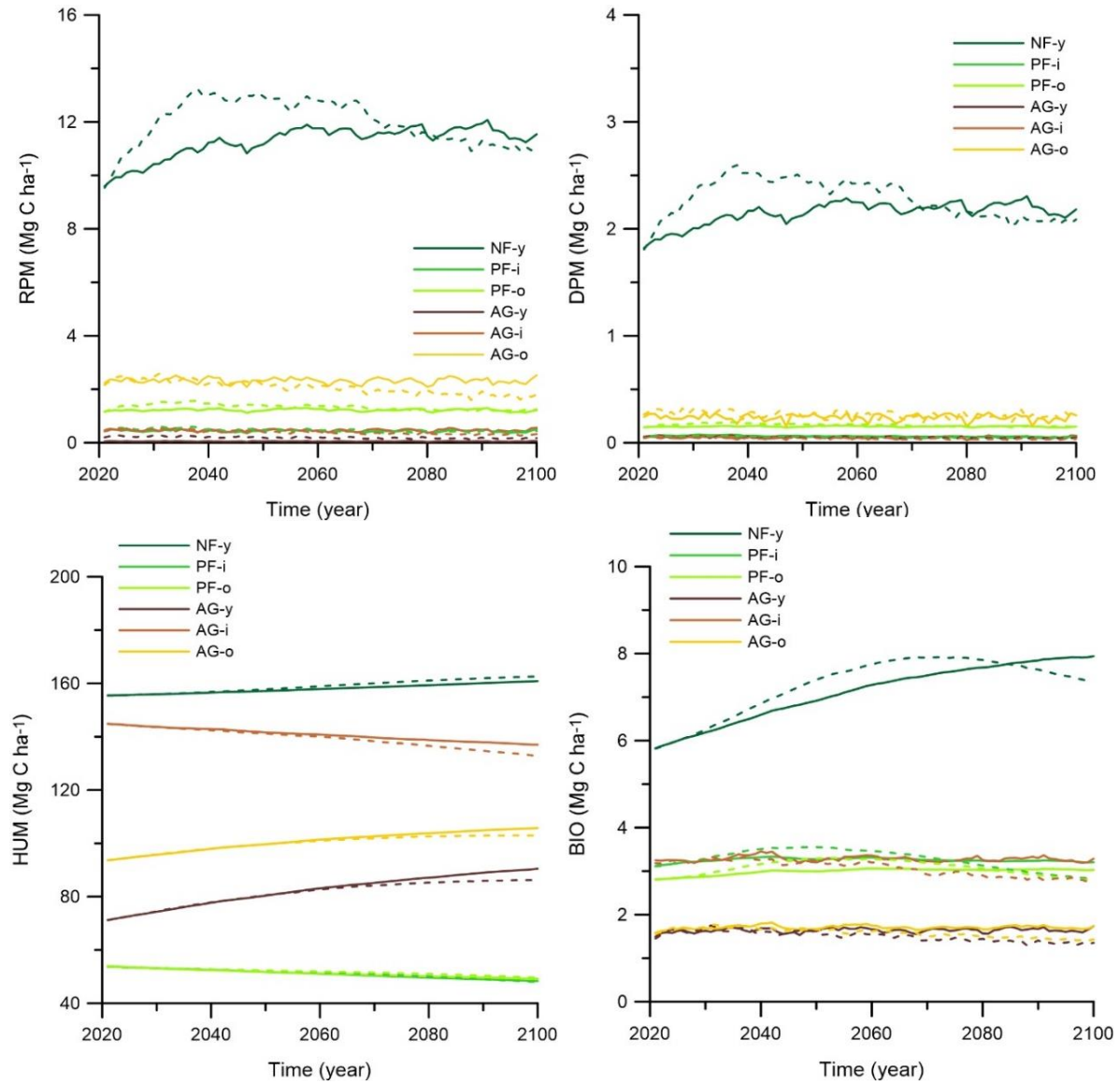


Figure 4-6 Simulation on the amount and distribution of each SOC pool i.e. RPM, DPM, HUM, BIO using site-specific calibration in response to different climate scenarios: RCP 2.6 (solid line) and RCP 8.5 (dashed line).

The responses of each SOC pool, i.e. RPM, DPM, HUM, and BIO pools using site-specific rates on different climate scenarios projection are in Fig. 4-6. There was no significant effect of global warming on the RPM and DPM pool sizes as anyhow the amount of SOC in these pools was generally small, except for at the NF-y site. In case of NF-y, the RPM and DPM pools initially increased but after several decades started to decrease under RCP 8.5. As the temperature continued to rise, the decomposition

rate outpaced rising carbon inputs with consequent declining SOC stock. The BIO pool in NF-y also showed a decreasing trend after year 2080 similar to the RPM and DPM pools, whereas there was a slight increase of the HUM pool. The latter might be due to initially more and thereafter less C-input to the BIO from decay of the likewise evolving RPM and DPM pools. At the agricultural sites, the effect of global warming on SOC was straightforward with a 2.6 – 4.6% lower HUM pool between in the RCP 8.5 than in the RCP 2.6 scenario and this lowering was more than in forest (< 1%). In addition, lower BIO pool was also observed in agricultural soils (16 – 22%) than in forest soils (7 – 11%) between RCP 2.6 and 8.5. Overall, the model suggests a relatively limited change in SOC pool partitioning to occur due to global warming in case of the forest sites and a shift towards mainly less C in the HUM and BIO pools for the agricultural sites. This preferential loss of stable SOC matches the higher predicted thermosensitivity of microbial decomposition of more recalcitrant organic matter (Davidson and Janssens, 2006).

4.3.5 Limitation of this study

For this study several assumptions and simplifications were made which may influence the interpretation of the results. (i) First, we used field estimated soil texture in the clay migration calibration with assumption that the high amount of clay particles (Anindita et al., 2022b) that are present as pseudo-sand and/or pseudo-silt will act as sand and silt with respect to the water flow (i.e. the particle does not easily break). (ii) As mentioned in section 4.3.1.2, the initially taken mineralogical composition can partly explain the difference of dissolution rate constant values between our study and literature. This initial amount of a given mineral is important to calculate its loss over time. Since there was no information on the amount of minerals in the parent materials and the presence of parent materials in field was obscure (no C-horizons), our reconstructed initial mineral composition may not have accurately reflected the actual (unknown) starting condition. In addition, this study was based on assumptions that there was no erosion or that no additional minerals entered from new eruptions since detailed information about these processes was limited for our study area. (iii) In the calibration processes, the difference between simulated and measured values was partially due to the selected interval range. A smaller interval will result to a more accurate calibration, but it will increase the amount of time spent on the calibration process. This limitation can partly be dealt with by making interpolations between best dissimilarity values or by more iteration steps. (iv) The geochemical rate modifier was determined from linear regression between the SOC decay rate and measured TRB as geochemical proxy. However, in reality, the amount of TRB changes with time. To have more accurate calibration simulation of geochemical proxy, the proxy would need to be dynamically included in the simulations. (v) In the projection simulation, we assume that there is no change on vegetation or occurrence of catastrophic events, like e.g. forest fire or volcanic eruptions. Such assumptions may not represent the real situation in the future. Another limitation is the used simple calculation of vegetation NPP and C-input responses to climate. Adaptation of the vegetation structure to climate change is likely with non-linear responses between the rise in MAT or MAP and C-inputs. The interaction mechanisms between climate and vegetation, and additional scenarios, e.g. a forest fire scenario, in the SoilGen model can be considered for future research.

4.4 Conclusions

In this study, the SoilGen2.25 model has been calibrated to reproduce the present SOC stock in 6 Andosol profiles at forested and agricultural sites and to estimate the future of SOC under different climate projection scenarios. Our results showed that:

1. Most of the selected parameters i.e. soil detachability coefficient, pressure head at which macropores empty, filter coefficient, particle splitting and soil temperature change, dissolution rate constants at acid and basic condition, and decay rate of RPM, DPM, HUM, and BIO pools responded to the calibration. Hence, SoilGen proved sensitive to the change of process parameters. Detailed information of initial parent material is important for the model accuracy, so the model can produce better calculation on weathering rates and the amount of cations released.
2. The calibration of SOC using a four-pool model, produces better simulation on total SOC than five-pool model (including inert pool) underlining the uncertainty of the presence of an inert pool over millenniums. We found that the application of site-specific rates to calculate the decay rate of SOC pools provides the best simulation to reproduce total SOC, with percentage differences between the measured and simulated SOC of about 1 – 10 %. These site-specific rates were also important for the SOC projection in the future. The use of generic rates, particularly using the same decay rate constant on different land uses will lead to a lower accuracy on the estimated SOC projections.
3. The use of a geochemical proxy (the total reserve of bases) improved the simulation of HUM pool. However overall, site-specific calibration was much better able to reproduce measured SOC stocks and pool partitioning. The benefit of using geochemical proxies in SOC modelling is observed at most study sites but more sites are required to confirm this.
4. The effect of global warming, represented by climate projection scenario RCP 8.5, on SOC stock was stronger in agricultural soils than in forest soils. There was a reduced SOC stock of about 3 – 5% compared to RCP 2.6 (i.e. no significant increase of temperature) in agricultural soils at the end of simulation (i.e. year 2100), whereas the SOC reduction was less than 2% in forest soils. This stronger global warming effect for agricultural sites is due to the substantial share of exogenous carbon to total soil carbon inputs, which do not lift alongside with a temperature rise.
5. As the impact of calibration method on simulated total SOC is much larger than that of the climate scenario, the need for a good calibration is found to be essential. Particularly so as the default kinetic decomposition rates of the DPM and RPM pools were inappropriate for over half of the concerned study sites with substantially overestimated carbon residing in both pools and SOC.

Authors contributions

Sastrika Anindita performed the research, data visualization, interpretation of the results and writing of the manuscript. Peter Finke conceptualized the soil modelling experiment, provided the software, reviewed, co-wrote the manuscript, and supervised the research. Steven Sleutel reviewed and co-wrote the manuscript, and supervised the research.

CHAPTER 5

GENERAL CONCLUSION, CHALLENGES, AND FUTURE
RESEARCH

5.1 General conclusions and discussion

Volcanic soils have been acknowledged for their ability to retain SOC. However, many of these soils under primary forest in the (sub)tropics are subject to land use change due to their inherently good physical and chemical soil properties, allowing high-yielding food or timber production. Conversion of land use in these soils as anywhere is likely to affect SOC stock on the relatively short term, i.e. on the course of decades to centuries. SOC stock is a function of climate, drainage, vegetation, and edaphic properties with the latter usually quite invariable at this time scale (except for bulk density, soil pH and contents of plant nutrients). However, the weathering of primary minerals and formation of secondary minerals including non-crystalline materials, could proceed rapidly in these volcanic soils, especially in tropical climate. The alteration of the geochemical composition as a consequence of land-use changes may have an impact on SOC dynamics, particularly in volcanic soils where organo-mineral association is a key SOC stabilizing mechanism. The overall aim of this thesis research was to understand the effects of land use on SOC through its relation to geochemical soil properties at present times and to explore future SOC under different climate scenarios. The PhD-research thus pursued several objectives: (i) to assess the effect of land use on weathering, soil geochemical properties and SOC, (ii) to analyse the effect of land use on quality and stability of SOC mediated by soil properties, (iii) to calibrate the important soil processes on volcanic soils, (iv) to assess the impact of different calibration approaches on the accuracy of simulated SOC, and (iv) to forecast the SOC stock and each pool under climate change. The major conclusions, challenges, and future research are summarized hereunder.

The effect of land use on geochemical properties and their controls on SOC was evaluated in volcanic soils near Mt. Tangkuban Perahu and Mt. Burangrang, Indonesia. The study covered six sites that have different ages based on a lithology map (Silitonga, 1973) and land use (tropical primary forest, secondary pine forest, and agricultural land). In **Chapter 2**, the effects of land use on geochemical properties were assessed. Results indicated that the site with primary forest contains different parent materials than the other five sites and thus was excluded from the comparison of soil properties. The inability to still find primary forest in the area with the same parent material and the difficulty to date and trace back the history of sites in the tropics, demonstrate how difficult it is to study land-use effects on soil development in practice. Nevertheless, the comparison of soils under pine forest and agricultural land uses using a weathering index, elemental analyses, and semi-quantitative XRD-based assessment of minerals showed a comparable weathering stage, total element content, and mineral content between these two land use types. We, therefore, concluded that the sites under pine forest and agricultural land have similar parent materials and formed a robust base to study land-use effects on SOC and geochemical soil properties in Indonesia.

A difference in soil properties was found after an agricultural period of < 50 years, as indicated by higher pH, exchangeable bases, and base saturation in agricultural soils compared to the pine forest soils. The high amount of these properties in agricultural soils could be expected as a result of liming and fertilizer application. However, there was also a contrast in the content of amorphous materials, with particularly higher levels of NH_4 -oxalate extractable aluminium (Al_o). These results underline the existence of phenofoms (management-related sub-soil type) within the general genoforms (genetic soil types), which was expressed in terms of soil classification by the WRB qualifiers *dystric* (pine forest

soil) and *eutric* (agricultural soil). Further, about equal SOC stock in the agricultural soils than in the pine forest soils was also remarkable, as land conversion to agriculture generally results in SOC depletion (Don et al., 2011). At this point, we concluded that the higher short-range order Al (hydr-) oxides (indicated by Al_o) under agricultural soil, which correlated well with soil specific area and micropore volume, partly contributed to higher SOC stock in agricultural soils. The role of Al_o in the capacity of volcanic soils to maintain high SOC stocks is well recognized and we hypothesized that formation of short-range order aluminium (Al_o) in agricultural soil would indirectly mediate SOC storage in these soils.

For the second objective (**Chapter 3**), the effects of land use on the storage and stability of SOC were analysed under the hypothesis developed in **Chapter 2** that Al_o had a role in SOC stabilization mechanisms. In this study, soils were separated into several fractions corresponding to different physical and chemical stabilising mechanisms. In this soil fractionation, we used the proposed method of Zimmermann et al. (2007). As further discussed under 5.2.2, it was modified for tropical Andosols. The results showed that most of the SOC in these soils ($\pm 78\%$) was present in the silt and clay fraction which represents SOC-mineral interactions. The Al_o showed a good negative correlation with the proportion of SOC that was oxidizable by 6% NaOCl, particularly at subsoil, but the difference of SOC content in silt-clay fraction between pine forest and agricultural land uses was not found. On the other hand, the SOC content in the sand-aggregate fraction showed a good correlation with some soil properties such as Al_o and amorphous materials. A higher amount of SOC in the sand-aggregate fraction was found in agriculture than in pine forest soils, in line with our experiment that showed a lower native SOC mineralised (%) in agricultural than pine forest soils ($p < 0.01$). These results did in fact support our view that Al_o plays an important role in SOC stabilization in Andosols (**Chapter 2**). This PhD research did underline the possible role of Al_o as a binding agent to stimulate the formation of stable aggregates in agricultural soil and the role of Al_o on SOC stabilization via organo-mineral association, specifically at subsoil. The conclusion was therefore drawn that agricultural practices stimulate the development of Al_o, which plays a role in the physical aggregation and protection of SOC in aggregates. However, we acknowledged that the occurrence of Al_o would not be the sole factor that determines the stability of aggregates and accumulation of SOC in agricultural soils. Other factors, such as clay content, type of crops, and tillage intensity, are expected to co-influence the stability of aggregates. In addition, high input of exogenous OM in the form of excessive manure amendments likely also contributed to the accumulation of SOC in the investigated agricultural sites. These conditions might also be the cause of large deviations between agricultural sites (e.g. the share of SOC in sand-aggregates fraction in agricultural soil was $32 \pm 25\%$).

Additionally, in **Chapter 3**, the degradability of native and exogenous SOC of topsoil (0 - 20 cm depth) was also tested under laboratory conditions in an incubation experiment). Land-use determines both SOC quality as well as soil geochemical properties and both jointly control degradability of SOC. This makes deconvolution of both land-use impacts on SOC stabilization difficult. By use of a single ¹³C-isotope labelled substrate, we could in isolation investigate if the decomposition of fresh OM is impacted by soil mineralogy or soil aggregation. We found no such influence, in fact, in contrast to our expectancy that enhanced soil aggregation and higher levels of Al_o and amorphous materials in the agricultural soils would promote stabilization of OM. However, in other research (e.g. Li et al., 2022),

it has been shown that factors such as soil texture actually bear no impact at all on the initial decomposition of POM, like the ryegrass substrate used here. On the contrary, longer-term stability of more transformed OM does depend on geochemical properties, texture, and structure. The negative correlation between the SOC proportion of the 400 J ml⁻¹ ultrasonic dispersion stable aggregates fraction and SOC mineralization supports this view. Thus, from this PhD research we may again add that SOC stabilization in these tropical Andosols is apparently regulated by soil aggregation to a significant degree, and not just by organo-mineral interaction.

Finally, objectives (III), (IV), and (V) were pursued in **Chapter 4**. This chapter evaluated the trend of SOC in volcanic soils with a process-based soil genesis model, SoilGen 2.25. Data collected from **Chapters 2 and 3** were used and converted as input and measured data in the SoilGen model. For the third objective, we calibrated some essential soil processes in volcanic soils to maximize the reliability of model output, viz. clay migration, weathering of primary minerals, and decay of SOC pools. The calibration results of the clay migration process were generally within the range of reference values. On the other hand, the optimum parameter values on the calibration of minerals weathering were generally not within the range of reference values. The average dissimilarities in these calibrations were between 0.2 – 0.4 ($\pm 20 - 40\%$ error). This is partly due to the uncertain, thus potentially inaccurate, initial input and limited soil processes coverage, such as the formation of secondary minerals in the SoilGen model (see sections 5.2.3 and 5.2.4). We, therefore, concluded that the results of minerals weathering calibration did show that the model can be successfully calibrated, but results were nevertheless uncertain because of the uncertain initial mineralogical composition and formation of secondary minerals.

For the fourth objective, we did more analyses on the calibration of the decay rate of SOC pools by comparing four-pool (without Inert Organic Matter) vs. five-pool models (including Inert Organic Matter) and evaluating three calibration approaches: a site-specific calibration, a generic calibration, and a generic calibration modified by a geochemical proxy. The geochemical proxy was applied to represent the effects of geochemical composition or mineral contents on the decay of SOC. Results indicated that total reserve base (TRB) was the best proxy, in contrast with our previous results regarding the role of Al_o in SOC stabilisation, as discussed in **Chapters 2 and 3**. The significant negative relation between TRB and the decay rate of SOC would underline the role of polyvalent cations as bridges between soil mineral surface and organic matter. However, with high OM inputs being accompanied by liming and use of mineral fertilizers following conversion to agricultural land, it is not possible to confirm that the observed positive relation between TRB and SOC was causal. It in fact seems doubtful that polyvalent 'basic' cations would have contributed strongly to soil aggregation and organo-mineral association considering the much higher levels of pedogenic Fe and Al. We neither found a significant correlation between Al_o and the decay rate of SOC in this study. Possibly absence of this relation might be partly due to the high clay content of the studied soils (27 - 67%) (**Chapter 2**), which acts as primary surfaces for organo-mineral association. However, a positive correlation was found between mineralization of native SOC (**Chapter 3**) and the decay rate of HUM pool with site-specific calibration (**Chapter 4**) ($r = 0.56$). This result indicated that the site-specific calibration of HUM pool at least to some extent reflected the combined effect of various SOC protection mechanism. Overall, the measured SOC pools and total SOC were better reproduced with a four-pool model and a

site-specific calibration, whereas calibration modified with a geochemical proxy generally improves the simulations of total SOC and HUM pool compared to calibration with a generic rate.

For the fifth objective, we analysed the effect of global warming on different land use using the three calibration approaches under different climate projection scenarios, RCP 2.6 and RCP 8.5. These climate projection scenarios were derived from Coordinated Regional Climate Downscaling Experiment (CORDEX) for South-East Asia (CORDEX-SEA) domain using climate model from MPI-ESM-LR_REMO2015. Results showed that simulations using a generic rate or a generic rate modified by geochemical proxy led to a different trend from the trend with local calibrated rates of total SOC stock in the future, and the effect of choosing a calibration approach to parametrize the projective simulations was larger than the effect of global warming (i.e. RCP 8.5). In addition, the effects of increased temperature (i.e. RCP 8.5) on total SOC, and the HUM and BIO SOC-model pools were stronger in agricultural than forest soils. The larger effects in agricultural soils are possibly due to the rapid decomposition of organic fertilizer, contrasting with the increased amount of plant carbon inputs in forest soils under increased temperatures. In conclusion, this study highlighted the importance of the calibration method in estimating future SOC and the susceptibility of agricultural soil and forest soil to global warming.

5.2 Challenges and recommendations

Challenges and limitations encountered while carrying out this PhD-research challenges are grouped into several sections, i.e. related to the applied (i) samples collection, (ii) laboratory methods and (iii) the SoilGen model, such as input data, process coverage, and model calibration. These challenges are discussed under the following subsections.

5.2.1 Samples collection

The samples were collected based on the estimated age between 8000 to 1000 years old, and our study in **Chapter 2** concluded that the weathering index and mineral contents in all sites were comparable, despite different lithology. However, there might be contamination of new materials derived from other volcanic eruptions which might slightly influence the minerals composition between sites. Since, to our knowledge, no information exist about recent or contaminated materials (e.g. the amount and chemical composition) from recent volcanic eruptions to the studied soils, this unknown information remains a limitation. Furthermore, regarding the agricultural land use, this study selected the land that have been farmed for long time (i.e. $\pm 30 - 50$ years). However, the tillage intensity, type of crops, and the amount of fertilizer is not exactly known and are different between agricultural sites. These differences possibly contributed to the variation of soil properties within agricultural sites.

5.2.2 Laboratory method

As Andosols generally contain substantial amounts of non-crystalline materials, some challenges were encountered, mainly related to particle size distribution. The dispersion of soil aggregates into distinct sand, silt, and clay-sized particles by chemical and physical treatments proved to be difficult because

volcanic ash soils are built up by highly stable aggregates. These aggregates can be formed due to (i) bonding between non-crystalline materials or oxides with organic matter (Alekseeva et al., 2009), or irreversible drying of non-crystalline materials that form stable sand and silt size aggregates (Kubota, 1972; Uehara and Gillman, 1981). Some methods were tried to quantify the real content of clay-sized particles, such as the combination of sodium hexametaphosphate, very strong ultrasonic dispersion (1600 J ml^{-1}), and pH adjustment (Silva et al., 2015) or the combination between sonication, Na^+ resin and pH adjustment (Bartoli et al., 1991; Delvaux et al., 1989; Rouiller et al., 1972). By using these two methods, we observed a big difference in the amount of clay fraction between field estimation and laboratory measurement (**Chapter 2**). In both cases, the importance of pH adjustment higher than 8 was underlined, in line with the study by Nakagawa and Ishiguro (1994). The measured clay content increases significantly with such pH adjustment. On the other hand, applying only high-energy of ultrasonication or Na^+ resin resulted in a lower amount of clay. In this case, surface charge plays a role in binding soil particles, particularly in soils with variable charge (Uehara and Gillman, 1981). Therefore, for volcanic or oxide-rich soils, we recommend using either high ultrasonic dispersion or sonication and Na^+ resin dispersion with pH adjustment higher than 8 for both methods rather than the regular pipette method.

For soil fractionation to isolate SOC fractions supposedly under various mode of protection against microbial mediated mineralization, some adjustments to existing methods were likewise needed to separate all the intended fractions (**Chapter 3**). We here used the Zimmermann et al. (2007) soil fractionation scheme as a link between the resulting SOC fractions proportions and SOC model pool sizes of the Roth-C model have previously been found, making it a useful method to test the value of various approaches to calibrate the SoilGen model that employs the Roth-C model pools. Steps in this fractionation scheme with respect to soil dispersion and density separation proved unfit for volcanic soils and had to be modified. Ultrasonic dispersion is the first step in the fractionation procedure and thus has a major effect on the overall SOC fractionation distribution. Ultrasonic energy applied at 22 J mL^{-1} (Zimmermann et al., 2007) was observed to be insufficient for separating sand-aggregates and silt-clay fractions in these volcanic soils. We tested energy levels of 200 and 300 J ml^{-1} , but a remnant of macroaggregates was still left. By modifying the applied an energy level to 400 J mL^{-1} , most macroaggregates dispersed and soil material ended up into s+c fractions ($< 63 \mu\text{m}$). A complete disruption of $> 63 \mu\text{m}$ aggregates using the energy level of 400 J mL^{-1} was not achieved since we previously found that complete separation of particles for soil texture analysis requires higher ultrasonication energy levels. However, such high energy levels would likely cause the release of mineral-bound organic carbon and the diminution of particulate organic carbon. We decided to use an energy level of 400 J ml^{-1} and isolated organic matter contained in highly stable soil aggregates in the sand-aggregates fraction. Nevertheless, from the similarity in contents of Fe and Al of obtained sand-aggregates and silt-clay fractions, it does seem that both fractions display overlap. A further testing of dispersion modes to isolate more distinct soil fractions: i.e. primarily organo-mineral associated OC and aggregate occluded OC would have been desirable, but out of scope here. Notwithstanding, with strong variation in soil texture between our sites, we would in practice only achieve setting an overall optimal mode of soil dispersion, that is not necessarily well suited for each of the study sites. It is because ideally the soil dispersion mode required to isolate mineral-bound OC from POM is set for each individual soil (Cerli et al., 2012). Another adjustment was also made with

the Sodium Polytungstate (SPT) density solution to separate free POM and the sand-aggregates fraction. The use of 1.8 g ml^{-1} did not completely separate these fractions, with many lighter, probably organo-mineral, soil particles ending up in the light fraction. A density solution of 1.5 g ml^{-1} was found to be best for separation of POM in these volcanic soils. Overall, the above illustrates that laboratory methods developed for upland soils in the temperate zone are not simply usable for other contexts. Development of specific robust SOC fractionation methods is needed to understand the relative importance of mineral association as opposed to aggregate-occlusion of OC in its stabilization in volcanic soils.

5.2.3 Model input data

One of the limitations of almost all mechanistic models is the need for a precise and large amount of input data (Sauer et al., 2012). The SoilGen model is a process-based soil genesis model. Thus, full information on soil forming factors (i.e. climate, organism, parent material, relief, and time) are required to run the model. However, such large amount of data is often scarce. In this study, the initial and boundary input data was collected from literature sources, field and laboratory measurements, climate model simulation, historical records, and queries to the government and farmers, which may be imprecise and influence the quality of the simulation.

As stated in **Chapter 4**, two limitations of this study are the imprecise quantity of parent materials and the use of field-estimated soil texture. Typically, parent material corresponds to C-horizon properties which are found to be unweathered at the bottom of the soil profile and used as the initial condition on a SoilGen simulation. In tropical climates, however, the weathering of volcanic ash typically occurs rapidly due to the high precipitation and warm climate. Thus, the C-horizon was no longer present in the field. In addition, there is no clear historical record on the number of minerals in parent materials and from eruptions that correspond to the present minerals in the study soils. The uncertainty of reconstructed parent materials could partly hinder the quality of the mineral calibration in the study. Thus, the need for the type and amount of parent material for input data is essential. Furthermore, using actual soil texture (i.e. laboratory soil data) in which the soils contain a high amount of clay particles will influence the hydrological processes (e.g. water flow and hydraulic conductivity) and ignore the occurrence of pseudo-sand and pseudo-silt microaggregates that influence both water retention and hydraulic conductivity. On the other hand, field-estimated soil texture is associated with uncertainty. Nevertheless, we found the optimum parameters in the clay migration process (e.g. $h-\theta$ macro, filter coefficient, and a maximum of splitting probability and soil temperature change) to be inside the range of reference values from literature. This indicates that field-estimated soil texture, whereby part of the fine material is assigned to (pseudo-)sand and silt can compensate the limitation of SoilGen to simulate pseudo-sand and pseudo-silt aggregates. The limitations regarding the uncertainty of initial soil formation and boundary conditions will influence SoilGen results and can partly explain the model deviation from measured data. More realistic input data will likely improve the quality and reliability of simulation output.

5.2.4 Model process coverage

Regarding the process coverage, the SoilGen model has been calibrated and encompassed sufficient soil processes in different climates and parent materials (e.g. Finke, 2010, 2012; Keyvanshokouhi et al., 2016; Ranathunga et al., 2022). In total, the SoilGen model is able to simulate 24 out of 32 reference soil groups (Opolot et al., 2015), to which we attempted to add the 25th: Andosols. However, some soil processes and features are not yet implemented in the current SoilGen model, such as the formation of secondary minerals and non-crystalline materials, vegetation development, and soil volume changes. These processes will be described sequentially in the following paragraphs.

The formation of non-crystalline materials is one of the main pedogenic processes in soils formed in volcanic materials (Shoji et al., 1993). The representation of non-crystalline materials, e.g. allophane, imogolite, and proto-imogolite, is essential in the simulation of volcanic soils due to their influence on the chemical and physical properties of these soils. Therefore, it is necessary to explore the formation of these minerals and their influence on other soil properties. The biggest challenge is related to the formation and chemistry of non-crystalline materials. Non-crystalline materials were formed after the release of elements, such as Si, Al, and Fe, from rapid weathering which is faster than the formation of crystalline minerals and results in the over-saturated metastable and non-crystalline materials in soil solution (Ugolini and Dahlgren, 2002). The preferential precipitation of non-crystalline materials is because the process of the nucleation of non-crystalline materials (more soluble) is kinetically preferred over crystalline minerals (less soluble phase) (Stumm, 1992). In addition, the structure of non-crystalline materials in volcanic soils is still under debate despite intensive research on this topic (Levard et al., 2012). The chemistry of non-crystalline materials and the conversion of the formation and development of non-crystalline materials to mathematical models are still limited and can be explored in future research. While the formation of secondary clay minerals in the SoilGen model has already been designed and studied by Opolot (2016), it still needs implementation and testing. The formation and presence of secondary minerals are important to be simulated as they influence cation exchange capacities, weathering of primary minerals, and clay migration process, so these processes should be incorporated. So far, the SoilGen model has been calibrated in various settings such as luvisols, alisols, calcisols and gypsisols in loess, cover sand and marine clays which indicates the ability of the model to simulate various primary and secondary minerals.

Regarding vegetation development, the annual plant biomass input (NPP) in the SoilGen model is estimated as a function of mean annual temperature and precipitation (Miami model; Lieth, 1975). In this model, currently, the relationships between soil properties and vegetation development are through annual litter input and plant uptake of cations (i.e. the relative amounts of K, Na, Mg, Ca, and Al taken up via transpiration stream). The effects of soil moisture, soil nutrient stress, and atmospheric CO₂ pressure to NPP were not simulated yet in the SoilGen model. Estimating the correct NPP is important as it affects the amount of carbon input into the soil and SOC stock. In SoilGen, NPP is estimated using Miami model, an empirical model predicting NPP from air temperature and precipitation). This model is simple and likely responses in vegetation NPP to climate change will be non-linear. In addition, the catastrophic event scenarios, e.g. forest fire, for the projection simulation might also be considered in the model. Integration of these processes into the SoilGen model will improve the model's ability to evaluate the effect of climate and land use on SOC. Such mechanisms

are important, particularly for forecasting future SOC. In general the amount and nature of below-ground C inputs is poorly known, although there is a growing consensus that these in particular contribute to formation of stable SOC. Rasse et al. (2005) already questioned in his landmark paper 'Is soil carbon mostly root carbon'? As a consequence, for any soil simulation exercise, including the one carried out in this PhD-research, more accurate knowledge on root biomass or more importantly rhizodeposition would be needed to improve reliability of model predictions.

Another challenge in most mechanistic soil models is the assumption that soil volume does not change over time (Sollins and Gregg, 2017). In a one-dimensional model, the volume change is indicated by the change in soil compartment thickness over time. Assuming a constant soil volume during the simulation of soil-forming processes can lead to a not negligible inaccuracy of the model output (Keyvanshokouhi et al., 2016). Generally, soil processes such as weathering, clay migration, or bioturbation will significantly affect bulk density. Thus, understanding the mechanisms that contribute to volume change and soil structure is required, and such mechanisms need to be incorporated into the SoilGen model. These processes will allow the model to simulate the influence of soil structure on SOC dynamics (e.g. physical protection of SOC in aggregates). In this study, the inaccuracy of simulated bulk density may partly influence SOC calibration, particularly for agricultural soil. However, this effect may not have a significant impact on the outcomes of this study because the soils contain highly stable aggregates and land use does not significantly affect bulk density (**Chapter 2**).

5.2.5 Model calibration

Calibrating soil formation over a long-time scale is challenging (Finke and Hutson, 2008; Minasny et al., 2015). In the SoilGen model, only two data points, e.g. initial (8000 yrs BP) and final state (0 yrs BP), are usually available, and the process parameters are usually adjusted to match the measured data in the final state. In our study, changing boundary conditions, e.g. land use, will affect the decay rate of SOC, thus the optimum calibrated parameters may not represent the decay rate of SOC in the intermediate stages. This effect may partially influence the results of the model. Short-time calibration or soil chrono-sequence studies are ways to address this challenge to avoid relying upon the result only in the final state.

5.3 Areas for future research

The research on the indirect effects of land use on SOC via geochemical properties in tropical volcanic soils is still limited and thus has great potential to be explored. Based on the results and conclusions obtained from this study, the following studies can be carried out.

5.3.1 Assessing the effect of different agricultural practices on geochemical soil properties.

As discussed in **Chapter 3**, the high amount of SOC in agricultural soils was possibly a result of the combination between the high amount of organic matter input (i.e. manure) and the role of short-range order aluminium. Agricultural practices have the potential to stimulate the formation of non-crystalline materials. However, detailed mechanisms on how agricultural practices stimulate the formation of non-crystalline materials are still unexplained, particularly in a tropical climate where

weathering and SOC decomposition occur fast. There may be important positive feedback between accumulation of SOM and formation of poorly crystalline Al in Andosols that has not been looked into to date. Borggaard et al. (1990) found that SOM has an inhibiting effect on the crystallization process of Al-oxides, similar to the anti-Gibbsitic effect, leading to polymerization rather than crystallization that is well-known for mineral surfaces. Kang et al. (2009) as well argued that SOM can inhibit the crystallization of Al, resulting in less crystalline Al-oxides, which are well known to be in turn adsorbents of organic matter. A study on the effect of different types of agricultural practices, particularly related to fertilizer and tillage intensity with similar climates and types of crops, may distinguish the effect of each agricultural practice on the presence of non-crystalline materials as well as SOC in tropical Andosols. In addition, it might be relevant to also include this double interaction between SOM and poorly crystalline Al in soil genesis simulation models, but such will firstly require further empirical proof.

5.3.2 Improving soil fractionation method and conversion of SOC fractions to SOC pool in the Roth-C model (Zimmermann et al., 2007) for tropical Andosols

The use of soil fractionation by Zimmermann et al. (2007) enables us to convert the SOC fractions into SOC pools in the Roth-C model. However, the procedure was not described precisely and led to individual laboratory-specific adjustments. Our experiment underlined some crucial steps that influence the quality and size of all fractions. However, limited samples in our study may not completely cover the variation of soil properties in tropical Andosols. By conducting analyses and experiments with more samples, the standard procedure of soil fractionation (Zimmermann et al., 2007) for tropical Andosols can be achieved. As explained in 5.2.1, steps that can be investigated are the application of different levels of ultrasonic energy, the minimum amount of water to isolate DOC, the density of SPT solution to separate POM and S+A fraction, and the concentration of NaOCl for isolating the rSOC fraction. Furthermore, a study on SOC equilibrium and model initialisation, e.g. the splitting ratio of DPM/RPM and BIO/HUM, for the Roth-C model in tropical Andosols can be a focus of future research. However, in the end, to test if measured soil fractions could be used to set SOC model pool partitioning or test model performance, we require long-term experiments in which management, climate, and importantly OC-inputs to soil are well described. Such experiments are still too scarce for tropical volcanic soils.

5.3.3 Calibrating of non-crystalline materials in tropical volcanic soil using chrono-sequence study

The occurrence and presence of non-crystalline materials are essential in modelling volcanic soils. Future studies can focus on defining the chemistry of non-crystalline materials, e.g. allophane and simulating the rate of elements released from weathering rock and the precipitation process. In addition, the simulated pH needs to mimic the pH in field conditions, as this property greatly contributes to the simulation of minerals weathering. The mechanism of pH dependent charge in a model context can also be investigated in future research. To validate the formation and development of non-crystalline materials, the study of soil in chrono-sequence on similar land use starting from the very young to intermediate age (e.g. recent eruption, 0.1, 0.5, 1, 2 kyr) can be conducted.

5.3.4 Improving soil-vegetation-climate simulation in the SoilGen model

The interactive mechanisms between soil, climate, and vegetation in the SoilGen model can be a focus for future research. Integrating a vegetation model into the SoilGen model is essential, particularly to forecast the future SOC. Some feedbacks that can be considered to be integrated in the SoilGen model are the impact of atmospheric CO₂ concentration on vegetation development and plant carbon input, the impact of changing vegetation on biogeochemical element cycling, the effect of evolving soil properties (e.g. pH, soil moisture) on vegetation development as well as the decay rate of SOC. These mechanisms certainly require collaboration with vegetation and climate modellers.

Authors contributions


This chapter was designed and written by Sastrika Anindita. Peter Finke and Steven Sleutel had a great contribution through providing extra materials for further referencing, interpreting the results, and reviewing this chapter.

Appendix for chapter 2

Table A2-1. Morphological properties of pedons in study soils

Horizon	Depth (cm)	Color (moist)	Texture ^a	Structure ^b	Consistency ^c	Boundary ^d	Special features
Primary forest (NF-y)		<i>dystric, sideralic, vitric, andic CAMBISOLS (aluminic, loamic)</i>					
Oe	-2-0					c, s	
Ah	0-8	7.5YR 1.7/1	ls	cr	vfr	c, s	
A2	8-17	10YR 3/4	sl	cr	vfr	c, s	Fine to medium gravel ± 5%
AE	17-27	10YR 4/4 and 10YR 6/1	l	1, gr	fr	c, s	Fine to medium gravel ± 5%
AB1	27-58	7.5YR 4/6	sil	1, gr	fr	g, w	
AB2	58-64	7.5YR 4/6	sil	2, gr	fi	g, s	
Bw	64-84	5YR 3/6	sil	2, gr + sb	fi	g, w	Very few black mottles (10YR2/1)
BC	84-118	7.5YR 5/8 and 10YR 6/8		3, r	efi	g, w	Concentration of boulders
2AB1	118-134	10YR 3/3	cl	2, sb	vfi	g, w	
2Bw	134-150	10YR 4/6	sil	2, sb	fi		

NF-y



Ah
AB
Bw
BC
2 AB

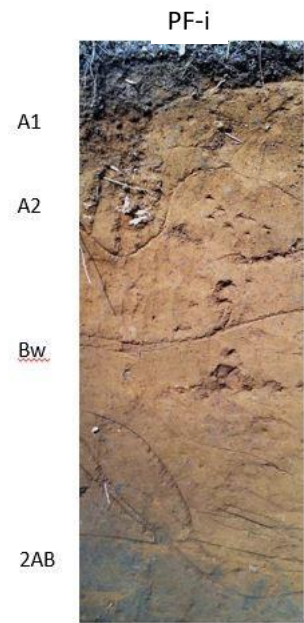
code: dy,se,vi,an CM (au,lo)

Horizon	Depth (cm)	Color (moist)	Texture ^a	Structure ^b	Consistency ^c	Boundary ^d	Special features	
Agriculture land (AG-y)		<i>eutric, aluandic ANDOSOLS (clayic, aric, sideralic)</i>						AG-y
Ap1	0-29	7.5YR 2/3	scl	1, gr	fr	c, s		Ap1
Ap2	29-45	10YR 4/4	sil	2, gr	fr	c, s	very few fine rounded Mn concretions	Ap2
Ap3	45-69	10YR 3/4	sil	2, gr	fr	g, w		
Bw	69-96	7.5YR 4/6	sil	1, sb	fi	c, s		
2AB	96-123	10YR 2/3	sc	1, sb	sfi	g, w		
2Bw1	123-148	10 YR 4/6	sc	2, gr	fi	g, w		
2Bw2	148-150	7.5YR 5/6	sil	2, gr	vfi			Bw
								2AB




code: eu,aa AN (ce,ai,se)

Horizon	Depth (cm)	Color (moist)	Texture ^a	Structure ^b	Consistency ^c	Boundary ^d	Special features
Pine forest (PF-i)		<i>dystric, sideralic, andic CAMBISOLS (alumic, clayic)</i>					
Oe	-3-0					c, s	
A1	0-15	10YR 3/3	sl	1, gr	vfr	g, s	
A2	15-45	7.5YR 4/3	sl	1, gr	fr	g, i	
Bw1	45-73	10YR 4/6	sil	2, gr	sfi	g, w	
Bw2	73-111	10YR 4/6	sil	2, sb	fi	g, i	Few (7.5YR 5/6) mottles, few medium Fe concretions
2AB1	111-139	10YR 3/3	scl	1, sb	sfi	c, s	Few (10YR 2/1) mottles
2AB2	139-150	10YR 2/2	sc	2, sb	fi	c, s	



code: dy,se,an CM (au,ce)

Horizon	Depth (cm)	Color (moist)	Texture ^a	Structure ^b	Consistency ^c	Boundary ^d	Special features	
Agriculture land (AG-i)		<i>eutric, aluandic ANDOSOLS (clayic, aric, sideralic)</i>						AG-i
Ap1	0-18	10YR 2/2	sl	1, gr	fr	g, s		
Ap2	18-54	10YR 2/3	scl	1, gr	sfi	g, w		
Bw	54-71	10YR 3/4	scl	1, sb	fi	c, s		
2AB	71-89	10YR1.7/1 and 10YR 2/3	sc	2, sb	fi	c, s		Few (10YR5/8) mottles
2Bw1	89-137	10YR ¾	scl	2, sb	fi	g, w		
2Bw2	137-152	10YR 4/6	scl	2, sb	fi	g, w		

code: eu,aa AN (ce,ai,se)

Horizon	Depth (cm)	Color (moist)	Texture ^a	Structure ^b	Consistency ^c	Boundary ^d	Special features
Pine forest (PF-o)		<i>dystric, aluandic ANDOSOLS (clayic, sideralic)</i>					
Oi	-2-0					c,s	
A1	0-9	7.5YR 3/4	sl	cr	vfr	c, s	
A2	9-27	7.5YR 4/6	scl	1, gr	fr	g, w	
AB1	27-66	10YR 5/6	scl	2, gr	sfi	g, w	Few (7.5YR 6/8) mottles
AB2	66-92	10YR 4/6	scl	2, sb	Fi	g, w	Few (7.5YR 5/6) mottles, few Mn concretions
2AB1	92-115	10YR 2/3	sil	1, sb	Fi	g, b	
2Bw1	115-121	10YR 5/6	scl	1, sb	Fi	g, w	
2Bw2	121-139	7.5YR 4/6	sc	1, sb	Fi	g, w	
2Bw3	139-175	10YR 4/6	sc	2, sb	vfi	g, s	Few (7.5YR 5/8) mottles



code: dy,aa AN (ce,se)

Horizon	Depth (cm)	Color (moist)	Texture ^a	Structure ^b	Consistency ^c	Boundary ^d	Special features
Agricultural land (AG-o)		<i>eutric, aluandic ANDOSOLS (clayic, aric, sideralic)</i>					
Ap1	0-13	7.5YR 2/3	sl	1, gr	fr	c, s	Presence of charcoal
Ap2	13-47	10YR 3/4	sl	1, gr	Fr	g, w	Few (10YR 6/8) mottles, presence of charcoal
Bw	47-81	7.5YR 5/6	sil	1, sb	Fi	g, w	
2AB	81-115	10YR 3/4	sil	2, sb	Fi	g, s	Few (10YR 5/8) mottles
2Bw	115-150	10YR 4/6	sil	2, sb	Fi		



code: eu,aa AN (ce,ai,se)

Abbreviations: ^aTexture: ls=loamy sand; sl=sandy loam; scl=sandy clay loam l-loam; sil=silt loam; sc=sandy clay; cl=clay loam. ^bStructure: 1=weak; 2=moderate; 3=strong; cr=crumb; gr=granular; sb=subangular blocky; r=rock. ^cConsistency: fr=friable; vfr=very friable; sfi=slightly firm; fi=firm; vfi=very firm; efi=extremely firm. ^dBoundary: a=abrupt; c=clear; g=gradual; d=diffuse; s=smooth; w=wavy; i=irregular. "code" refers to WRB2015 codes.

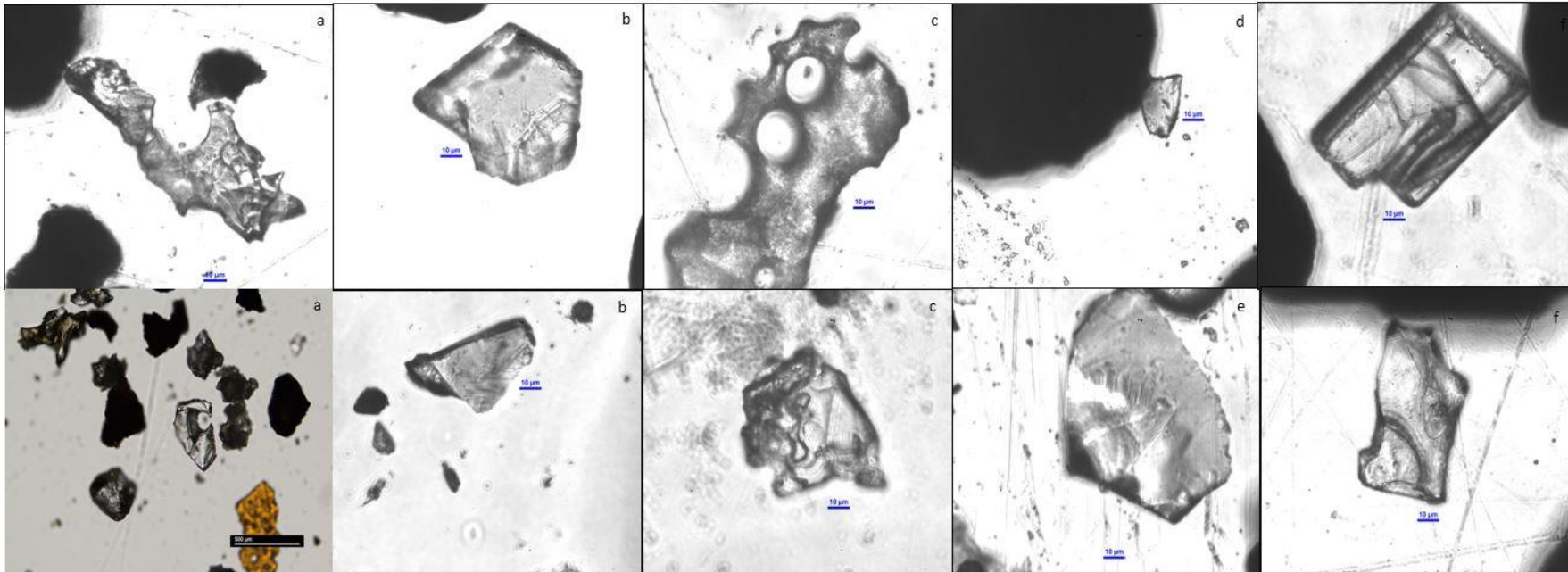


Figure A2-1. Volcanic glass found in topsoils at sites NF-y (a), AG-y (b), PF-i (c), AG-I (d), AG-o (d), PF-o (e) and AG-o (f)

Appendix for chapter 3

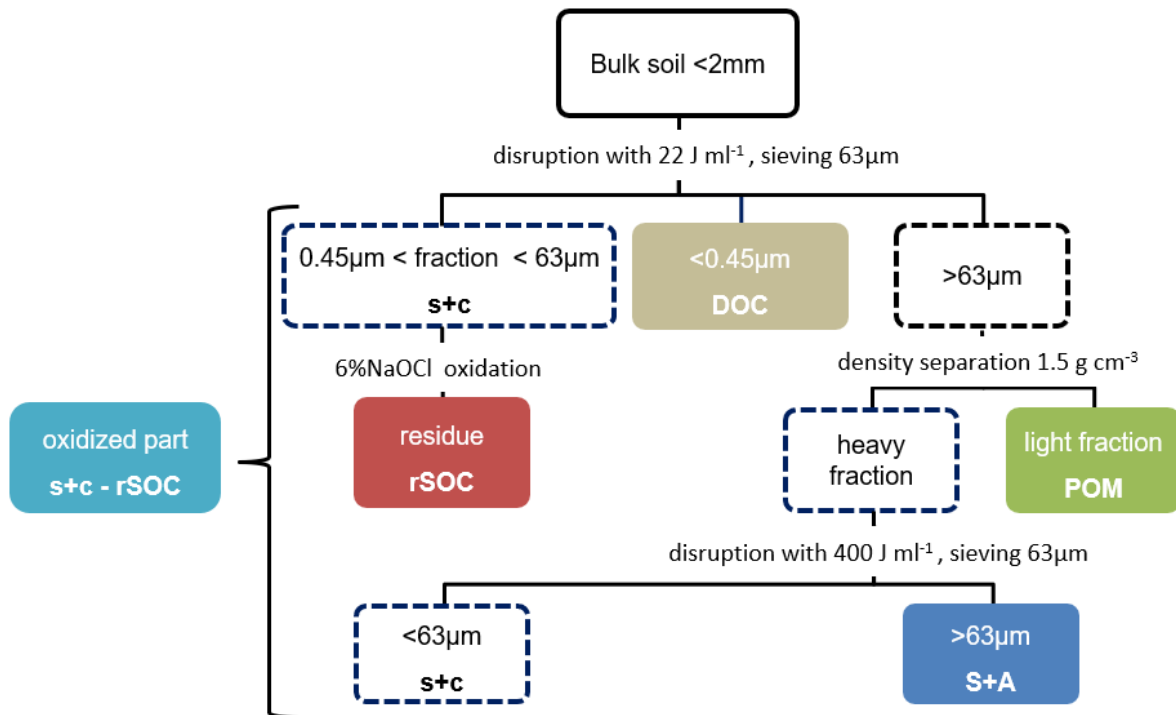


Figure A3-1. Schematic of the used soil fractionation procedure, based on the procedure by Zimmerman et al. (2007) but adapted to use with volcanic soils: 1) Free particulate organic matter (POM) in the > 63 µm fraction is separated by density at 1.5 g cm⁻³ instead of 1.8 g cm⁻³; 2) a second stronger ultrasonic dispersion step was introduced to separate the considerable > 63 µm heavy fraction into silt and clay (s+c) and sand and stable aggregates (S+A). The amount of chemically oxidizable C contained in silt and clay is not measured but calculated from the difference in C contained in both isolated s+c fractions and the C in the 6%NaOCl oxidation residue.

Appendix for chapter 4

Table A4-1. Plot and initial soil data

Sites	Current Landuse	Coordinate	Slope angle	Field estimated soil texture				Exchangeable cations					ECEC
				Sand	Silt	Clay	OC	Ca	K	Mg	Na	Al	
			°	Mass%fine earth				mmol kg ⁻¹ soil					
NF-y	Primary forest	6°46'15.69"S 107°37'21.98"E	15	40	46	14	0.001	1.27	0.13	0.42	0.30	20.56	22.70
PF-i	Pine forest	6°47'54.80"S 107°37'21.50"E	18	20	55	25	0.001	2.21	0.23	0.74	0.53	35.82	39.54
PF-o	Pine forest	6°45'38.50"S 107°31'3.00"E	18	50	20	30	0.001	2.66	0.28	0.89	0.30	20.56	47.45
AG-y	Agriculture	6°48'9.00"S 107°35'47.60"E	15	20	55	25	0.001	2.21	0.23	0.74	0.53	35.82	39.54
AG-i	Agriculture	6°48'48.60"S 107°38'30.30"E	16	40	35	25	0.001	2.21	0.23	0.74	0.53	35.82	39.54
AG-o	Agriculture	6°46'26.80"S 107°31'20.30"E	14	25	60	20	0.001	1.78	0.19	0.60	0.42	28.65	31.65

Table A4-2. Estimated plant carbon input and fertilization data

Sites	Time (yearsBP)	Plant input	Manure input	Fertilizer (organic+inorganic) input				Land use
				Ca	Mg	K	SO ₄	
		Mg ha ⁻¹ yr ⁻¹		Mol m ⁻² yr ⁻¹				
NF-y	8000 - 0	9.3 ¹	0					Deciduous forest
PF-i	8000 - 59	9.3	0					Deciduous forest
	58 - 0	6.5 ²	0					Coniferous forest
PF-o	10000 - 59	9.3	0					Deciduous forest
	59 - 49	8.0	0					Agroforestry: pine forest and coffee plantation
	49 - 0	6.5	0					Coniferous forest
AG-y	8000 - 103	9.3	0					Deciduous forest
	102 - 73	3.9 ³	0					Bamboo forest
	72 - 50	4 ⁴	0					Coffee plantation
	49 - 29	1.76	5.78	0.08	3.2	0.23	0.01	Agriculture
	28 - 10	1.76	9.63	0.14	5.39	0.32	0.02	Agriculture
	9 - 0	1.76	11.6	0.16	6.42	0.36	0.02	Agriculture
	AG-i	8000 - 103	9.3	0				Deciduous forest
	102 - 73	3.9	0					Bamboo forest
	72 - 40	4	0					Coffee plantation
	39 - 29	1.57	2.1	0.02	1.31	0.12	0.002	Agriculture
	28 - 14	1.57	4.2	0.05	2.63	0.19	0.005	Agriculture
AG-o	13 - 0	1.57	6.4	0.07	4.01	0.26	0.007	Agriculture
	10000 - 103	9.3	0					Deciduous wood
	102 - 73	6.5	0					Deciduous forest
	72 - 32	4	0					Coffee plantation
	31 - 25	1	2.2	0.02	1.41	0.10	0.002	Agriculture

	24 - 9	1	4.4	0.04	2.87	0.18	0.004	Agriculture
	9 - 0	1	6.8	0.07	4.45	0.27	0.006	Agriculture

¹Guillaume et al. (2018), Hertel et al. (2009); ²Bruijnzeel (1985); ³Christanty et al. (1996); ⁴Hairiah et al. (2006), Kumar (2008)

Table A4-3. The initial percentage of SOC pool in five and four-pool models

Sites	Five-pool model					Four pool model			
	DPM	RPM	HUM	BIO	IOM	DPM	RPM	HUM	BIO
	%								
NF-y	0.71	5.23	38.64	0.97	54.47	0.71	5.23	91.96	2.11
PF-i	0.09	0.66	49.88	1.05	48.33	0.09	0.66	97.21	2.05
PF-o	0.19	1.37	42.44	0.89	55.12	0.19	1.37	96.42	2.03
AG-y	0.02	0.15	60.65	1.27	37.90	0.02	0.15	97.77	2.06
AG-i	0.02	0.18	70.72	1.49	27.59	0.02	0.18	97.74	2.06
AG-o	0.16	1.16	60.17	1.27	37.25	0.16	1.16	96.66	2.03

Table A4-4. Initial mineral data

Minerals(%)	NF-y	PF-i	PF-o	AG-y	AG-i	AG-o
Quartz ¹	45.81	13.82	11.31	13.03	8.42	12.00
Hornblende	1.82	6.35	-	-	3.18	0.92
Gibbsite	0.51	7.25	14.01	2.79	9.40	1.86
Kaolinite	7.74	25.62	23.02	29.23	10.66	30.54
Anorthite ²	3.63	-	-	-	-	-
Albite	6.92	-	-	1.43	5.64	4.50
Alunite/Magnetite ³	5.43	4.21	2.18	-	3.37	2.21
Amorphous materials ⁴	28.13	42.76	48.28	53.53	60.53	47.97

¹Quartz mineral is a sum of tridymite, quartz, and cristobalite minerals

² Anorthite is only in site NF-y, it is the result of re-calculation of Andesine, which was classified into anorthite and albite

³Alunite is only in site NF-y, whereas in PFi, AGi, Pfo, and AGo have magnetite

⁴Amorphous materials are the amount of amorphous fraction estimated from the difference between obtained and the real amount of internal standard (Zincite 20%) after semi-quantification of crystalline minerals using BGMN Rietveld and Profex as user interface.

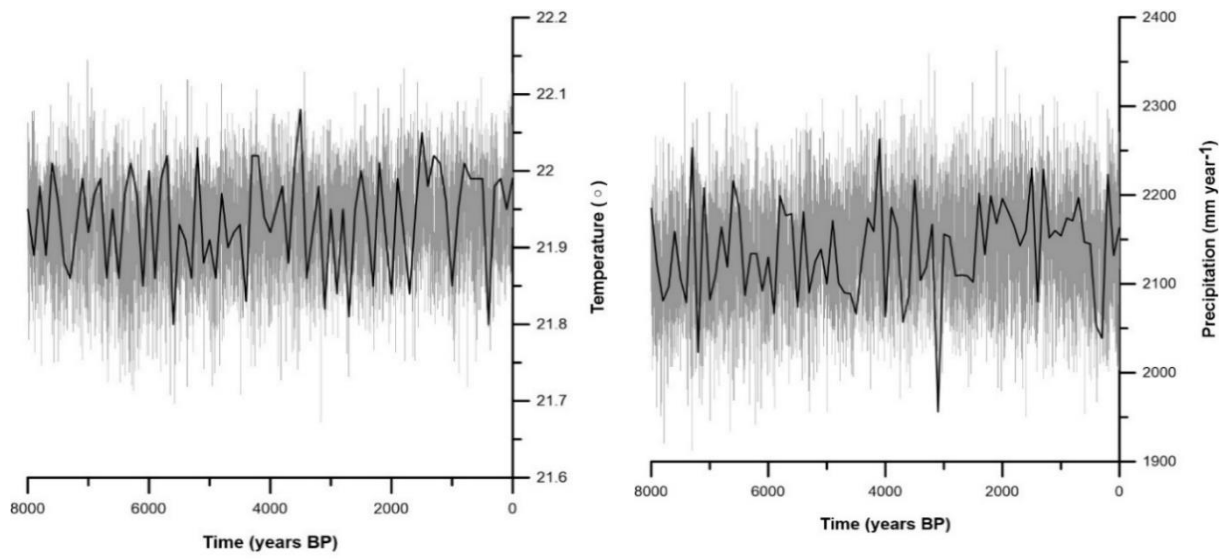


Figure A4-1. The average of temperature (left) and sum of precipitation (right) per year over all study sites from 8000 years BP until present time (0; year 2020). The black line showed the trend of temperature and precipitation per 100 years.

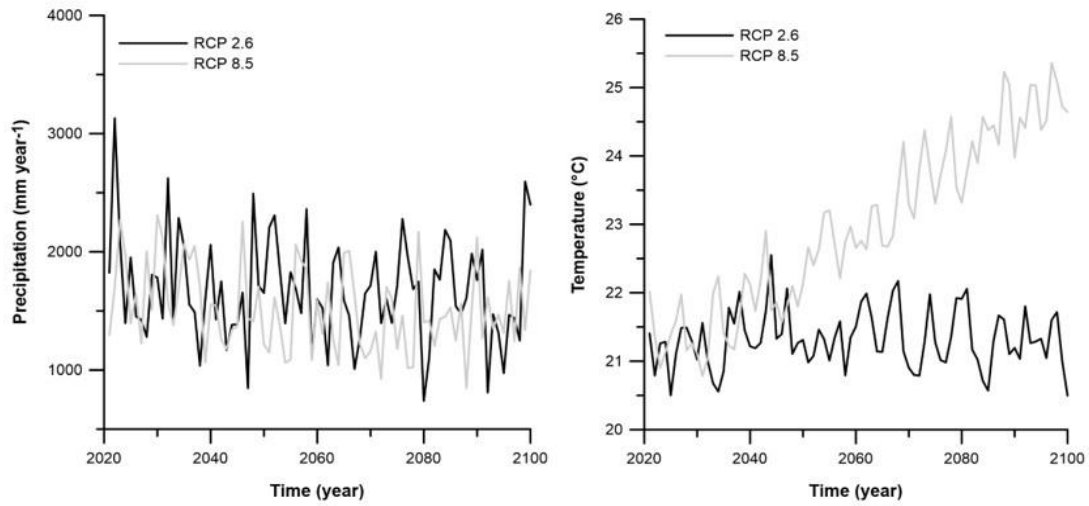


Figure A4-2. Projection of average precipitation and temperature under climate scenarios RCP 2.6 and RCP 8.5 in the study area

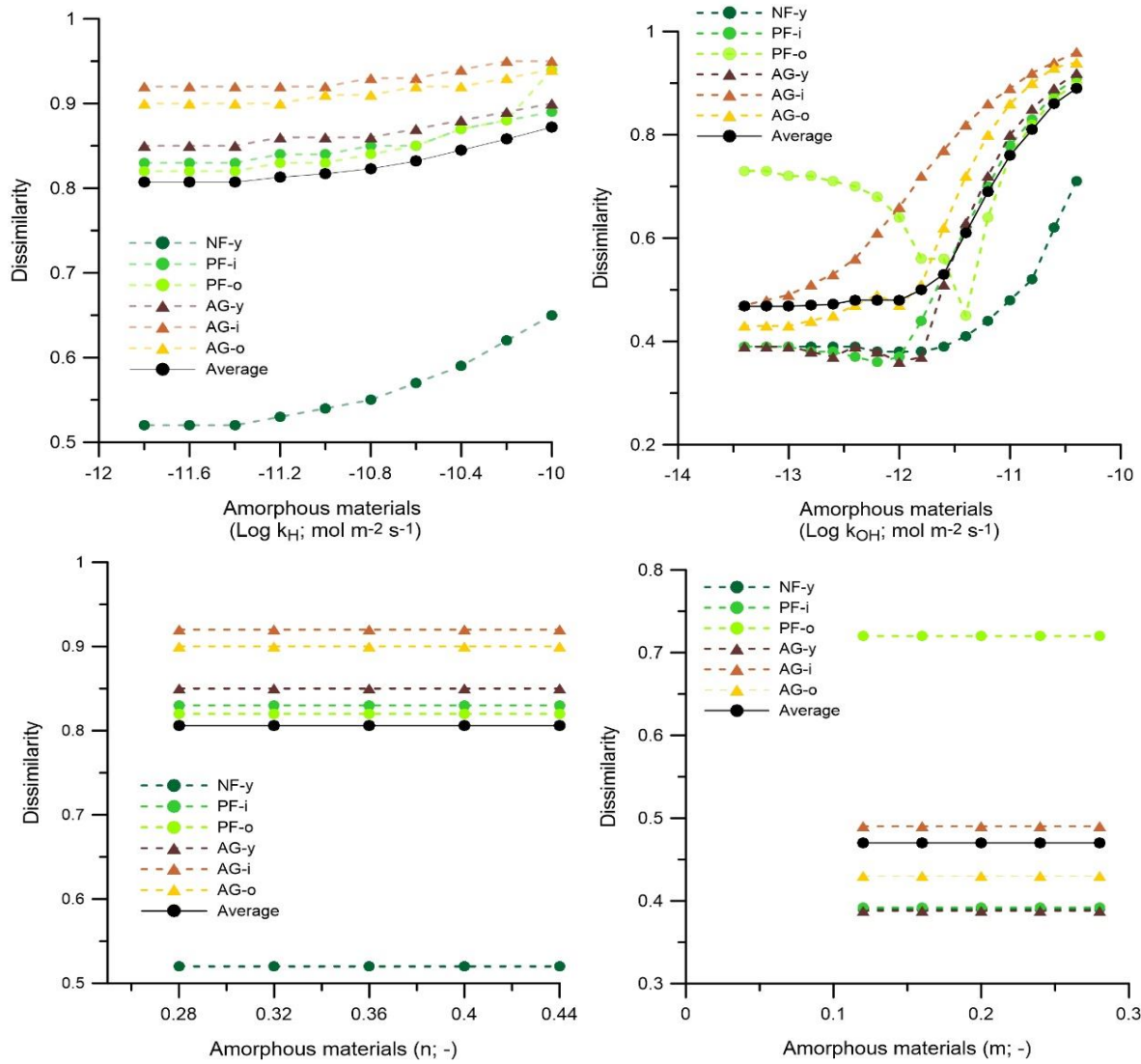


Figure A4-3. Variation of scaled dissimilarities in the calibration of amorphous materials weathering.

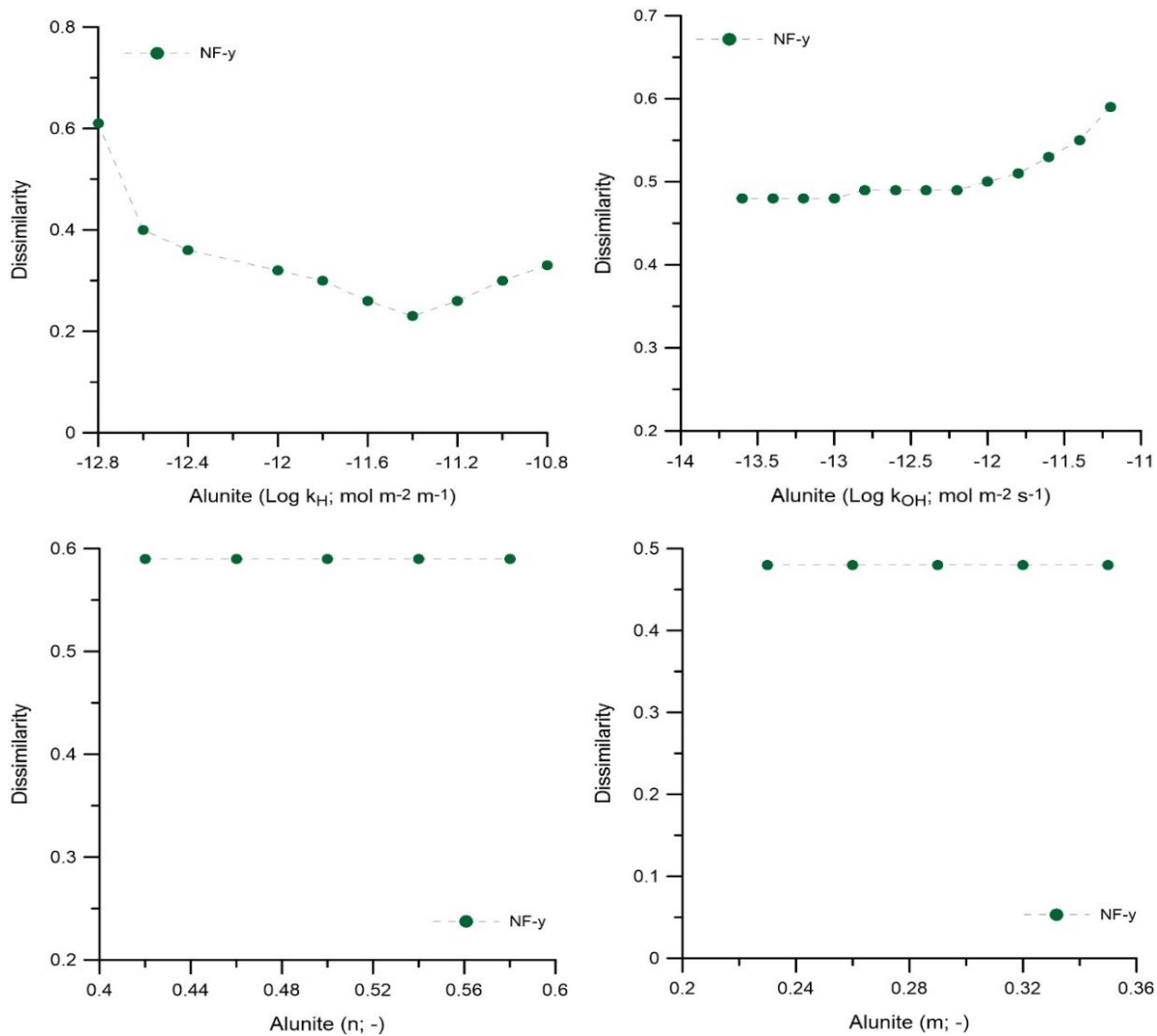


Figure A4-4. Variation of scaled dissimilarities in the calibration of alunite weathering

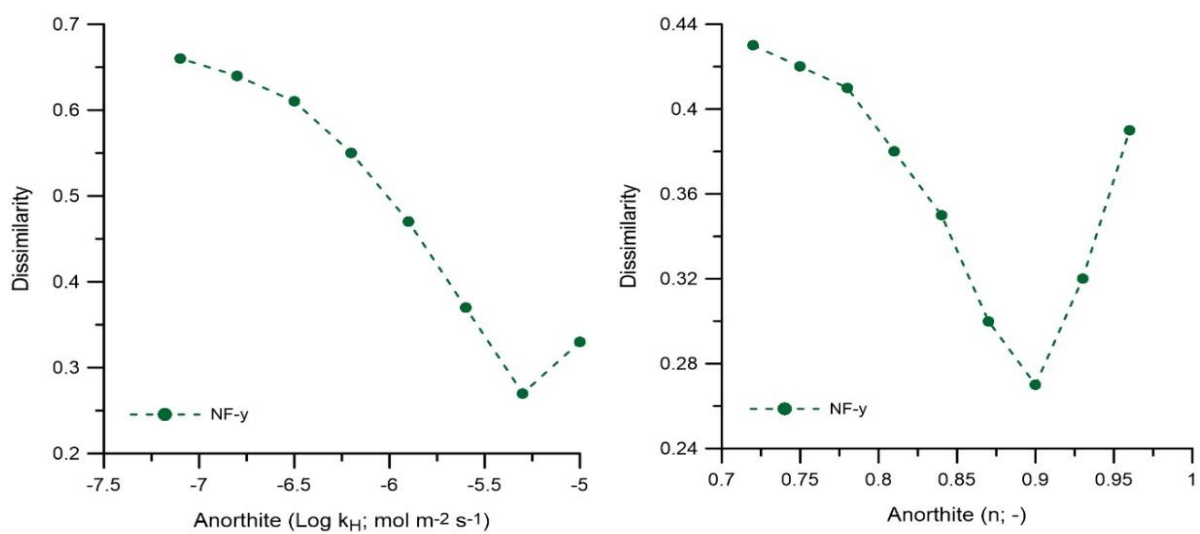


Figure A4-5. Variation of scaled dissimilarities in the calibration of anorthite weathering.

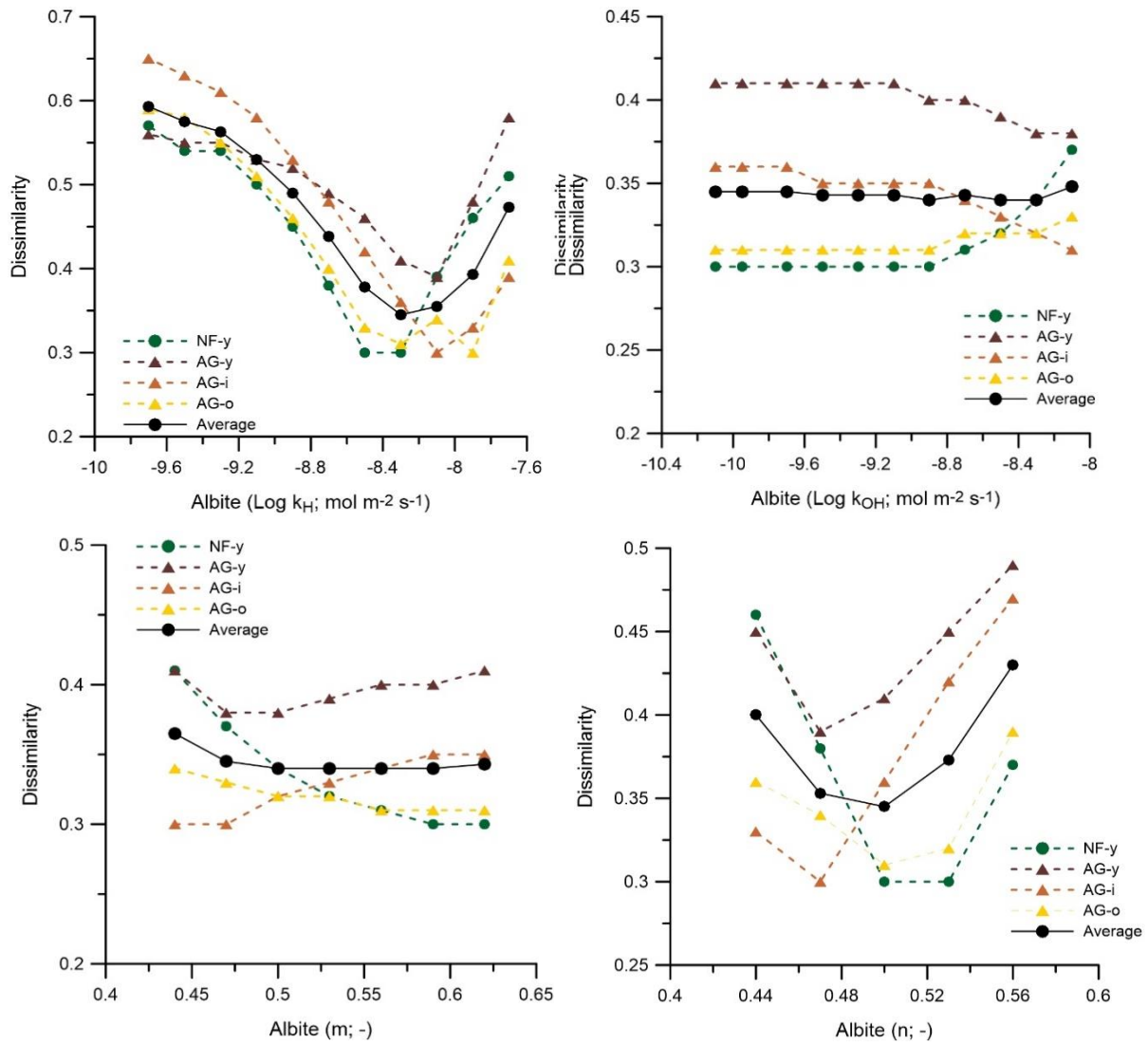


Figure A4-6. Variation of scaled dissimilarities in the calibration of albite weathering

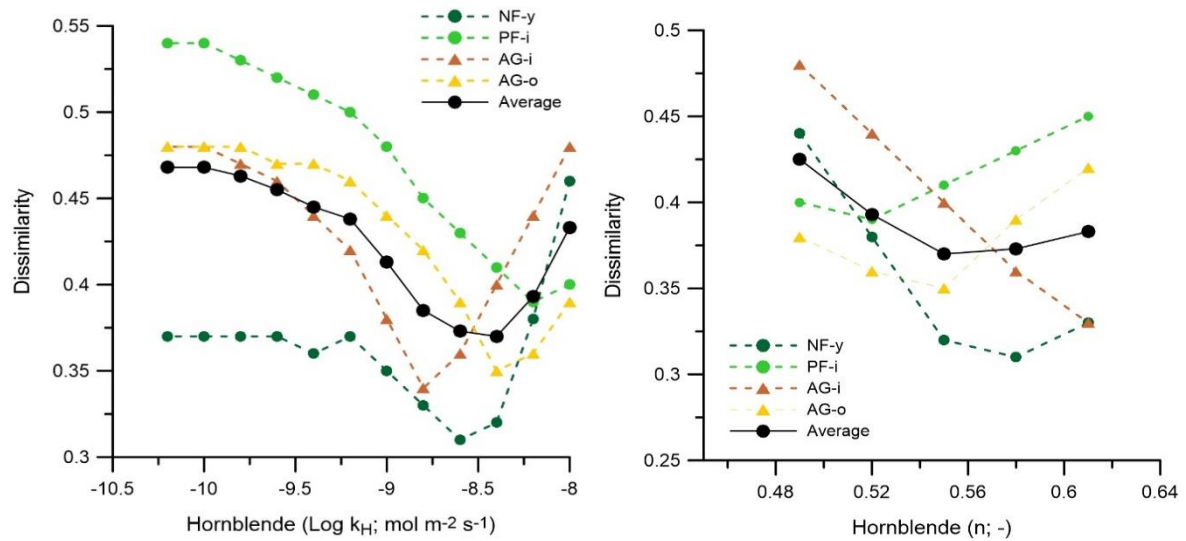


Figure A4-7. Variation of scaled dissimilarities in the calibration of hornblende weathering

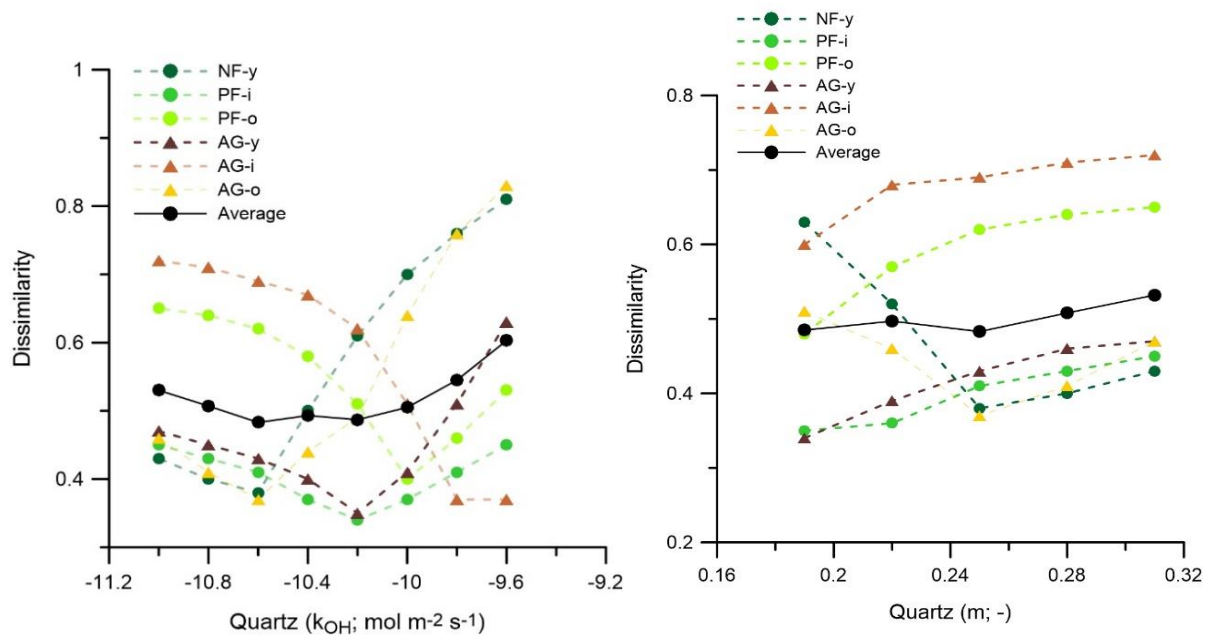


Figure A4-7. Variation of scaled dissimilarities in the calibration of quartz weathering

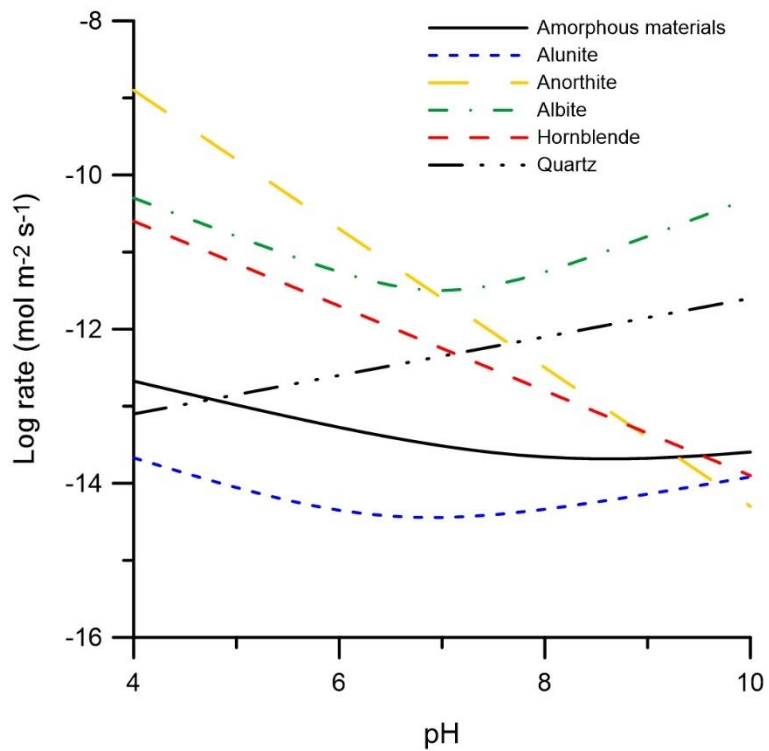


Figure A4-8. Comparison of calibrated weathering rates of primary minerals in the study soils at 25°C.

References

- Abera, G., Wolde-Meskel, E., 2013. Soil Properties, and Soil Organic Carbon Stocks of Tropical Andosol under Different Land Uses. *Open J. Soil Sci.* 03, 153–162. <https://doi.org/10.4236/ojss.2013.33018>
- Alekseeva, T. V., Sokolowska, Z., Hajnos, M., Alekseev, A.O., Kalinin, P.I., 2009. Water stability of aggregates in subtropical and tropical soils (Georgia and China) and its relationships with the mineralogy and chemical properties. *Eurasian Soil Sci.* 42, 415–425. <https://doi.org/10.1134/S1064229309040085>
- Anda, M., Dahlgren, R.A., 2020. Long-term response of tropical Andisol properties to conversion from rainforest to agriculture. *Catena* 194, 104679. <https://doi.org/10.1016/j.catena.2020.104679>
- Anda, M., Sarwani, M., 2012. Mineralogy, Chemical Composition, and Dissolution of Fresh Ash Eruption: New Potential Source of Nutrients. *Soil Sci. Soc. Am. J.* 76, 733–747. <https://doi.org/10.2136/sssaj2011.0305>
- Anderson, J.U., 1961. An Improved Pretreatment for Mineralogical Analysis of Samples Containing Organic Matter1. *Clays Clay Miner.* 10, 380–388. <https://doi.org/10.1346/ccmn.1961.0100134>
- Anindita, S., Finke, P., Sleutel, S., 2022a. Tropical Andosol organic carbon quality and degradability in relation to soil geochemistry as affected by land use. *SOIL* 1–23. <https://doi.org/https://doi.org/10.5194/soil-2022-13>
- Anindita, S., Sleutel, S., Vandenberghe, D., Grave, J. De, Vandenhende, V., Finke, P., 2022b. Land use impacts on weathering, soil properties, and carbon storage in wet Andosols, Indonesia. *Geoderma* 423, 115963. <https://doi.org/10.1016/j.geoderma.2022.115963>
- Araujo, M.A., Zinn, Y.L., Lal, R., 2017. Soil parent material, texture and oxide contents have little effect on soil organic carbon retention in tropical highlands. *Geoderma* 300, 1–10. <https://doi.org/10.1016/j.geoderma.2017.04.006>
- Arifin, M., 1994. Pedogenesis andisol berbahan induk abu vulkan andesit dan basalt pada beberapa zona agroklimat di daerah perkebunan teh Jawa Barat. Institut Pertanian Bogor.
- Asano, M., Wagai, R., 2015. Distinctive organic matter pools among particle-size fractions detected by solid-state ^{13}C -NMR, $\delta^{13}\text{C}$ and $\delta^{15}\text{N}$ analyses only after strong dispersion in an allophanic andisol. *Soil Sci. Plant Nutr.* 61, 242–248. <https://doi.org/10.1080/00380768.2014.982492>
- Asano, M., Wagai, R., 2014. Evidence of aggregate hierarchy at micro- to submicron scales in an allophanic andisol. *Geoderma* 216, 62–74. <https://doi.org/10.1016/j.geoderma.2013.10.005>
- Asano, M., Wagai, R., Yamaguchi, N., Takeichi, Y., Maeda, M., Suga, H., Takahashi, Y., 2018. In search of a binding agent: Nano-scale evidence of preferential carbon associations with poorly-crystalline mineral phases in physically-stable, clay-sized Aggregates. *Soil Syst.* 2, 32. <https://doi.org/10.3390/soilsystems2020032>
- Asio, V.B., Jahn, R., Stahr, K., 1999. Changes in the properties of a volcanic soil (Andisol) in Leyte due to conversion of forest to other land uses. *Philipp. J. Sci.* 128, 1–13.
- Balai Besar Litbang Sumberdaya Lahan Pertanian (BBSDLP), 2017. ATLAS PETA TANAH SEMI DETAIL Skala 1:50.000 Kabupaten Bandung Barat Provinsi Jawa Barat. Balai Besar Litbang Sumberdaya Lahan Pertanian, Bogor.
- Baldock, J.A., 2007. Composition and Cycling of Organic Carbon in Soil, in: Marschner, P., Rengel, Z. (Eds.), *Nutrient Cycling in Terrestrial Ecosystems*. Springer Berlin, Heidelberg, pp. 1–35. https://doi.org/10.1007/978-3-540-68027-7_1
- Bandstra, J.Z., Brantley, S.L., 2008. Data Fitting Techniques with Applications to Mineral Dissolution Kinetics, in: Brantley, S.L., Kubicki, J.D., White, A.F. (Eds.), *Kinetics of Water-Rock Interaction*. New York, pp. 211–257. https://doi.org/https://doi.org/10.1007/978-0-387-73563-4_6
- Bandyopadhyay, K.K., 2019. Effect of tillage on soil carbon sequestration, in: Ghosh, P., Mahanta, S., Mandal, D., Mandal, B., Ramakrishnan, S. (Eds.), *Carbon Management in Tropical and Sub-Tropical Terrestrial Systems*. Springer, Singapore, pp. 213–229. https://doi.org/10.1007/978-981-13-9628-1_13
- Bartoli, F., Burtin, G., Herbillon, A.J., 1991. Disaggregation and clay dispersion of Oxisols: Na resin, a

- recommended methodology. *Geoderma* 49, 301–317. [https://doi.org/10.1016/0016-7061\(91\)90082-5](https://doi.org/10.1016/0016-7061(91)90082-5)
- Basile-Doelsch, I., Amundson, R., Stone, W.E.E., Borschneck, D., Bottero, J.Y., Moustier, S., Masin, F., Colin, F., 2007. Mineral control of carbon pools in a volcanic soil horizon. *Geoderma* 137, 477–489. <https://doi.org/10.1016/j.geoderma.2006.10.006>
- Basile-Doelsch, I., Amundson, R., Stone, W.E.E., Masiello, C.A., Bottero, J.Y., Colin, F., Masin, F., Borschneck, D., Meunier, J.D., 2005. Mineralogical control of organic carbon dynamics in a volcanic ash soil on La Réunion. *Eur. J. Soil Sci.* 56, 689–703. <https://doi.org/10.1111/j.1365-2389.2005.00703.x>
- Basile-Doelsch, I., Balesdent, J., Rose, J., 2015. Are interactions between organic compounds and nanoscale weathering minerals the key drivers of carbon storage in soils? *Environ. Sci. Technol.* 49, 3997–3998. <https://doi.org/10.1021/acs.est.5b00650>
- Beare, M.H., McNeill, S.J., Curtin, D., Parfitt, R.L., Jones, H.S., Dodd, M.B., Sharp, J., 2014. Estimating the organic carbon stabilisation capacity and saturation deficit of soils: A New Zealand case study. *Biogeochemistry* 120, 71–87. <https://doi.org/10.1007/s10533-014-9982-1>
- Berg, B., McClaugherty, C., 2003. *Plant litter: decomposition, humus formation, carbon sequestration*, Third. ed. Springer Berlin Heidelberg, Berlin, Heidelberg.
- Bergmann, J., Fridel, P., Kleeberg, R., 1998. BGMN- a new fundamental parameter based Rietveld program for laboratory X-ray sources, its use in quantitative analysis and structure investigations. *CPD Newsletter, Comm. Powder Diffraction, Int. Union Crystallogr.* 20, 5–8.
- Besnard, E., Chenu, C., Balesdent, J., Puget, P., Arrouays, D., 1996. Fate of particulate organic matter in soil aggregates during cultivation. *Eur. J. Soil Sci.* 47, 495–503. <https://doi.org/10.1111/j.1365-2389.1996.tb01849.x>
- Bétard, F., 2021. Insects as zoogeomorphic agents: an extended review. *Earth Surf. Process. Landforms* 46, 89–109. <https://doi.org/10.1002/esp.4944>
- Birkeland, P.W., 1999. *Soils and Geomorphology*, 3rd ed. Oxford University Press, New York.
- Blagodatskaya, E., Khomyakov, N., Myachina, O., Bogomolova, I., Blagodatsky, S., Kuzyakov, Y., 2014. Microbial interactions affect sources of priming induced by cellulose. *Soil Biol. Biochem.* 74, 39–49. <https://doi.org/10.1016/j.soilbio.2014.02.017>
- Blake, G.R., Hartge, K.H., 1986. Bulk density, in: Klute, A. (Ed.), *Methods of Soil Analysis, Part I. Physical and Mineralogical Methods*. ASA SSSA, Madison, WI, pp. 74–75. <https://doi.org/10.2136/sssabookser5.1.2ed.c13>
- Blakemore, L., Searle, P., Daly, B., 1981. *Methods for chemical analysis of soils*. <https://doi.org/10.1111/aos.12317>
- Blanco-Canqui, H., Lal, R., 2004. Mechanisms of carbon sequestration in soil aggregates. *CRC. Crit. Rev. Plant Sci.* 23, 481–504. <https://doi.org/10.1080/07352680490886842>
- Boddy, E., Roberts, P., Hill, P.W., Farrar, J., Jones, D.L., 2008. Turnover of low molecular weight dissolved organic C (DOC) and microbial C exhibit different temperature sensitivities in Arctic tundra soils. *Soil Biol. Biochem.* 40, 1557–1566. <https://doi.org/10.1016/j.soilbio.2008.01.030>
- Borggaard, O.K., Jørgensen, S.S., Møberg, J.P., Raben-Lange, B., 1990. Influence of organic matter on phosphate adsorption by aluminium and iron oxides in sandy soils. *J. Soil Sci.* 41, 443–449. <https://doi.org/10.1111/j.1365-2389.1990.tb00078.x>
- Brahy, V., Deckers, J., Delvaux, B., 2000. Estimation of soil weathering stage and acid neutralizing capacity in a toposequence Luvisol-Cambisol on loess under deciduous forest in Belgium. *Eur. J. Soil Sci.* 51, 1–13. <https://doi.org/10.1046/j.1365-2389.2000.00285.x>
- Brantley, S.L., 2008. Kinetics of mineral dissolution, in: Brantley, S., Kubicki, J., White, A. (Eds.), *Kinetics of Water-Rock Interaction*. Springer, New York, pp. 151–210. https://doi.org/10.1007/978-0-387-73563-4_5
- Brantley, S.L., 2003. Reaction Kinetics of Primary Rock-forming Minerals under Ambient Conditions. *Treatise on Geochemistry* 5–9, 73–117. <https://doi.org/10.1016/B0-08-043751-6/05075-1>
- Brantley, S.L., Mellott, N.P., 2000. Surface Area and Porosity of Silicates. *Am. Mineral.* 85, 1767–1783.

- Brown, L.C., Foster, G.R., 1986. Storm erosivity using idealized intensity distributions. *Trans. ASAE* 30, 379–386. <https://doi.org/http://dx.doi.org/10.13031/2013.31957>
- Brubaker, S.C., Holzhey, C.S., Brasher, B.R., 1992. Estimating the Water-Dispersible Clay Content of Soils. *Soil Sci. Soc. Am. J.* 56, 1226–1232. <https://doi.org/10.2136/sssaj1992.03615995005600040036x>
- Bruijnzeel, L.A., 1985. Nutrient Content of Litterfall in Coniferous Forest Plantations in Central Java, Indonesia. *J. Trop. Ecol.* 1, 353–372.
- Bruun, T.B., Elberling, B., Christensen, B.T., 2010. Lability of soil organic carbon in tropical soils with different clay minerals. *Soil Biol. Biochem.* 42, 888–895. <https://doi.org/10.1016/j.soilbio.2010.01.009>
- Candan, F., Broquen, P., 2009. Aggregate stability and related properties in NW Patagonian Andisols. *Geoderma* 154, 42–47. <https://doi.org/10.1016/j.geoderma.2009.09.010>
- Cerli, C., Celi, L., Kalbitz, K., Guggenberger, G., Kaiser, K., 2012. Separation of light and heavy organic matter fractions in soil - Testing for proper density cut-off and dispersion level. *Geoderma* 170, 403–416. <https://doi.org/10.1016/j.geoderma.2011.10.009>
- Chadwick, O.A., Gavenda, R.T., Kelly, E.F., Ziegler, K., Olson, C.G., Crawford Elliott, W., Hendricks, D.M., 2003. The impact of climate on the biogeochemical functioning of volcanic soils. *Chem. Geol.* 202, 195–223. <https://doi.org/10.1016/j.chemgeo.2002.09.001>
- Chartres, C.J., Van Reuler, H., 1985. Mineralogical changes with depth in a layered Andosol near Bandung, Java (Indonesia). *J. Soil Sci.* 36, 173–186. <https://doi.org/https://doi.org/10.1111/j.1365-2389.1985.tb00322.x>
- Chen, R., Senbayram, M., Blagodatsky, S., Myachina, O., Dittert, K., Lin, X., Blagodatskaya, E., Kuzyakov, Y., 2014. Soil C and N availability determine the priming effect: Microbial N mining and stoichiometric decomposition theories. *Glob. Chang. Biol.* 20, 2356–2367. <https://doi.org/10.1111/gcb.12475>
- Chenu, C., Angers, D.A., Barré, P., Derrien, D., Arrouays, D., Balesdent, J., 2019. Increasing organic stocks in agricultural soils: Knowledge gaps and potential innovations. *Soil Tillage Res.* 188, 41–52. <https://doi.org/10.1016/j.still.2018.04.011>
- Chenu, C., Plante, A.T., 2006. Clay-sized organo-mineral complexes in a cultivation chronosequence: Revisiting the concept of the “primary organo-mineral complex.” *Eur. J. Soil Sci.* 57, 596–607. <https://doi.org/10.1111/j.1365-2389.2006.00834.x>
- Churchman, G.J., Lowe, D.J., 2012. Alteration, formation, and occurrence of minerals in soils, in: Huang, P.M., Li, Y., Sumner, M.E. (Eds.), *Handbook of Soil Sciences*. CRC Press (Taylor & Francis), Boca Raton, FL, pp. 20.1-20.72.
- Churchman, G.J., Singh, M., Schapel, A., Sarkar, B., Bolan, N., 2020. Clay Minerals As the Key To the Sequestration of Carbon in Soils. *Clays Clay Miner.* 68, 135–143. <https://doi.org/10.1007/s42860-020-00071-z>
- Coleman, K., Jenkinson, D.S., 1999. RothC 26.3 - A Model for the turnover of carbon in soil: Model description and Windows Users Guide. Harpenden. https://doi.org/10.1007/978-3-642-61094-3_17
- Conant, R.T., Ryan, M.G., Ågren, G.I., Birge, H.E., Davidson, E.A., Eliasson, P.E., Evans, S.E., Frey, S.D., Giardina, C.P., Hopkins, F.M., Hyvönen, R., Kirschbaum, M.U.F., Lavelle, J.M., Leifeld, J., Parton, W.J., Megan Steinweg, J., Wallenstein, M.D., Martin Wetterstedt, J.Å., Bradford, M.A., 2011. Temperature and soil organic matter decomposition rates - synthesis of current knowledge and a way forward. *Glob. Chang. Biol.* 17, 3392–3404. <https://doi.org/10.1111/j.1365-2486.2011.02496.x>
- Cornu, S., Montagne, D., Hubert, F., Barré, P., Caner, L., 2012. Evidence of short-term clay evolution in soils under human impact. *Comptes Rendus - Geosci.* 344, 747–757. <https://doi.org/10.1016/j.crte.2012.09.005>
- Covalada, S., Gallardo, J.F., García-Oliva, F., Kirchmann, H., Prat, C., Bravo, M., Etchevers, J.D., 2011. Land-use effects on the distribution of soil organic carbon within particle-size fractions of

- volcanic soils in the Transmexican Volcanic Belt (Mexico). *Soil Use Manag.* 27, 186–194. <https://doi.org/10.1111/j.1475-2743.2011.00341.x>
- Cox, P.M., Betts, R.A., Jones, C.D., Spall, S.A., Totterdell, I.J., 2000. Acceleration of global warming due to carbon-cycle feedbacks in a coupled climate model. *Nature* 408, 184–187. <https://doi.org/https://doi.org/10.1038/35041539>
- Craswell, E.T., Lefroy, R.D.B., 2001. The role and function of organic matter in tropical soils. *Nutr. Cycl. Agroecosystems* 61, 7–18. <https://doi.org/10.1023/A:1013656024633>
- Cronan, C.S., 2018. *Ecosystem Biogeochemistry*, *Ecosystem Biogeochemistry*. Springer, Orono, USA.
- Crowther, T.W., Todd-Brown, K.E.O., Rowe, C.W., Wieder, W.R., Carey, J.C., MacHmuller, M.B., Snoek, B.L., Fang, S., Zhou, G., Allison, S.D., Blair, J.M., Bridgham, S.D., Burton, A.J., Carrillo, Y., Reich, P.B., Clark, J.S., Classen, A.T., Dijkstra, F.A., Elberling, B., Emmett, B.A., Estiarte, M., Frey, S.D., Guo, J., Harte, J., Jiang, L., Johnson, B.R., Kroël-Dulay, G., Larsen, K.S., Laudon, H., Lavalley, J.M., Luo, Y., Lupascu, M., Ma, L.N., Marhan, S., Michelsen, A., Mohan, J., Niu, S., Pendall, E., Peñuelas, J., Pfeifer-Meister, L., Poll, C., Reinsch, S., Reynolds, L.L., Schmidt, I.K., Sistla, S., Sokol, N.W., Templer, P.H., Treseder, K.K., Welker, J.M., Bradford, M.A., 2016. Quantifying global soil carbon losses in response to warming. *Nature* 540, 104–108. <https://doi.org/10.1038/nature20150>
- Cusack, D.F., Chadwick, O.A., Ladefoged, T., Vitousek, P.M., 2013. Long-term effects of agriculture on soil carbon pools and carbon chemistry along a Hawaiian environmental gradient. *Biogeochemistry* 112, 229–243. <https://doi.org/10.1007/s10533-012-9718-z>
- Cyle, K.T., Hill, N., Young, K., Jenkins, T., Hancock, D., Schroeder, P.A., Thompson, A., 2016. Substrate quality influences organic matter accumulation in the soil silt and clay fraction. *Soil Biol. Biochem.* 103, 138–148. <https://doi.org/10.1016/j.soilbio.2016.08.014>
- Dahlgren, R.A., Saigusa, M., Ugolini, F.C., 2004. The Nature, Properties and Management of Volcanic Soils. *Adv. Agron.* 82, 113–182. [https://doi.org/10.1016/S0065-2113\(03\)82003-5](https://doi.org/10.1016/S0065-2113(03)82003-5)
- Dam, M.A.C., Suparan, P., Nossin, J.J., Voskuil, R.P.G.A., GTL Group, 1996. A chronology for geomorphological developments in the greater Bandung area, West-Java, Indonesia, *Journal of Southeast Asian Earth Sciences*. [https://doi.org/10.1016/S0743-9547\(96\)00069-4](https://doi.org/10.1016/S0743-9547(96)00069-4)
- Davidson, E.A., Janssens, I.A., 2006. Temperature sensitivity of soil carbon decomposition and feedbacks to climate change. *Nature* 440, 165–173. <https://doi.org/10.1038/nature04514>
- De Clercq, T., Heiling, M., Dercon, G., Resch, C., Aigner, M., Mayer, L., Mao, Y., Elsen, A., Steier, P., Leifeld, J., Merckx, R., 2015. Predicting soil organic matter stability in agricultural fields through carbon and nitrogen stable isotopes. *Soil Biol. Biochem.* 88, 29–38. <https://doi.org/10.1016/j.soilbio.2015.05.011>
- Dec, D., Dörner, J., Balocchi, O., López, I., 2012. Temporal dynamics of hydraulic and mechanical properties of an Andosol under grazing. *Soil Tillage Res.* 125, 44–51. <https://doi.org/10.1016/j.still.2012.05.018>
- Delvaux, B., Herbillon, A.J., Vielvoye, L., 1989. Characterization of a weathering sequence of soils derived from volcanic ash in Cameroon. Taxonomic, mineralogical and agronomic implications. *Geoderma* 45, 375–388. [https://doi.org/10.1016/0016-7061\(89\)90017-7](https://doi.org/10.1016/0016-7061(89)90017-7)
- Derrien, D., Plain, C., Courty, P.E., Gelhaye, L., Moerdijk-Poortvliet, T.C.W., Thomas, F., Versini, A., Zeller, B., Koutika, L.S., Boschker, H.T.S., Epron, D., 2014. Does the addition of labile substrate destabilise old soil organic matter? *Soil Biol. Biochem.* 76, 149–160. <https://doi.org/10.1016/j.soilbio.2014.04.030>
- Di, J., Feng, W., Zhang, W., Cai, A., Xu, M., 2017. Soil organic carbon saturation deficit under primary agricultural managements across major croplands in China. *Ecosyst. Heal. Sustain.* 3. <https://doi.org/10.1080/20964129.2017.1364047>
- Doebelin, N., Kleeberg, R., 2015. Profex: A graphical user interface for the Rietveld refinement program BGMN. *J. Appl. Crystallogr.* 48, 1573–1580. <https://doi.org/10.1107/S1600576715014685>
- Doetterl, S., Berhe, A.A., Arnold, C., Bodé, S., Fiener, P., Finke, P., Fuchslueger, L., Griepentrog, M., Harden, J.W., Nadeu, E., Schnecker, J., Six, J., Trumbore, S., Van Oost, K., Vogel, C., Boeckx, P.,

2018. Links among warming, carbon and microbial dynamics mediated by soil mineral weathering. *Nat. Geosci.* 11, 589–593. <https://doi.org/10.1038/s41561-018-0168-7>
- Doetterl, S., Stevens, A., Six, J., Merckx, R., Van Oost, K., Casanova Pinto, M., Casanova-Katny, A., Muñoz, C., Boudin, M., Zagal Venegas, E., Boeckx, P., 2015. Soil carbon storage controlled by interactions between geochemistry and climate. *Nat. Geosci.* 8, 780–783. <https://doi.org/10.1038/ngeo2516>
- Don, A., Schumacher, J., Freibauer, A., 2011. Impact of tropical land-use change on soil organic carbon stocks - a meta-analysis. *Glob. Chang. Biol.* <https://doi.org/10.1111/j.1365-2486.2010.02336.x>
- Dörner, J., Dec, D., Feest, E., Vásquez, N., Díaz, M., 2012. Dynamics of soil structure and pore functions of a volcanic ash soil under tillage. *Soil Tillage Res.* 125, 52–60. <https://doi.org/10.1016/j.still.2012.05.019>
- Droogers, P., Bouma, J., 1997. Soil Survey Input in Exploratory Modeling of Sustainable Soil Management Practices. *Soil Sci. Soc. Am. J.* 61, 1704–1710. <https://doi.org/10.2136/sssaj1997.03615995006100060023x>
- Du, Z. liu, Wu, W. liang, Zhang, Q. zhong, Guo, Y. bin, Meng, F. qiao, 2014. Long-Term Manure Amendments Enhance Soil Aggregation and Carbon Saturation of Stable Pools in North China Plain. *J. Integr. Agric.* 13, 2276–2285. [https://doi.org/10.1016/S2095-3119\(14\)60823-6](https://doi.org/10.1016/S2095-3119(14)60823-6)
- Dümig, A., Smittenberg, R., Kögel-Knabner, I., 2011. Concurrent evolution of organic and mineral components during initial soil development after retreat of the Damma glacier, Switzerland. *Geoderma* 163, 83–94. <https://doi.org/10.1016/j.geoderma.2011.04.006>
- Dungait, J.A.J., Hopkins, D.W., Gregory, A.S., Whitmore, A.P., 2012. Soil organic matter turnover is governed by accessibility not recalcitrance. *Glob. Chang. Biol.* 18, 1781–1796. <https://doi.org/10.1111/j.1365-2486.2012.02665.x>
- Edwards, A.P., Bremner, J.M., 1967. Dispersion of soil particles by sonic vibration. *J. Soil Sci.* 18, 47–63. <https://doi.org/https://doi.org/10.1111/j.1365-2389.1967.tb01487.x>
- Eswaran, H., Berg, E. Van Den, Reich, P., 1993. Organic carbon in soils of the world. *Soil Sci. Am. J.* 57, 192–194.
- Ferguson, J.H.A., 1954. Growth and yield of *Pinus merkusii* in Indonesia. *Netherlands J. Agric. Sci.* 2, 197–208. <https://doi.org/10.18174/njas.v2i3.17843>
- Finke, P., 2010. Modelling soil formation along a loess toposequence, in: *World Congress of Soil Science, Soil Solutions for a Changing World*. Brisbane.
- Finke, P., Opolot, E., Balesdent, J., Berhe, A.A., Boeckx, P., Cornu, S., Harden, J., Hatté, C., Williams, E., Doetterl, S., 2019. Can SOC modelling be improved by accounting for pedogenesis? *Geoderma* 338, 513–524. <https://doi.org/10.1016/j.geoderma.2018.10.018>
- Finke, P.A., 2012. Modeling the genesis of luvisols as a function of topographic position in loess parent material. *Quat. Int.* 265, 3–17. <https://doi.org/10.1016/j.quaint.2011.10.016>
- Finke, P.A., Hutson, J.L., 2008. Modelling soil genesis in calcareous loess. *Geoderma* 145, 462–479. <https://doi.org/10.1016/j.geoderma.2008.01.017>
- Finke, P.A., Samouëlian, A., Suarez-Bonnet, M., Laroche, B., Cornu, S.S., 2015. Assessing the usage potential of SoilGen2 to predict clay translocation under forest and agricultural land uses. *Eur. J. Soil Sci.* 66, 194–205. <https://doi.org/10.1111/ejss.12190>
- Fornara, D.A., Steinbeiss, S., Mcnamara, N.P., Gleixner, G., Oakley, S., Poulton, P.R., Macdonald, A.J., Bardgett, R.D., 2011. Increases in soil organic carbon sequestration can reduce the global warming potential of long-term liming to permanent grassland. *Glob. Chang. Biol.* 17, 1925–1934. <https://doi.org/10.1111/j.1365-2486.2010.02328.x>
- Gerzabek, M.H., Bajraktarevic, A., Keiblinger, K., Mentler, A., Rechberger, M., Tintner, J., Wriessnig, K., Gartner, M., Valenzuela, X.S., Troya, A., Couenberg, P.M., Jäger, H., Carrión, J.E., Zehetner, F., 2019. Agriculture changes soil properties on the Galápagos Islands-two case studies. *Soil Res.* 57, 201–214. <https://doi.org/10.1071/SR18331>
- Gijsman, A.J., Sanz, J.I., 1998. Soil organic matter pools in a volcanic-ash soil under fallow or cultivation with applied chicken manure. *Eur. J. Soil Sci.* 49, 427–436. <https://doi.org/10.1046/j.1365->

2389.1998.4930427.x

- Gillman, G.P., Sumpter, E.A., 1986. Modification to the compulsive exchange method for measuring exchange characteristics of soils. *Aust. J. Soil Res.* 24, 61–66. <https://doi.org/10.1071/SR9860061>
- Giorgetta, M.A., Jungclaus, J., Reick, C.H., Legutke, S., Bader, J., Böttinger, M., Brovkin, V., Crueger, T., Esch, M., Fieg, K., Glushak, K., Gayler, V., Haak, H., Hollweg, H.-D., Ilyina, T., Kinne, S., Kornblueh, L., Matei, D., Mauritsen, T., Mikolajewicz, U., Mueller, W., Notz, D., Pithan, F., Raddatz, T., Rast, S., Redler, R., Roeckner, E., Schmidt, H., Schnur, R., Segschneider, J., Six, K.D., Stockhause, M., Timmreck, C., Wegner, J., Widmann, H., Wieners, K.-H., Claussen, M., Marotzke, J., Stevens, B., 2013. Climate and carbon cycle changes from 1850 to 2100 in MPI-ESM simulations for the Coupled Model Intercomparison Project phase 5. *J. Adv. Model. Earth Syst.* 5, 572–597. <https://doi.org/10.1002/jame.20038>
- Godde, C.M., Thorburn, P.J., Biggs, J.S., Meier, E.A., 2016. Understanding the impacts of soil, climate, and farming practices on soil organic carbon sequestration: A simulation study in Australia. *Front. Plant Sci.* 7, 1–15. <https://doi.org/10.3389/fpls.2016.00661>
- Goddéris, Y., François, L.M., Probst, A., Schott, J., Moncoulon, D., Labat, D., Viville, D., 2006. Modelling weathering processes at the catchment scale: The WITCH numerical model. *Geochim. Cosmochim. Acta* 70, 1128–1147. <https://doi.org/10.1016/j.gca.2005.11.018>
- Goosse, H., Brovkin, V., Fichefet, T., Haarsma, R., Huybrechts, P., Jongma, J., Mouchet, A., Selten, F., Barriat, P.Y., Campin, J.M., Deleersnijder, E., Driesschaert, E., Goelzer, H., Janssens, I., Loutre, M.F., Morales Maqueda, M.A., Opsteegh, T., Mathieu, P.P., Munhoven, G., Pettersson, E.J., Renssen, H., Roche, D.M., Schaeffer, M., Tartinville, B., Timmermann, A., Weber, S.L., 2010. Description of the Earth system model of intermediate complexity LOVECLIM version 1.2. *Geosci. Model Dev.* 3, 603–633. <https://doi.org/10.5194/gmd-3-603-2010>
- Gottschalk, P., Smith, J.U., Wattenbach, M., Bellarby, J., Stehfest, E., Arnell, N., Osborn, T.J., Jones, C., Smith, P., 2012. How will organic carbon stocks in mineral soils evolve under future climate? Global projections using RothC for a range of climate change scenarios. *Biogeosciences* 9, 3151–3171. <https://doi.org/10.5194/bg-9-3151-2012>
- Gower, J.C., 1971. A General Coefficient of Similarity and Some of Its Properties. *Int. Biometrics Soc.* 27, 857–874. <https://doi.org/https://doi.org/10.2307/2528823>
- Gray, J.M., Bishop, T.F.A., Wilson, B.R., 2016. Factors Controlling Soil Organic Carbon Stocks with Depth in Eastern Australia. *Soil Sci. Soc. Am. J.* 79, 1741–1751. <https://doi.org/10.2136/sssaj2015.06.0224>
- Gross, A., Glaser, B., 2021. Meta-analysis on how manure application changes soil organic carbon storage. *Sci. Rep.* 11, 5516. <https://doi.org/10.1038/s41598-021-82739-7>
- Guillaume, T., Kotowska, M.M., Hertel, D., Knohl, A., Krashevskaya, V., Murtillaksono, K., Scheu, S., Kuzyakov, Y., 2018. Carbon costs and benefits of Indonesian rainforest conversion to plantations. *Nat. Commun.* 9. <https://doi.org/10.1038/s41467-018-04755-y>
- Gulde, S., Chung, H., Amelung, W., Chang, C., Six, J., 2008. Soil Carbon Saturation Controls Labile and Stable Carbon Pool Dynamics. *Soil Sci. Soc. Am. J.* 72, 605–612. <https://doi.org/10.2136/sssaj2007.0251>
- Guo, L.B., Gifford, R.M., 2002. Soil carbon stocks and land use change: A meta analysis. *Glob. Chang. Biol.* 8, 345–360. <https://doi.org/10.1046/j.1354-1013.2002.00486.x>
- Guo, Y., Fan, R., Zhang, X., Zhang, Y., Wu, D., McLaughlin, N., Zhang, S., Chen, X., Jia, S., Liang, A., 2020. Tillage-induced effects on SOC through changes in aggregate stability and soil pore structure. *Sci. Total Environ.* 703, 134617. <https://doi.org/10.1016/j.scitotenv.2019.134617>
- Hall, S.J., Huang, W., Timokhin, V.I., Hammel, K.E., 2020. Lignin lags, leads, or limits the decomposition of litter and soil organic carbon. *Ecology* 101, 1–7. <https://doi.org/10.1002/ecy.3113>
- Handley, H.K., 2006. Geochemical and Sr-Nd-Hf-O isotopic constraints on volcanic petrogenesis at the Sunda Arc, Indonesia. Durham University.
- Harrington, C.D., Whitney, J.W., 1987. Scanning electron microscope method for rock-varnish dating. *Geology* 15, 967–970. [https://doi.org/10.1130/0091-7613\(1987\)15<967:SEMMFR>2.0.CO;2](https://doi.org/10.1130/0091-7613(1987)15<967:SEMMFR>2.0.CO;2)

- Hartley, I.P., Hill, T.C., Chadburn, S.E., Hugelius, G., 2021. Temperature effects on carbon storage are controlled by soil stabilisation capacities. *Nat. Commun.* 12, 1–7. <https://doi.org/10.1038/s41467-021-27101-1>
- Herbillon, 1986. Chemical estimation of weatherable minerals present in the diagnostic horizons of low activity clay soils, in: Beinroth, F., Camargo, M., Eswaran, H. (Eds.), *Proceedings of the 8th International Clay Classification Workshop: Classification, Characterization and Utilization of Oxisols (Part 1)*. Rio de Janeiro, pp. 39–48.
- Hernández, Z., Almendros, G., Carral, P., Álvarez, A., Knicker, H., Pérez-Trujillo, J.P., 2012. Influence of non-crystalline minerals in the total amount, resilience and molecular composition of the organic matter in volcanic ash soils (Tenerife Island, Spain). *Eur. J. Soil Sci.* 63, 603–615. <https://doi.org/10.1111/j.1365-2389.2012.01497.x>
- Hertel, D., Moser, G., Culmsee, H., Erasmi, S., Horna, V., Schuldt, B., Leuschner, C., 2009. Below- and above-ground biomass and net primary production in a paleotropical natural forest (Sulawesi, Indonesia) as compared to neotropical forests. *For. Ecol. Manage.* 258, 1904–1912. <https://doi.org/10.1016/j.foreco.2009.07.019>
- Högberg, M.N., Högberg, P., Myrold, D.D., 2007. Is microbial community composition in boreal forest soils determined by pH, C-to-N ratio, the trees, or all three? *Oecologia* 150, 590–601. <https://doi.org/10.1007/s00442-006-0562-5>
- Holz, D.J., Williard, K.W.J., Edwards, P.J., Schoonover, J.E., 2015. Soil Erosion in Humid Regions: A Review. *J. Contemp. Water Res. Educ.* 154, 48–59. <https://doi.org/10.1111/j.1936-704x.2015.03187.x>
- Hou, R., Ouyang, Z., Maxim, D., Wilson, G., Kuzyakov, Y., 2016. Lasting effect of soil warming on organic matter decomposition depends on tillage practices. *Soil Biol. Biochem.* 95, 243–249. <https://doi.org/10.1016/j.soilbio.2015.12.008>
- Hoyos, N., Comerford, N.B., 2005. Land use and landscape effects on aggregate stability and total carbon of Andisols from the Colombian Andes. *Geoderma* 129, 268–278. <https://doi.org/10.1016/j.geoderma.2005.01.002>
- Hutson, J.L., Wagenet, R.J., 1995. LEACHM: Leaching Estimation And Chemistry Model: A process-based model of water and solute movement, transformations, plant uptake and chemical reactions in the unsaturated zone, in: Loeppert, R.H., Schwab, P., Goldberg, S. (Eds.), *Chemical Equilibrium and Reaction Models*. Soil Science Society of America, Inc and American Society of Agronomy, Inc., Ithaca, NY, pp. 409–422. <https://doi.org/10.2136/sssaspecpub42>
- Huygens, D., Boeckx, P., Van Cleemput, O., Godoy, R., Oyarzun, C., 2005. Aggregate structure and stability linked to carbon dynamics in a south Chilean Andisol. *Biogeosciences Discuss.* 2, 203–238. <https://doi.org/10.5194/bgd-2-203-2005>
- Imanuddin, R., Hidayat, A., Rachmat, H.H., Turjaman, M., Pratiwi, Nurfatriani, F., Indrajaya, Y., Susilowati, A., 2020. Reforestation and sustainable management of pinus merkusii forest plantation in indonesia: A review. *Forests* 11, 1–22. <https://doi.org/10.3390/f11121235>
- IPCC WGI, 2001. *Climate change 2001: The scientific basis*, Cambridge University Press. Cambridge, UK.
- IUSS, 2015. *World Reference Base for Soil Resources 2014, update 2015 International soil classification system for naming soils and creating legends for soil map*, World Soil Resources Reports No. 106. Rome. <https://doi.org/10.1017/S0014479706394902>
- Jarvis, N.J., Villholth, K.G., Ulén, B., 1999. Modelling particle mobilization and leaching in macroporous soil. *Eur. J. Soil Sci.* 50, 621–632. <https://doi.org/10.1046/j.1365-2389.1999.00269.x>
- Jobbágy, E.G., Jackson, R.B., 2000. The vertical distribution of soil organic carbon and its relation to climate and vegetation. *Ecol. Appl.* 10, 423–436. [https://doi.org/10.1890/1051-0761\(2000\)010\[0423:TVDOSO\]2.0.CO;2](https://doi.org/10.1890/1051-0761(2000)010[0423:TVDOSO]2.0.CO;2)
- Jones, R.C., Babcock, C.J., Knowlton, W.B., 2000. Estimation of the Total Amorphous Content of Hawai'i Soils by the Rietveld Method. *Soil Sci. Soc. Am. J.* 64, 1100–1108. <https://doi.org/10.2136/sssaj2000.6431100x>

- Kaiser, M., Ellerbrock, R.H., Wulf, M., Dultz, S., Hierath, C., Sommer, M., 2012. The influence of mineral characteristics on organic matter content, composition, and stability of topsoils under long-term arable and forest land use. *J. Geophys. Res. Biogeosciences* 117, 1–16. <https://doi.org/10.1029/2011JG001712>
- Kallenbach, C.M., Grandy, A.S., Frey, S.D., Diefendorf, A.F., 2015. Microbial physiology and necromass regulate agricultural soil carbon accumulation. *Soil Biol. Biochem.* 91, 279–290. <https://doi.org/10.1016/j.soilbio.2015.09.005>
- Kang, J., Hesterberg, D., Osmond, D.L., 2009. Soil Organic Matter Effects on Phosphorus Sorption: A Path Analysis. *Soil Sci. Soc. Am. J.* 73, 360–366. <https://doi.org/10.2136/sssaj2008.0113>
- Kartadinata, M., Okuno, M., Nakamura, T., Kobayashi, T., 2002. Eruptive history of Tangkuban Perahu Volcano, West Java, Indonesia: A preliminary report. *J. Geog.* 111, 404–409. <https://doi.org/10.1017/cbo9781316155530.002>
- Keeling, D., 1958. The concentration and isotopic abundances of atmospheric carbon dioxide in rural areas. *Geochim. Cosmochim. Acta* 13, 322–334. [https://doi.org/https://doi.org/10.1016/0016-7037\(58\)90033-4](https://doi.org/https://doi.org/10.1016/0016-7037(58)90033-4)
- Kershaw, A.P., van der Kaars, S., Flenley, J.R., 2007. The Quaternary history of Far Eastern rainforests, in: Mason, J. (Ed.), *Tropical Rainforest Responses to Climatic Change*. Springer Berlin, Heidelberg, pp. 85–123. https://doi.org/10.1007/978-3-642-05383-2_4
- Keyvanshokouhi, S., Cornu, S., Samouëlian, A., Finke, P., 2016. Evaluating SoilGen2 as a tool for projecting soil evolution induced by global change. *Sci. Total Environ.* 571, 110–123. <https://doi.org/10.1016/j.scitotenv.2016.07.119>
- Kleber, M., Eusterhues, K., Keiluweit, M., Mikutta, C., Mikutta, R., Nico, P.S., 2015. Mineral-Organic Associations: Formation, Properties, and Relevance in Soil Environments, in: Sparks, D. (Ed.), *Advances in Agronomy*. Elsevier Ltd, pp. 1–140. <https://doi.org/10.1016/bs.agron.2014.10.005>
- Köppen, W., 1936. Das geographische system der Klimate, in: Köppen, W., Geiger, R. (Eds.), *Handbuch Der Klimatologie*. Gebrüder Borntraeger, Berlin, pp. 1–44. <https://doi.org/10.2307/200498>
- Kramer, M.G., Sanderman, J., Chadwick, O.A., Chorover, J., Vitousek, P.M., 2012. Long-term carbon storage through retention of dissolved aromatic acids by reactive particles in soil. *Glob. Chang. Biol.* 18, 2594–2605. <https://doi.org/10.1111/j.1365-2486.2012.02681.x>
- Kubota, T., 1972. Aggregate-formation of allophanic soils: Effect of drying on the dispersion of the soils. *Soil Sci. Plant Nutr.* 18, 79–97. <https://doi.org/10.1080/00380768.1972.10433277>
- Kuzyakov, Y., Zamanian, K., 2019. Reviews and syntheses: Agropedogenesis-Humankind as the sixth soil-forming factor and attractors of agricultural soil degradation. *Biogeosciences* 16, 4783–4803. <https://doi.org/10.5194/bg-16-4783-2019>
- La Manna, L., Gaspar, L., Rostagno, C.M., Quijano, L., Navas, A., 2018. Soil changes associated with land use in volcanic soils of Patagonia developed on dynamic landscapes. *Catena* 166, 229–239. <https://doi.org/10.1016/j.catena.2018.03.025>
- Lal, R., 2003. Global potential of soil carbon sequestration to mitigate the greenhouse effect. *CRC. Crit. Rev. Plant Sci.* 22, 151–184. <https://doi.org/10.1080/713610854>
- Lange, M., Eisenhauer, N., Sierra, C.A., Bessler, H., Engels, C., Griffiths, R.I., Mellado-Vázquez, P.G., Malik, A.A., Roy, J., Scheu, S., Steinbeiss, S., Thomson, B.C., Trumbore, S.E., Gleixner, G., 2015. Plant diversity increases soil microbial activity and soil carbon storage. *Nat. Commun.* 6, 6707. <https://doi.org/10.1038/ncomms7707>
- Lawrence, C.R., Harden, J.W., Xu, X., Schulz, M.S., Trumbore, S.E., 2015. Long-term controls on soil organic carbon with depth and time: A case study from the Cowlitz River Chronosequence, WA USA. *Geoderma* 247–248, 73–87. <https://doi.org/10.1016/j.geoderma.2015.02.005>
- Lehmann, J., Kinyangi, J., Solomon, D., 2007. Organic matter stabilization in soil microaggregates: Implications from spatial heterogeneity of organic carbon contents and carbon forms. *Biogeochemistry* 85, 45–57. <https://doi.org/10.1007/s10533-007-9105-3>
- Lehmann, J., Kleber, M., 2015. The contentious nature of soil organic matter. *Nature* 528, 60–68. <https://doi.org/10.1038/nature16069>

- Lemenih, M., Karlun, E., Olsson, M., 2005. Assessing soil chemical and physical property responses to deforestation and subsequent cultivation in smallholders farming system in Ethiopia. *Agric. Ecosyst. Environ.* 105, 373–386. <https://doi.org/10.1016/j.agee.2004.01.046>
- Levard, C., Doelsch, E., Basile-Doelsch, I., Abidin, Z., Miche, H., Masion, A., Rose, J., Borschneck, D., Bottero, J.Y., 2012. Structure and distribution of allophanes, imogolite and proto-imogolite in volcanic soils. *Geoderma* 183–184, 100–108. <https://doi.org/10.1016/j.geoderma.2012.03.015>
- Li, H., Van den Bulcke, J., Mendoza, O., Deroo, H., Haesaert, G., Dewitte, K., De Neve, S., Sleutel, S., 2022. Soil texture controls added organic matter mineralization by regulating soil moisture—evidence from a field experiment in a maritime climate. *Geoderma* 410, 115690. <https://doi.org/10.1016/j.geoderma.2021.115690>
- Li, J., Du, J., Zhong, S., Ci, E., Wei, C., 2021. Changes in the profile properties and chemical weathering characteristics of cultivated soils affected by anthropic activities. *Sci. Rep.* 11, 20822. <https://doi.org/10.1038/s41598-021-00302-w>
- Lieth, H., 1975. Modeling the primary productivity of the world, in: Lieth, H., Whittaker, R.H. (Eds.), *Primary Productivity of the Biosphere*. Springer - Verlag, Berlin, Heidelberg, New York, pp. 237–263. <https://doi.org/10.1007/978-3-642-80915-6>
- Linlin, G., Taku, N., Hiromi, I., Zhigang, S., 2016. Carbon Mineralization Associated with Soil Aggregates as Affected by Short-Term Tillage. *J. Resour. Ecol.* 7, 101–106. <https://doi.org/10.5814/j.issn.1674-764x.2016.02.004>
- Liu, X.J.A., Sun, J., Mau, R.L., Finley, B.K., Compson, Z.G., van Gestel, N., Brown, J.R., Schwartz, E., Dijkstra, P., Hungate, B.A., 2017. Labile carbon input determines the direction and magnitude of the priming effect. *Appl. Soil Ecol.* 109, 7–13. <https://doi.org/10.1016/j.apsoil.2016.10.002>
- Lu, M., Zhou, X., Yang, Q., Li, H., Luo, Y., Fang, C., Chen, J., Yang, X., Li, B., 2013. Responses of ecosystem carbon cycle to experimental warming: A meta-analysis. *Ecology* 94, 726–738. <https://doi.org/10.1890/12-0279.1>
- Lumbanraja, J., Syam, T., Nishide, H., Mahi, A.K., Utomo, M., Sarno, Kimura, M., 1998. Deterioration of soil fertility by land use changes in South Sumatra, Indonesia: from 1970 to 1990. *Hydrol. Process.* 12, 2003–2013. [https://doi.org/10.1002/\(sici\)1099-1085\(19981030\)12:13/14<2003::aid-hyp715>3.0.co;2-d](https://doi.org/10.1002/(sici)1099-1085(19981030)12:13/14<2003::aid-hyp715>3.0.co;2-d)
- Lützw, M. V., Kögel-Knabner, I., Ekschmitt, K., Matzner, E., Guggenberger, G., Marschner, B., Flessa, H., 2006. Stabilization of organic matter in temperate soils: Mechanisms and their relevance under different soil conditions - A review. *Eur. J. Soil Sci.* 57, 426–445. <https://doi.org/10.1111/j.1365-2389.2006.00809.x>
- Lyu, H., Watanabe, T., Kilasara, M., Hartono, A., Funakawa, S., 2021. Soil organic carbon pools controlled by climate and geochemistry in tropical volcanic regions. *Sci. Total Environ.* 761, 143277. <https://doi.org/10.1016/j.scitotenv.2020.143277>
- Madani, N., Kimball, J.S., Ballantyne, A.P., Affleck, D.L.R., Van Bodegom, P.M., Reich, P.B., Kattge, J., Sala, A., Nazeri, M., Jones, M.O., Zhao, M., Running, S.W., 2018. Future global productivity will be affected by plant trait response to climate. *Sci. Rep.* 8, 1–10. <https://doi.org/10.1038/s41598-018-21172-9>
- Maillard, É., Angers, D.A., 2014. Animal manure application and soil organic carbon stocks: A meta-analysis. *Glob. Chang. Biol.* 20, 666–679. <https://doi.org/10.1111/gcb.12438>
- Malik, A.A., Puissant, J., Buckeridge, K.M., Goodall, T., Jehmlich, N., Chowdhury, S., Gweon, H.S., Peyton, J.M., Mason, K.E., van Agtmaal, M., Blaud, A., Clark, I.M., Whitaker, J., Pywell, R.F., Ostle, N., Gleixner, G., Griffiths, R.I., 2018. Land use driven change in soil pH affects microbial carbon cycling processes. *Nat. Commun.* 9, 1–10. <https://doi.org/10.1038/s41467-018-05980-1>
- Matus, F., Amigo, X., Kristiansen, S.M., 2006. Aluminium stabilization controls organic carbon levels in Chilean volcanic soils. *Geoderma* 132, 158–168. <https://doi.org/10.1016/j.geoderma.2005.05.005>
- Matus, F., Rumpel, C., Neculman, R., Panichini, M., Mora, M.L., 2014. Soil carbon storage and stabilisation in andic soils: A review. *Catena* 120, 102–110.

<https://doi.org/10.1016/j.catena.2014.04.008>

- Mayer, L.M., Xing, B., 2001. Organic Matter-Surface Area Relationships in Acid Soils. *Soil Sci. Soc. Am. J.* 65, 250–258. <https://doi.org/10.2136/sssaj2001.651250x>
- Mayes, M., Marin-Spiotta, E., Szymanski, L., Akif Erdoğan, M., Ozdoğan, M., Clayton, M., 2014. Soil type mediates effects of land use on soil carbon and nitrogen in the Konya Basin, Turkey. *Geoderma* 232–234, 517–527. <https://doi.org/10.1016/j.geoderma.2014.06.002>
- McKeague, J.A., 1967. An evaluation of 0.1 M pyrophosphate and pyrophosphate-dithionite in comparison with oxalate as extractants of the accumulation products in podzols and some other soils. *Can. J. Soil Sci.* 47, 95–99. <https://doi.org/10.4141/cjss67-017>
- McNally, S.R., Beare, M.H., Curtin, D., Meenken, E.D., Kelliher, F.M., Calvelo Pereira, R., Shen, Q., Baldock, J., 2017. Soil carbon sequestration potential of permanent pasture and continuous cropping soils in New Zealand. *Glob. Chang. Biol.* 23, 4544–4555. <https://doi.org/10.1111/gcb.13720>
- McTiernan, K.B., Coûteaux, M.M., Berg, B., Berg, M.P., De Anta, R.C., Gallardo, A., Kratz, W., Piusi, P., Remacle, J., De Santo, A.V., 2003. Changes in chemical composition of *Pinus sylvestris* needle litter during decomposition along a European coniferous forest climatic transect. *Soil Biol. Biochem.* 35, 801–812. [https://doi.org/10.1016/S0038-0717\(03\)00107-X](https://doi.org/10.1016/S0038-0717(03)00107-X)
- Mehra, O.P., Jackson, M.L., 1958. Iron Oxide Removal from Soils and Clays by a Dithionite-Citrate System Buffered with Sodium Bicarbonate. *Clays Clay Miner.* 7, 317–327. <https://doi.org/10.1346/ccmn.1958.0070122>
- Meier, I.C., Leuschner, C., 2010. Variation of soil and biomass carbon pools in beech forests across a precipitation gradient. *Glob. Chang. Biol.* 16, 1035–1045. <https://doi.org/10.1111/j.1365-2486.2009.02074.x>
- Mendoza, O., De Neve, S., Deroo, H., Sleutel, S., 2022. Mineralisation of ryegrass and soil organic matter as affected by ryegrass application doses and changes in soil structure. *Biol. Fertil. Soils* 58, 679–691. <https://doi.org/10.1007/s00374-022-01654-9>
- Mikha, M.M., Rice, C.W., 2004. Tillage and Manure Effects on Soil and Aggregate-Associated Carbon and Nitrogen. *Soil Sci. Soc. Am. J.* 68, 809–816. <https://doi.org/10.2136/sssaj2004.8090>
- Mikutta, R., Kleber, M., Torn, M.S., Jahn, R., 2006. Stabilization of soil organic matter: Association with minerals or chemical recalcitrance? *Biogeochemistry* 77, 25–56. <https://doi.org/10.1007/s10533-005-0712-6>
- Mikutta, R., Schaumann, G.E., Gildemeister, D., Bonneville, S., Kramer, M.G., Chorover, J., Chadwick, O.A., Guggenberger, G., 2009. Biogeochemistry of mineral-organic associations across a long-term mineralogical soil gradient (0.3–4100 kyr), Hawaiian Islands. *Geochim. Cosmochim. Acta* 73, 2034–2060. <https://doi.org/10.1016/j.gca.2008.12.028>
- Miller, J.L., Elwood Madden, A.S., Phillips-Lander, C.M., Pritchett, B.N., Elwood Madden, M.E., 2016. Alunite dissolution rates: Dissolution mechanisms and implications for Mars. *Geochim. Cosmochim. Acta* 172, 93–106. <https://doi.org/10.1016/j.gca.2015.10.001>
- Minasny, B., Malone, B.P., McBratney, A.B., Angers, D.A., Arrouays, D., Chambers, A., Chaplot, V., Chen, Z.S., Cheng, K., Das, B.S., Field, D.J., Gimona, A., Hedley, C.B., Hong, S.Y., Mandal, B., Marchant, B.P., Martin, M., McConkey, B.G., Mulder, V.L., O'Rourke, S., Richer-de-Forges, A.C., Odeh, I., Padarian, J., Paustian, K., Pan, G., Poggio, L., Savin, I., Stolbovoy, V., Stockmann, U., Sulaeman, Y., Tsui, C.C., Vågen, T.G., van Wesemael, B., Winowiecki, L., 2017. Soil carbon 4 per mille. *Geoderma* 292, 59–86. <https://doi.org/10.1016/j.geoderma.2017.01.002>
- Minasny, B., Sulaeman, Y., Mcbratney, A.B., 2011. Is soil carbon disappearing? The dynamics of soil organic carbon in Java. *Glob. Chang. Biol.* 17, 1917–1924. <https://doi.org/10.1111/j.1365-2486.2010.02324.x>
- Miyazawa, M., Takahashi, T., Sato, T., Kanno, H., Nanzyo, M., 2013. Factors controlling accumulation and decomposition of organic carbon in humus horizons of Andosols: A case study for distinctive non-allophanic Andosols in northeastern Japan. *Biol. Fertil. Soils* 49, 929–938. <https://doi.org/10.1007/s00374-013-0792-8>

- Morgan, R.P.C., 2001. A simple approach to soil loss prediction: A revised Morgan-Morgan-Finney model. *Catena* 44, 305–322. [https://doi.org/10.1016/S0341-8162\(00\)00171-5](https://doi.org/10.1016/S0341-8162(00)00171-5)
- Morris, S.J., Bohm, S., Haile-mariam, S., Paul, E.A., 2007. Evaluation of carbon accrual in afforested agricultural soils. *Glob. Chang. Biol.* 13, 1145–1156. <https://doi.org/10.1111/j.1365-2486.2007.01359.x>
- Murty, D., Kirschbaum, M.U.F., McMurtrie, R.E., McGilvray, H., 2002. Does conversion of forest to agricultural land change soil carbon and nitrogen? a review of the literature. *Glob. Chang. Biol.* 8, 105–123. <https://doi.org/10.1046/j.1354-1013.2001.00459.x>
- Nakagawa, T., Ishiguro, M., 1994. Hydraulic Conductivity of an Allophanic Andisol as Affected by Solution pH. *J. Environ. Qual.* 23, 208–210. <https://doi.org/10.2134/jeq1994.00472425002300010032x>
- Nanzyo, M., Dahlgren, R., Shoji, S., 1993a. Chemical Characteristics of Volcanic Ash Soils, in: Shoji, S., Nanzyo, M., Dahlgren, R. (Eds.), *Volcanic Ash Soils. Genesis, Properties and Utilization*. Elsevier, Tokyo, Japan, pp. 145–187. [https://doi.org/10.1016/S0166-2481\(08\)70267-8](https://doi.org/10.1016/S0166-2481(08)70267-8)
- Nanzyo, M., Shoji, S., Dahlgren, R., 1993b. Physical Characteristics of Volcanic Ash Soils, in: Shoji, Sadao, Nanzyo, Masami, Dahlgren, Randy (Eds.), *Volcanic Ash Soils. Genesis, Properties and Utilization*. Elsevier, pp. 189–207. [https://doi.org/10.1016/S0166-2481\(08\)70268-X](https://doi.org/10.1016/S0166-2481(08)70268-X)
- Nasution, A., Kartadinata, M., Kobayashi, T., Siregar, D., Sutaningsih, E., Hadisantono, R., Kadarstia, E., 2004. Geology, age dating, and geochemistry of Tangkuban perahu. *J. Geotherm. Res. Soc. Japan* 26, 285–303.
- Nawaz, R., Parkpian, P., Arshad, M., Ahmad, F., Garivait, H., Ali, A.S., 2013. Mobilization and leaching of trace elements (Fe, Al and Mn) in agricultural soils as affected by simulated acid rain. *Asian J. Chem.* 25, 9891–9896. <https://doi.org/10.14233/ajchem.2013.15560>
- Nesbitt, H.W., Young, G.M., 1982. Early proterozoic climates and plate motions inferred from major element chemistry of lutites. *Nature* 299, 715–717. <https://doi.org/10.1038/299715a0>
- Nguyen, P.L., Bador, M., Alexander, L. V., Lane, T.P., Ngo-Duc, T., 2022. More intense daily precipitation in CORDEX-SEA regional climate models than their forcing global climate models over Southeast Asia. *Int. J. Climatol.* 1–25. <https://doi.org/10.1002/joc.7619>
- Niu, S., Wu, M., Han, Y., Xia, J., Li, L., Wan, S., 2008. Water-mediated responses of ecosystem carbon fluxes to climatic change in a temperate steppe. *New Phytol.* 177, 209–219. <https://doi.org/10.1111/j.1469-8137.2007.02237.x>
- Nur'utami, M.N., Hidayat, R., 2016. Influences of IOD and ENSO to Indonesian Rainfall Variability: Role of Atmosphere-ocean Interaction in the Indo-pacific Sector. *Procedia Environ. Sci.* 33, 196–203. <https://doi.org/10.1016/j.proenv.2016.03.070>
- Opolot, E., 2016. Modelling soil evolution to assess soil system behaviour under global change. Ghent University.
- Opolot, E., Finke, P.A., 2015. Evaluating sensitivity of silicate mineral dissolution rates to physical weathering using a soil evolution model (SoilGen2.25). *Biogeosciences* 12, 6791–6808. <https://doi.org/10.5194/bg-12-6791-2015>
- Opolot, E., Yu, Y.Y., Finke, P.A., 2015. Modeling soil genesis at pedon and landscape scales: Achievements and problems. *Quat. Int.* 376, 34–46. <https://doi.org/10.1016/j.quaint.2014.02.017>
- Ouédraogo, R.A., Chartin, C., Kambiré, F.C., van Wesemael, B., Delvaux, B., Milogo, H., Bielders, C.L., 2020. Short and long-term impact of urban gardening on soil organic carbon fractions in Lixisols (Burkina Faso). *Geoderma* 362, 114110. <https://doi.org/10.1016/j.geoderma.2019.114110>
- Palandri, J., Kharaka, Y., 2004. A compilation of rate parameters of water-mineral interaction kinetics for application to geochemical modeling, U.S. Geological Survey Open File Report 2004 - 1068. California.
- Parfitt, R.L., 2009. Allophane and imogolite: role in soil biogeochemical processes. *Clay Miner.* 44, 135–155. <https://doi.org/10.1180/claymin.2009.044.1.135>
- Parfitt, R.L., Russel Milton, Orbell, G.E., 1983. Weathering sequence of soils from volcanic ash involving

- allophane and halloysite New Zealand. *Geoderma* 29, 41–57. [https://doi.org/10.1016/0016-7061\(83\)90029-0](https://doi.org/10.1016/0016-7061(83)90029-0)
- Parkhurst, D., Appelo, C.A., 1999. User's guide to PHREEQC (ver 2) - A computer program for speciation, batch-reaction, one-dimensional transport, and inverse geochemical calculations. Denver, Colorado.
- Parton, W.J., 1996. The CENTURY model, in: Powlson, D.S., Smith, P., Smith, J.U. (Eds.), *Evaluation of Soil Organic Matter Models*. Springer - Verlag, Berlin Heidelberg, pp. 283–291. https://doi.org/10.1007/978-3-642-61094-3_23
- Paustian, K., Andr n, O., Janzen, H.H., Lal, R., Smith, P., Tian, G., Tiessen, H., Van Noordwijk, M., Woomer, P.L., 1997. Agricultural soils as a sink to mitigate CO₂ emissions. *Soil Use Manag.* 13, 230–244.
- Peltre, C., Christensen, B.T., Dragon, S., Icard, C., K tterer, T., Houot, S., 2012. RothC simulation of carbon accumulation in soil after repeated application of widely different organic amendments. *Soil Biol. Biochem.* 52, 49–60. <https://doi.org/10.1016/j.soilbio.2012.03.023>
- Pendall, E., Rustad, L., Schimel, J., 2008. Towards a predictive understanding of belowground process responses to climate change: Have we moved any closer? *Funct. Ecol.* 22, 937–940. <https://doi.org/10.1111/j.1365-2435.2008.01506.x>
- Percival, H.J., Parfitt, R.L., Scott, N.A., 2000. Factors Controlling Soil Carbon Levels in New Zealand Grasslands Is Clay Content Important? *Soil Sci. Soc. Am. J.* 64, 1623–1630. <https://doi.org/10.2136/sssaj2000.6451623x>
- Perdrial, N., Perdrial, J.N., Delphin, J.E., Elsass, F., Liewig, N., 2010. Temporal and spatial monitoring of mobile nanoparticles in a vineyard soil: Evidence of nanoaggregate formation. *Eur. J. Soil Sci.* 61, 456–468. <https://doi.org/10.1111/j.1365-2389.2010.01263.x>
- Perhutani, 2014. Rencana pengaturan kelestarian hutan; Jangka perusahaan 1 Januari 2012/31 Desember 2021 (In Indonesia).
- Phillips, J.D., 2007. Development of texture contrast soils by a combination of bioturbation and translocation. *Catena* 70, 92–104. <https://doi.org/10.1016/j.catena.2006.08.002>
- Poeplau, C., Don, A., 2015. Carbon sequestration in agricultural soils via cultivation of cover crops - A meta-analysis. *Agric. Ecosyst. Environ.* 200, 33–41. <https://doi.org/10.1016/j.agee.2014.10.024>
- Poeplau, C., Don, A., Dondini, M., Leifeld, J., Nemo, R., Schumacher, J., Senapati, N., Wiesmeier, M., 2013. Reproducibility of a soil organic carbon fractionation method to derive RothC carbon pools. *Eur. J. Soil Sci.* 64, 735–746. <https://doi.org/10.1111/ejss.12088>
- Poeplau, C., K tterer, T., Leblans, N.I.W., Sigurdsson, B.D., 2017. Sensitivity of soil carbon fractions and their specific stabilization mechanisms to extreme soil warming in a subarctic grassland. *Glob. Chang. Biol.* 23, 1316–1327. <https://doi.org/10.1111/gcb.13491>
- Poirier, V., Basile-Doelsch, I., Balesdent, J., Borschneck, D., Whalen, J.K., Angers, D.A., 2020. Organo-Mineral Interactions Are More Important for Organic Matter Retention in Subsoil Than Topsoil. *Soil Syst.* 4, 4. <https://doi.org/10.3390/soilsystems4010004>
- Post, W.M., Kwon, K.C., 2000. Soil carbon sequestration and land-use change: Processes and potential. *Glob. Chang. Biol.* 6, 317–327. <https://doi.org/10.1046/j.1365-2486.2000.00308.x>
- Pronk, G.J., Heister, K., Ding, G.C., Smalla, K., K gel-Knabner, I., 2012. Development of biogeochemical interfaces in an artificial soil incubation experiment; aggregation and formation of organo-mineral associations. *Geoderma* 189–190, 585–594. <https://doi.org/10.1016/j.geoderma.2012.05.020>
- Qiao, N., Schaefer, D., Blagodatskaya, E., Zou, X., Xu, X., Kuzyakov, Y., 2014. Labile carbon retention compensates for CO₂ released by priming in forest soils. *Glob. Chang. Biol.* 20, 1943–1954. <https://doi.org/10.1111/gcb.12458>
- Quideau, S.A., 2006. Organic matter accumulation, in: Lal, R. (Ed.), *Encyclopedia of Soil Science*. Taylor & Francis. <https://doi.org/10.1081/E-ESS3>
- Rabbi, S.M.F., Daniel, H., Lockwood, P. V., Macdonald, C., Pereg, L., Tighe, M., Wilson, B.R., Young, I.M., 2016. Physical soil architectural traits are functionally linked to carbon decomposition and

- bacterial diversity. *Sci. Rep.* 6. <https://doi.org/10.1038/srep33012>
- Ranathunga, K.N., Finke, P.A., Yin, Q., Yu, Y., 2022. Calibrating SoilGen2 for interglacial soil evolution in the Chinese Loess Plateau considering soil parameters and the effect of dust addition rhythm. *Quat. Int.* 607, 100–112. <https://doi.org/10.1016/j.quaint.2021.08.019>
- Rasmussen, C., Heckman, K., Wieder, W.R., Keiluweit, M., Lawrence, C.R., Berhe, A.A., Blankinship, J.C., Crow, S.E., Druhan, J.L., Hicks Pries, C.E., Marin-Spiotta, E., Plante, A.F., Schädel, C., Schimel, J.P., Sierra, C.A., Thompson, A., Wagai, R., 2018. Beyond clay: towards an improved set of variables for predicting soil organic matter content. *Biogeochemistry* 137, 297–306. <https://doi.org/10.1007/s10533-018-0424-3>
- Rasmussen, C., Matsuyama, N., Dahlgren, R.A., Southard, R.J., Brauer, N., 2007. Soil Genesis and Mineral Transformation Across an Environmental Gradient on Andesitic Lahar. *Soil Sci. Soc. Am. J.* 71, 225–237. <https://doi.org/10.2136/sssaj2006.0100>
- Rasmussen, C., Torn, M.S., Southard, R.J., 2005. Mineral Assemblage and Aggregates Control Carbon Dynamics in a California Conifer Forest. *Soil Sci. Soc. Am. J.* 69, 1711–1721. <https://doi.org/10.2136/sssaj2005.0040>
- Rasse, D.P., Rumpel, C., Dignac, M.F., 2005. Is soil carbon mostly root carbon? Mechanisms for a specific stabilisation. *Plant Soil* 269, 341–356. <https://doi.org/10.1007/s11104-004-0907-y>
- Reichenbach, M., Fiener, P., Garland, G., Griepentrog, M., Six, J., Doetterl, S., 2021. The role of geochemistry in organic carbon stabilization against microbial decomposition in tropical rainforest soils. *Soil* 7, 453–475. <https://doi.org/10.5194/soil-7-453-2021>
- Remedio, A.R., Teichmann, C., Bunttemeyer, L., Sieck, K., Weber, T., Rechid, D., Hoffmann, P., Nam, C., Kotova, L., Jacob, D., 2019. Evaluation of new CORDEX simulations using an updated köppen-trewartha climate classification. *Atmosphere (Basel)*. 10, 1–25. <https://doi.org/10.3390/atmos10110726>
- Richardson, J.B., Petrenko, C.L., Friedland, A.J., 2017. Base cations and micronutrients in forest soils along three clear-cut chronosequences in the northeastern United States. *Nutr. Cycl. Agroecosystems* 109, 161–179. <https://doi.org/10.1007/s10705-017-9876-4>
- Richter, D.D.B., 2007. Humanity's transformation of earth's soil: Pedology's new frontier. *Soil Sci.* 172, 957–967. <https://doi.org/10.1097/ss.0b013e3181586bb7>
- Richter, D.D.B., Bacon, A.R., Brecheisen, Z., Mobley, M.L., 2015. Soil in the Anthropocene. *IOP Conf. Ser. Earth Environ. Sci.* 25. <https://doi.org/10.1088/1755-1315/25/1/012010>
- Riggers, C., Poeplau, C., Don, A., Frühauf, C., Dechow, R., 2021. How much carbon input is required to preserve or increase projected soil organic carbon stocks in German croplands under climate change? *Plant Soil* 460, 417–433. <https://doi.org/10.1007/s11104-020-04806-8>
- Rocci, K.S., Lavallee, J.M., Stewart, C.E., Cotrufo, M.F., 2021. Soil organic carbon response to global environmental change depends on its distribution between mineral-associated and particulate organic matter: A meta-analysis. *Sci. Total Environ.* 793, 148569. <https://doi.org/10.1016/j.scitotenv.2021.148569>
- Rossiter, D.G., Bouma, J., 2018. A new look at soil phenofoms – Definition, identification, mapping. *Geoderma* 314, 113–121. <https://doi.org/10.1016/j.geoderma.2017.11.002>
- Rouiller, J., Burtin, G., Souchier, B., 1972. La dispersion des sols dans l'analyse granulométrique. Méthode utilisant les résines échangeuses d'ions. *Bull. ENSAIA Nancy* 194–205.
- Rowley, M.C., Grand, S., Verrecchia, É.P., 2018. Calcium-mediated stabilisation of soil organic carbon. *Biogeochemistry* 137, 27–49. <https://doi.org/10.1007/s10533-017-0410-1>
- Rustad, L.E., Campbell, J.L., Marion, G.M., Norby, R.J., Mitchell, M.J., Hartley, A.E., Cornelissen, J.H.C., Gurevitch, J., Alward, R., Beier, C., Burke, I., Canadell, J., Callaghan, T., Christensen, T.R., Fahnestock, J., Fernandez, I., Harte, J., Hollister, R., John, H., Ineson, P., Johnson, M.G., Jonasson, S., John, L., Linder, S., Lukewille, A., Masters, G., Melillo, J., Mickelsen, A., Neill, C., Olszyk, D.M., Press, M., Pregitzer, K., Robinson, C., Rygielwicz, P.T., Sala, O., Schmidt, I.K., Shaver, G., Thompson, K., Tingey, D.T., Verburg, P., Wall, D., Welker, J., Wright, R., 2001. A meta-analysis of the response of soil respiration, net nitrogen mineralization, and aboveground plant growth to

- experimental ecosystem warming. *Oecologia* 126, 543–562. <https://doi.org/10.1007/s004420000544>
- Ruswandi, A., Rustiadi, E., Mudikdjo, K., 2007. Agricultural Land Conversion and Land Use Change Dynamics in North Bandung Area. *J. Ilmu Tanah dan Lingkungan* 9, 63–70. <https://doi.org/10.29244/jitl.9.2.63-70>
- Samouëlian, A., Finke, P., Goddèris, Y., Cornu, S., 2012. Hydrologic information in pedologic model, in: Lin, H. (Ed.), *Hydropedology*. Elsevier B.V., Amsterdam, pp. 595–636. <https://doi.org/10.1016/B978-0-12-386941-8.00019-6>
- Sanderman, J., Baisden, W.T., Fallon, S., 2016. Redefining the inert organic carbon pool. *Soil Biol. Biochem.* 92, 149–152. <https://doi.org/10.1016/j.soilbio.2015.10.005>
- Sanderman, J., Hengl, T., Fiske, G.J., 2017. Soil carbon debt of 12,000 years of human land use. *Proc. Natl. Acad. Sci. U. S. A.* 114, 9575–9580. <https://doi.org/10.1073/pnas.1706103114>
- Sanderman, J., Kramer, M.G., 2017. Dissolved organic matter retention in volcanic soils with contrasting mineralogy: a column sorption experiment. *Biogeochemistry* 135, 293–306. <https://doi.org/10.1007/s10533-017-0374-1>
- Schimel, D.S., 1995. Terrestrial ecosystems and the carbon cycle. *Glob. Chang. Biol.* 1, 77–91. <https://doi.org/https://doi.org/10.1111/j.1365-2486.1995.tb00008.x>
- Schmidt, M.W.I., Torn, M.S., Abiven, S., Dittmar, T., Guggenberger, G., Janssens, I.A., Lehmann, J., Manning, D.A.C., Nannipieri, P., Rasse, D.P., Kleber, M., Ko, I., 2011. Persistence of soil organic matter as an ecosystem property. *Nature* 478, 49–56. <https://doi.org/10.1038/nature10386>
- Schneider, M.P.W., Scheel, T., Mikutta, R., van Hees, P., Kaiser, K., Kalbitz, K., 2010. Sorptive stabilization of organic matter by amorphous Al hydroxide. *Geochim. Cosmochim. Acta* 74, 1606–1619. <https://doi.org/10.1016/j.gca.2009.12.017>
- Seguel, O., Horn, R., 2005. Mechanical behavior of a volcanic ash soil (Typic Hapludand) under static and dynamic loading. *Soil Tillage Res.* 82, 109–116. <https://doi.org/10.1016/j.still.2005.01.010>
- Sémah, A.M., Sémah, F., 2012. The rain forest in Java through the Quaternary and its relationships with humans (adaptation, exploitation and impact on the forest). *Quat. Int.* 249, 120–128. <https://doi.org/10.1016/j.quaint.2011.06.013>
- Shahbaz, M., Kuzjakov, Y., Heitkamp, F., 2017. Decrease of soil organic matter stabilization with increasing inputs: Mechanisms and controls. *Geoderma* 304, 76–82. <https://doi.org/10.1016/j.geoderma.2016.05.019>
- Shen, Y., McLaughlin, N., Zhang, X., Xu, M., Liang, A., 2018. Effect of tillage and crop residue on soil temperature following planting for a Black soil in Northeast China. *Sci. Rep.* 8, 1–9. <https://doi.org/10.1038/s41598-018-22822-8>
- Shirato, Y., Hakamata, T., Taniyama, I., 2004. Modified rothamsted carbon model for andosols and its validation: Changing humus decomposition rate constant with pyrophosphate-extractable Al. *Soil Sci. Plant Nutr.* 50, 149–158. <https://doi.org/10.1080/00380768.2004.10408463>
- Shoji, S., Dahlgren, R., Nanzyo, M., 1993. Genesis of Volcanic Ash Soils, in: Shoji, S., Nanzyo, M., Dahlgren, R. (Eds.), *Volcanic Ash Soils - Genesis, Properties and Utilization*. Elsevier Science, pp. 37–71. [https://doi.org/10.1016/S0166-2481\(08\)70264-2](https://doi.org/10.1016/S0166-2481(08)70264-2)
- Shoji, S., Takahashi, T., 2002. Environmental and Agricultural Significance of Volcanic Ash Soils. *Glob. J. Environ. Res.* 6, 113–135.
- Silitonga, P.H., 1973. Peta geologi Lembar Bandung, Djawa (Geologic map of the Bandung Quadrangle, Java), scale 1:100 000.
- Silva, J.H.S., Deenik, J.L., Yost, R.S., Bruland, G.L., Crow, S.E., 2015. Improving clay content measurement in oxidic and volcanic ash soils of Hawaii by increasing dispersant concentration and ultrasonic energy levels. *Geoderma* 237, 211–223. <https://doi.org/10.1016/j.geoderma.2014.09.008>
- Sing, K.S., Everett, D., Haul, R.A., Moscou, L., Pierotti, R., Rouquerol, J., Siemieniowska, T., 1985. Reporting physisorption data for gas/solid systems with special reference to the determination of surface area and porosity. *Pure Appl. Chem.* 57, 603–619.

- Six, J., Conant, R.T., Paul, E.A., Paustian, K., 2002. Stabilization mechanisms of soil organic matter: Implications for C-saturation of soils. *Plant Soil* 241, 155–176. <https://doi.org/10.1023/A:1016125726789>
- Six, J., Elliott, E.T., Paustian, K., 2000a. Soil macroaggregate turnover and microaggregate formation: A mechanism for C sequestration under no-tillage agriculture. *Soil Biol. Biochem.* 32, 2099–2103. [https://doi.org/10.1016/S0038-0717\(00\)00179-6](https://doi.org/10.1016/S0038-0717(00)00179-6)
- Six, J., Paustian, K., Elliott, E.T., Combrink, C., 2000b. Soil Structure and Organic Matter I. Distribution of Aggregate-Size Classes and Aggregate-Associated Carbon. *Soil Sci. Soc. Am. J.* 64, 681–689. <https://doi.org/10.2136/sssaj2000.642681x>
- Sleutel, S., De Neve, S., Hofman, G., 2007. Assessing causes of recent organic carbon losses from cropland soils by means of regional-scaled input balances for the case of Flanders (Belgium). *Nutr. Cycl. Agroecosystems* 78, 265–278. <https://doi.org/10.1007/s10705-007-9090-x>
- Smith, P., Davies, C.A., Ogle, S., Zanchi, G., Bellarby, J., Bird, N., Boddey, R.M., McNamara, N.P., Powlson, D., Cowie, A., van Noordwijk, M., Davis, S.C., Richter, D.D.B., Kryzanowski, L., van Wijk, M.T., Stuart, J., Kirton, A., Eggar, D., Newton-Cross, G., Adhya, T.K., Braimoh, A.K., 2012. Towards an integrated global framework to assess the impacts of land use and management change on soil carbon: Current capability and future vision. *Glob. Chang. Biol.* 18, 2089–2101. <https://doi.org/10.1111/j.1365-2486.2012.02689.x>
- Smith, P., Falloon, P., Szabó, J., Smith, J., Marshall, S., Coleman, K., 1998. Regional estimates of carbon sequestration potential : linking the Rothamsted Carbon Model to GIS databases. *Biol. Fertil. Soils* 27, 236–241.
- Smith, P., Smith, J., Wattenbach, M., Meyer, J., Lindner, M., Zaehle, S., Niederer, R., Jones, R.J.A., Montanarella, L., Rounsevell, M., Reginster, I., Kankaanpää, S., 2006. Projected changes in mineral soil carbon of European forests, 1990-2100. *Can. J. Soil Sci.* 86, 159–169. <https://doi.org/10.4141/s05-078>
- Smith, W., Cleveland, C., Reed, S., Running, S., 2014. Agricultural conversion without external water and nutrient inputs reduces terrestrial vegetation productivity. *Geophys. Prospect.* 6298–6305. <https://doi.org/10.1002/2013GL058857>. Received
- Soeria-Atmadja, R., Noeradi, D., 2005. Distribution of early tertiary volcanic rocks in south Sumatra and west Java. *Isl. Arc* 14, 679–686. <https://doi.org/10.1111/j.1440-1738.2005.00476.x>
- Soil Survey Staff, 2014. Keys to soil taxonomy, 12th ed, Soil Conservation Service. USDA-Natural Resources Conservation Service, Washington, DC.
- Soleimani, A., Hosseini, S.M., Massah Bavani, A.R., Jafari, M., Francaviglia, R., 2017. Simulating soil organic carbon stock as affected by land cover change and climate change, Hyrcanian forests (northern Iran). *Sci. Total Environ.* 599–600, 1646–1657. <https://doi.org/10.1016/j.scitotenv.2017.05.077>
- Solleiro-Rebolledo, E., Sedov, S., Cabadas-Báez, H., 2015. Use of soils and palaeosols on volcanic materials to establish the duration of soil formation at different chronological scales. *Quat. Int.* 376, 5–18. <https://doi.org/10.1016/j.quaint.2014.12.002>
- Sollins, P., Gregg, J.W., 2017. Soil organic matter accumulation in relation to changing soil volume, mass, and structure: Concepts and calculations. *Geoderma* 301, 60–71. <https://doi.org/10.1016/j.geoderma.2017.04.013>
- Sosnowska, A., 2012. Land use change impact on soil organic matter. Loess landscape case study. *Misc. Geogr.* 16, 11–15. <https://doi.org/10.2478/v10288-012-0027-0>
- Stuble, K.L., Ma, S., Liang, J., Luo, Y., Classen, A.T., Souza, L., 2019. Long-term impacts of warming drive decomposition and accelerate the turnover of labile, not recalcitrant, carbon. *Ecosphere* 10. <https://doi.org/10.1002/ecs2.2715>
- Stuitjs, I., Newsome, J., Flenley, J.R., 1988. Evidence for Late Quaternary Vegetational Change. *Rev. Palaeobot. Palynol.* 55, 207–216.
- Stumm, W., 1992. Chemistry solid-water interface. John Wiley & Sons, Inc, New York.
- Sunardy, E., Kimura, J., 1998. Temporal chemical variations in late Cenozoic volcanic rocks around The

- Bandung Basin, West Java, Indonesia. *J. Min. Petr. Econ. Geol* 93, 103–128. <https://doi.org/10.2465/GANKO.93.103>
- Surmayadi, M., Sumintadireja, P., Irawan, D., Arisbaya, I., 2011. Dinamika vulkanisme Gunung Api Tangkuban Parahu, in: Joint Convention HAGI-IAGI. Makasar. <https://doi.org/10.13140/RG.2.1.3527.4088>
- Tamrat, W., Rose, J., Grauby, O., Doelsch, E., Levard, C., Chaurand, P., Basile-Doelsch, I., 2019. Soil organo-mineral associations formed by co-precipitation of Fe, Si and Al in presence of organic ligands. *Geochim. Cosmochim. Acta* 260, 15–28. <https://doi.org/https://doi.org/10.1016/j.gca.2019.05.043>
- Tangang, F., Chung, J.X., Juneng, L., Supari, Salimun, E., Ngai, S.T., Jamaluddin, A.F., Mohd, M.S.F., Cruz, F., Narisma, G., Santisirisomboon, J., Ngo-Duc, T., Van Tan, P., Singhruck, P., Gunawan, D., Aldrian, E., Sopaheluwakan, A., Grigory, N., Remedio, A.R.C., Sein, D. V., Hein-Griggs, D., McGregor, J.L., Yang, H., Sasaki, H., Kumar, P., 2020. Projected future changes in rainfall in Southeast Asia based on CORDEX–SEA multi-model simulations. *Clim. Dyn.* 55, 1247–1267. <https://doi.org/10.1007/s00382-020-05322-2>
- Taylor, M.D., Lowe, D.J., Hardi, P., Smidt, G.A., Schnug, E., 2016. Comparing volcanic glass shards in unfertilised and fertilised Andisols derived from rhyolitic tephras, New Zealand: Evidence for accelerated weathering and implications for land management. *Geoderma* 271, 91–98. <https://doi.org/10.1016/j.geoderma.2016.01.035>
- Thommes, M., Kaneko, K., Neimark, A. V., Olivier, J.P., Rodriguez-Reinoso, F., Rouquerol, J., Sing, K.S.W., 2015. Physisorption of gases, with special reference to the evaluation of surface area and pore size distribution (IUPAC Technical Report). *Pure Appl. Chem.* 87, 1051–1069. <https://doi.org/10.1515/pac-2014-1117>
- Tonneijck, F.H., Jansen, B., Nierop, K.G.J., Verstraten, J.M., Sevink, J., De Lange, L., 2010. Towards understanding of carbon stocks and stabilization in volcanic ash soils in natural Andean ecosystems of northern Ecuador. *Eur. J. Soil Sci.* 61, 392–405. <https://doi.org/10.1111/j.1365-2389.2010.01241.x>
- Topographical Service Batavia, 1941. Topographical map West Java 1:50,000 (Goenoeng Tangkoebanprahoe).
- Torn, M.S., Trumbore, S., Chadwick, O.A., Vitousek, P.M., Hendricks, D., 1997. Mineral control of soil organic carbon storage and turnover. *Nature* 389, 170–173. <https://doi.org/https://doi.org/10.1038/38260>
- Totsche, K.U., Amelung, W., Gerzabek, M.H., Guggenberger, G., Klumpp, E., Knief, C., Lehndorff, E., Mikutta, R., Peth, S., Prechtel, A., Ray, N., Kögel-Knabner, I., 2018. Microaggregates in soils. *J. Plant Nutr. Soil Sci.* 181, 104–136. <https://doi.org/10.1002/jpln.201600451>
- Uehara, G., Gillman, G., 1981. The mineralogy, chemistry, and physics of tropical soils with variable charge clays. Westview Press, Inc., Colorado.
- Ugolini, F.C., Dahlgren, R.A., 2002. Soil development in volcanic ash. *Glob. Environ. Res.* 6, 69–81.
- Utami, S.R., Mees, F., Dumon, M., Qafoku, N.P., Van Ranst, E., 2019. Charge fingerprint in relation to mineralogical composition of Quaternary volcanic ash along a climatic gradient on Java Island, Indonesia. *Catena* 172, 547–557. <https://doi.org/10.1016/j.catena.2018.09.024>
- Van Bemmelen, R., 1949. The Geology of Indonesia. Vol. IA: General Geology of Indonesia and Adjacent Archipelagoes. The Hague, Jakarta. <https://doi.org/10.1144/gospp>
- Van Breemen, N., Mulder, J., Driscoll, C., 1983. Acidification and alkalinization of soils. *Plant Soil* 75, 283–308.
- Van Der Kaars, S., Dam, R., 1997. Vegetation and climate change in West-Java, Indonesia during the last 135,000 years. *Quat. Int.* 37, 67–71. [https://doi.org/10.1016/1040-6182\(96\)00002-x](https://doi.org/10.1016/1040-6182(96)00002-x)
- Vander Linden, C., Delvaux, B., 2019. The weathering stage of tropical soils affects the soil-plant cycle of silicon, but depending on land use. *Geoderma* 351, 209–220. <https://doi.org/10.1016/j.geoderma.2019.05.033>
- Vander Linden, C., Li, Z., Iserentant, A., Van Ranst, E., de Tombeur, F., Delvaux, B., 2021. Rainfall is the

- major driver of plant Si availability in perudic gibbsitic Andosols. *Geoderma* 404, 115295. <https://doi.org/10.1016/j.geoderma.2021.115295>
- Veenstra, J.J., Lee Burras, C., 2012. Effects of agriculture on the classification of black soils in the midwestern United States. *Can. J. Soil Sci.* 92, 403–411. <https://doi.org/10.4141/CJSS2010-018>
- Veldkamp, E., Schmidt, M., Powers, J.S., Corre, M.D., 2020. Deforestation and reforestation impacts on soils in the tropics. *Nat. Rev. Earth Environ.* 1, 590–605. <https://doi.org/10.1038/s43017-020-0091-5>
- Violette, A., Godd ris, Y., Mar chal, J.C., Riotte, J., Oliva, P., Kumar, M.S.M., Sekhar, M., Braun, J.J., 2010. Modelling the chemical weathering fluxes at the watershed scale in the Tropics (Mule Hole, South India): Relative contribution of the smectite/kaolinite assemblage versus primary minerals. *Chem. Geol.* 277, 42–60. <https://doi.org/10.1016/j.chemgeo.2010.07.009>
- von L tzow, M., K gel-Knabner, I., 2009. Temperature sensitivity of soil organic matter decomposition-what do we know? *Biol. Fertil. Soils* 46, 1–15. <https://doi.org/10.1007/s00374-009-0413-8>
- von L tzow, M., K gel-Knabner, I., Ekschmitt, K., Flessa, H., Guggenberger, G., Matzner, E., Marschner, B., 2007. SOM fractionation methods: Relevance to functional pools and to stabilization mechanisms. *Soil Biol. Biochem.* 39, 2183–2207. <https://doi.org/10.1016/j.soilbio.2007.03.007>
- Wagai, R., Kajiura, M., Uchida, M., Asano, M., 2018. Distinctive roles of two aggregate binding agents in allophanic andisols: Young carbon and poorly-crystalline metal phases with old carbon. *Soil Syst.* 2, 1–23. <https://doi.org/10.3390/soilsystems2020029>
- Wagai, R., Mayer, L.M., 2007. Sorptive stabilization of organic matter in soils by hydrous iron oxides. *Geochim. Cosmochim. Acta* 71, 25–35. <https://doi.org/10.1016/j.gca.2006.08.047>
- Wagai, R., Mayer, L.M., Kitayama, K., 2009. Extent and nature of organic coverage of soil mineral surfaces assessed by a gas sorption approach. *Geoderma* 149, 152–160. <https://doi.org/10.1016/j.geoderma.2008.11.032>
- Wang, B., Gray, J.M., Waters, C.M., Rajin Anwar, M., Orgill, S.E., Cowie, A.L., Feng, P., Li Liu, D., 2022. Modelling and mapping soil organic carbon stocks under future climate change in south-eastern Australia. *Geoderma* 405, 115442. <https://doi.org/10.1016/j.geoderma.2021.115442>
- Wei, C., Ni, J., Gao, M., Xie, D., Hasegawa, S., 2006. Anthropogenic pedogenesis of purple rock fragments in Sichuan Basin, China. *Catena* 68, 51–58. <https://doi.org/10.1016/j.catena.2006.04.022>
- Wei, X., Shao, M., Gale, W., Li, L., 2014. Global pattern of soil carbon losses due to the conversion of forests to agricultural land. *Sci. Rep.* 4, 6–11. <https://doi.org/10.1038/srep04062>
- Werth, M., Kuz'yakov, Y., 2010. 13C fractionation at the root-microorganisms-soil interface: A review and outlook for partitioning studies. *Soil Biol. Biochem.* 42, 1372–1384. <https://doi.org/10.1016/j.soilbio.2010.04.009>
- White, A.F., Brantley, S.L., 2003. The effect of time on the weathering of silicate minerals: Why do weathering rates differ in the laboratory and field? *Chem. Geol.* 202, 479–506. <https://doi.org/10.1016/j.chemgeo.2003.03.001>
- Wiesmeier, M., H bner, R., Barthold, F., Sp rlein, P., Geu , U., Hangen, E., Reischl, A., Schilling, B., von L tzow, M., K gel-Knabner, I., 2013. Amount, distribution and driving factors of soil organic carbon and nitrogen in cropland and grassland soils of southeast Germany (Bavaria). *Agric. Ecosyst. Environ.* 176, 39–52. <https://doi.org/10.1016/j.agee.2013.05.012>
- Wiesmeier, M., Urbanski, L., Hobbey, E., Lang, B., von L tzow, M., Marin-Spiotta, E., van Wesemael, B., Rabot, E., Lie , M., Garcia-Franco, N., Wollschl ger, U., Vogel, H.J., K gel-Knabner, I., 2019. Soil organic carbon storage as a key function of soils - A review of drivers and indicators at various scales. *Geoderma* 333, 149–162. <https://doi.org/10.1016/j.geoderma.2018.07.026>
- Wiseman, C.L.S., P ttmann, W., 2005. Soil organic carbon and its sorptive preservation in central Germany. *Eur. J. Soil Sci.* 56, 65–76. <https://doi.org/10.1111/j.1351-0754.2004.00655.x>
- Witzgall, K., Vidal, A., Schubert, D.I., H schen, C., Schweizer, S.A., Buegger, F., Pouteau, V., Chenu, C., Mueller, C.W., 2021. Particulate organic matter as a functional soil component for persistent soil organic carbon. *Nat. Commun.* 12, 1–10. <https://doi.org/10.1038/s41467-021-24192-8>

- Woignier, T., Primera, J., Duffours, L., Dieudonné, P., Raada, A., 2008. Preservation of the allophanic soils structure by supercritical drying. *Microporous Mesoporous Mater.* 109, 370–375. <https://doi.org/10.1016/j.micromeso.2007.05.019>
- Wolff-Boenisch, D., Gislason, S.R., Oelkers, E.H., Putnis, C. V., 2004. The dissolution rates of natural glasses as a function of their composition at pH 4 and 10.6, and temperatures from 25 to 74°C. *Geochim. Cosmochim. Acta* 68, 4843–4858. <https://doi.org/10.1016/j.gca.2004.05.027>
- Yigini, Y., Panagos, P., 2016. Assessment of soil organic carbon stocks under future climate and land cover changes in Europe. *Sci. Total Environ.* 557–558, 838–850. <https://doi.org/10.1016/j.scitotenv.2016.03.085>
- Yu, G., Xiao, J., Hu, S., Polizzotto, M.L., Zhao, F., McGrath, S.P., Li, H., Ran, W., Shen, Q., 2017. Mineral availability as a key regulator of soil carbon storage. *Environ. Sci. Technol.* 51, 4960–4969. <https://doi.org/10.1021/acs.est.7b00305>
- Yu, H., Ding, W., Luo, J., Geng, R., Ghani, A., Cai, Z., 2012. Effects of long-term compost and fertilizer application on stability of aggregate-associated organic carbon in an intensively cultivated sandy loam soil. *Biol. Fertil. Soils* 48, 325–336. <https://doi.org/10.1007/s00374-011-0629-2>
- Yu, L., Gu, F., Huang, M., Tao, B., Hao, M., Wang, Z., 2020. Impacts of 1.5 °C and 2 °C global warming on net primary productivity and carbon balance in China’s terrestrial ecosystems. *Sustain.* 12, 1–17. <https://doi.org/10.3390/su12072849>
- Yu, Y.Y., Finke, P.A., Wu, H.B., Guo, Z.T., 2013. Sensitivity analysis and calibration of a soil carbon model (SoilGen2) in two contrasting loess forest soils. *Geosci. Model Dev.* 6, 29–44. <https://doi.org/10.5194/gmd-6-29-2013>
- Yuan, G., Theng, B.K.G., Parfitt, R.L., Percival, H.J., 2000. Interactions of allophane with humic acid and cations. *Eur. J. Soil Sci.* 51, 35–41. <https://doi.org/10.1046/j.1365-2389.2000.00295.x>
- Zhang, J., Xiao, J., Li, S., Ran, W., 2017. Manure amendment increases the content of nanomineral allophane in an acid arable soil. *Sci. Rep.* 7. <https://doi.org/10.1038/s41598-017-14445-2>
- Zhao, F., Wu, Y., Hui, J., Sivakumar, B., Meng, X., Liu, S., 2021. Projected soil organic carbon loss in response to climate warming and soil water content in a loess watershed. *Carbon Balance Manag.* 16, 1–14. <https://doi.org/10.1186/s13021-021-00187-2>
- Zheng, H., Liu, W., Zheng, J., Luo, Y., Li, R., Wang, H., Qi, H., 2018. Effect of long-term tillage on soil aggregates and aggregate-associated carbon in black soil of northeast China. *PLoS One* 13, 1–18. <https://doi.org/10.1371/journal.pone.0199523>
- Zimmerman, A.R., Chorover, J., Goynes, K.W., Brantley, S.L., 2004. Protection of mesopore-adsorbed organic matter from enzymatic degradation. *Environ. Sci. Technol.* 38, 4542–4548. <https://doi.org/10.1021/es035340+>
- Zimmermann, M., Leifeld, J., Schmidt, M.W.I., Smith, P., Fuhrer, J., 2007. Measured soil organic matter fractions can be related to pools in the RothC model. *Eur. J. Soil Sci.* 58, 658–667. <https://doi.org/10.1111/j.1365-2389.2006.00855.x>

Curriculum vitae

Sastrika Anindita was born on 12 May 1990 in Bandung, West Java, Indonesia. In 2012, she graduated her bachelor's degree in Soil Science from Universitas Padjadjaran, Indonesia. During her study, she received a scholarship two times from The Ministry of Education, Culture, Research, and Technology, Indonesia, for academic merit. During this period, she did a research internship at Research Institute for Tea and Cinchona, and she wrote a scientific paper in the national journal about the distribution of *Azotobacter sp.* and organic matter in various slopes on tea plantations. She was also involved in the land restoration project in the former Kareumbi plantation. She received a VLIR-UOS scholarship in 2014 to pursue her master's degree in the Physical Land Resources program at Ghent University, Belgium. Her engagement with volcanic soils started after joining voluntary work with farmers in the area of Mt. Tangkuban Perahu. She found that the volcanic soils have unique characteristics that even after long intensive cultivation, the farmers still produce a good quantity of agricultural products from this soil, although it may not persist for a long time. This experience brings an idea for her thesis entitled "Analysing land use effects on soil development at Lembang, Bandung district, Indonesia". The thesis was evaluated as the best MSc thesis in her program and was presented at National Conference in Yogyakarta. In 2018, she received a full scholarship from Indonesia Endowment Fund for Education (LPDP) for a doctoral program at Ghent University. She continued her PhD research on volcanic soils, specifically on the effect of land use on soil organic carbon mediated by soil properties. During her doctoral program, she has an article published in a scientific peer-reviewed journal. She presented her research at the European Geoscience Union (EGU) and the National Symposium of Applied Biological Science. She also joined a workshop on BGMN-Profex software for minerals quantification and several transferable skills organised by Ghent University.